

Strategies to Improve Adenovirus and Reovirus Vectors for Oncolytic Virotherapy

Sanne K. van den Hengel

ISBN: 978-94-6299-151-4

Cover: Sanne van den Hengel

Lay-out: Nikki Vermeulen - Ridderprint BV - www.ridderprint.nl

Printed: Ridderprint BV - www.ridderprint.nl

Copyright © Sanne van den Hengel, 2015

Strategies to Improve Adenovirus and Reovirus Vectors for Oncolytic Virotherapy

Het verbeteren van adenovirus en reovirus vectoren
voor oncolytische virustherapie

Proefschrift

ter verkrijging van de graad van doctor aan de
Erasmus Universiteit Rotterdam

op gezag van de rector magnificus
Prof.dr. H.A.P. Pols
en volgens besluit van het College voor Promoties.

De openbare verdediging zal plaatsvinden op
woensdag 16 september 2015 om 15.30 uur

door

Sanne Klaassiena van den Hengel

geboren te Groningen

Erasmus University Rotterdam

The logo of Erasmus University, featuring the word "Erasmus" in a stylized, cursive script.

Promotiecommissie

Promotoren:

Prof.dr. P.A.E. Sillevius Smitt

Prof.dr. R.C. Hoeben

Overige leden:

Prof.dr. C.M.F. Dirven

Prof.dr. C.H. Bangma

Dr. G. van der Pluijm

The studies described in this thesis were performed at the Department of Neurology of the Erasmus University Medical Center (Rotterdam, The Netherlands) and the Department of Molecular Biology of the Leiden University Medical Center (Leiden, The Netherlands).

CONTENTS

Part I	Introduction	7
Chapter 1	General introduction	9
Chapter 2	Adenovirus	17
Chapter 3	Reovirus	31
	<i>References I</i>	65
Part II	Adenovirus	81
Chapter 4	Enhanced transduction of CAR-negative cells by protein IX-gene deleted adenovirus 5 vectors	83
Chapter 5	Truncating the i-leader open reading frame enhances release of human adenovirus type 5 in glioma cells	105
	<i>References II</i>	123
Part III	Reovirus	131
Chapter 6	A strategy for genetic modification of the spike-encoding segment of human reovirus T3D for reovirus targeting	133
Chapter 7	Isolation of reovirus T3D mutants capable of infecting human tumor cells independent of junction adhesion molecule-A	157
Chapter 8	Heterogeneous reovirus susceptibility in human glioblastoma stem-like cell cultures	185
Chapter 9	Mesenchymal stromal cells as carriers for oncolytic reoviruses: an <i>in vitro</i> feasibility study	201
	<i>References III</i>	221
Part IV	Summary, discussion and conclusion	233
Chapter 10	Summary and discussion	235
Chapter 11	Conclusion	243
Chapter 12	Nederlandse samenvatting	247
	<i>References IV</i>	257
	<i>List of Publications</i>	269
	<i>PhD portfolio</i>	275
	<i>About the Author</i>	281
	<i>Dankwoord</i>	285

CHAPTER 1

GENERAL INTRODUCTION



BACKGROUND

The goal of this thesis is to explore new methods for improving adenovirus and reovirus vectors for oncolytic virus therapy. Oncolytic virus therapy aims at treating malignancies with viruses that preferentially replicate in cancer cells. Oncolytic virotherapy can use both natural unmodified viruses as well as engineered viruses. The general concept to use viruses for eradication of malignancies dates back to the late 1800s and early 1900s [1]. In the first case reports, patients, most often suffering from hematological malignancies, went into remission after contracting an infectious disease, presumably of viral origin. Unfortunately remissions were often short-lived [1-3] and the cause of the remission remained vague. Physical evidence for the existence of viruses was not acquired until later in the 20th century. Around the 1950s developments in cell and tissue culture techniques led to the ability to propagate viruses *in vitro*. This allowed an increase in the general knowledge of virus biology and resulted in the evaluation of the oncolytic potential of a range of viruses on malignancies of different origins in cell and tissue cultures. Subsequently, studies in animal models and even humans were performed. Although there was anecdotal evidence of tumor remission in humans, the side effects, virus elimination by the immune system, and a number of ethical concerns together with the beginning of the era of chemotherapy resulted in a decrease of interest in oncolytic virotherapy [2-5].

Renewed interest in oncolytic viruses arose in the early 1990s with the rise of recombinant DNA techniques and the increased knowledge in virus biology obtained in the previous decades [6]. The major breakthrough was the development of a thymidine kinase-negative herpes simplex-1 mutant with reduced neurovirulence which showed to be active in a murine glioblastoma model [7]. After the first encouraging paper more reports about genetically engineered viruses followed [8,9] and provided the field with new know-how in virus biology, virus-cell interactions, replication cycles, and also virus modification strategies. In the same period general knowledge about cancer biology increased enormously. This increased knowledge of both virus and cancer biology resulted in a long list of potential oncolytic viruses, some of which even reached the clinic (reviewed in [4,5]). The first genetically modified oncolytic virus registered for clinical use is an adenovirus based vector. It was approved in China in 2005 for the treatment of head and neck cancers [10].

However, in Europe and the USA no vector has yet been registered for oncolytic virotherapy and the road to develop effective oncolytic vectors has been more difficult than was expected in the beginning of this research era.

Nevertheless, the field has made enormous progress. For a number of viruses safety profiles were excellent, and the viruses could be produced in high titer at clinical grade. In addition the development and applicability of modifications strategies is facilitating new vector development. Currently, the major drawbacks in oncolytic virotherapy are insufficient tumor tropism and tumor cell-specificity, inefficient replication in tumor cells and limited spread in the tumor. In addition viruses can be rapidly cleared by the immune system and scavenged by non-target cells. In this thesis research is focused on getting solutions for some of these issues.

AIMS

The general aim of this thesis is to overcome some of the bottlenecks that limit efficacy of oncolytic virotherapy. We focused on four different approaches to generate more effective viruses and to obtain more reliable parameters of anticancer efficacy.

1. Modification of capsid proteins to alter the tropism of the wild-type virus.
2. Forward-genetic strategies were used to obtain more potent viruses.
3. The modified viruses, obtained with the help of forward genetics, have been analyzed and compared with wild-type viruses on primary cultures and stem-like cultures.
4. Mesenchymal stromal cells (MSC) were evaluated as carrier cells for reovirus delivery to cancer cells.

Standard testing of oncolytic viruses is performed mainly on established cell lines. In the last decade, the appropriateness of established cell lines for predicting the effects on genuine tumor cells has been increasingly challenged. Primary cultures and tumor stem cells cultures have a closer resemblance to tumors than conventional serum cultured cell lines [11,12]. It is therefore suggested that primary and tumor stem cells cultures are better models to predict of the clinical efficacy. So in this thesis two of the modified viruses were tested on primary cultures obtained from resected glioblastomas. Glioblastoma is the most aggressive form of brain cancer and even with the current treatment regimens the median survival is only between 12-15 months [6,13]. The poor prognosis is due to the rapid growth and invasive nature of the tumor and to its resistance to chemotherapeutic drugs and radiation therapy. Despite the extensive research of the last decades, only limited improvements in survival rate have been obtained [14]. In the quest to curative treatment modalities for this disease, oncolytic virus therapy has been heralded as a promising therapeutic agent. The

factors which make oncolytic virus therapy an ideal candidate for treatment of glioblastoma are 1) that the tumors are located in an enclosed environment and 2) metastases outside the skull almost never occur. Additionally, the tumors are often surrounded by post mitotic cells, which have the advantages that viruses which require active cell division cannot replicate in these cells. At least fourteen oncolytic viruses have already been selected as candidate viruses for glioma therapy (listed in table 1.1) (reviewed in [15,16]). Seven of these viruses have been or are currently evaluated in clinical trials and case studies. Data of the completed studies provide evidence for the safety of the approach and, so far, the maximum tolerated dose has not been reached. Unfortunately the data reporting evidence significant therapeutic impact have been limited (reviewed in [15-17]). This demonstrates that new preclinical research is warranted to improve the therapeutic efficacy. Only then, the oncolytic viruses can be a useful addition to the armamentarium to combat this devastating disease (reviewed in [15]).

Table 1.1 Candidate viruses for oncolytic virus therapy for glioma. Table adapted from Wollman *et al.* [15]

Virus	Virus family	Phase of development relating to glioma
Herpes simplex virus 1	<i>Herpesviridae</i>	Clinical phase I/II
Newcastle Disease virus	<i>Paramyxoviridae</i>	Clinical phase I/II
Adenovirus	<i>Adenoviridae</i>	Clinical phase I
Reovirus	<i>Reoviridae</i>	Clinical phase I
H1 Parvovirus	<i>Parvoviridae</i>	Clinical phase I
Poliovirus	<i>Picornaviridae</i>	Clinical phase I
Measles virus	<i>Paramyxoviridae</i>	Clinical phase I
Vaccinia virus	<i>Poxviridae</i>	Preclinical <i>in vivo</i>
Myxoma virus	<i>Poxviridae</i>	Preclinical <i>in vivo</i>
Vesicular Stomatitis Virus	<i>Rhabdoviridae</i>	Preclinical <i>in vivo</i>
Pseudorabies virus	<i>Herpesviridae</i>	Preclinical <i>in vitro</i>
Minute Virus of Mice	<i>Parvoviridae</i>	Preclinical <i>in vitro</i>
Sindbis virus	<i>Togaviridae</i>	Preclinical <i>in vitro</i>
Seneca Valley virus	<i>Picornaviridae</i>	Preclinical <i>in vitro</i>

OUTLINE

Part I is divided in three chapters. After a general introduction to oncolytic virotherapy and the aim of this thesis, a brief introduction into the adenovirus biology and the development of recombinant vectors is provided. The third

chapter focuses on reovirus. Here, shortly, the structure, replication biology and genetic modification strategies of reovirus are discussed. This chapter ends with the motivation why reovirus is of interest as oncolytic agent.

Part II focuses on genetic modifications of the adenovirus in order to obtain an adenoviral vector with improved oncolytic efficacy. In **chapter 4** the effect of deleting the minor capsid protein IX is investigated. As described in chapter 2 the function of protein IX is still not fully clear. However, deleting this protein makes the particle more susceptible to heat and decreases the maximum genome size which can be packaged [18]. Here it is shown that deletion of protein IX expands the cell tropism but also the virus became more susceptible to the innate immune system in mice. These data provide more insight into the biological role of protein IX and can be of value for the development of oncolytic vectors. In **chapter 5** the effect of truncating the adenovirus i-leader open reading frame (orf) on glioma cell lines and primary high-grade glioma cultures is described. Already in previous studies it was shown that truncating mutations in this i-leader region improved the cytopathic activity of human adenovirus-5 (HAdV-5) in a panel of tumor cell lines [19,20]. Unfortunately, no glioma cultures were included in the published study. Here, the generation of the replication-competent vector containing the single i-leader point mutation is described. After verification of the vector, the cytopathic effect is analyzed using cell based assays. It is shown that the cytopathic activity in glioma cultures increases by truncation of the i-leader orf. Although these are preliminary results and no *in vivo* data is presented it is important knowledge which may be implemented in future vectors.

Part III concentrates on reovirus as oncolytic vector. As described in chapter 3, reovirus has a natural preference for transformed cell. Unfortunately its clinical efficacy as oncolytic agent is still limited. The first two chapters of section 3 focus on genetic modification of reovirus in order to modify the tropism. In **chapter 6** a strategy to replace the wild-type spike by a modified spike-protein with short peptide ligand is described. This strategy makes use of a helper cell line expressing the modified segment as conventional RNA polymerase II transcript which leads to the replacement of the wild-type segment by the modified segment. In **chapter 7** modifications are based on classical forward-genetics strategies. Reovirus RNA-dependent RNA polymerase lacks the proofreading ability and therefore genomic mutations are easily introduced. Adaptation of wild-type reovirus to replicate on a cell line which does not express the reovirus high affinity receptor junction adhesion molecule-A (JAM-A) yields mutants with a modified tropism (JAM-A independent (*jln*) mutants). Additional genomic

analysis of the *jin* mutants indicates that mutations in the S1 segment, encoding the spike protein $\sigma 1$, is responsible for the expanded tropism. These mutants could be of great interest as oncolytic agents for the treatment of tumors that lack JAM-A on the cell surface.

In the last decades, enormous progress has been made in elucidating cancer biology. Cancer stem-like cells have been assigned as a cell type which play an important role in the recurrence and metastases of tumors. In addition, these cells possess a high resistance to radiation and chemotherapy (reviewed in [21-23]). Therefore an efficient therapy requires the removal of these cells. In order to determine the susceptibility of human glioblastoma stem-like cell (GSC) cultures to reovirus a panel of GSC was exposed to reovirus (**chapter 8**). Because of a high variation of JAM-A expression between GSC cultures determined by flow cytometry, both wild-type as well as mutant *jin-1* were applied. In this study it was shown that GSC were more susceptible to *jin-1* than wild-type in monolayer experiments. However, in 3-dimensional (3D) tumor cell spheroids the viruses were equally effective.

A major bottleneck of oncolytic virus therapy is neutralization and scavenging of the virus by immune cells or non-target tissue reducing the effective dose. Hiding the virus from these factors and in the meantime delivering the virus to the target site could make the oncolytic virus therapy more effective. Of several cell types it is known that they home to tumors such as dendritic cells, T cells, NK cells, macrophages and several stem cell types [24]. In **chapter 9** it is investigated whether mesenchymal stromal cells (MSC) can be potential carriers for reovirus. Since JAM-A is almost absent on MSC, wild-type reovirus and *jin-1* were applied to MSC cultures. Here it is shown that, although replication was not supported in MSC, these cells could still hand-off the virus to neighboring cells in monolayer and in 3D tumor cell spheroids. These results support the development of human MSC as cellular vehicles for the delivery of oncolytic reoviruses.

CHAPTER 2

ADENOVIRUS



BIOLOGY

One of the most popular viruses for the use in oncolytic virus therapy is the human adenovirus [3,25,26]. This virus was first isolated in the 1950s from cell cultures derived from adenoid-tissue [27,28]. In the same period the research on the use of viruses as oncolytic agent was expanding [3,4]. Therefore it is not surprising that not long after the initial isolation of adenovirus it was evaluated as a candidate in pre-clinical and clinical studies. Administration of adenovirus to cancer patients caused only modest side effects, but unfortunately survival of the patients was only minimally prolonged and infections were quickly abolished by the immune system (reviewed in [3]). In the consecutive years adenoviruses have been very important for unraveling the principles of RNA splicing [29] and for developing techniques for naked-DNA transfer such as the calcium phosphate DNA-transfection method [30]. In addition, the study of adenoviruses has been instrumental for acquiring knowledge on fundamental viral processes and basic aspects of cell biology (reviewed in [31,32]). Together with the upcoming recombinant DNA techniques in the 1980s, the relative ease of the genetic modification of viruses, the high-titers of adenovirus vector batches, and the good safety profiles seen in clinical trials have made adenoviral vectors one of the most frequently used vectors in vaccine development, gene delivery, and oncolytic areas [25,33].

The human adenoviruses belong to the family *Adenoviridae* and the genus *Mastoadenovirus*. Over 60 serotypes of human adenoviruses have been identified which are classified in seven species, A to G [34]. Depending on the serotype human adenovirus can cause respiratory, enteric, eye or urinary tract infections. However usually these infections are mild and self-limiting, and result in life-long immunity [25]. Serotype 2 and 5 of species C are among the first adenoviruses to be discovered. Most studies have used these serotypes and therefore most knowledge has been obtained on these serotypes. In this thesis we focus on modifying serotype 5 for generating vectors with potency in oncolytic virotherapy.

The human adenovirus 5 (HAAdV-5) is a non-enveloped icosahedral virus of approximately 90 nm. The capsid is composed of three major proteins, hexon, penton and fiber, and four minor proteins IIIa, VI, VIII and IX (figure 2.1). Minor capsid protein IX it is the smallest capsid protein and a virion contains 240 copies of this protein in the capsid. Protein IX consists of 3 conserved domains, the amino-terminal domain which is embedded in the capsid, the central-part and the carboxyl-terminal (C-terminal) domain. The exact function of protein IX is unknown, but vectors lacking this protein are more heat sensitive and unable

to package a full genome length. Therefore a cementing function have been assigned to protein IX. When only the C-terminal domain is removed less clear effects are demonstrated [35].

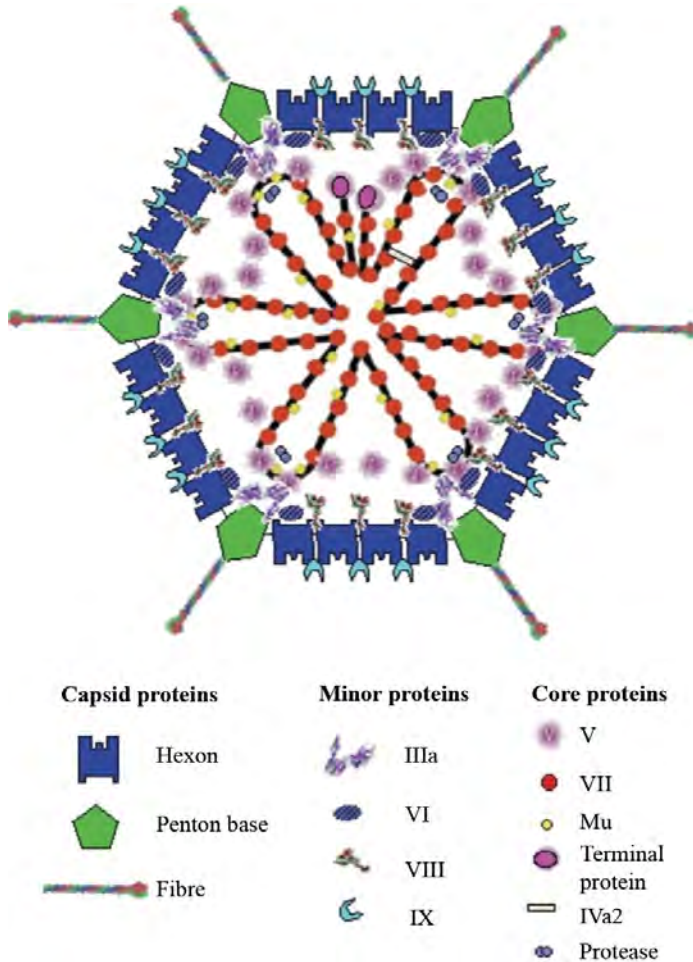


Figure 2.1 Schematic representation of the adenovirus. Adopted from Russell [36].

Recently, by Cryo-electron microscopy (Cryo-EM), high resolution images of the adenovirus capsid have been made. These images reveal the interactions between the capsid proteins [37]. Hexon, the first animal virus protein which was crystallized [38], is the main building block of the capsid and serves mainly for stability. Furthermore, hexon plays an important role in establishing the immune

response and in 2008 the liver tropism of several human adenoviruses could be assigned to binding of coagulation factor X to the hexon [39,40]. The second major capsid protein, penton base proteins, form a pentameric structure, which, together with the fiber forms the pentons on the 12 vertices of viral capsid. The vertices are sensitive to heat fluctuations and pH changes and define the weakest part of the capsid. Penton-base contains a RGD-motif to which is important for the binding to cellular integrins during cell attachment. From the penton-base structure, the trimeric fiber extrude. Fiber is composed of three of three domains 1) the N-terminal tail domain which is anchored in the penton base, 2) the shaft, existing of repeating motifs, and 3) the C-terminal domain which forms a globular head domain. The globular head-domain binds to the cellular high-affinity receptor. For HAdV-5 and most other adenovirus serotypes the main high-affinity receptor is the coxsackie and adenovirus receptor (CAR) which is a transmembrane protein of the immunoglobulin superfamily associated with the formation of tight junctions. Docking to CAR is the first interaction between the virus and the cell in the multistep attachment process [32,36]. The next step is the association the RGD-motif located at the penton to cellular integrins which facilitate entry via the clathrin coated pits. This is the main entry route of adenovirus species C however there is also an alternative CAR-independent route via attachment of the shaft to heparin sulphate glycosoaminoglycans [32,36]. Acidification of the endosomes triggers the disassembly of the virion and release of the virus core into the cytoplasm. The virus core contains several viral proteins including IVa2, V, VII, terminal protein (TP), μ (mu), the adenovirus protease, and the adenovirus double stranded DNA genome. HAdV-5 the genome length is 36 kb and is imported in the nucleus where transcription of viral genes is initiated. Adenovirus transcription is a tightly regulated process of early (E1-E4), intermediate (protein IX and IV2a) and late genes (L1-L5) and includes transcription of both strands and complex RNA splicing [41].

Approximately 5-6 hrs after infection the transcription of the viral genes is initiated. The early genes prepare the cell for adenovirus replication. In addition, these gene products will inhibit the immune responses against the infected cell. The whole cascade starts with the transcription of the immediate early gene E1A, which force the cell to shift to S-phase of the cell cycle, which is the ideal environmental state for ensuing viral replication. In addition E1A activates the transcription of the other early genes. The E1B proteins play an important anti-apoptotic role. The E2 proteins, the pre-terminal protein, the DNA-polymerase, and the single stranded DNA binding protein, have multiple functions all concerning viral transcription, mRNA transport, and replication. Transcripts of

the E3 unit act as important as down regulators of the host immune response against HAdV. The E4 proteins are involved in regulating the viral transcription and mRNA transport. After the initiation of the viral replication, the transcription shifts to the late genes which encode mostly the capsid proteins. Assembly of the particles starts already around 8 hrs after infection and after 30-40 hrs the cell will lyse initiated by de adenovirus death protein releasing all particles to the environment [25,42].

VECTOR BIOLOGY

Despite replication and cell lysis of HAdV-5 is not restricted to tumor cells it is still considered as potential virus for oncolytic virus therapy. Reasons to choose for HAdV-5 as vector are the wealth of fundamental knowledge. Furthermore, these viruses are able to infect dividing and quiescent cells and do not integrate their genome in the host genome, HAdV-5 can be produced at high-titer in clinical-grade quality and the safety profiles obtained from clinical trials have been good. In addition, in the last decades several methods are developed which make it possible to produce replication deficient vectors or vectors which specifically replicate in tumor cells, vectors with an expanded tropism or armed vectors with therapeutic genes. A number of these methods will be discussed in the next sections.

Replication deficient vectors

The first generation replication-deficient adenovirus vectors were E1 deleted. As described earlier E1 has an important function for the initiation of the viral transcription and deletion of this sequence yielded a transcription and replication-impaired adenoviruses [41,43]. E1-deleted vectors are produced on a helper cell lines that complement for E1 functions *in trans*. The first established cell line expressing the HAd5-E1 sequence was the 293 cell line, a human embryonic kidney line transformed with sheared HAdV5 DNA [44]. Unfortunately, as results of homologues recombination between E1 region and the E1-deleted adenovirus vector contamination of replication-competent adenoviruses (RCAs) occurred in produced batches [45]. To reduce the risk of RCA formation, new cell helper lines, containing a smaller region of overlap between the E1 regions in the vector and in the helper cells, were developed [46,47]. This cell line, PER.C6, reduces the risk of RCA formation and together with the 293 and 911 helper cell lines are the most used cell lines for the production of first-generation vectors. Additionally, the E3 region which is involved in evasion of the cellular-immune response

and which is not essential for replication, was deleted from these vectors and generated more space for transgene inserts. Although the first generation of vectors was highly promising and proved to be safe, it induced a strong cellular immune response leading to a rapid eradication of the transduced cells. In reaction to this, a second-generation vector was developed by deleting the E2 and/or E4 sequences. These vectors induced a reduced immune response [41,43] and therefore the transduced cells persisted longer than those transduced with first generation vectors. Subsequently, a third generation vector was developed [41,43]. In this vector all viral protein-coding sequences are removed except the sequences encompassing the inverted terminal repeats and the packaging signal. These vectors are also called gutless vectors or high capacity vectors. The benefits of these vectors are that the transgene insert can be up to ~35 kb in length, and the expression of the transgene is long-lasting also in immune competent animals as the absence of viral genes prevents triggering the immune system. Production of progeny virus requires the presence of a helper virus for providing all the gene products necessary for replication and packaging. A critical note which has to be made is that the produced vector batches can be contaminated with helper-virus. Contamination can be reduced by introducing site-directed recombination sites flanking the packaging signals of the helper virus. These method reduced the recombination events [41].

All three replication-deficient vectors described above have their own pros and cons. The preferred vector depends on the goal to achieve, long-term or short-term expression, insertion of a large or small transgenes and is activation of the immune system appreciated. In most studies activation of the immune system is seen as a negative side effect however there are studies which indicate that oncolytic virotherapy can lead to cancer immunotherapy (reviewed in [48]). How the immune system is stimulated by virotherapy to effectively target the tumor cells still needs to be solved, however it is worthwhile to investigate this further.

Conditionally replicating adenoviruses (CrAds)

Previously the development of replication deficient vectors is discussed. A disadvantage of these vectors is that after the initial infection no new progeny virus is produced. To overcome this hurdle conditional replication adenovirus vectors (CrAds) have been generated. Several strategies can be employed to generate these vectors such as genomic deletions or insertion of tissue-specific promoters.

In most tumors, cell division is impaired and cell-division checkpoints are defective. Wild-type adenovirus will drive cells into S-phase to initiate replication.

This knowledge was used to construct adenovirus which replicate selective in tumor cells. Typical adjustments are modifications of genetic elements which are involved in driving cells into S-phase which results in a vector which can only replicate in transformed cells. The archetype of such a vector is HAdV-5 dl1520, its commercial name is Onyx-015. In this vector the E1B-55k gene is disrupted [49]. A function of E1-55k is to inactivate p53. The cellular p53 is a tumor suppressor protein and defective in almost all tumors. This resulted in a vector which preferentially replicated and killed tumor cells although additional research showed that the mechanism of replication is more complex and does not solely rely on the p53 status [50,51]. Subsequently vectors containing deletions in the E1A-encoding sequence were generated. E1A is known to bind the retinoblastoma protein (Rb) family members, which are also tumor suppressor proteins. A 24-bp deletion in the E1A sequence impairs the binding to Rb. Therefore the vectors are not able to drive cells into S-phase and replication is inhibited in poorly dividing and quiescent cells [52] (reviewed in [25]). Both of these vectors are subjected to extensive clinical trial research. Results of these trials demonstrated a good safety profile and tumor-selective replication unfortunately the antitumor response was limited [25].

Using the characteristics of tumor biology to generate tumor-specific vectors is one way. Another approach is to generate vectors in which essential viral genes are under control of a tissue or tumor-specific promoter. For example placing E1A region under transcriptional control of the tissue-specific glial fibrillary acidic protein (GFAP) promoter resulted in efficient and specific replication in malignant glioma cells *in vitro* and *in vivo* [53]. Disadvantages of this approaches are that the size of the tissue specific promoter is restricted and the occurrence of leakage of E1A regulatory functions resulting in non-specific replication. The last disadvantages can be solved by placing E1A in the reverse orientation, or by placing other essential viral genes under control of a specific promoter (reviewed in [25])

Modification of the exterior

Effective treatment relies not only on effective oncolysis but also on effective infection of the target tumor. There are a number of factors inhibiting the infection of tumor cells, including infection of non-target CAR-expressing tissue, and the absence of CAR on the target tumor. But also rapid removal of the vector after intravenously administration is a major problem. Vectors in the blood stream will effectively transduce liver cells by binding to coagulation factor X (FX) and Kupffer cells. Furthermore the particles will be scavenged by other blood factors

or neutralized by the immune system. To increase the targeting of the tumor cell and reduce virus sequestering and to evade neutralization of the immune system different strategies have been developed to reduce these effects such as modification of the capsid proteins and shielding the particle.

Retargeting of the vector

To overcome the issue of the absence of CAR on target cells the therapeutic adenovirus has been subjected to retargeting strategies. Most of these strategies resulted in an expanded tropism of the vector. Retargeting can be achieved by modifying capsid proteins. The main focus have been on fiber protein modifications since this is the major attachment protein. In this perspective three different strategies are described. First fibers have been swapped by fibers of other adenovirus serotypes but also synthetic fibers and fiber-like proteins of other viruses have been used to replace the wild-type fiber. Secondly, adenovirus have been subjected to studies replacing only the fiber knob and knob-shaft domains by knobs or knob-shafts of other serotypes. Finally, also the CAR-binding sequences in the knob has been replaced by short peptide sequences such as the integrin-binding Arg-Gly-Asp (RGD)-motif. Other capsid proteins used for retargeting are hexon, penton base, and the minor capsid proteins IIIa and IX (reviewed in [25,54-56]). And although protein IX is the smallest capsid protein, the exposure at the exterior of the capsid and the abundant number in the capsid makes protein IX an interesting anchor for fusing targeting polypeptides [35]. It was shown that incorporation of peptide ligands on protein IX had no effect on the viral titers and stability of the virus [18]. Improvement of the presentation of the ligand was accomplished by inserting an alpha-helical spacer before the ligand [57]. In addition, a protein IX-producing helper cell line system have been developed for protein IX-pseudotyping as an alternative for genetic modification of the vector [58].

A non-capsid modifying retargeting strategy for adenovirus delivery is the adaptor strategy. Bi-functional antibodies bridge between the vector and the target cell. The strategies is copied from the chemical anti-cancer delivery strategies and proved to be useful for adenovirus targeting [55]. Advantages of this strategy are that modification of the adenovirus genome is not necessary and high titer production, and purification protocols do not need to be adapted. But to guarantee clinical efficacy extensive test studies need to be performed since the therapy is dependent on two separate factors. The modification is lost after replication, just as by the capsid-protein pseudotyping.

Reduction of scavenging

Most of the capsid modifications resulted in an altered tropism, but unfortunately scavenging by non-target tissue was not solved. It was only in 2008 that scavenging of adenovirus via coagulation FX was described [39,40]. Binding to FX mediates the uptake by hepatocytes in the liver. The adenovirus capsid protein responsible for binding to FX is hexon. Genetically modifications of the amino acids responsible for the binding resulted in a decreased liver transduction *in vivo* [59]. The prevention of sequestration by other blood factors, such as erythrocytes, neutralizing antibodies, and kupffer cells still needs to be solved.

Vectors can also be coated by polymers or taken up by carriers to shield them from scavenging factors. Shielding adenovirus particles increases the circulation in time in the blood stream and reduced liver toxicity in animal models. Polymer shielding of vectors have been taken from the drug carrier industry. Different polymers have been subjected of which polyethylene (PEG) and poly-[2-(2-hydroxypropyl) methacrylamide] (pHPMA) are the most studied. The advantages of coating are that it occurs after the virus production and purification and retargeting to tumor-targets is relatively straight forward [60]. The counterpart of chemical shielding is biological shielding. Adenovirus particles can be "loaded" onto carrier cells. Loading can be achieved by infecting but also by attaching to the carrier cell, the main goal is that vectors are hidden from the blood stream. Important is that the cellular carriers deliver the load to the tumor-target. Tumor homing has been shown for immune cells such as dendritic-cells and T-cells, but also stem cells home to tumors. Studies with mesenchymal stromal cells have shown great promise but more research needs to be done [61,62] (reviewed in [25,55]). Both methods, the chemical shielding and the biological shielding, have as disadvantages that it shields only the vector for the first replication round.

Increasing efficacy

Adenovirus vectors have been armed with therapeutic genes to increase the spread after the initial infection. These therapeutic genes can roughly divided in four groups, apoptosis inducers, gene repair mechanisms, immune modulators and angiogenesis inhibitor and prodrug-converting enzymes [25,63]. Probably the best known therapeutic gene is the suicide gene also called prodrug-converting enzyme thymidin3e-kinase of the herpes simplex virus (HSV-tk). The enzyme thymidine-kinase is of itself not toxic, but it can convert ganciclovir (GCV) into a toxic product. Expression of HSV-tk followed by GCV administration kills cells selectively [63,64]. A promising replication deficient adenovirus vector encoding

the HSV-tk gene is sitimagene ceradenovec or Cerepro® (Ark Therapeutics Group plc, UK and Finland). This vector was conducted in phase III clinical trials for the treatment of primary high grade gliomas [65]. Yet not approved, the committee for Medicinal Products for Human use (CHMP) reviewed the effect of Cerepro® of the phase III trials as not significantly effective. Furthermore, treatment was associated with increased risk of side effects such as paralysis and seizures. Therefore it was recommended that Ark Therapeutic need to conduct further clinical evaluation before the vector can be approved into the clinic [63].

Random modification

Most of the above described modifications strategies are based on *in silico* design of the vectors. Since there is so much knowledge about adenovirus and the current techniques available this was also the most obvious way to perform the research. Recently random modification approaches gained more interest in the oncolytic adenovirus field. Reports describing improved oncolytic vectors obtained by chemical virus treatment followed by bioselection on a target cell line obtained unexpected mutations [19,20,66]. Alternatively, directed evolution or making use of a sloppy-polymerase can be instrumental in genetic diversification.

In chapter 5 the oncolytic efficiency of adenovirus mutant containing a point mutation in the i-leader sequence is investigated on glioblastoma cells. This point mutation was identified by Yan *et al.* [20]. They subjected adenovirus to a chemical treatment followed by selection for mutants on a human colorectal cancer cell line. The selected mutants, which replicated more rapidly, were subjected to detailed analyzes. Although two of the mutants contained several mutations the mutation in the i-leader region was shared. Further analysis confirmed that truncation of the i-leader region resulted in the enhanced oncolytic efficacy. Similarly, an i-leader mutant was isolated after UV-treatment and bioselection on epithelial cancer cell lines by Subramanian *et al.* [19]. This confirmed that truncation of the i-leader protein could be relevant for the development of oncolytic vectors. According a similar approach a vector with enhanced antitumor activity was isolated by Gros *et al.* This mutant contained a mutation in the E3/19K protein which enhanced the viral release and improved the anti-tumor efficacy [66].

Very differently to the previous approach are the following modification strategies described. Kuhn *et al.* made us of the 'directed evolution' approach. First they pooled different adenovirus serotypes and passaged them under conditions that stimulated the rearrangements of the genes. After harvesting,

the progeny were subjected to stringent culture conditions which yielded potent anticancer vectors [67]. Alternatively, the strategy pursued by Uil *et al.* was to cripple the adenovirus polymerase, making it more error-prone, followed by adaptation of the vector to the target cell line [68]. This approach has a lot of similarities with the adaptation strategies performed with RNA viruses which naturally lack the polymerase proofreading resulting in a high mutation rate [69]. Also this strategy yielded a mutants with improved cytolytic activity. Also here the regions affected by the mutations were never considered or described during *in silico* vector design experiments.

Altogether, this proves that the random mutagenesis approach, also called directed evolution, is a powerful strategy for isolating novel and improved oncolytic vectors.

CHAPTER 3

REOVIRUS



This section is compiled out the following sources

Genetic modification in mammalian orthoreoviruses

S.K. van den Hengel, I.J.C. Dautzenberg, D.J.M. van den Wollenberg,
P.A.E. Sillevis Smitt, R.C. Hoeben
Reverse Genetics of RNA viruses – applications and perspectives.
Wiley-Blackwell (2013); Chapter 10, p289-317

**Modification of mammalian reoviruses for use
as oncolytic agents**

D.J.M. van den Wollenberg, S.K. van den Hengel, I.J.C. Dautzenberg,
O. Kranenburg, R.C. Hoeben
Expert.Opin.Biol.Ther. (2009) 9: 1509-1520

BIOLOGY

Mammalian reoviruses are members of the *orthoreovirus* genus of the family of *Reoviridae*. They were first isolated from the gastrointestinal and respiratory tracts of healthy and sick humans in the early 1950s (reviewed by [70]). The name reovirus is an acronym of **R**espiratory and **E**nteric **O**rphan virus. The term 'orphan' is used to indicate that no serious disease is linked to this virus in humans, given that a large proportion of the human population has been exposed to the virus and built neutralizing immunity to reoviruses [71,72]. The *orthoreoviruses* have a wide geographic distribution and are isolated from a broad range of mammals, birds and reptiles. Although in humans the mammalian *orthoreoviruses* are non-pathogenic, in newborn mice they can cause severe disease [73].

The capsid of the *orthoreovirus* is a non-enveloped icosahedral structure composed of outer and inner protein shell. In 1963 it was discovered that the genome consists of double-stranded RNA (dsRNA) [74], and soon after it was found that the genome of mammalian *orthoreoviruses* consist of 10 distinct genome segments [75].

Taxonomy

To date three *orthoreovirus* species groups are recognized. In this manuscript we will focus on the mammalian *orthoreoviruses*. In this species group three serotype strains of mammalian *orthoreoviruses* have been identified, with the type 1 Lang (T1L), type 2 Jones (T2J), type 3 Abney (T3A) and type 3 Dearing (T3D) as the prototypical representatives. The serotypes are classified according to their neutralization by specific antibodies and by the classical hemagglutination inhibition assay [76,77]. Genomic variation between the serotypes is found for all segments. The S1 segments, coding for the $\sigma 1$ attachment protein, has the largest sequence divergence. The sequence variations can have biological consequences [73]. It was observed by reassortment studies between T1L and T3D that the S1 segments define the pathology. While the serotypes T1L and T3D both infect the central nervous system (CNS) in new born mice, their routes of infection differ. T1L causes hydrocephalus by spreading hematogenously in the CNS by infecting ependymal cells. In contrast, T3D causes viral encephalitis by spreading via the neural routes in the CNS [78]. In this thesis we focus on T3D as oncolytic vector therefore the 'term' reovirus is limited to serotype T3D.

Genome segments and their proteins

Structural proteins

The genome of the reovirus consists of 10 dsRNA segments with a total size of 23.5 kb. The segments are named according to their sizes [75]. There are three large segments (L1, L2 and L3) ranging in size from 3854 to 3916 nt, three medium segments (M1, M2 and M3) with sizes between 2206 to 2304 nt, and four small segments (S1, S2, S3 and S4) varying from 1196 to 1416 nt [73,79]. Each segment encodes a single protein, with as a sole exception the S1 segment which encodes two proteins [80,81]. The proteins are named and numbered according to their apparent molecular weight on SDS-PAGE. The names are derived from the Greek character of the segment it was translated from, the L segments code for the λ proteins, the M segments code for the μ proteins, and the S segments encode the σ proteins. The numbering of the proteins does not always correspond to the genome size of the segment from which they are transcribed [73]. An overview of the segments, and the proteins that they code for is provided in table 3.1.

The non-enveloped icosahedral outer capsid is about 70 nm in diameter. The inner capsid or core structure is about 52 nm in diameter. Together, these capsids are composed of eight structural proteins (figure 3.1). The five structural proteins forming the inner core structure are $\lambda 1$, $\lambda 2$, $\lambda 3$, $\mu 2$ and $\sigma 2$. The $\lambda 1$ protein is encoded by L3 segment and is a major structural protein of the inner capsid. This protein is involved in transcription. The $\lambda 2$ protein is translated from L2 RNA and forms the pentameric turrets of the core structure. During primary transcription this protein adds a methylated cap structure to nascent plus-strand RNA (discussed below). The $\lambda 3$ protein is encoded by L1 segment and functions as the RNA-dependent RNA polymerase (RdRp) and it transcribes the plus and the minus strands [82]. The exact function and location in the core of the $\mu 2$ protein, encoded by the M1 segment, is still unknown. However it has been suggested as a cofactor or second subunit of RdRp. The $\sigma 2$ protein, encoded by the S2 segment, is involved in the assembly of the core particles. This protein decorates the $\lambda 1$ shell (reviewed by [73,79]).

Table 3.1 Overview of the genome segments, proteins and prototypes of the various ts mutants.

	Segment				Protein				ts mutant		
	Total size	ORF (nt)	Size (aa)	Location	Group	Prototype	ssRNA	Phenotype	Protein	dsRNA	
L1	3854	19-3819	λ3	Core	D	tsD357	+/-	+		-	
L2	3916	14-3880	λ2	Core	B	tsB352	+	+		+	
L3	2901	14-3838	λ1	Core	I	tsI138	?	+		-	
M1	2304	14-221	μ2	Core	H	tsH11.2	++	-		-	
M2	2203	30-2153	μ1	Outer capsid	A	tsA201	++	++		++	
M3	2241	19-2181	μNS	NS	F	tsF556 ¹	++	++		++	
			μNSC	NS							
S1	1416	13-1377	σ1	Outer capsid	J	tsJ128	?	?		?	
		71-430	σ1s	NS							
S2	1331	19-1272	σ2	Core	C	tsC447	?	?		-	
S3	1198	28-1125	σNS	NS	E	tsE320	+/-	+		-	
S4	1196	33-1127	σ3	Outer capsid	G	tsG453	+	+		+	

Note: ORF – Open Reading Frame; nt – nucleotide; aa – amino acids; ¹ Tentative, leaky mutant; ++ (almost) as wild type; + less than 50% of wild type; +/- less than 10% of wild type; - less than 1 % of wild type

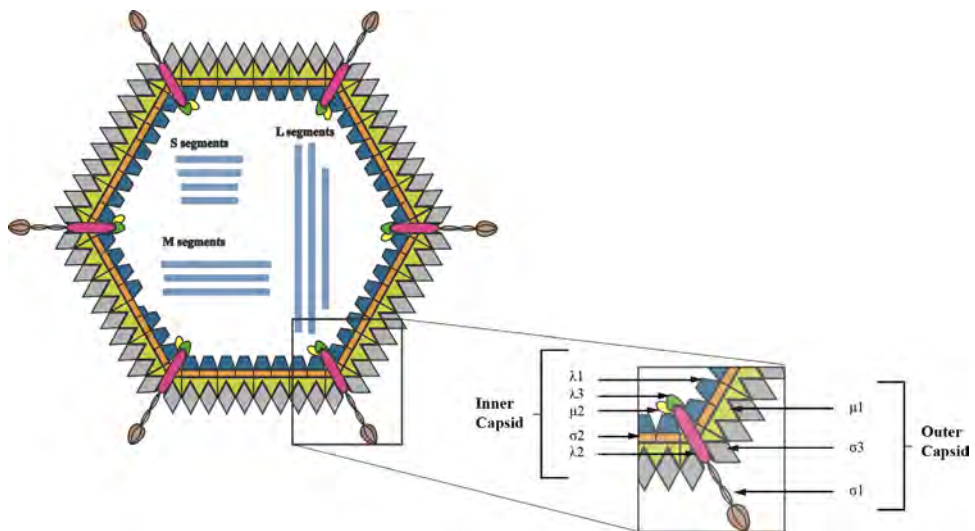


Figure 3.1 Schematic representation of the mammalian orthoreovirus. The virus contains a non-enveloped icosahedral capsid, containing 10 dsRNA segments. These encode the structural proteins: five proteins comprise the inner capsid, and the three others form the outer capsid. The positions of the various capsid components are indicated.

The outer capsid is composed of three structural proteins. The two major outer-capsid constituents are $\sigma 3$ and $\mu 1$ proteins. The third minor outer-capsid protein $\sigma 1$ forms the spikes at the vertices of the icosahedron and functions as the attachment protein. The $\sigma 3$ protein is encoded by the S4 segment and provides stability to the capsid and functions as a shield for $\mu 1$. Removal of $\sigma 3$ protein occurs through proteolytic cleavage upon entrance. The $\mu 1$ protein is encoded by the M2 segment and provides stability to the outer capsid. This protein is by proteolysis cleaved during viral entry to yield the $\mu 1N$ and $\mu 1C$ proteins. This is an important process during replication. Removal of $\sigma 3$ and cleavage of $\mu 1$ yield a partially uncoated particle, the so-called intermediate subviral particles (ISVP). These ISVPs have the capacity to disrupt cellular membranes and may function in endosomal escape. Moreover, ISVPs generated *in vitro* by treatment of purified reovirus particles with chymotrypsin or *in vivo* in the lumen or small intestines by proteases, yields particles that retain their infectivity, and can enter the cell independent of the presence of the canonical reovirus receptor JAM-A (also known as junction adhesion molecule 1, or JAM-1) (reviewed by Coombs (2006) and Tyler and Fields (2001)).

Trimers of $\sigma 1$ proteins encoded by S1 segment form the spikes on the vertices of the icosahedral capsid (see representative figure at Viralzone, 2011 [83]). The

spikes contain a tail and a head domain and interacts with cellular receptors. Furthermore, the spike is anchored in the $\lambda 2$ protein turret. Through removal of $\sigma 1$ protein during virus entry, the $\lambda 2$ turrets undergo a conformational change and becomes active.

Non-structural proteins

At least three nonstructural proteins are generated during infection. The $\sigma 1NS$ is translated from the second open reading frame of the S1 mRNA. This is a nonessential protein which causes cell cycle arrest during infection [80,81]. The second nonstructural protein, σNS , is encoded by the S3 segment. This protein has a strong affinity with single stranded RNA (ssRNA) [84]. It is suggested that it plays a role in replication and assembly of core particles [85]. Furthermore it associates with μNS and $\mu 2$ to form inclusion domains or viral factories.

The μNS protein is encoded by the M3 segment. It is the third nonstructural protein and associates with the viral mRNA shortly after transcription, and to viral cores, probably to anchor viral components needed for assembly or replication [86-89]. In addition, by proteolytic cleavage of μNS μNSC is generated. The precise function of this protein is unknown [73].

Replication

Receptors

Wild-type reovirus T3D binding to target cells is a multistep attachment process [90]. Initially a low-affinity interaction is established with sialic acid residues on the cell surface via interactions with the tail of the spike. Sialic acids were the first molecules identified to bind reovirus T3D [91,92]. Subsequently, high-affinity interactions can establish between the head domain of the spike and JAM-A. Campbell and colleagues defined that only JAM-A and not JAM-B or JAM-C can serve as a receptor for reovirus type 1, 2 and 3 [93,94]. Transient expression of JAM-A renders reovirus-resistant cells sensitive to infection [93]. Subsequently, Arg-Gly-Asp (RGD) domains in the $\lambda 2$ protein bind $\beta 1$ -integrins on the cell surface and mediate particle entry by endocytosis [95,96].

Entry and uncoating

As for most RNA viruses, genome replication of reoviruses takes place in the cytoplasm, schematic represented in figure 3.2. First reoviruses are internalized into the endosomes. Upon acidification, the particles are partially uncoated, yielding so called ISVPs. The uncoating process includes removal and proteolytic cleavage of $\sigma 3$ and $\mu 1$ and subsequent detachment of $\sigma 1$ molecules. The

hydrophobic peptides of $\mu 1$ penetrate and locally disrupt the membrane initiating the escape of the activated particles from the endosomes [97]. Through removal of $\mu 1$ and $\sigma 1$ the $\lambda 3$ RdRp is activated and initiates transcription, yielding full-length plus-strand RNA molecules. The conformational change of $\lambda 2$ pentamers, through removal of $\sigma 1$, turns them into channels for the release of plus-strand mRNA into the cytosol. In addition, the $\lambda 2$ turrets add a methylated cap structure to the 5' end of the plus-strand RNAs [98-100]. On these transcripts the 3' end remains non-poly-adenylated. The methylated cap structure (7-methyl guanosine triphosphate (m7G(5')ppp)) is identical to the cap structures of cellular mRNAs and is therefore recognized by the host ribosomes and translated. Initially the four segments L1, M3, S3 and S4 are transcribed and translated which stimulates subsequent transcription and translation of all segments [78,101-103]. At this stage in the replication cycle translation of viral and host proteins occurs simultaneously.

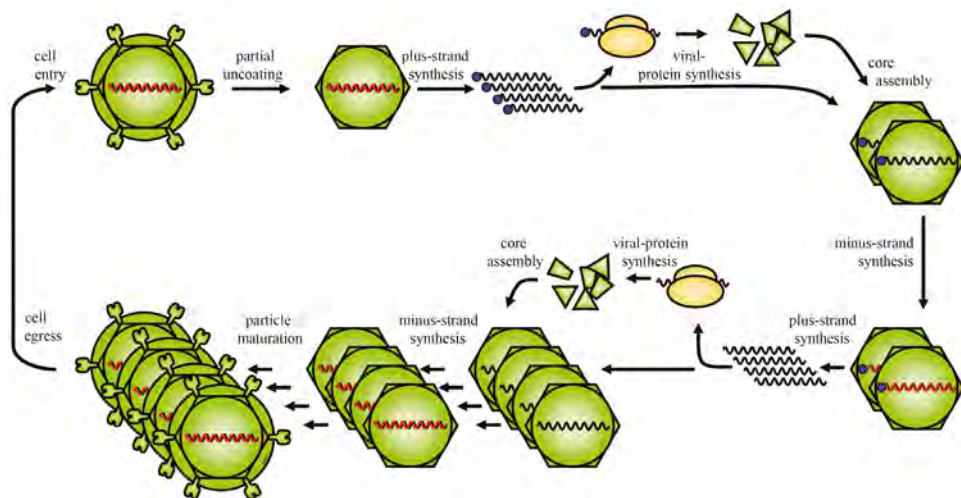


Figure 3.2 Schematic representation of the reovirus' genome replication. After cell entry the viral particle is partially uncoated, and penetrates the endosomal-membrane. In the cytoplasm the primary transcription process yields capped plus-strand RNA molecules, which are translated and can associate with the newly assembled cores. In the cores these transcripts serve as templates for minus-strand synthesis yielding double-stranded RNA. Subsequently the secondary transcription process yields uncapped transcripts which are translated and associate with the new core particles. Minus-strand synthesis proceeds to yield double-stranded RNA genome segments. The particles mature and egress from the cells. In the figure only one of the genome segments is drawn.

The assembly of new particles occurs in newly formed non-membranous structures in the cytoplasm, the so-called viral factories. These may aid in shielding the viral processes from the host cell's components of the innate immune system. The plus-strand transcripts are incorporated into these new cores. Within the core-particles the minus-strand synthesis takes place to yield dsRNA [85,104]. In the newly formed core particles, a secondary round of plus-strand synthesis initiates, yielding uncapped viral transcripts. The uncapped viral transcripts are translated very efficiently since the reoviruses employ a mechanism to modify the ribosomes in such a way that non-capped transcripts are preferentially translated. At this point the host cell protein synthesis is shutdown. This mechanism ensures that the host cell's protein synthesising machinery is used for synthesis of viral proteins rather than for cellular proteins (reviewed in [79]).

Lytic infection

Reoviruses normally cause a lytic infection in permissive host cells. The reovirus-induced cell death is independent of productive infection. Exposure of cells to UV-inactivated virus particles can still induce apoptosis. The primary determinants of reovirus induced-apoptosis are associated with the outer capsid protein $\mu 1$, although attachment of $\sigma 1$ to the cell surface strongly enhances the apoptotic signal. The cleavage of the $\mu 1$ protein during internalisation is essential for the induction of apoptosis. If the disassembly of the viral particles is blocked by monoclonal antibodies against $\sigma 3$ or $\mu 1$, apoptosis is not initiated. Also monoclonal antibodies against $\sigma 1$ inhibit apoptosis; however the mechanism here is prevention of binding to the cells surface. Pro-apoptotic signals are generated by binding of the attachment protein to sialic acid and JAM-A. Reovirus mutants lacking the sialic acid binding capacity are still able to induce apoptosis albeit to a lesser extent [78,105-107].

Cis-acting sequences

Knowledge in the replicative cycle of reoviruses has been essential for the development of a reverse genetics system. The essential *cis*-acting sequences that reside in the genome segments need to be identified. Such sequences include the elements required for the initiation of plus and minus-strand synthesis, the sequences in the plus-strand RNA that function as segment-identity labels, and the sequences that are required for incorporating the plus strand RNA's into the newly formed cores. Also it is crucial to identify other constraints that may limit the incorporation of heterologous sequences in reovirus genome segments. In

the following paragraphs we will describe the functional elements identified in reovirus genome segments.

Non-translated regions

The particle to infectious unit ratio of reoviruses is low [108], indicating that the assembly of new particles is effective and precise and the infection process is highly efficient. The encapsidation involves assembly of 8 structural proteins with one copy of each of the 10 segments. The precise sorting mechanism which directs one copy of each segment into the particle is not yet well understood. Sequences contained within the 130 nt at the 5' terminus serve as identity label for each of the segments [109,110]. The termini of all segments contain relatively short (15-33 nt) non-translated region (NTR) with short (4-5 nt) identical sequences at the extreme ends. The 5' end of the plus-strand RNA starts with the tetranucleotide sequence GCUA- and the sequence at the 3' end is a pentanucleotide -UCAUC. No other sequence homology exists in the NTR regions of the segment termini [104,111,112].

Assortment of the segments

The first indications that the 5' and 3' ends of the segments are important for replication and assembly stem from work by Schlesinger *et al.* (1977), and later by Zou and Brown (1992). In these studies deletion mutants were used. These deletions mutants were formed spontaneously when T3D was passaged at a high multiplicity of infection and contained deletions in the middle of the segments. The deleted segments were replicated and encapsidated in new particles although the presence of helper virus was required. It led to the hypothesis that sequences near the 3' end are necessary to function as promoter for the RdRp and that the termini are needed for the assembly of new particles [113,114].

By employing a reverse genetics system for inserting a chloramphenicol acetyl transferase (CAT) reporter gene in different genome segments (discussed below) more information on the required *cis*-acting sequences at the 5' and 3' ends was obtained [115]. From three segments, e.g. S2, M1 and L1, the regions which are important for assembly have been determined. The lengths of these regions were identified through varying the length of the 5' and 3' ends and measuring the CAT activity of the progeny virus. The lengths of the elements required for encapsidation correlated with the lengths of the genome segments. L1 required the longest 5' and 3' regions (i.e. respectively 129 nt and 139 nt) while S2 needed the shortest regions, at the 5' end 96 nt and at the 3' end 98 nt. The M1 segment required at the 5' end 124 nt and 172 nt at the 3' end [109,110].

These results indicate that the *cis*-acting sequences do not only encompass the non-translated regions, but extend into the coding regions of the segments. Furthermore, Roner *et al.*, in 2004 and 2006, demonstrated that the signals at the 5' end act independently from the signal at the 3' end. In the process the signals at the 5' end function as the segment-identity labels. This became apparent from the observation that chimeric segments, containing the 5' end of S2 or M1 and the 3' end of L1 are incorporated as S2 or M1 segments, not as a L1 segment [104,116].

Genome-size constraints

The genome of the mammalian reoviruses is packaged within the 52 nm inner core. In comparison to other RNA viruses, reoviruses have one of the most densely packaged genomes [110]. Experiments of the group of Roner and colleagues indicate that the maximum amount of RNA that can be included into the core is almost reached. They showed with their reverse genetics system that upon increasing the length of L1 with 726 nt this segment was still incorporated. However, when creating chimeric segments with the 5' end of M1 or S2 and the 3' end of L1, and increasing the size of the resulting segments by 2307 nt or 2500 nt respectively, full incorporation of these segments was inhibited. The modified 5'-L1.CAT.3'-S2, 5'-M1.CAT.3'-S2 and 5'-S2.CAT.3'-L1 segments, in which the sizes were decreased by approximately 980 bp, were still packaged [110]. These data suggest that there are limitations to the packaging capacity of reoviruses. Such limitations are important if one considers developing heterologous transgene-containing reoviruses.

GENETIC MODIFICATION

In virology, reverse genetics has been extremely useful for delineating the functions of individual viral genes. More recently, reverse genetics have allowed rational design of improved viruses for use in clinical applications such as vaccination and experimental oncolytic-virus therapy. In Reoviridae, the development of reverse-genetic strategies has been thwarted by their segmented double-stranded RNA genomes. Therefore, much of the knowledge on reovirus biology has been derived from the studies involving the more classical forward-genetics techniques. The latter studies employed reassortants, chemical-induced mutagenesis and spontaneous mutants, as well as bioselection strategies. In these studies, the mammalian *orthoreoviruses* have often served as a model for the family. While these approaches have been extremely rewarding and yielded

a wealth of information, efficient reverse genetics techniques are still needed for further identification of segment functions and for improving the reovirus based oncolytic virus therapies. Several groups have reported the generation of genetically modified human reoviruses by reverse genetics. In this section we will review the systems used, and discuss the strengths and weaknesses of each of these.

Forward-genetics in orthoreoviruses

In forward-genetics studies aberrant phenotypes are isolated followed by the identification of the mutation responsible for this phenotype. One of the strategies used most commonly was the selection of temperature-sensitive mutants after chemical mutagenesis. This method was often used in combination with the use of reassortants. A third strategy discussed here is the selection of natural mutants.

Temperature-sensitive mutants

The initial isolation of many reovirus temperature sensitive (*ts*) mutants was after chemical mutagenesis of reovirus stocks. The mutated reoviruses were plated and propagated at a low permissive temperature (usually 32°C), yielding virus which could efficiently replicate at this temperature. Subsequently, clones were isolated that exhibited an impaired growth at a higher temperature (often 39°C was used).

With this strategy large series of mutants with aberrant phenotypes have been generated, and designated as *ts* mutants. These *ts* mutants were classified in complementation groups on basis of the absence of complementation between pairs of *ts* mutants. Subsequently these complementation groups could be assigned to the different genome segments of the reovirus (reviewed by [79]). A summary of the different groups and the segments to which they have been mapped is provided in table 3.1.

The phenotypes of these mutants have been instrumental in defining the roles of the individual viral proteins in the infectious pathways of the human reoviruses [79].

Reassortants

In addition to *ts* mutants, reassortment strategies were applied. The reassortants can arise during co-infections of cells with two different *ts* mutants or between different *orthoreovirus* serotypes. Co-infection can lead to exchange of entire genome segments between the viruses. During co-infection, a reassorted genome can be detected in up to 15 % of the progeny viruses [117].

Natural selection/bioselection

A third forward-genetics strategy is the isolation of spontaneous mutants and naturally occurring reoviruses [118,119]. The absence of proofreading in the reoviral RdRp leads to a high mutation rate [120]. This leads to rapid adaptation of the reoviruses and the selective outgrowth of mutants that have favorably adapted to the host [69,121].

What did we learn?

A key role of $\sigma 1$ in cell binding

Since the early sixties it was well established that Reovirus T3D, but not T1L, could hemagglutinate bovine erythrocytes [122]. Reassortment studies identified $\sigma 1$ protein as haemagglutinin. In these studies T1L x T3D reassortants were generated and by using serotype-specific $\sigma 1$ antisera it was demonstrated that the capacity to haemagglutinate the bovine erythrocytes was strictly correlated with the presence of the $\sigma 1$ protein of T3D [76,77,123,124]. Further studies using these reassortants and serotype specific sera pinpointed $\sigma 1$ also as the protein responsible for infection of permissive nucleated cells [125].

Sialic acids play an important role

Attachment studies of the T3D virus to different cell types (erythrocytes, L cells, lymphocytes and murine erythroleukaemia (MEL) cells) made clear that haemagglutination (HA) in erythrocytes is caused by binding to terminal sialic acids of glycoproteins on the cell surface [122,126-129]. Sialic acid is a generic term for the *N*- or *O*-substituted derivatives of neuraminic acid and also the name of the most common neuraminic acid, the terminal *N*-acetylneuraminic acid (NeuAc). With S1 reassorted viruses of T3D and T1L (reassortants T1L+S1-T3D (1HA3) and T3D+S1-T1L (3HA1)) it was demonstrated that reovirus attachment to sialylated oligosaccharides on glycoproteins was solely mediated by the $\sigma 1$ attachment protein [130].

The $\sigma 1$ protein is present as a homo-trimer [131,132] at the vertices of the viral particle. It has a distinct 'head' and 'tail' region [133,134]. The domains that interact with cellular receptors have been identified. The knowledge of the interaction of the $\sigma 1$ protein with cellular sialic acids was derived from studies employing reovirus T3D field isolates that differ in their capacity to agglutinate human and bovine erythrocytes and to bind sialic acids. Sequence analyses of the S1 genes of the different virus isolates revealed single point mutations that only cause weak haemagglutination and which are unable to bind sialic acids. These mutations all cluster in one region in the $\sigma 1$ tail, residue 198-204, which

demonstrated that not only the head but also the tail region of the spike is exposed on the capsid in such a way that it can interact with cellular receptors [135].

The phenomenon that only T3D and 1HA3 and not T1L viruses could infect MEL cells was exploited in studies that mapped the sialic-acid binding-domain of $\sigma 1$. The capacity of the viruses to infect MEL cells is strictly correlated with the viruses' capacity to haemagglutinate erythrocytes. This suggested sialylated proteins to be involved in MEL cell binding [136]. To further identify the receptor binding region of the $\sigma 1$ tail, reovirus type 3 field isolates which were unable to bind sialic acids were adapted by serial passaging to grow in MEL cells. Sequence analyses of these MEL adapted (MA) viruses revealed point mutations that were clustered near the residues 198-204 that had previously been identified as the sialic acid binding region of the $\sigma 1$ tail. These data demonstrated that this part of the tail of the spike is involved in sialic-acids binding [118].

Similarly, T3D reoviruses were selected for growth in the presence of a monoclonal antibody that inhibited haemagglutination. This selection yielded mutants that exhibit a strongly reduced neurovirulence upon inoculation of newborn mice [119]. These data demonstrate the relative ease with which reovirus mutants can be obtained by conventional forward genetics strategies.

Junction adhesion molecule-A is essential

JAM-A, the canonical reovirus receptor, is a 25kDa type I transmembrane protein with two extracellular Ig domains (D1 and D2) and a short cytoplasmic tail. The protein is concentrated at the apical region of intercellular tight junctions of epithelial and endothelial cells (for reviews [137-139]). And the membrane distal extracellular domain (D1) forms a homodimer [137].

Structure-guided mutational analysis revealed three amino acids located in the D1 domain of JAM-A which are individually required to bind $\sigma 1$. The amino acids Glu⁶¹ and Lys⁶³ participate in salt bridges with opposing amino acids and thereby have a role in stabilization of the D1 dimer. The amino acid Leu⁷² is part of a hydrophobic interaction with a residue of the opposing dimer [95]. Since all amino acids required for binding $\sigma 1$ were located in the dimeric interface of the D1 domain, it was reasoned that $\sigma 1$ first disrupts the JAM-A dimer and then binds to the monomeric form of the D1 domain. Binding studies indeed showed that the binding affinity between $\sigma 1$ and the monomeric form of the D1 domain is higher than between the JAM-A homodimers. In addition using cryocrystallography it was clearly demonstrated that only monomers of JAM-A were bound by $\sigma 1$ [140]. Insight in the amino acid residues important for

binding JAM-A was obtained by using the helper-free reverse-genetics system (see below) [141]. The engineered reoviruses with mutant forms of $\sigma 1$ revealed that the JAM-A binding domain is located at the lower part of the head domain. Moreover, one reovirus $\sigma 1$ molecule can bind three JAM-A monomers [140] (Picture of JAM in [95] and JAM- $\sigma 1$ interaction in [140]).

The knowledge of reovirus T3D binding to its cellular receptors culminated in a multi-step binding model in which attachment protein $\sigma 1$ first engages sialic acids on the cell surface in a low-affinity interaction and subsequently binds JAM-A with high affinity [141,142]. The virion is internalized via clathrin-mediated endocytosis upon interaction between $\beta 1$ -integrins on the cell surface with the capsid protein $\lambda 2$ [96]. This has been suggested since $\lambda 2$ contains the integrin binding sequences Arg-Gly-Asp (RGD) [96]. Furthermore, $\beta 1$ integrins contain a cytoplasmic domain containing two Asn-Pro-any amino acid-Tyr (NPXY) motifs which are required for functional reovirus entry [143].

Persistent infection

Rather than causing a lytic infection, the T3D reovirus can establish a persistent infection. The initial observations stem from experimental infections of cultured human embryonic cells [144]. Infectious virus could be recovered from the cultures after 9-12 passages without appearance of overt cytopathic effects.

Taber and colleagues (1976) isolated a culture of persistently infected CHO cells. In these cultures a large number of cells were infected, and the cultures produced reoviruses that were cytopathic for the parental CHO cell line [145]. This suggests that the persistently infected cell lines adapted to resist the reovirus-induced cytopathic effects. Ahmed and coworkers (1981) demonstrated in an L-cell system that the persistently infected cells as well as the reoviruses propagated in the persistently infected cultures acquire changes and thus eventually differs from the parental virus and host cells. The L cells cured from the persistent infection had an increased resistance to wild-type T3D viruses, suggesting that the cells adapted by genetic or epigenetic mechanisms, leading to increased virus resistance [146]. More recently it was demonstrated that persistently infected cells express reduced amounts of the cathepsins B and L, which are known to be involved in reovirus uncoating [147-149]. These data suggest a co-evolution of host and virus to eventually reach a state of a stable but dynamic equilibrium.

Persistently infected L-cell cultures obtained after co-infections with T2J, which does not result in persistent infections, together with T3D, which is able to give persistent infections, yielded various hybrid recombinant mutants containing all

the S4 segment of T3D. This suggested that sequences in this segment underlie the capacity of the virus to establish a latent infection [150]. Via a similar approach the capacity of human reoviruses to inhibit host cell RNA and protein synthesis was also been mapped to the S4 segment [151]. Taken together, these data imply that persistent infection can only exist if the host cells retain the capacity to synthesize proteins. Strong inhibition, as is the case upon infection with T2J, would be incompatible with such persistence. Furthermore, sequence analyses of the persistent infections demonstrated acquisition of additional mutations in the S4 segment and an increased resistance to ammonium chloride, a weak base that inhibits the pH decrease in endosomes and lysosomes. This again suggests that the viruses adapted to selective pressure operating at the level of cell entry.

In addition to alterations in S4, sequence analyses of the viruses causing persistent infection also revealed mutations in the S1 segment, encoding the spike protein [150,152-154]. The $\sigma 1$ protein is known to be involved in the induction of apoptosis in reovirus infected cells [78]. Isolation of an S1 attenuated reovirus mutant form from persistently infected cells, revealed that although virus replication was maintained the apoptotic potential was reduced. Sequence analysis revealed that the most significant mutation was a nonsense mutation which truncated the $\sigma 1$ protein, however it could not be ruled out that other mutations in S1 and S4 too are involved in this phenomenon [152]. It would therefore be interesting to test whether the mutations found in the S1 segments of the persistently infected viruses affect the capacity of $\sigma 1$ to bind sialylated proteins and to induce apoptosis [155,156].

In the preceding section the conventional forward-genetics strategies have been discussed as well as some of their applications. Although they have been instrumental for determining the functions of the different segments, these techniques have their limitations. No directed mutations can be introduced. Therefore, reverse genetics systems have been developed, facilitating not only new studies into the functions of individual reovirus proteins, as well as the development of new reoviruses for use as oncolytic agents.

Reverse-genetics in orthoreoviruses

So far development of reverse genetic systems for reoviruses has been notoriously difficult. Although in 1982 the cDNAs of all the genome segments had been cloned for the purpose of sequencing [157], the first reverse genetics system was only described in 1990 [158]. Genetically modified particles were generated with the aid of helper reoviruses. In 2007 the first helper-free system

was described [141]. To date, three different systems have been developed which have all their merits and weaknesses.

The Infectious-RNA system

The first method for reverse genetics in reovirus T3D employs RNA transfections of all the 10 genome segments, a cell-free translation system, and helper reoviruses [158].

Active core structures, generated by *in vitro* disassembly of reoviral particles, were used for transcription of plus-strand RNA's *in vitro*. The RNA transcripts were translated using a rabbit reticulocyte lysates (RRL) system. While this step was not essential, it increased the efficiency by 2-3 orders of magnitude. The newly translated viral proteins, together with dsRNA, and ssRNA, were introduced into mouse L fibroblasts by lipofection. Usage of only ssRNA or dsRNA in this mixture is possible but less efficient. A few hrs later the helper virus, which can be either serotype 1 or serotype 2, is added to the cultures. Between 24 to 48 hrs post infection, virus can be harvested. Either plaque purification, or the use of serotype-specific neutralizing antisera, was required to eliminate the helper-viruses [158,159].

This technique was used to generate a compound *ts* mutant. Two *ts* mutants were chosen both of which contain a *ts* mutation albeit on different genome segments (genome segment M2 coding for μ 1 and segment S2 encoding σ 2). These segments were jointly incorporated in progeny virions generating the compound double *ts* mutant. Creating these double *ts* mutant required removal of the corresponding wild-type segments from transfected RNA pool. This can be accomplished by sequence-specific degradation of the wild-type segments through addition of complementary oligonucleotides and RNase H treatment. This enzyme degrades the RNA-strand in complementary DNA/RNA duplexes. Analysis of the double mutant showed that the *ts* phenotype was enhanced compared to the parental single *ts* mutants. Furthermore, exposure of mice revealed that the double *ts* mutant was less pathogenic than the parental viruses, while protective neutralizing immunity was still induced [160].

Transgene-containing reoviruses

The first example of the introduction of a heterologous transgene gene in the reovirus genome was described by Roner and Joklik in 2001. To this end the infectious RNA-system was used. In this experiment the S2 segment was replaced by an S2 segment modified to include the chloramphenicol acetyl transferase (CAT) gene, as a reporter. The coding sequence of the CAT gene is

smaller than the coding sequence of $\sigma 2$ (753 nt versus 1331 nt, respectively), and its activity can be easily monitored in cell lysates [115].

The CAT gene was placed in-frame in the S2 open reading frame. The total lengths of the S2 sequences flanking the CAT gene were 198 nt at the 5' end and 284 nt at the 3' end. The modification inactivated the $\sigma 2$ open reading frame. Therefore all experiments were performed in helper cells that expressed an intact copy of S2 to trans-complement the missing $\sigma 2$ protein. To generate infectious virus with the modified S2 gene, the wild-type S2 was removed from viral RNA preparation by addition of an oligodeoxyribonucleotide complementary to the S2-transcript and RNase-H treatment. To provide the modified S2 transcripts, the capped S2-CAT RNA was generated by transcribing a cloned version of this S2-CAT segment by T7 RNA polymerase. After removal of the wild-type S2 RNA and addition of capped S2-CAT RNA the mixture was lipofected into helper cells, yielding reoviruses carrying the CAT gene in their S2 segment.

This system was used to identify the regions that are essential for replication and packaging of the segments. These regions were mapped at the segment termini. In an experiment in which the CAT gene was inserted between the 5' terminal end of the L1 segment and 3' terminal of the S2 segment, the CAT containing segment was found to replace the L1 segment, but not the S2 segment. Similarly, a chimeric 5'-S2.CAT.L1-3' segment and a 5'-M1.CAT.L1-3' replace the S2 and M1 segments, respectively. These data indicate that the 5' terminus determines the segment identity in the segment assortment. Moreover the 5' and 3' termini act independently [110].

In similar studies, the size constraints were established for packaging and replication as discussed in genome-size constraints. These data show that although the size of the segments can be increased by inserting heterologous sequences, the capacity is limited [110].

The infectious-RNA method has been effectively used to engineer alterations in the reovirus genome. However, the method is technically demanding. The RNase H procedure is not fully efficient, resulting in the presence of residual RNA of the targeted segment, and appearance of viruses with wild-type segments. In addition, the requirement of helper viruses during the generation of the modified viruses is undesirable. The helper virus may yield the formation of reassortants between the 'helper' viruses and the generated virus, although the use of T2J as helper reduces the magnitude of the problem [159]. Despite these weaknesses, the results obtained with this system have been extremely informative.

The segment-replacement technique

Van den Wollenberg *et al.* recently described an alternative approach for generating genetically modified reoviruses (chapter 6). In an effort to modify the $\sigma 1$ spike, an S1 segment was generated encoding a $\sigma 1$ that harbors a C-terminal histidine-tag. The presence of this tag would allow particles to infect JAM-A-negative cells that express on their surface a single-chain antibody recognizing the His-tag, as an artificial receptor [161].

This strategy was based on experiments by Rouault and Lemay [162]. These authors expressed modified versions $\sigma 1$, $\mu 1$, and $\sigma 3$ and used these proteins to recoat reovirus ISVPs and cores *in vitro* [163-165] to study reovirus capsid protein structures and functions. In a proof of principle study a foreign epitope, viz. a hexa-histidine tag, was added to the amino terminus of $\sigma 3$ [162]. For recoating, purified wild-type virions were treated with chymotrypsin to generate ISVPs. The ISVPs were incubated with cellular extracts that contain mutant $\sigma 3$ proteins. Free $\sigma 3$ proteins were removed from the re-coated ISVPs and by immunoblotting procedure the modified $\sigma 3$ on the re-coated ISVPs could be detected. While this strategy can be used to introduce modified proteins in the capsid, the modification will not persist upon replication since the viral genome is not modified.

Van den Wollenberg *et al.* produced particles with modified proteins incorporated in their capsid by propagating reoviruses on helper cell lines that synthesize modified reoviral proteins. These modified proteins would be incorporated in the capsid during replication of the reovirus. In a first series of experiments reoviruses were propagated on modified cells that express a S1 segment that included a His-tag at the carboxyl terminus of the $\sigma 1$ -encoding open reading frame. It was anticipated that the viruses harvested from these cells would carry the $\sigma 1$ -His in their capsid, but would not carry the modified S1-His segment. However, the authors noted that propagation of wild-type reoviruses on cells expressing the $\sigma 1$ -His-encoding segment as a conventional RNA polymerase II transcript led to frequent replacement of the wild-type genome segment with the modified version. The resulting viruses could be serially passaged on JAM-A-deficient U118MG cells that were modified to express the single-chain Fv capable of binding a His-tag. Hence, this technique allowed generating reoviruses that are genetically retargeted. It also demonstrates that the C-terminus of the $\sigma 1$ protein is a suitable location for the insertion of oligopeptide ligands and shows that it is possible to use genetic modification to retarget the infection of reoviruses [161].

The precise mechanism by which the modified segment is incorporated is still unclear. Two mechanisms could be envisaged. In a first mechanism, the RNA-polymerase II transcript that contains the modified S1 segment, associates with newly formed core particle despite the presence of the long 3' extension and a poly-A tail. In the core particle the minus-strand synthesis would start even with the 3' extension and poly-A tail. This would yield a partially double-stranded RNA copy of the polymerase II transcript. If this dsRNA copy serves as template for secondary plus-strand synthesis, new plus strands would be generated that harbor the modified $\sigma 1$ open reading frame, but are otherwise identical to the wild-type S1 segment. Alternatively, one could anticipate a mechanism that would involve RNA recombination or a template switch during replication of the reovirus genomes. Future studies will aim at resolving the mechanism for the replacement of genetic information.

The segment-replacement system is relatively straightforward, as it is based on the selective advantage for the modified $\sigma 1$ over the wild-type $\sigma 1$. The selection is essential for selectively expanding the viruses that have the wild-type genome segment replaced by the modified version. Unfortunately, this method is thwarted by the fact that, with a low frequency, mutants arise in these cultures that have the capacity to infect the U118MG cells independent of JAM-A and the His-tag-specific scFV. This leads to the occurrence of replicating reoviruses that do not carry the desired mutation. Therefore plaque purification and screening is important to characterize and purify the desired mutants.

A helper-free reverse-genetics systems

A fully helper-free system for reverse genetics was described by Kobayashi and colleagues. It employs 10 different plasmids, each containing a single cloned genome segment. The method starts with infection of susceptible cells with an attenuated vaccinia virus expressing the T7 RNA polymerase, and is followed by naked-DNA transfection of the 10 plasmids encoding each of the genome segments. The genome segments are inserted in the plasmid as full-length cDNA clones derived from the wild-type T3D. These cloned segments are inserted downstream of a bacteriophage T7 promoter. The 3' terminus of each cloned segment was fused to the hepatitis delta virus (HDV) ribozyme, which generates native 3' ends without poly-A tail by self-cleavage of the RNA transcript, and by a T7-terminator sequence. The attenuated vaccinia virus is replication-deficient and serves to express the T7 RNA polymerase at high level. The supernatants of the transfected cultures were plaque assayed on L-cells and replication-competent viruses could be isolated. The method is robust and productive, viral infection

could be established in approximately 1 in 10^5 – 10^6 cells transfected. This system was validated to confirm that a single amino acid change in $\sigma 1$ conferred resistance of $\sigma 1$ to trypsin cleavage, and that a single amino acid change in $\sigma 3$ accelerates proteolytic disassembly of the reovirus. Furthermore, with this system the functional domains in $\mu 1$ responsible for the induction of reovirus apoptosis in host cells could be mapped [106,166]. Introduction of the enhanced green fluorescent protein (eGFP) gene into the S4 segment demonstrated that the technology allowed the incorporation of heterologous transgenes into the reovirus genome. Since this virus lacks a normal S4 segment, the $\sigma 3$ encoded by S4 needs to be provided in *trans*. Therefore the T3D/S4-GFP virus could only be propagated in cells genetically modified to produce the $\sigma 3$ protein [141]. Taken together, these data show that this helper-free reverse genetics method can be used for generating viruses with single amino-acid changes as well as for generating viruses carrying heterologous transgenes.

The advantage in comparison of the two other systems is that there is no requirement for helper viruses. The system is easily amendable for the introduction of various kinds of mutations. However, the efficiency may need further improvement since it is estimated that about 1 in 10^5 – 10^6 transfected cells can establish viral progeny. As a first step of improvement, instead of inserting the genome segments in 10 separated plasmids, the system has been amended to four plasmids including all the 10 segments. Each plasmid contains the cDNAs of two or four of the reovirus genome segments. In these plasmids each of the cloned genome segments is preceded by the T7 promoter, and succeeded by the HDV ribozyme and T7 terminator sequences. Furthermore, instead of using the attenuated vaccinia virus, BHK cells stably expressing the T7 polymerase under control of cytomegalovirus promoter can be used, further simplifying the technology [167]. With these improvements, the reverse genetics system is more effective in generating progeny virus.

Rotavirus

Rotaviruses are classified in a separate genus of the *Reoviridae*. Unlike the mammalian *orthoreoviruses*, the human rotaviruses are very pathogenic, causing severe diarrhoea, especially in young children [168]. It is a major health problem, particularly in developing countries [169]. At this moment attenuated live virus is used as vaccine [170]. The development of a reverse genetics system would allow gaining more knowledge about the biology of rotaviruses.

Rotaviruses are very similar to the mammalian *orthoreoviruses*. They contain 11 dsRNA genome segments encoding 13 proteins, and they have a

non-enveloped three-layer icosahedral capsid structure [171]. Although they resemble reovirus, the development of a reverse genetics system is even more difficult.

So far attempts to generate a plasmid-based reverse genetics system have remained unsuccessful. A first reverse-genetics system was described in 2006 by Komoto *et al.* [172]. These authors managed to replace the spike-encoding segment of a human rotavirus by that of a simian homologue. The system employed resembles *the segment-replacement technique* described above, except the cDNA of the simian spike-encoding segment was flanked by a T7 promoter and the HDV ribozyme. Infection of a vaccinia virus vector expressing T7 polymerase was required to provide the T7 polymerase. Selection of the modified virus employed neutralizing antibodies against the human spike-protein, selectively enriching the virus population for the viruses containing the simian spike-protein [172]. So far this method relied on a high selective pressure for the modified rotavirus which limits the application of the technique.

More recently, Troupin *et al.* describe a modified version of the Komoto method to generate a recombinant rotavirus carrying an artificially rearranged rotavirus segment 7, coding for non-structural protein 3 (NSP3) [173]. Their method is based on the observation that rearranged segments 7 and 11 are preferentially packaged [174]. The usefulness of this system is under debate [175], since it requires extended passaging at a high multiplicity of infection to recover the recombinant virus.

The latest development on rotavirus reverse genetics is based on the method of Komoto *et al.* together with a dual selection mechanism [175]. Trask *et al.* combined a *ts* mutation of non-structural protein 2 (NSP2), with RNAi-mediated degradation of NSP2 transcripts to select for a recombinant rotavirus evading both mechanisms, *ts* and RNAi degradation. Therefore, the recombinant segment 8 cDNA, coding for NSP2, was modified to contain silent mutations in the region targeted by the RNAi to avoid degradation. The combination of the *ts* helper virus with the RNAi-mediated selection significantly improved the recovery of the recombinant rotavirus. An analysis demonstrated that eight of eight rotavirus isolates contained the recombinant segment 8.

This “two-hit” method may enhance the efficiency of recombinant virus recovery. One limitation for this system is the requirement for gene-specific RNAi, which may not equally effective for all the 11 segments of the rotavirus.

So far, reverse genetic systems for introduction a foreign gene in rotaviruses have not been reported.

Concluding remarks

To date, several reverse-genetics systems have been described for manipulation of mammalian *orthoreovirus* genomes. These systems have already proven their effectiveness and were used to reveal new viral functions and facilitated the introduction of modified genome segments. Nevertheless, the robustness of these techniques should be further improved to make them more widely applicable. Some of these systems require selection methods to enrich the mutant viruses. The developments of genetically modified variants should be accompanied by the parallel development of procedures to make the mutant reoviruses a safe pharmaceutical product. This requires manufacturing processes that prevent reversion of the mutants to wild-type viruses. To ensure that the mutations are retained during the prolonged passaging that is required for production of large clinical-grade batches, the production systems should be developed in parallel. Such systems must provide a continued positive-selection pressure for the presence of mutations or modifications. Only if the development of reverse genetics systems goes hand in hand with the development of dedicated production systems, the new technology can be employed to generate improved mammalian *orthoreoviruses* for clinical application.

REOVIRUS AS ONCOLYTIC AGENT

The human reovirus Type 3 Dearing is an interesting candidate for oncolytic virotherapy because of its well documented inherent preference for replication in transformed cells. Reovirus type 3 was isolated from the intestinal tract from an apparently health individual. Serology demonstrates that most humans are exposed to human reoviruses before that age of 5, presumably with an asymptomatic infection [73,176]. The impetus for the use of human reovirus T3D as an oncolytic agent has been the observation that although reovirus T3D is non-pathogenic, it preferentially lyses tumor cells, especially those with an activated Ras signaling pathway. The human reovirus' preference for replication in transformed cells has been much studied [176]. A hallmark study was published by Patrick Lee's group which showed that activation of the Ras signaling pathway can sensitize cells to reovirus replication [177]. This study revealed the essential role of the double-stranded-RNA-dependent protein kinase (PKR). In normal cells, the double-stranded reovirus RNA activates a PKR response and leads to PKR phosphorylation. This triggers phosphorylation of eukaryotic initiation factor 2a, which in turn, inhibits translation of mRNA. Strong and coworkers demonstrated that Ras signaling inhibits PKR phosphorylation,

allowing translation of the reovirus plus-strand RNAs [177]. Further studies implicated the Ras/RaIGEF/p38 signaling in the regulation of reovirus replication and cytolysis [178]. These data offered an explanation for the reovirus' preferential cytolysis effects on transformed cells. This renewed the interest in the use of reovirus as oncolytic agents. Already in 1978, Theiss, Stoner and Kniazeff reported that infusion of reovirus type 3 into the lungs of mice reduced the progression of chemically induced pulmonary adenomas, and that multiple infusions enhanced the antitumor effect [179]. More elaborate studies confirmed the feasibility of reovirus based cancer therapeutics [180,181], and boosted the interest in developing reoviruses as an oncolytic agent [182], as is evident from an increase in the number of publications on this topic figure 3.3. In Canada, the company *Oncolytics Biotech, Inc.* was founded, which is committed to exploring the oncolytic capability of reovirus as oncolytic agent [183].

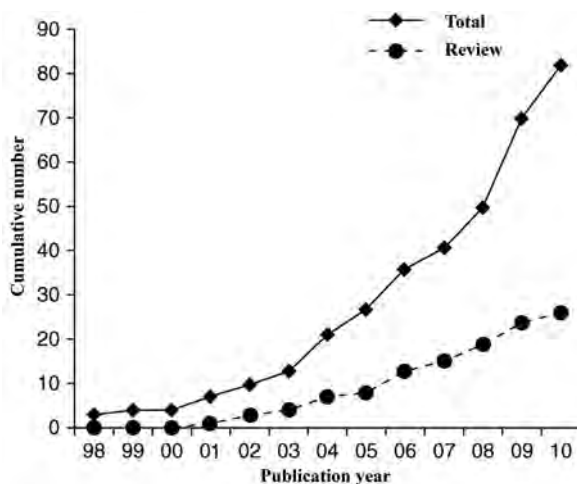


Figure 3.3 Cumulative number of entries found in PubMed using (reovirus AND oncoly*) as search term. The Y axis represents the number of entries with a publication date before January 1st of the indicated year. The diamonds and the solid line represent the total number of publications and the circles and dashed line indicated the number of reviews on this topic. Note that approximately 30% of the publications represent review papers. *Data gathered on August 25, 2009.*

The relationship between Ras signaling and reovirus replication has been much debated [184-186]. The PKR relation should not be taken too dogmatically as also other steps in the replication cycle may determine the cell's susceptibility to reovirus-mediated cytolysis. Kranenburg and collaborators demonstrated that activation of the Ras pathway sensitized the cells to reovirus-induced apoptosis,

both in mouse [187] and in human tumor models [188]. However, virus yield was not affected by ras status. Reovirus T3D was strongly cytopathogenic in cells with activated Kras, but not in cells in which the Kras gene was inactivated. Similarly, viral uncoating is critical in determining the cells sensitivity to reovirus infection. Efficient uncoating is dependent on cellular proteases, such as cathepsin B and L. The expression of these proteases is often upregulated in tumor cells [189,190]. Conversely, down regulation of cathepsin L leads to reovirus resistance as this thwarts reovirus disassembly [149]. Also late events in the reovirus life cycle, such as the assembly of infectious viral particles, are correlated with Ras status [191]. It should be noted here, that it is probable that not the Ras-status itself, but rather the functional consequences of Ras signaling, are sensed by the reoviruses. Rubin and collaborators set up a gene-trap method to identify cellular genes involved in virus infection and cell killing. Intriguingly, the screen suggests that expression of the IGF-II gene could confer resistance to reovirus infection [192,193]. Along similar lines the reovirus S4 gene may affect the efficiency of virus replication in Ras transformed cells [194].

Clinical studies: limited efficacy

The preference for transformed cells plus the absence of significant pathology in humans made reoviruses excellent candidates for oncolytic virus therapies. The Canadian company *Oncolytics Biotech, Inc.* initiated several clinical trials with their lead product, Reolysin, which based on the wild-type T3D strain. At this moment at least 24 clinical trials are active or completed in the UK, US, Canada, and Belgium. The indications comprise a range of cancer types, including prostate cancer, malignant gliomas, pancreatic cancer, lung cancer, head and neck cancer [195]. Initially, the virus was administered as mono-therapy but in more recent clinical trials reoviruses are combined with more conventional treatment modalities. In these studies no dose-limiting toxicity was reached, underscoring the safety of reovirus-based oncolytic virus therapy [196]. Despite anecdotal evidence of antitumor activity, the efficacy has been limited. Currently, several factors such as insufficient tumor penetration of the therapeutic virus, limited spread of the virus within the tumor cell mass, insufficient expression of the reovirus receptor JAM-A on tumor cells, and preexisting humoral immunity, have been proffered to explain the limited tumor-cell transduction [24]. It is anticipated that technology to modify reovirus genomes by reverse genetics may aid the generation of new mutants that overcome these current limitations.

Optimizing reovirus therapy

While the reovirus receptor is widely expressed in several tissues, some tumor cells may have downregulated the receptors on their cell surface. For instance, Kranenburg and collaborators described that none of the 13 freshly isolated tumor fragments from patients with colorectal metastases were susceptible to reovirus T3D infection [197]. This is probably due to absence or inaccessibility of the reovirus receptor JAM-A on the tumor cells. Immunohistochemistry on tissue microarrays showed that JAM-A was expressed at very low levels in liver metastases and improperly localized in the cytoplasm of colorectal tumor cells. Remarkably, tissue fragments and single-cell populations isolated from human colorectal tumor biopsies were susceptible to ISVPs, which have the capacity to directly penetrate the cell membrane independent of reovirus receptors [197]. Similarly, infectivity of the non-permissive human glioblastoma cell line U118MG could be restored by transfer and expression of a JAM-A cDNA clone [161]. This confirms that the receptor scarcity contributes to the resistance of tumor cells to reovirus T3D. This may be specific to particular tumor types. A recent study shows that reovirus T3D induces regression of human breast cancer primary tumor samples xenografted in immunodeficient mice. In addition, reoviruses not only eradicated the differentiated breast tumor cells, but also the cancer stem cells [198]. Interestingly, expression of the JAM-A molecule has suggested as a prognostic factor in breast cancer. JAM-A has been suggested to function as a key negative regulator of cell migration and invasion. While JAM-A is robustly expressed in normal human mammary epithelium, its expression is downregulated in metastatic breast cancer tumors. MDA-MB-231 cells, which are highly migratory, expresses low amounts of JAM-A. Forced overexpression of JAM-A in MDA-MB-231 cells inhibited both migration and invasion through collagen gels, whereas knockdown of JAM-A using siRNAs enhanced the invasiveness. These data suggest that JAM-A serves as a negative regulator of breast cancer cell invasion and possibly metastasis [199]. Similarly, recent data suggest a role for JAM-A in progression of renal cell carcinoma [200] and endometrial carcinoma [201]. In contrast, based on patient survival studies and *in vitro* studies, McSherry and collaborators came to the opposite conclusion [202]. They suggest a correlation between increased JAM-A expression and reduced survival of breast cancer patients.

Taken together the data summarized above demonstrate that particular aspects of tumor biology, such as receptor availability, Ras signaling, cathepsin expression, antiviral immunity, etcetera, may affect the anti-tumor efficacy of reovirus-mediated oncolytic strategies. So how do we go from here, and how can we generate modified reoviruses with enhanced anti-tumor efficacy?

Generating improved oncolytic reoviruses

Bioselection

In virology two approaches are available to isolate viruses with distinct phenotypes. The classic approach involves bioselection for the desired phenotype, and subsequent characterization of the mutants, including the characterization of the genetic changes that underlie the new phenotype. In human reoviruses this method has been employed successfully, and has been used to select receptor mutants, interferon-resistant mutants, and temperature-sensitive mutants [118,203]. Studies on such mutants provided insight in the biology of reoviruses. As described in the chapter section '*Sialic acids play an important role*' starting with an isolate of T3D that could not be passaged in murine erythroleukemia (MEL) cells, Dermody and colleagues isolated mutants that were adapted to grow in MEL cells [118]. These studies demonstrated that receptor mutants of reoviruses can be selected for with relative ease. However, it should be noted that in these studies for a phenotype was selected that is present in many of the T3D isolates. Therefore it remains to be seen whether reoviruses with completely novel receptor specificities can be isolated with similar ease. Along similar lines Lemay and colleagues isolated T3D mutants with varying interferon sensitivity. One of the mutants had an interferon-hypersensitive phenotype. Interestingly this mutant was more dependent on Ras signaling than other viral isolates [204]. These data demonstrate that bioselection may be used to isolate reovirus mutants that are more efficient as oncolytic agent.

Alternatively, reverse genetics strategies can be used to genetically modified reoviruses. As described in the chapter section '*Reverse-genetics in orthoreoviruses*' viruses can be modified to encode new receptor-binding ligands in one of their capsid proteins. In this approach the lessons learned from generating adenovirus-C mutants that bypass the dependency of the adenovirus receptor, can be very helpful. Adenovirus-C is widely studied as oncolytic virus. The attachment protein of adenovirus-C, fiber, recognizes the coxsackie and adenovirus receptor (CAR) receptor. Although the adenovirus fiber and the reovirus spike have no sequence similarity, their 3-dimensional (3D) structures are remarkably similar [94,205]. In the adenovirus fiber protein a wide variety of ligands have been inserted. Such ligands include single-chain Fv domains, single-chain T-cell receptors, so called affibody™ molecules, and integrin-binding RGD motifs. This successfully changed the cellular tropism of the adenoviruses [206-208]. It remains to be determined whether the same approach is equally effective in modifying the cellular tropism of reoviruses.

In the chapter section '*The segment-replacement technique*' it was already mentioned that the N-terminus of $\sigma 3$ and the C-terminus of $\sigma 1$ are promising

locations for insertion of heterologous peptides. Such peptides sequences could act as alternative receptors but are also attractive for small targeting peptides. Such peptides could be the integrinbinding 'RGD'-containing oligopeptides that have been inserted successfully in the fiber of the adenovirus and facilitate adenovirus-receptor-independent infection of cells [209]. It remains to be determined, however, whether these sites tolerate insertion of larger targeting peptides. If this proves feasible, then targeting ligands that have been successfully incorporated in the capsids of other non-enveloped oncolytic viruses may be incorporated in reoviruses. Such ligands could include single-chain Fv domains, single-chain T-cell receptors, or so-called affibodies [208].

Not only the infection efficiency, but also the tumor-cell specificity of infection can be enhanced. To avoid the infection of non-target cells expressing JAM-A, the $\sigma 1$ protein can be modified to ablate its association with JAM-A. As discussed in section 'What did we learn?' reovirus S1 mutants were generated which strongly reduced JAM-A binding in surface plasma resonance analyses, as well as to neuraminidase treated HeLa cells [140,141]. Interestingly, these mutants were viable and could be propagated on L929 cells, infecting the cells presumably via direct association with sialic acid residues. Furthermore, viruses with reduced JAM-A binding have been isolated [140,152], these mutants were still viable and infected cells presumably via binding to sialic acid residues [140]. The mutant with the truncated $\sigma 1$, isolated by Kim and colleagues, still preferentially targeted tumor cells, however, it showed a reduced toxicity *in vivo*. Also exposure of naive mice to this virus still resulted in the induction of neutralizing immune response. Such viruses may facilitate the development of more efficacious tumor-cell selective reoviruses for application as oncolytic agent.

Where do we go from here?

With these tools and techniques available and with evidence of excellent safety of the wild-type reoviruses in clinical studies we may further define key factors that may limit clinical efficacy. In what fields are new developments necessary to fulfill the promise of efficacious cancer-targeted reovirus vectors?

Cells for delivery

Many preclinical and clinical studies have demonstrated that delivery of viral vectors to the tumor is often disappointingly inefficient. As outlined above, the expression of the reovirus receptor JAM-A may be low, or the receptor proteins are inaccessible to the virus particles. In addition, the high interstitial fluid pressure within most tumors causes a convective flow away from the tumor.

This inhibits the passive diffusion of viral particles into the tumor. Moreover, the extracellular matrix may form physical barriers that prevent efficient spread of viral vectors [210,211].

Given the inefficiency of virus delivery to tumor cells, new delivery methods are essential. An attractive option is to use cells with the capacity to migrate to tumors as delivery vehicles of oncolytic viruses. In this strategy the tumor targeting cells are loaded with viruses and administered to the patient. After migration, the cells should hand off the cell-associated viruses to the tumor cells. Several cell types can migrate to tumors *in vivo*, including cytokine induced-killer cells, tumor-antigen-specific T cells, macrophages, endothelial progenitor cells, and mesenchymal stem cells [212].

Cellular delivery may also circumvent the effects of neutralizing immunity [213,214]. This is evidenced in a recent study that employed human reovirus T3D as oncolytic agent. In reovirus-naive mice with B16tk lymph node melanoma metastases, free reovirus or reovirus delivered through mature dendritic cells (DC) or T cells was detected in the tumor-draining lymph nodes three days after treatment. Here, these viruses could eradicate local tumor cells. Only T cells carrying reovirus generated anti-tumor immune responses and long-term tumor clearance. In reovirus-immune mice, however, the results were different. Delivery of free reovirus was ineffective as a therapy, but if mature DC as well as T cells were used as carriers, reovirus was effectively delivered to melanoma *in vivo* [213]. These data show that whereas systemically administered reoviruses may not be suitable for therapy, DC may be an appropriate vehicle for delivery of significant amounts of reovirus to tumors. This and several other studies suggest that cellular delivery is feasible and may be applicable for delivery of viral oncolytic agents at the tumor sites. However, cellular delivery also adds a new level of complexity to the clinical studies, and is logistically challenging.

Which cells to target?

With the aid of genetic modification and bioselection strategies new reovirus-derived cancer gene therapeutics can be developed that ensure efficient infection of cells within the tumor. It is known that tumors are usually markedly heterogeneous, consisting of complex mixtures of cancer cells with various grades of differentiation. A cell type that has attracted much attention in recent years is the tumor-initiating cell, or cancer stem cell. The tumor-initiating cell is a cell with the capacity to self-renew and differentiate into any of the lineages of cancer cells that comprise a tumor [215]. Presumably the tumor-initiating cells are derived from organ stem cells [216]. The latter are long-lived and

change over the course of time by accumulating (epi)genetic alterations. In this model, the characteristics of cancer-initiating cells and therefore of the resulting tumor, depend (in part) on these alterations. The cancer stem cell population in a tumor may not only govern tumor progression, but may also be responsible for the establishment of distant clones (metastases) [215,217]. Therapeutic efficacy may therefore be directly related to the efficiency with which a particular treatment eradicates the cancer stem cell population. It may therefore be important to ensure that new reoviral oncolytic agents have the capacity to transduce and kill cancer stem cells [198]. It may even be desirable to generate reovirus variants that specifically target the cancer stem cell population, rather than the more differentiated tumor cells.

Conclusion

Recent years have witnessed a reemergence of the oncolytic virus approach to cancer treatment. Initial clinical safety studies have demonstrated the validity of the concept, and feasibility of current approaches. The reovirus T3D used in the clinical studies reported on so far are well tolerated and safe. In recent years the knowledge of mammalian reoviruses, their biology and their interaction with the host have expanded rapidly. Whereas genetic modification of reoviruses' segmented double-stranded RNA genomes was notoriously difficult, new techniques facilitate the development of genetically modified variants. These techniques can be used to generate new tumor-targeted oncolytic reoviruses that will hopefully be as safe as current ones, but more efficacious.

Expert opinion

Reovirus-based oncolytic virus therapies have been safe, but so far the efficacy is limited. As with other oncolytic viruses the efficacy may be enhanced by combining the oncolytic virus approach with more conventional therapeutic approaches such as radiation and chemotherapy [218,219]. This concept is now being explored clinically [220].

In parallel, the new techniques for reverse genetics together with more classical genetic approaches can be used to overcome some of the hurdles that thwart efficacious oncolytic virus therapy. Several factors limit the efficacy of treatment with oncolytic viruses. These include the inefficient delivery of oncolytic viruses to the tumors, the limited infectivity of the cancer cells within the tumors, preexisting immunity in the patient population, and the marked heterogeneity of many tumor types. With the new (reverse-) genetics techniques, new tumor-targeted oncolytic reoviruses can be generated with

improved efficacy and applicability. Hereby, the gene therapist can be guided by our knowledge in parallel fields. In this respect, the large body of knowledge on oncolytic adenoviruses may be extremely valuable. Despite the differences in their genomic constitution, adenoviruses and reoviruses have several aspects in common. Although reovirus T3D and human adenovirus-C recognize different receptors, there are overt structural similarities between the T3D spike and the adenovirus fiber [205,221]. Hence for developing tumor-targeted reoviruses it may be useful to parallel the approaches that have been explored so successfully in the oncolytic adenovirus field [206-208].

Transient immune suppression may overcome immunological barriers that impede effective reovirus delivery [222,223], although it should be realized that this approach should be employed with caution. Reovirus infection can be associated with severe morbidity in immune compromised NOD/SCID mice [224]. Interestingly, it may be possible to select mutants with significantly reduced viral pathogenesis in immune compromised animals [225]. On the other hand, the immune system is an important mediator of anti-tumor activity, and the oncolytic virus infection may activate antitumor immune activity [48,226].

Reverse genetic techniques can be used to generate reoviruses carrying heterologous genes [115,141]. Transgenes may be included to arm the oncolytic viruses, for instance by including transgenes encoding cytokines for activating the immune system. This may increase the anti-tumor efficacy [227]. Also the replication of reoviruses may be reduced by insertion of microRNA target sequences, similar to the method used to prevent replication of adenoviruses in hepatocytes [228,229]. Already, Dermody and colleagues demonstrated that RNA interference can be used to inhibit reovirus replication [230]. It remains to be established whether reoviruses carrying foreign sequences (i.e., transgenes, microRNA targets) are genetically stable enough to allow production of clinical-grade batches.

In cases where the use of mutants may be ineffective, other changes to the virus particles could be used. One such hurdle is the occurrence of reovirus immunity in the human population. While it is unlikely that mutants can be isolated that are insensitive to preexisting immunity, polymer shielding may be used to mask the epitopes in the capsid. This approach has been found to be extremely effective to protect adenovirus vectors, and it seems reasonable to anticipate that this strategy will also be effective in reoviruses [60].

Despite the new opportunities there is one factor that may limit use of genetically targeted reoviruses. Reoviruses display a high mutation rate compared with many DNA viruses. As a result, during prolonged passage reovirus mutants have a tendency to change or revert, forming so-called

quasispecies. This genetic drift may be reduced by propagating the viruses under appropriate selective pressure. For large-scale production of reoviruses for clinical use, product consistency is important. Therefore, it is essential to design culture conditions that limit the expansion of mutants or revertants in the vector preparation. It remains to be seen whether that is feasible for novel tumor-targeted oncolytic reoviruses with new phenotypes. It is anticipated that the development of new production systems may be necessary, and should be developed in parallel with appropriate pre-clinical testing methods. This can warrant safe clinical application of new oncolytic reoviruses. With these we can keep the gene therapists' promise of providing new and effective treatment for malignant neoplastic disease.

REFERENCES I

INTRODUCTION



1. **Dock, G.** The influence of complicating diseases upon leukemia. *Am.J.Med.Sci.* 1904; **127**:563-592.
2. **Hammill, A.M., Conner, J., and Cripe, T.P.** Oncolytic virotherapy reaches adolescence. *Pediatr.Blood Cancer* 2010; **55**:1253-1263.
3. **Kelly, E. and Russell, S.J.** History of oncolytic viruses: genesis to genetic engineering. *Mol.Ther.* 2007; **15**:651-659.
4. **Russell, S.J., Peng, K.W., and Bell, J.C.** Oncolytic virotherapy. *Nat.Biotechnol.* 2012; **30**:658-670.
5. **Vaha-Koskela, M.J., Heikkila, J.E., and Hinkkanen, A.E.** Oncolytic viruses in cancer therapy. *Cancer Lett.* 2007; **254**:178-216.
6. **Wirth, T., Parker, N., and Yla-Herttuala, S.** History of gene therapy. *Gene* 2013; **525**:162-169.
7. **Martuza, R.L., Malick, A., Markert, J.M., et al.** Experimental therapy of human glioma by means of a genetically engineered virus mutant. *Science* 1991; **252**:854-856.
8. **Kay, M.A., Glorioso, J.C., and Naldini, L.** Viral vectors for gene therapy: the art of turning infectious agents into vehicles of therapeutics. *Nat.Med.* 2001; **7**:33-40.
9. **Robbins, P.D. and Ghivizzani, S.C.** Viral vectors for gene therapy. *Pharmacol. Ther.* 1998; **80**:35-47.
10. **Garber, K.** China approves world's first oncolytic virus therapy for cancer treatment. *J.Natl.Cancer Inst.* 2006; **98**:298-300.
11. **Lee, J., Kotliarova, S., Kotliarov, Y., et al.** Tumor stem cells derived from glioblastomas cultured in bFGF and EGF more closely mirror the phenotype and genotype of primary tumors than do serum-cultured cell lines. *Cancer Cell* 2006; **9**:391-403.
12. **Vik-Mo, E.O., Sandberg, C., Olstorn, H., et al.** Brain tumor stem cells maintain overall phenotype and tumorigenicity after *in vitro* culturing in serum-free conditions. *Neuro.Oncol.* 2010; **12**:1220-1230.
13. **Ohgaki, H. and Kleihues, P.** Epidemiology and etiology of gliomas. *Acta Neuropathol.* 2005; **109**:93-108.
14. **Ricard, D., Idbah, A., Ducray, F., et al.** Primary brain tumours in adults. *Lancet* 2012; **379**:1984-1996.
15. **Wollmann, G., Ozduman, K., and van den Pol, A.N.** Oncolytic virus therapy for glioblastoma multiforme: concepts and candidates. *Cancer J.* 2012; **18**:69-81.
16. **Zemp, F.J., Corredor, J.C., Lun, X., et al.** Oncolytic viruses as experimental treatments for malignant gliomas: using a scourge to treat a devil. *Cytokine Growth Factor Rev.* 2010; **21**:103-117.
17. **Murphy, A.M. and Rabkin, S.D.** Current status of gene therapy for brain tumors. *Transl.Res.* 2013; **161**:339-354.
18. **Vellinga, J., van den Wollenberg, D.J., van der Heijdt, S., et al.** The coiled-coil domain of the adenovirus type 5 protein IX is dispensable for capsid incorporation and thermostability. *J.Virol.* 2005; **79**:3206-3210.
19. **Subramanian, T., Vijayalingam, S., and Chinnadurai, G.** Genetic identification of adenovirus type 5 genes that influence viral spread. *J.Virol.* 2006; **80**:2000-2012.
20. **Yan, W., Kitzes, G., Dormishian, F., et al.** Developing novel oncolytic adenoviruses through bioselection. *J.Virol.* 2003; **77**:2640-2650.
21. **Jordan, C.T., Guzman, M.L., and Noble, M.** Cancer stem cells. *N.Engl.J.Med.* 2006; **355**:1253-1261.

22. **O'Connor, M.L., Xiang, D., Shigdar, S., et al.** Cancer stem cells: A contentious hypothesis now moving forward. *Cancer Lett.* 2014; **344**:180-187.
23. **Vescovi, A.L., Galli, R., and Reynolds, B.A.** Brain tumour stem cells. *Nat.Rev. Cancer* 2006; **6**:425-436.
24. **van den Wollenberg, D.J., van den Hengel, S.K., Dautzenberg, I.J., et al.** Modification of mammalian reoviruses for use as oncolytic agents. *Expert.Opin.Biol. Ther.* 2009; **9**:1509-1520.
25. **Toth, K., Dhar, D., and Wold, W.S.** Oncolytic (replication-competent) adenoviruses as anticancer agents. *Expert.Opin.Biol. Ther.* 2010; **10**:353-368.
26. **Patel, M.R. and Kratzke, R.A.** Oncolytic virus therapy for cancer: the first wave of translational clinical trials. *Transl.Res.* 2013; **161**:355-364.
27. **Rowe, W.P., Huebner, R.J., Gilmore, L.K., et al.** Isolation of a cytopathogenic agent from human adenoids undergoing spontaneous degeneration in tissue culture. *Proc.Soc.Exp.Biol.Med.* 1953; **84**:570-573.
28. **Hilleman, M.R. and Werner, J.H.** Recovery of new agent from patients with acute respiratory illness. *Proc.Soc.Exp.Biol.Med.* 1954; **85**:183-188.
29. **Berget, S.M., Moore, C., and Sharp, P.A.** Spliced segments at the 5' terminus of adenovirus 2 late mRNA. *Proc.Natl.Acad.Sci.U.S.A* 1977; **74**:3171-3175.
30. **Graham, F. and van der Eb, A.** A new technique for the assay of infectivity of human adenovirus 5 DNA. *Virology* 1973; **52**:456-467.
31. **Berk, A.J.** Recent lessons in gene expression, cell cycle control, and cell biology from adenovirus. *Oncogene* 2005; **24**:7673-7685.
32. **Rux, J.J. and Burnett, R.M.** Adenovirus structure. *Hum.Gene Ther.* 2004; **15**:1167-1176.
33. **Lasaro, M.O. and Ertl, H.C.** New insights on adenovirus as vaccine vectors. *Mol. Ther.* 2009; **17**:1333-1339.
34. **Robinson, C.M., Singh, G., Lee, J.Y., et al.** Molecular evolution of human adenoviruses. *Sci.Rep.* 2013; **3**:1812.
35. **Parks, R.J.** Adenovirus protein IX: a new look at an old protein. *Mol.Ther.* 2005; **11**:19-25.
36. **Russell, W.C.** Adenoviruses: update on structure and function. *J.Gen.Virol.* 2009; **90**:1-20.
37. **Liu, H., Jin, L., Koh, S.B., et al.** Atomic structure of human adenovirus by cryo-EM reveals interactions among protein networks. *Science* 2010; **329**:1038-1043.
38. **Pereira, H.G., Valentine, R.C., and Russell, W.C.** Crystallization of an adenovirus protein (the hexon). *Nature* 1968; **219**:946-947.
39. **Kalyuzhniy, O., Di Paolo, N.C., Silvestry, M., et al.** Adenovirus serotype 5 hexon is critical for virus infection of hepatocytes *in vivo*. *Proc.Natl.Acad.Sci.U.S.A* 2008; **105**:5483-5488.
40. **Waddington, S.N., McVey, J.H., Bhella, D., et al.** Adenovirus serotype 5 hexon mediates liver gene transfer. *Cell* 2008; **132**:397-409.
41. **McConnell, M.J. and Imperiale, M.J.** Biology of adenovirus and its use as a vector for gene therapy. *Hum.Gene Ther.* 2004; **15**:1022-1033.
42. **Branton, P. E.** 1999. Early gene expression, p. 39-55. *In:* p. Seth (ed.), *Adenoviruses: Basic Biology to Gene Therapy*.
43. **Douglas, J.T.** Adenoviral vectors for gene therapy. *Mol.Biotechnol.* 2007; **36**:71-80.

44. **Graham, F.L., Smiley, J., Russell, W.C., and Nairn, R.** Characteristics of a human cell line transformed by DNA from human adenovirus type 5. *J.Gen.Virol.* 1977; **36**:59-74.
45. **Lochmuller, H., Jani, A., Huard, J., et al.** Emergence of early region 1-containing replication-competent adenovirus in stocks of replication-defective adenovirus recombinants (delta E1 + delta E3) during multiple passages in 293 cells. *Hum. Gene Ther.* 1994; **5**:1485-1491.
46. **Fallaux, F.J., Bout, A., van de Velde, I., et al.** New helper cells and matched early region 1-deleted adenovirus vectors prevent generation of replication-competent adenoviruses. *Hum.Gene Ther.* 1998; **9**:1909-1917.
47. **Gao, G.P., Engdahl, R.K., and Wilson, J.M.** A cell line for high-yield production of E1-deleted adenovirus vectors without the emergence of replication-competent virus. *Hum.Gene Ther.* 2000; **11**:213-219.
48. **Prestwich, R.J., Errington, F., Diaz, R.M., et al.** The case of oncolytic viruses versus the immune system: waiting on the judgment of Solomon. *Hum.Gene Ther.* 2009; **20**:1119-1132.
49. **Barker, D.D. and Berk, A.J.** Adenovirus proteins from both E1B reading frames are required for transformation of rodent cells by viral infection and DNA transfection. *Virology* 1987; **156**:107-121.
50. **Goodrum, F.D. and Ornelles, D.A.** p53 status does not determine outcome of E1B 55-kilodalton mutant adenovirus lytic infection. *J.Virol.* 1998; **72**:9479-9490.
51. **Turnell, A.S., Grand, R.J., and Gallimore, P.H.** The replicative capacities of large E1B-null group A and group C adenoviruses are independent of host cell p53 status. *J.Virol.* 1999; **73**:2074-2083.
52. **Fueyo, J., Gomez-Manzano, C., Alemany, R., et al.** A mutant oncolytic adenovirus targeting the Rb pathway produces anti-glioma effect *in vivo*. *Oncogene* 2000; **19**:2-12.
53. **Horst, M., Brouwer, E., Verwijnen, S., et al.** Targeting malignant gliomas with a glial fibrillary acidic protein (GFAP)-selective oncolytic adenovirus. *J.Gene Med.* 2007; **9**:1071-1079.
54. **Bachtarzi, H., Stevenson, M., and Fisher, K.** Cancer gene therapy with targeted adenoviruses. *Expert.Opin.Drug Deliv.* 2008; **5**:1231-1240.
55. **Glasgow, J.N., Everts, M., and Curiel, D.T.** Transductional targeting of adenovirus vectors for gene therapy. *Cancer Gene Ther.* 2006; **13**:830-844.
56. **Nandi, S. and Lesniak, M.S.** Adenoviral virotherapy for malignant brain tumors. *Expert.Opin.Biol.Ther.* 2009; **9**:737-747.
57. **Vellinga, J., Rabelink, M.J., Cramer, S.J., et al.** Spacers increase the accessibility of peptide ligands linked to the carboxyl terminus of adenovirus minor capsid protein IX. *J.Virol.* 2004; **78**:3470-3479.
58. **Vellinga, J., Uil, T.G., de Vrij, J., et al.** A system for efficient generation of adenovirus protein IX-producing helper cell lines. *J.Gene Med.* 2006; **8**:147-154.
59. **Alba, R., Bradshaw, A.C., Coughlan, L., et al.** Biodistribution and retargeting of FX-binding ablated adenovirus serotype 5 vectors. *Blood* 2010; **116**:2656-2664.
60. **Kreppel, F. and Kochanek, S.** Modification of adenovirus gene transfer vectors with synthetic polymers: a scientific review and technical guide. *Mol.Ther.* 2008; **16**:16-29.
61. **Komarova, S., Kawakami, Y., Stoff-Khalili, M.A., et al.** Mesenchymal progenitor cells as cellular vehicles for delivery of oncolytic adenoviruses. *Mol.Cancer Ther.* 2006; **5**:755-766.

62. **Studený, M., Marini, F.C., Champlin, R.E., et al.** Bone marrow-derived mesenchymal stem cells as vehicles for interferon-beta delivery into tumors. *Cancer Res.* 2002; **62**:3603-3608.
63. **van Putten, E.H., Dirven, C.M., van den Bent, M.J., and Lamfers, M.L.** Sitimagene ceradenovec: a gene-based drug for the treatment of operable high-grade glioma. *Future.Oncol.* 2010; **6**:1691-1710.
64. **Trask, T.W., Trask, R.P., Aguilar-Cordova, E., et al.** Phase I study of adenoviral delivery of the HSV-tk gene and ganciclovir administration in patients with current malignant brain tumors. *Mol.Ther.* 2000; **1**:195-203.
65. **Westphal, M., Yla-Herttuala, S., Martin, J., et al.** Adenovirus-mediated gene therapy with sitimagene ceradenovec followed by intravenous ganciclovir for patients with operable high-grade glioma (ASPECT): a randomised, open-label, phase 3 trial. *Lancet Oncol.* 2013; **14**:823-833.
66. **Gros, A., Martinez-Quintanilla, J., Puig, C., et al.** Bioreselection of a gain of function mutation that enhances adenovirus 5 release and improves its antitumoral potency. *Cancer Res.* 2008; **68**:8928-8937.
67. **Kuhn, I., Harden, P., Bauzon, M., et al.** Directed evolution generates a novel oncolytic virus for the treatment of colon cancer. *PLoS.One.* 2008; **3**:e2409.
68. **Uil, T.G., Vellinga, J., de Vrij, J., et al.** Directed adenovirus evolution using engineered mutator viral polymerases. *Nucleic Acids Res.* 2011; **39**:e30.
69. **Domingo, E. and Holland, J.J.** RNA virus mutations and fitness for survival. *Annu. Rev.Microbiol.* 1997; **51**:151-178.
70. **Joklik, W.K.** Structure and function of the reovirus genome. *Microbiol.Rev.* 1981; **45**:483-501.
71. **Minuk, G.Y., Paul, R.W., and Lee, P.W.** The prevalence of antibodies to reovirus type 3 in adults with idiopathic cholestatic liver disease. *J.Med.Virol.* 1985; **16**:55-60.
72. **Minuk, G.Y., Rascanin, N., Paul, R.W., et al.** Reovirus type 3 infection in patients with primary biliary cirrhosis and primary sclerosing cholangitis. *J.Hepatol.* 1987; **5**:8-13.
73. **Tyler, K. L. and B. N. Fields.** 2001. Mammalian Reoviruses, p. 1729-1745. *In:* D. M. Knipe and P. M. Howely (eds.), *Fields Virology*. 4 th ed. Lippincott, Williams & Wilkins, Philadelphia.
74. **Gomatos, P.J. and Tamm, I.** THE SECONDARY STRUCTURE OF REOVIRUS RNA. *Proc.Natl.Acad.Sci.U.S.A* 1963; **49**:707-714.
75. **Shatkin, A.J., Sipe, J.D., and Loh, P.** Separation of ten reovirus genome segments by polyacrylamide gel electrophoresis. *J.Virol.* 1968; **2**:986-991.
76. **Weiner, H.L., Drayna, D., Averill, D.R., Jr., and Fields, B.N.** Molecular basis of reovirus virulence: role of the S1 gene. *Proc.Natl.Acad.Sci.U.S.A* 1977; **74**:5744-5748.
77. **Weiner, H.L. and Fields, B.N.** Neutralization of reovirus: the gene responsible for the neutralization antigen. *J.Exp.Med.* 1977; **146**:1305-1310.
78. **Tyler, K.L., Squier, M.K., Rodgers, S.E., et al.** Differences in the capacity of reovirus strains to induce apoptosis are determined by the viral attachment protein sigma 1. *J.Virol.* 1995; **69**:6972-6979.
79. **Coombs, K.M.** Reovirus structure and morphogenesis. *Curr.Top.Microbiol.Immunol.* 2006; **309**:117-167.

80. **Jacobs, B.L. and Samuel, C.E.** Biosynthesis of reovirus-specified polypeptides: the reovirus s1 mRNA encodes two primary translation products. *Virology* 1985; **143**:63-74.
81. **Sarkar, G., Pelletier, J., Bassel-Duby, R., et al.** Identification of a new polypeptide coded by reovirus gene S1. *J. Virol.* 1985; **54**:720-725.
82. **Starnes, M.C. and Joklik, W.K.** Reovirus protein lambda 3 is a poly(C)-dependent poly(G) polymerase. *Virology* 1993; **193**:356-366.
83. ViralZone. Orthoreovirus. http://expasy.org/viralzone/all_by_species/105.html . 30-5-2011.
Ref Type: Online Source
84. **Huismans, H. and Joklik, W.K.** Reovirus-coded polypeptides in infected cells: isolation of two native monomeric polypeptides with affinity for single-stranded and double-stranded RNA, respectively. *Virology* 1976; **70**:411-424.
85. **Antczak, J.B. and Joklik, W.K.** Reovirus genome segment assortment into progeny genomes studied by the use of monoclonal antibodies directed against reovirus proteins. *Virology* 1992; **187**:760-776.
86. **Becker, M.M., Peters, T.R., and Dermody, T.S.** Reovirus sigma NS and mu NS proteins form cytoplasmic inclusion structures in the absence of viral infection. *J. Virol.* 2003; **77**:5948-5963.
87. **Broering, T.J., McCutcheon, A.M., Centonze, V.E., and Nibert, M.L.** Reovirus nonstructural protein muNS binds to core particles but does not inhibit their transcription and capping activities. *J. Virol.* 2000; **74**:5516-5524.
88. **Kobayashi, T., Ooms, L.S., Chappell, J.D., and Dermody, T.S.** Identification of functional domains in reovirus replication proteins muNS and mu2. *J. Virol.* 2009; **83**:2892-2906.
89. **Mora, M., Partin, K., Bhatia, M., et al.** Association of reovirus proteins with the structural matrix of infected cells. *Virology* 1987; **159**:265-277.
90. **Barton, E.S., Connolly, J.L., Forrest, J.C., et al.** Utilization of sialic acid as a coreceptor enhances reovirus attachment by multistep adhesion strengthening. *J. Biol. Chem.* 2001; **276**:2200-2211.
91. **Chappell, J.D., Duong, J.L., Wright, B.W., and Dermody, T.S.** Identification of carbohydrate-binding domains in the attachment proteins of type 1 and type 3 reoviruses. *J. Virol.* 2000; **74**:8472-8479.
92. **Nibert, M. L. and L. A. Schiff.** 2001. Reovirus and their replication, p. 1679-1728. *In*: D. M. Knipe and P. M. Howely (eds.), *Field Virology*. 4th ed. Lippincott Williams & Wilkins, Philadelphia.
93. **Barton, E.S., Forrest, J.C., Connolly, J.L., et al.** Junction adhesion molecule is a receptor for reovirus. *Cell* 2001; **104**:441-451.
94. **Campbell, J.A., Schelling, P., Wetzell, J.D., et al.** Junctional adhesion molecule a serves as a receptor for prototype and field-isolate strains of mammalian reovirus. *J. Virol.* 2005; **79**:7967-7978.
95. **Guglielmi, K.M., Johnson, E.M., Stehle, T., and Dermody, T.S.** Attachment and cell entry of mammalian orthoreovirus. *Curr. Top. Microbiol. Immunol.* 2006; **309**:1-38.
96. **Maginnis, M.S., Forrest, J.C., Kopecky-Bromberg, S.A., et al.** Beta1 integrin mediates internalization of mammalian reovirus. *J. Virol.* 2006; **80**:2760-2770.
97. **Ivanovic, T., Agosto, M.A., Zhang, L., et al.** Peptides released from reovirus outer capsid form membrane pores that recruit virus particles. *EMBO J.* 2008; **27**:1289-1298.

98. **Chow, N.L. and Shatkin, A.J.** Blocked and unblocked 5' termini in reovirus genome RNA. *J.Virol.* 1975; **15**:1057-1064.
99. **Furuichi, Y., Muthukrishnan, S., and Shatkin, A.J.** 5'-Terminal m-7G(5')ppp(5') G-m-p *in vivo*: identification in reovirus genome RNA. *Proc.Natl.Acad.Sci.U.S.A* 1975; **72**:742-745.
100. **Miura, K., Watanabe, K., Sugiura, M., and Shatkin, A.J.** The 5'-terminal nucleotide sequences of the double-stranded RNA of human reovirus. *Proc.Natl.Acad.Sci.U.S.A* 1974; **71**:3979-3983.
101. **Nonoyama, M., Millward, S., and Graham, A.F.** Control of transcription of the reovirus genome. *Nucleic Acids Res.* 1974; **1**:373-385.
102. **Spandidos, D.A., Krystal, G., and Graham, A.F.** Regulated transcription of the genomes of defective virions and temperature-sensitive mutants of reovirus. *J.Virol.* 1976; **18**:7-19.
103. **Watanabe, Y., Millward, S., and Graham, A.F.** Regulation of transcription of the Reovirus genome. *J.Mol.Biol.* 1968; **36**:107-123.
104. **Roner, M.R., Bassett, K., and Roehr, J.** Identification of the 5' sequences required for incorporation of an engineered ssRNA into the Reovirus genome. *Virology* 2004; **329**:348-360.
105. **Connolly, J.L. and Dermody, T.S.** Virion disassembly is required for apoptosis induced by reovirus. *J.Virol.* 2002; **76**:1632-1641.
106. **Danthi, P., Kobayashi, T., Holm, G.H., et al.** Reovirus apoptosis and virulence are regulated by host cell membrane penetration efficiency. *J.Virol.* 2008; **82**:161-172.
107. **Tyler, K.L., Squier, M.K., Brown, A.L., et al.** Linkage between reovirus-induced apoptosis and inhibition of cellular DNA synthesis: role of the S1 and M2 genes. *J.Virol.* 1996; **70**:7984-7991.
108. **Spendlove, R.S., McClain, M.E., and Lennette, E.H.** Enhancement of reovirus infectivity by extracellular removal or alteration of the virus capsid by proteolytic enzymes. *J.Gen.Virol.* 1970; **8**:83-94.
109. **Roner, M.R. and Steele, B.G.** Localizing the reovirus packaging signals using an engineered m1 and s2 ssRNA. *Virology* 2007; **358**:89-97.
110. **Roner, M.R. and Steele, B.G.** Features of the mammalian orthoreovirus 3 Dearing I1 single-stranded RNA that direct packaging and serotype restriction. *J.Gen.Virol.* 2007; **88**:3401-3412.
111. **Antczak, J.B., Chmelo, R., Pickup, D.J., and Joklik, W.K.** Sequence at both termini of the 10 genes of reovirus serotype 3 (strain Dearing). *Virology* 1982; **121**:307-319.
112. **Gaillard, R.K., Li, J.K., Keene, J.D., and Joklik, W.K.** The sequence at the termini of four genes of the three reovirus serotypes. *Virology* 1982; **121**:320-326.
113. **Schlesinger, R.W., Stollar, V., Guild, G.M., et al.** The significance and nature of defective interfering viruses. *Bull.Schweiz.Akad.Med.Wiss.* 1977; **33**:229-242.
114. **Zou, S. and Brown, E.G.** Identification of sequence elements containing signals for replication and encapsidation of the reovirus M1 genome segment. *Virology* 1992; **186**:377-388.
115. **Roner, M.R. and Joklik, W.K.** Reovirus reverse genetics: Incorporation of the CAT gene into the reovirus genome. *Proc.Natl.Acad.Sci.U.S.A* 2001; **98**:8036-8041.
116. **Roner, M.R. and Roehr, J.** The 3' sequences required for incorporation of an engineered ssRNA into the Reovirus genome. *Viol.J.* 2006; **3**:1.

117. **Joklik, W.K.** Assembly of the reovirus genome. *Curr.Top.Microbiol.Immunol.* 1998; **233**:57-68.
118. **Chappell, J.D., Gunn, V.L., Wetzel, J.D., et al.** Mutations in type 3 reovirus that determine binding to sialic acid are contained in the fibrous tail domain of viral attachment protein sigma1. *J.Virol.* 1997; **71**:1834-1841.
119. **Spriggs, D.R. and Fields, B.N.** Attenuated reovirus type 3 strains generated by selection of haemagglutinin antigenic variants. *Nature* 1982; **297**:68-70.
120. **Steinhauer, D.A., Domingo, E., and Holland, J.J.** Lack of evidence for proofreading mechanisms associated with an RNA virus polymerase. *Gene* 1992; **122**:281-288.
121. **Novella, I.S., Duarte, E.A., Elena, S.F., et al.** Exponential increases of RNA virus fitness during large population transmissions. *Proc.Natl.Acad.Sci.U.S.A* 1995; **92**:5841-5844.
122. **Gomatos, P.J. and Tamm, I.** Reactive sites of reovirus type 3 and their interaction with receptor substances. *Virology* 1962; **17**:455-461.
123. **Weiner, H.L., Ramig, R.F., Mustoe, T.A., and Fields, B.N.** Identification of the gene coding for the hemagglutinin of reovirus. *Virology* 1978; **86**:581-584.
124. **Weiner, H.L., Ault, K.A., and Fields, B.N.** Interaction of reovirus with cell surface receptors. I. Murine and human lymphocytes have a receptor for the hemagglutinin of reovirus type 3. *J.Immunol.* 1980; **124**:2143-2148.
125. **Lee, P.W., Hayes, E.C., and Joklik, W.K.** Protein sigma 1 is the reovirus cell attachment protein. *Virology* 1981; **108**:156-163.
126. **Armstrong, G.D., Paul, R.W., and Lee, P.W.** Studies on reovirus receptors of L cells: virus binding characteristics and comparison with reovirus receptors of erythrocytes. *Virology* 1984; **138**:37-48.
127. **Co, M.S., Gaulton, G.N., Fields, B.N., and Greene, M.I.** Isolation and biochemical characterization of the mammalian reovirus type 3 cell-surface receptor. *Proc.Natl.Acad.Sci.U.S.A* 1985; **82**:1494-1498.
128. **Gentsch, J.R. and Pacitti, A.F.** Effect of neuraminidase treatment of cells and effect of soluble glycoproteins on type 3 reovirus attachment to murine L cells. *J.Virol.* 1985; **56**:356-364.
129. **Paul, R.W. and Lee, P.W.** Glycophorin is the reovirus receptor on human erythrocytes. *Virology* 1987; **159**:94-101.
130. **Pacitti, A.F. and Gentsch, J.R.** Inhibition of reovirus type 3 binding to host cells by sialylated glycoproteins is mediated through the viral attachment protein. *J.Virol.* 1987; **61**:1407-1415.
131. **Leone, G., Duncan, R., Mah, D.C., et al.** The N-terminal heptad repeat region of reovirus cell attachment protein sigma 1 is responsible for sigma 1 oligomer stability and possesses intrinsic oligomerization function. *Virology* 1991; **182**:336-345.
132. **Strong, J.E., Leone, G., Duncan, R., et al.** Biochemical and biophysical characterization of the reovirus cell attachment protein sigma 1: evidence that it is a homotrimer. *Virology* 1991; **184**:23-32.
133. **Bassel-Duby, R., Jayasuriya, A., Chatterjee, D., et al.** Sequence of reovirus haemagglutinin predicts a coiled-coil structure. *Nature* 1985; **315**:421-423.
134. **Nibert, M.L., Dermody, T.S., and Fields, B.N.** Structure of the reovirus cell-attachment protein: a model for the domain organization of sigma 1. *J.Virol.* 1990; **64**:2976-2989.

135. **Dermody, T.S., Nibert, M.L., Bassel-Duby, R., and Fields, B.N.** A sigma 1 region important for hemagglutination by serotype 3 reovirus strains. *J.Virol.* 1990; **64**:5173-5176.
136. **Rubin, D.H., Wetzel, J.D., Williams, W.V., et al.** Binding of type 3 reovirus by a domain of the sigma 1 protein important for hemagglutination leads to infection of murine erythroleukemia cells. *J.Clin.Invest* 1992; **90**:2536-2542.
137. **Severson, E.A. and Parkos, C.A.** Structural determinants of Junctional Adhesion Molecule A (JAM-A) function and mechanisms of intracellular signaling. *Curr.Opin. Cell Biol.* 2009; **21**:701-707.
138. **Martin-Padura, I., Lostaglio, S., Schneemann, M., et al.** Junctional adhesion molecule, a novel member of the immunoglobulin superfamily that distributes at intercellular junctions and modulates monocyte transmigration. *J.Cell Biol.* 1998; **142**:117-127.
139. **Liu, Y., Nusrat, A., Schnell, F.J., et al.** Human junction adhesion molecule regulates tight junction resealing in epithelia. *J.Cell Sci.* 2000; **113 (Pt 13)**:2363-2374.
140. **Kirchner, E., Guglielmi, K.M., Strauss, H.M., et al.** Structure of reovirus sigma1 in complex with its receptor junctional adhesion molecule-A. *PLoS.Pathog.* 2008; **4**:e1000235.
141. **Kobayashi, T., Antar, A.A., Boehme, K.W., et al.** A plasmid-based reverse genetics system for animal double-stranded RNA viruses. *Cell Host.Microbe* 2007; **1**:147-157.
142. **Danthi, P., Guglielmi, K.M., Kirchner, E., et al.** From touchdown to transcription: the reovirus cell entry pathway. *Curr.Top.Microbiol.Immunol.* 2010; **343**:91-119.
143. **Maginnis, M.S., Mainou, B.A., Derdowski, A., et al.** NPXY motifs in the beta1 integrin cytoplasmic tail are required for functional reovirus entry. *J.Virol.* 2008; **82**:3181-3191.
144. **Bell, T.M. and Ross, M.G.** Persistent latent infection of human embryonic cells with reovirus type 3. *Nature* 1966; **212**:412-414.
145. **Taber, R., Alexander, V., and Whitford, W.** Persistent reovirus infection of CHO cells resulting in virus resistance. *J.Virol.* 1976; **17**:513-524.
146. **Ahmed, R., Canning, W.M., Kauffman, R.S., et al.** Role of the host cell in persistent viral infection: coevolution of L cells and reovirus during persistent infection. *Cell* 1981; **25**:325-332.
147. **Ebert, D.H., Deussing, J., Peters, C., and Dermody, T.S.** Cathepsin L and cathepsin B mediate reovirus disassembly in murine fibroblast cells. *J.Biol.Chem.* 2002; **277**:24609-24617.
148. **Ebert, D.H., Kopecky-Bromberg, S.A., and Dermody, T.S.** Cathepsin B Is Inhibited in Mutant Cells Selected during Persistent Reovirus Infection. *J.Biol.Chem.* 2004; **279**:3837-3851.
149. **Baer, G.S., Ebert, D.H., Chung, C.J., et al.** Mutant cells selected during persistent reovirus infection do not express mature cathepsin L and do not support reovirus disassembly. *J.Virol.* 1999; **73**:9532-9543.
150. **Ahmed, R. and Fields, B.N.** Role of the S4 gene in the establishment of persistent reovirus infection in L cells. *Cell* 1982; **28**:605-612.
151. **Sharpe, A.H. and Fields, B.N.** Reovirus inhibition of cellular RNA and protein synthesis: role of the S4 gene. *Virology* 1982; **122**:381-391.

152. **Kim, M., Garant, K.A., zur Nieden, N.I., et al.** Attenuated reovirus displays oncolysis with reduced host toxicity. *Br.J.Cancer* 2011; **104**:290-299.
153. **Wilson, G.J., Wetzel, J.D., Puryear, W., et al.** Persistent reovirus infections of L cells select mutations in viral attachment protein sigma1 that alter oligomer stability. *J.Virol.* 1996; **70**:6598-6606.
154. **Wetzel, J.D., Wilson, G.J., Baer, G.S., et al.** Reovirus variants selected during persistent infections of L cells contain mutations in the viral S1 and S4 genes and are altered in viral disassembly. *J.Virol.* 1997; **71**:1362-1369.
155. **Tyler, K.L., Clarke, P., Debiasi, R.L., et al.** Reoviruses and the host cell. *Trends Microbiol.* 2001; **9**:560-564.
156. **Connolly, J.L., Barton, E.S., and Dermody, T.S.** Reovirus binding to cell surface sialic acid potentiates virus-induced apoptosis. *J.Virol.* 2001; **75**:4029-4039.
157. **Cashdollar, L.W., Esparza, J., Hudson, G.R., et al.** Cloning the double-stranded RNA genes of reovirus: sequence of the cloned S2 gene. *Proc.Natl.Acad.Sci.U.S.A* 1982; **79**:7644-7648.
158. **Roner, M.R., Sutphin, L.A., and Joklik, W.K.** Reovirus RNA is infectious. *Virology* 1990; **179**:845-852.
159. **Joklik, W.K. and Roner, M.R.** What reassorts when reovirus genome segments reassort? *J.Biol.Chem.* 1995; **270**:4181-4184.
160. **Roner, M.R., Nepliouev, I., Sherry, B., and Joklik, W.K.** Construction and characterization of a reovirus double temperature-sensitive mutant. *Proc.Natl.Acad.Sci.U.S.A* 1997; **94**:6826-6830.
161. **van den Wollenberg, D.J., van den Hengel, S.K., Dautzenberg, I.J., et al.** A strategy for genetic modification of the spike-encoding segment of human reovirus T3D for reovirus targeting. *Gene Ther.* 2008; **15**:1567-1578.
162. **Rouault, E. and Lemay, G.** Incorporation of epitope-tagged viral sigma3 proteins to reovirus virions. *Can.J.Microbiol.* 2003; **49**:407-417.
163. **Chandran, K., Walker, S.B., Chen, Y., et al.** *In vitro* recoating of reovirus cores with baculovirus-expressed outer-capsid proteins mu1 and sigma3. *J.Virol.* 1999; **73**:3941-3950.
164. **Chandran, K., Zhang, X., Olson, N.H., et al.** Complete *in vitro* assembly of the reovirus outer capsid produces highly infectious particles suitable for genetic studies of the receptor-binding protein. *J.Virol.* 2001; **75**:5335-5342.
165. **Jane-Valbuena, J., Nibert, M.L., Spencer, S.M., et al.** Reovirus virion-like particles obtained by recoating infectious subvirion particles with baculovirus-expressed sigma3 protein: an approach for analyzing sigma3 functions during virus entry. *J.Virol.* 1999; **73**:2963-2973.
166. **Danthi, P., Coffey, C.M., Parker, J.S., et al.** Independent regulation of reovirus membrane penetration and apoptosis by the mu1 phi domain. *PLoS.Pathog.* 2008; **4**:e1000248.
167. **Kobayashi, T., Ooms, L.S., Ikizler, M., et al.** An improved reverse genetics system for mammalian orthoreoviruses. *Virology* 2010; **398**:194-200.
168. **Dennehy, P.H.** Transmission of rotavirus and other enteric pathogens in the home. *Pediatr.Infect.Dis.J.* 2000; **19**:S103-S105.
169. **Simpson, E., Wittet, S., Bonilla, J., et al.** Use of formative research in developing a knowledge translation approach to rotavirus vaccine introduction in developing countries. *BMC.Public Health* 2007; **7**:281.
170. **Bernstein, D.I.** Rotavirus overview. *Pediatr.Infect.Dis.J.* 2009; **28**:S50-S53.

171. **Pesavento, J.B., Crawford, S.E., Estes, M.K., and Prasad, B.V.** Rotavirus proteins: structure and assembly. *Curr.Top.Microbiol.Immunol.* 2006; **309**:189-219.
172. **Komoto, S., Sasaki, J., and Taniguchi, K.** Reverse genetics system for introduction of site-specific mutations into the double-stranded RNA genome of infectious rotavirus. *Proc.Natl.Acad.Sci.U.S.A* 2006; **103**:4646-4651.
173. **Troupin, C., Dehee, A., Schnuriger, A., et al.** Rearranged genomic RNA segments offer a new approach to the reverse genetics of rotaviruses. *J.Virol.* 2010; **84**:6711-6719.
174. **Gault, E., Schnepf, N., Poncet, D., et al.** A human rotavirus with rearranged genes 7 and 11 encodes a modified NSP3 protein and suggests an additional mechanism for gene rearrangement. *J.Virol.* 2001; **75**:7305-7314.
175. **Trask, S.D., Taraporewala, Z.F., Boehme, K.W., et al.** Dual selection mechanisms drive efficient single-gene reverse genetics for rotavirus. *Proc.Natl.Acad.Sci.U.S.A* 2010; **107**:18652-18657.
176. **Shmulevitz, M., Marcato, P., and Lee, P.W.** Unshackling the links between reovirus oncolysis, Ras signaling, translational control and cancer. *Oncogene* 2005; **24**:7720-7728.
177. **Strong, J.E., Coffey, M.C., Tang, D., et al.** The molecular basis of viral oncolysis: usurpation of the Ras signaling pathway by reovirus. *EMBO J.* 1998; **17**:3351-3362.
178. **Norman, K.L., Hirasawa, K., Yang, A.D., et al.** Reovirus oncolysis: the Ras/RalGEF/p38 pathway dictates host cell permissiveness to reovirus infection. *Proc.Natl.Acad.Sci.U.S.A* 2004; **101**:11099-11104.
179. **Theiss, J.C., Stoner, G.D., and Kniazeff, A.J.** Effect of reovirus infection on pulmonary tumor response to urethan in strain A mice. *J.Natl.Cancer Inst.* 1978; **61**:131-134.
180. **Coffey, M.C., Strong, J.E., Forsyth, P.A., and Lee, P.W.** Reovirus therapy of tumors with activated Ras pathway. *Science* 1998; **282**:1332-1334.
181. **Norman, K.L. and Lee, P.W.** Reovirus as a novel oncolytic agent. *J.Clin.Invest* 2000; **105**:1035-1038.
182. **Norman, K.L. and Lee, P.W.** Not all viruses are bad guys: the case for reovirus in cancer therapy. *Drug Discov.Today* 2005; **10**:847-855.
183. **Stoeckel, J. and Hay, J.G.** Drug evaluation: Reolysin--wild-type reovirus as a cancer therapeutic. *Curr.Opin.Mol.Ther.* 2006; **8**:249-260.
184. **Lemay, G., Tumilasci, V., and Hiscott, J.** Uncoating reo: uncovering the steps critical for oncolysis. *Mol.Ther.* 2007; **15**:1406-1407.
185. **Shmulevitz, M., Marcato, P., and Lee, P.W.** Activated Ras signaling significantly enhances reovirus replication and spread. *Cancer Gene Ther.* 2010; **17**:69-70.
186. **Song, L., Ohnuma, T., Gelman, I.H., and Holland, J.F.** Reovirus infection of cancer cells is not due to activated Ras pathway. *Cancer Gene Ther.* 2009; **16**:382.
187. **Smakman, N., van den Wollenberg, D.J., Borel Rinkes, I.H., et al.** Sensitization to apoptosis underlies KrasD12-dependent oncolysis of murine C26 colorectal carcinoma cells by reovirus T3D. *J.Virol.* 2005; **79**:14981-14985.
188. **Smakman, N., van den Wollenberg, D.J., Elias, S.G., et al.** KRAS(D13) Promotes apoptosis of human colorectal tumor cells by ReovirusT3D and oxaliplatin but not by tumor necrosis factor-related apoptosis-inducing ligand. *Cancer Res.* 2006; **66**:5403-5408.
189. **Alain, T., Kim, T.S., Lun, X., et al.** Proteolytic disassembly is a critical determinant for reovirus oncolysis. *Mol.Ther.* 2007; **15**:1512-1521.

190. **Kim, M., Egan, C., Alain, T., et al.** Acquired resistance to reoviral oncolysis in Ras-transformed fibrosarcoma cells. *Oncogene* 2007; **26**:4124-4134.
191. **Marcato, P., Shmulevitz, M., Pan, D., et al.** Ras transformation mediates reovirus oncolysis by enhancing virus uncoating, particle infectivity, and apoptosis-dependent release. *Mol. Ther.* 2007; **15**:1522-1530.
192. **Organ, E.L., Sheng, J., Ruley, H.E., and Rubin, D.H.** Discovery of mammalian genes that participate in virus infection. *BMC. Cell Biol.* 2004; **5**:41.
193. **Sheng, J., Organ, E.L., Hao, C., et al.** Mutations in the IGF-II pathway that confer resistance to lytic reovirus infection. *BMC. Cell Biol.* 2004; **5**:32.
194. **Roner, M.R. and Mutsoli, C.** The use of monoreassortants and reverse genetics to map reovirus lysis of a ras-transformed cell line. *J. Virol. Methods* 2007; **139**:132-142.
195. Oncolytics Biotech Inc. Clinical Trials. <http://www.oncolyticsbiotech.com/clinical.html>. 23-5-2011.
Ref Type: Online Source
196. **Lal, R., Harris, D., Postel-Vinay, S., and de, B.J.** Reovirus: Rationale and clinical trial update. *Curr. Opin. Mol. Ther.* 2009; **11**:532-539.
197. **van Houdt, W.J., Smakman, N., van den Wollenberg, D.J., et al.** Transient infection of freshly isolated human colorectal tumor cells by reovirus T3D intermediate subviral particles. *Cancer Gene Ther.* 2008; **15**:284-292.
198. **Marcato, P., Dean, C.A., Giacomantonio, C.A., and Lee, P.W.** Oncolytic reovirus effectively targets breast cancer stem cells. *Mol. Ther.* 2009; **17**:972-979.
199. **Naik, M.U., Naik, T.U., Suckow, A.T., et al.** Attenuation of junctional adhesion molecule-A is a contributing factor for breast cancer cell invasion. *Cancer Res.* 2008; **68**:2194-2203.
200. **Gutwein, P., Schramme, A., Voss, B., et al.** Downregulation of junctional adhesion molecule-A is involved in the progression of clear cell renal cell carcinoma. *Biochem. Biophys. Res. Commun.* 2009; **380**:387-391.
201. **Koshiha, H., Hosokawa, K., Kubo, A., et al.** Junctional adhesion molecule: an expression in human endometrial carcinoma. *Int. J. Gynecol. Cancer* 2009; **19**:208-213.
202. **McSherry, E.A., McGee, S.F., Jirstrom, K., et al.** JAM-A expression positively correlates with poor prognosis in breast cancer patients. *Int. J. Cancer* 2009; **125**:1343-1351.
203. **Bergeron, J., Mabrouk, T., Garzon, S., and Lemay, G.** Characterization of the thermosensitive ts453 reovirus mutant: increased dsRNA binding of sigma 3 protein correlates with interferon resistance. *Virology* 1998; **246**:199-210.
204. **Rudd, P. and Lemay, G.** Correlation between interferon sensitivity of reovirus isolates and ability to discriminate between normal and Ras-transformed cells. *J. Gen. Virol.* 2005; **86**:1489-1497.
205. **Stehle, T. and Dermody, T.S.** Structural evidence for common functions and ancestry of the reovirus and adenovirus attachment proteins. *Rev. Med. Virol.* 2003; **13**:123-132.
206. **Arnberg, N.** Adenovirus receptors: implications for tropism, treatment and targeting. *Rev. Med. Virol.* 2009; **19**:165-178.
207. **Lindholm, L., Henning, P., and Magnusson, M.K.** Novel strategies in tailoring human adenoviruses into therapeutic cancer gene-therapy vectors. *Future Virol* 2008; **3**:45-59.


208. **Waehler, R., Russell, S.J., and Curiel, D.T.** Engineering targeted viral vectors for gene therapy. *Nat.Rev.Genet.* 2007; **8**:573-587.
209. **Dmitriev, I., Krasnykh, V., Miller, C.R., et al.** An adenovirus vector with genetically modified fibers demonstrates expanded tropism via utilization of a coxsackievirus and adenovirus receptor-independent cell entry mechanism. *J.Virol.* 1998; **72**:9706-9713.
210. **Kuppen, P.J., van der Eb, M.M., Jonges, L.E., et al.** Tumor structure and extracellular matrix as a possible barrier for therapeutic approaches using immune cells or adenoviruses in colorectal cancer. *Histochem.Cell Biol.* 2001; **115**:67-72.
211. **Mok, W., Boucher, Y., and Jain, R.K.** Matrix metalloproteinases-1 and -8 improve the distribution and efficacy of an oncolytic virus. *Cancer Res.* 2007; **67**:10664-10668.
212. **Power, A.T. and Bell, J.C.** Taming the Trojan horse: optimizing dynamic carrier cell/oncolytic virus systems for cancer biotherapy. *Gene Ther.* 2008; **15**:772-779.
213. **Ilett, E.J., Prestwich, R.J., Kottke, T., et al.** Dendritic cells and T cells deliver oncolytic reovirus for tumour killing despite pre-existing anti-viral immunity. *Gene Ther.* 2009; **16**:689-699.
214. **Power, A.T., Wang, J., Falls, T.J., et al.** Carrier cell-based delivery of an oncolytic virus circumvents antiviral immunity. *Mol.Ther.* 2007; **15**:123-130.
215. **Lobo, N.A., Shimono, Y., Qian, D., and Clarke, M.F.** The biology of cancer stem cells. *Annu.Rev.Cell Dev.Biol.* 2007; **23**:675-699.
216. **Dick, J.E.** Stem cell concepts renew cancer research. *Blood* 2008; **112**:4793-4807.
217. **Visvader, J.E. and Lindeman, G.J.** Cancer stem cells in solid tumours: accumulating evidence and unresolved questions. *Nat.Rev.Cancer* 2008; **8**:755-768.
218. **Bryson, J.S. and Cox, D.C.** Characteristics of reovirus-mediated chemoimmunotherapy of murine L1210 leukemia. *Cancer Immunol.Immunother.* 1988; **26**:132-138.
219. **Twigger, K., Vidal, L., White, C.L., et al.** Enhanced *in vitro* and *in vivo* cytotoxicity of combined reovirus and radiotherapy. *Clin.Cancer Res.* 2008; **14**:912-923.
220. **Sei, S., Mussio, J.K., Yang, Q.E., et al.** Synergistic antitumor activity of oncolytic reovirus and chemotherapeutic agents in non-small cell lung cancer cells. *Mol.Cancer* 2009; **8**:47.
221. **Chappell, J.D., Prota, A.E., Dermody, T.S., and Stehle, T.** Crystal structure of reovirus attachment protein sigma1 reveals evolutionary relationship to adenovirus fiber. *EMBO J.* 2002; **21**:1-11.
222. **Qiao, J., Wang, H., Kottke, T., et al.** Cyclophosphamide facilitates antitumor efficacy against subcutaneous tumors following intravenous delivery of reovirus. *Clin.Cancer Res.* 2008; **14**:259-269.
223. **Smakman, N., van der Bilt, J.D., van den Wollenberg, D.J., et al.** Immunosuppression promotes reovirus therapy of colorectal liver metastases. *Cancer Gene Ther.* 2006; **13**:815-818.
224. **Loken, S.D., Norman, K., Hirasawa, K., et al.** Morbidity in immunosuppressed (SCID/NOD) mice treated with reovirus (dearing 3) as an anti-cancer biotherapeutic. *Cancer Biol.Ther.* 2004; **3**:734-738.
225. **Kim, M., Chung, Y.H., and Johnston, R.N.** Reovirus and tumor oncolysis. *J.Microbiol.* 2007; **45**:187-192.

-
226. **Prestwich, R.J., Ilett, E.J., Errington, F., et al.** Immune-mediated antitumor activity of reovirus is required for therapy and is independent of direct viral oncolysis and replication. *Clin.Cancer Res.* 2009; **15**:4374-4381.
 227. **Cattaneo, R., Miest, T., Shashkova, E.V., and Barry, M.A.** Reprogrammed viruses as cancer therapeutics: targeted, armed and shielded. *Nat.Rev.Microbiol.* 2008; **6**:529-540.
 228. **Cawood, R., Chen, H.H., Carroll, F., et al.** Use of tissue-specific microRNA to control pathology of wild-type adenovirus without attenuation of its ability to kill cancer cells. *PLoS.Pathog.* 2009; **5**:e1000440.
 229. **Ylosmaki, E., Hakkarainen, T., Hemminki, A., et al.** Generation of a conditionally replicating adenovirus based on targeted destruction of E1A mRNA by a cell type-specific MicroRNA. *J.Virol.* 2008; **82**:11009-11015.
 230. **Kobayashi, T., Chappell, J.D., Danthi, P., and Dermody, T.S.** Gene-specific inhibition of reovirus replication by RNA interference. *J.Virol.* 2006; **80**:9053-9063.



CHAPTER 4

ENHANCED TRANSDUCTION OF CAR-NEGATIVE CELLS BY PROTEIN IX-GENE DELETED ADENOVIRUS 5 VECTORS



J. de Vrij
S.K. van den Hengel
T.G. Uil
D. Koppers-Lalic
I.J.C. Dautzenberg
O.M.J.A. Stassen
M. Bárcena
M. Yamamoto
C.M.A. de Ridder
R. Kraaij
K.M. Kwappenberg
M.W. Schilham
R.C. Hoeben

Virology (2011) **410**: 192–200.

INTRODUCTION

Protein IX is a non-essential protein in the capsid of human adenoviruses (HAdV). The protein has a size of 14.3 kDa, is present at 240 copies per virion, and has three highly conserved regions present in the amino (N) terminus, the central part (alanine-rich), and the carboxy (C) terminus (leucine-rich). The location and function of protein IX in the virus capsid has been the subject of investigation and debate for many years [1]. Recent work by different groups has brought consensus on its location and topology in the capsid [2,3]. The N-terminus of the protein is located in between hexon cavities of the groups of nine (GON) hexons, presumably stabilizing the GONs. The C-terminus of the protein forms an alpha-helix and is exposed on the capsid surface in close contact with hexon hypervariable region 4 (HVR4) [3]. C-terminal domains of three protein IX molecules associate in a parallel orientation, whereas a fourth domain binds in an antiparallel orientation [2]. The role of protein IX in the capsid remains enigmatic. *In vitro* analysis revealed the N-terminus of protein IX to confer a thermostable phenotype on HAdV-5 capsids [4]. Propagation of protein IX gene deleted HAdV-5 in cell culture yields wild-type like virus titers, demonstrating that protein IX is dispensable for virus replication *in vitro*.

Protein IX has potential as an anchor for the attachment of different types of polypeptides to the viral capsid. Targeting of HAdV-5 to tumor cells has been achieved by genetically fusing protein IX to a single-chain T cell receptor directed against MHC class I in complex with MAGE-A1 peptides [5]. Similarly, integrin-binding Arg-Gly-Asp (RGD) peptides, as well as single-chain antibody fragments have been incorporated in this way [6,7]. Alternatively, targeting ligands can be coupled to protein IX via the genetic inclusion of cysteine residues and subsequent chemical coupling of ligands to the reactive thiol groups [8]. Multiple polypeptides can be incorporated simultaneously [9]. A triple-mosaic HAdV-5 vector was developed with a poly-lysine motif, the herpes simplex virus type 1 (HSV-1) thymidine kinase, and the monomeric red fluorescent protein fused with protein IX, thereby combining targeting, therapeutic, and imaging modalities. Recently, it was demonstrated that HAdV-5 vaccine vectors with pathogen-specific antigens fused to protein IX can stimulate robust protective immune responses in animals, suggesting a new route for the development of improved HAdV-5 based recombinant vaccines [10,11].

Here we report on the enhanced delivery of transgenes into CAR-negative cell lines as a result of protein IX-gene deletion from a HAdV-5-based vector. Furthermore, the protein IX-deficient particles demonstrated enhanced activation of peripheral blood mononuclear cells (PBMCs), and had a different

in vivo distribution after intravenous delivery in a mouse model. The exact molecular mechanism behind this 'ΔpIX effect' remains to be delineated. Our data suggest that protein IX can affect the cell tropism of HAdV-5, and may function to dampen the innate immune responses against HAdV particles.

MATERIALS AND METHODS

Cell lines

All cell lines were maintained as monolayers at 37°C in a humidified atmosphere of 5% CO₂. The human cell lines HeLa (cervical cancer), A549 (carcinomic alveolar epithelium), MEL2A (melanoma), MZ2-MEL3.0 (melanoma) [5], VH10 (primary foreskin fibroblasts) [12], HepG2 (hepatocellular carcinoma), and 911 cells (HAdV-5 E1-transformed human embryonic retinoblasts) [13] were maintained in Dulbecco's Modified Eagle's Medium (DMEM) (Gibco-BRL, Breda, The Netherlands) supplemented with 8% fetal bovine serum (FBS) (Gibco-BRL, Breda, The Netherlands) and penicillin–streptomycin mixture.

Lentivirus transduction was used to create a MZ2-MEL3.0 cell line stably expressing human CAR. To this end, the CAR gene was PCR-amplified by using primers 1 and 2 (table 4.1) from plasmid pCMV_hCAR (kindly provided by Dr. J.M. Bergelson [14]). The *Pst*I + *Nhe*I digested PCR product was ligated in between the corresponding restriction sites of pLV.CMV.IRES.PURO [15], resulting in pLV.CMV.CAR.IRES.PURO. The virus LV.CMV.CAR.IRES.PURO was produced by a previously described procedure involving cotransfection of pLV.CMV.CAR.IRES.PURO together with 'helper' plasmids encoding HIV-1 gag-pol, HIV-1 rev, and the VSV-G envelope [16]. The methods for determining the titer of the LV.CMV.CAR.IRES.PURO vector stock and the procedures for transduction of the MZ2-MEL3.0 cells have been described before [15]. Selection for antibiotic resistance was achieved by seeding the cells in medium with 0.6 μg/ml puromycin (MP Biomedicals, Amsterdam, The Netherlands).

Viruses

The vectors HAdV-5.CMV.GFP/LUC (Vellinga *et al.*, 2006) (Ad5ΔE1+pIX) and HAdV-5ΔpIX.CMV.GFP/LUC [17] (Ad5ΔE1ΔpIX) contain a green fluorescent protein (GFP) gene as well as a firefly luciferase (LUC) gene, which are both driven by a human cytomegalovirus (CMV) promoter. The vector HAdV-5pIXΔ100-114.CMV.LUC (Ad5ΔE1pIX^{ΔLEU}), encoding LUC only, was described previously as well [4]. Titration of the vector stocks was performed by a PicoGreen-DNA binding assay to determine the concentration in physical vector particles per ml (pp/ml)

[18]. A standard agar overlay plaque assay on 911 cells was used to determine the infectious virus concentration in plaque forming units per ml (pfu/ml) [13]. The pp/pfu ratios of the three vectors were very similar, within the range of 10 to 12.

The replication-competent viruses HAdV-5.ΔE3.ADP.eGFP (Ad5+pIX) and HAdV-5.ΔE3.ADP.eGFP.ΔpIX (Ad5ΔpIX) were constructed by recombination of the shuttle plasmids pShuttle+E1+pIX (pSh+pIX) and pShuttle+E1ΔpIX (pShΔpIX) with a HAdV-5 backbone plasmid containing the eGFP gene in the E3 region (pBB). The plasmids pSh+pIX, pShΔpIX and pBB were constructed as follows. The wild-type HAdV-5 *BsrGI*–*MfeI* fragment containing the E1 genes (nucleotides 193–3925) was isolated from pTG3602 (kindly provided by Dr. M. Luski, Transgene, Strasbourg, France), and cloned into the *BsrGI*–*MfeI* digested pTrackCMV-GFP/LUC [17], thereby replacing the GFP/LUC genes with the HAdV-5 E1 region. By using site-directed mutagenesis (QuikChange site-directed mutagenesis kit; Stratagene) (primers 3, 4, 5, 6 (table 4.1)) two restriction sites were introduced in the protein IX gene; a *Scal* site at the start codon of protein IX and a *SpeI* site upstream of the protein IX stop codon, thereby creating pShuttle+E1+pIX^{Scal/SpeI}. Next, the pShΔpIX plasmid was constructed by *Scal/SpeI* digestion and re-ligation of the protein IX-gene-deleted fragment. The pSh+pIX plasmid was created by introducing the protein IX sequence (amplified from pAd5pIX [6] by using primers 7 and 8 (table 4.1)) into the *Scal/SpeI* linearized pShuttle+E1+pIX^{Scal/SpeI}. The *Scal*-site was restored to the wild-type HAdV-5 sequence by exchanging the *Scal*-overlapping *MfeI/HindIII* fragment with the corresponding fragment from pTG3602. The *SpeI* site and the downstream 'pIX-remainder sequence' were left intact, since part of this sequence forms a hairpin-loop structure situated over the polyA site of the E1B transcript, which might be essential for efficient polymerase slippage needed for polyadenylation [19].

Table 4.1 Oligonucleotide used in the cloning procedure

	Name	Sequence 5'-3'
1	FWD CAR_ <i>PstI</i>	5'-GATGTACTGCAGATGGCGCTCCTGCTGTG-3'
2	REV CAR_ <i>NheI</i>	5'-CGACGCTAGCTATACTATAGACCCATCCTTGCTCTG-3'
3	FWD <i>Scal</i> _correct	5'-TTGCAGCAGCCGCCGCCAGTACTAGCACCAACTCGTTTGATGG-3'
4	REV <i>Scal</i> _correct	5'-CCATCAAACGAGTTGGTGCTAGTACTGGCGCGCGGCTGCTGCAA-3'
5	FWD <i>SpeI</i> _correct	5'-GGTTTCTGCCCTGAAGGCTTACTAGTCTCCCAATGCGGTTTAAAC-3'
6	REV <i>SpeI</i> _correct	5'-GTTTTAAACCGCATTGGGAGACTAGTAAGCCTTCAGGGCAGAAACC-3'
7	FWD pIX_ <i>Scal</i>	5'-CGCGGAAGTACTATGAGCACCAACTCGTTTGATGG-3'
8	REV pIX_ <i>SpeI</i>	5'-CGCACTAGTTTAAACCGCATTGGGAGGGGAGG-3'

The pBB backbone plasmid was constructed by replacing the E3-lacking *SpeI*–*PacI* fragment (nucleotides 27238–33443) of pAdEasy-1 [20] with the corresponding *SpeI*–*PacI* fragment of pShuttle- Δ E3-ADP-EGFP-F2 [21], thereby introducing eGFP in the E3 region under control of the viral major late promoter. The coding sequence for the E3 Adenovirus Death Protein (ADP) was retained. The kanamycin resistance gene (inserted with the pShuttle- Δ E3-ADP-EGFP-F2 fragment) was removed by *ClaI* digestion and re-ligation of the two largest fragments.

Recombination of pBB with pSh+pIX and pSh Δ pIX in *E. coli* and subsequent virus rescue in A549 cells were performed as described elsewhere [20]. Virus was purified by a standard double cesium chloride gradient protocol, dialyzed against sucrose buffer (5% sucrose, 140 mM NaCl, 5 mM Na₂HPO₄·2H₂O, 1.5 mM KH₂PO₄) and stored at -80°C. The virus titer was determined by the PicoGreen-DNA binding assay [18] (for pp/ml measurement), and a plaque assay on A549 cells [13] (for pfu/ml measurement). For analysis of virus spread, GFP-positive plaques were photographed (Olympus Camedia Digital Camera C-3030, installed on an Olympus CK40 microscope) and the plaque size was determined in arbitrary units (Olympus DP-soft v.5.0 Soft imaging System software). The median plaque size of Ad5 Δ pIX was normalized to the plaque size for Ad5+pIX.

Analysis of CAR presentation on the cell surface

Flow cytometry was performed to determine the levels of CAR presentation on the cell surface. Cells in suspension (in PBS with 0.5% bovine serum albumin and 0.02% sodium azide) were incubated with mouse monoclonal anti-CAR antibody (clone RmcB, Upstate Biotechnology, Lake Placid, NY, diluted 1:1000) for 30 min on ice, followed by incubation with phycoerythrin (PE)-conjugated rabbit-anti-mouse secondary antibody (Caltac Laboratories, Burlingame, CA, USA) for 30 min on ice. Flow cytometry data were analyzed with CellQuest software (Becton Dickinson).

Immunohistochemistry was performed on the cell line MZ2-MEL3.0/CAR. After washing with phosphate-buffered saline (PBS), the cells were fixed in acetone/methanol (1:1) for 10 min at room temperature. Staining was performed with the anti-CAR antibody (clone RmcB, Upstate Biotechnology, Lake Placid, NY, diluted 1:500). Fluorescein isothiocyanate (FITC)-conjugated rabbit-anti-mouse antibody (Jackson ImmunoResearch, France) was used as secondary antibody.

Virus transduction assays

Luciferase expression

The transduction efficiency of CAR-positive (HeLa, A549, MEL2A, MZ2-MEL3.0/ CAR) and CAR-negative (MZ2-MEL3.0, VH10) cell lines by Ad5 Δ E1+pIX and Ad5 Δ E1 Δ pIX was compared by measuring luciferase expression. Transduction was performed in triplicate in 24-well plate wells in 500 μ l DMEM/8% FBS. After a two-hr incubation the virus-containing medium was replaced with fresh medium without virus. At 24 hrs post transduction the cells were washed once with PBS and lysed in 100 μ l LUC-lysis mix (25 mM Tris-phosphate (pH 7.8), 2 mM CDTA, 2 mM DTT, 10% glycerol and 1% Triton-X in PBS). Luciferase production was determined with the Promega Luciferase Assay by adding 25 μ l luciferase assay reagent to 10 μ l lysate. Light intensity measurement was performed in a Victor Wallac 2 microplate reader (PerkinElmer, Inc., Waltham, MA, USA).

4

Integrin blocking

Indirect blocking of integrin-mediated virus uptake was performed by incubating cells with EDTA. MZ2-MEL3.0 cells were harvested from semi-confluent tissue culture plates, washed three times in PBS with 5 mM EDTA, and resuspended in standard PBS or PBS supplemented with 0.9 mM CaCl₂ and 0.5 mM MgCl₂ (PBS⁺⁺). The Ad5 Δ E1+pIX and Ad5 Δ E1 Δ pIX stocks were adjusted to equal pp concentrations by adding sucrose buffer and were diluted 1:1 in a 5 mM EDTA solution in PBS. Virus (100 pp/cell) was added to 5x10⁵ cells in 1 ml PBS or PBS⁺⁺ and incubation was performed for 60 min at 37°C under constant agitation. Subsequently, the cells were pelleted by centrifugation, dissolved in 5 ml medium and transferred to 24-well plate wells (500 μ l per well). Cells were incubated for 24 hrs and analyzed for GFP expression by flow cytometry. Data were analyzed with CellQuest software (Becton Dickinson).

The anti-human CD51/61 monoclonal antibody (MAb LM609), an $\alpha_v\beta_3$ integrin antagonist, and MAb P1F6, an $\alpha_v\beta_5$ integrin antagonist (both obtained from Millipore) were used to test the inhibitory effect of anti-integrin antibodies on virus transduction. Cells grown as monolayers were pre-incubated with medium only or with medium containing integrin function-blocking MAbs (10 mg/ml). After 30 min of incubation, the excess antibody was removed by gentle washing followed by virus transduction (100 pp/cell). Reporter gene expression was measured 24 hrs post transduction by performing a standard luciferase assay.

Virus incubation with coagulation factor X

HepG2 and A549 cells were plated in 24-well plate wells. After a PBS wash step, Ad5ΔE1+pIX or Ad5ΔE1ΔpIX (100 pp/cell) was added in serum-free medium containing 8 μg/ml factor X (FX) (HCX-0050, Haematologic Technologies Inc.), 8 μg/ml Gla-domainless factor X (FX^{MUT}) (HCX-GD, Haematologic Technologies Inc.) or no FX/FX^{MUT}. After 2 hrs the medium was replaced by normal medium. Luciferase expression was measured 24 hrs post transduction.

Immunoblot analysis and electron microscopy

Immunoblot analyses were performed to assess the incorporation of proteins into the capsid of Ad5ΔE1+pIX and Ad5ΔE1ΔpIX. The western blotting and detection procedures were described previously [5]. Virus lysates were prepared by adding 5×10^9 virus particles directly to western sample buffer. Capsid proteins were visualized with rabbit polyclonal anti-protein IX serum (1:2000) [22] goat polyclonal anti-hexon (1:1000, ab19998, Abcam, Cambridge, UK), and mouse monoclonal anti-fiber (1:5000, 4D2, Abcam) [23]. Secondary antibodies were horseradish peroxidase (HRP)-conjugated goat-anti-rabbit and rabbit-anti-mouse (Santa Cruz Biotechnology, Inc., Santa Cruz, CA, USA).

Electron microscopy was performed on Ad5ΔE1+pIX and Ad5ΔE1ΔpIX samples adsorbed into glow-discharged carbon coated copper grids and negatively stained for 30 sec with 2% phosphotungstic acid (pH 7). The viruses were examined with a FEI Tecnai Spirit BioTwin transmission electron microscope operating at 120 kV. Images were recorded on a 4k × 4k Eagle CCD camera.

PBMC analysis

Buffy coats were obtained from healthy donors after consent (Sanquin Bloodbank, Leiden, The Netherlands) and centrifuged on a Ficoll gradient to obtain PBMC. PBMC (1×10^6) were added to a well of a 24-well plate in 0.5 ml medium (RPMI/10% FCS) and virus was added at the indicated MOI in 0.5 ml medium. After incubation at 37°C and 5% CO₂ for two days, the supernatants were isolated for interferon gamma (IFN-γ) measurement, and the cells were prepared for flow cytometry analysis. Cells were washed twice with PBS/0.02% sodium azide, fixed for 10 min in 4% paraformaldehyde, washed twice with PBS/0.5% BSA/0.02 sodium azide, and stained with antibodies. Antibodies used were anti-CD3-PerCP-Cy5.5, anti-CD4-PE, anti-CD14-APC, anti-CD14-PerCP-Cy5.5, anti-CD19-PE, anti-CD19-PerCP-Cy5.5, anti-CD69-PE and anti-CD86-PE (Becton Dickinson, Franklin Lakes, NJ, USA), anti-CD8-APC and anti-CD56-APC (Beckman Coulter, Brea, CA, USA). Activation of NK cells was evaluated

as increased CD69 expression on CD3⁻, CD14⁻, CD19⁻, CD56⁺ cells. Monocyte activation was analyzed as increased CD86 expression on CD3⁻, CD19⁻, CD14⁺ cells. Fluorescence was measured by flow cytometry on a FACS Calibur (Becton Dickinson) and data were analyzed with CellQuest software (Becton Dickinson). IFN- γ in supernatants was measured by ELISA using the PeliPair reagent set for human IFN- γ (Sanquin, Amsterdam, NL).

Viral distribution after intravenous delivery

Ad5 Δ E1+pIX or Ad5 Δ E1 Δ pIX (10^9 pp) was injected in the tail vein of 6-week-old athymic nude mice (NMRI nu/nu; Taconic M&B A/S, Ry, Denmark), followed by sacrificing the animals and harvesting of multiple organs at 3 days post injection. Four hrs before Ad5 Δ E1+pIX and Ad5 Δ E1 Δ pIX injection, pre-dosing was performed with the empty vector HAdV-5.CMV (replication-deficient and not encoding a transgene) (5×10^{10} pp) to saturate Kupffer cell macrophages. Tissue samples from each organ were lysed in LUC-lysis mix and the luciferase expression was measured according to the Promega Luciferase Assay. The protein concentration in the lysates was determined by using the bicinchoninic acid protein assay (Pierce, Perbio Science BV, Etten-Leur, The Netherlands), enabling the calculation of luciferase expression per total protein. The experiment was performed under the Dutch Experiments on Animals Act that serves the implementation of "Guidelines on the protection of experimental animals" by the Council of Europe (1986), Directive 86/609/EC, and only after a positive recommendation by the Animal Experiments Committee.

4

RESULTS

Enhanced transgene expression in CAR-negative cells with Ad5 Δ E1 Δ pIX

To study the role of protein IX in the HAdV-5 transduction of cells, we compared the vectors Ad5 Δ E1+pIX and Ad5 Δ E1 Δ pIX for luciferase transgene expression in a panel of cell lines (figure 4.1 A). Cell lines with varying expression levels of CAR were included (figure 4.1 B). Whereas similar expression levels were obtained with both vectors in the CAR-positive cell lines HeLa, A549, and MEL2A, the vector Ad5 Δ E1 Δ pIX yielded higher levels than Ad5 Δ E1+pIX in the CAR-negative cell lines MZ2-MEL3.0 and VH10. Since these results suggested a specific role of the protein IX lacking vector in mediating relatively higher transduction in the absence of CAR, Ad5 Δ E1+pIX and Ad5 Δ E1 Δ pIX were analyzed for reporter gene expression in MZ2-MEL3.0 cells versus MZ2-MEL3.0/CAR cells (figure

4.2 B). MZ2-MEL3.0/ CAR cells stably expressed CAR via transduction with a recombinant lentivirus, which was confirmed by flow cytometry and immune fluorescence staining (figure 4.2 A). In MZ2-MEL3.0 cells the reporter gene expression upon infection with Ad5ΔE1ΔpIX was found to be ten-fold increased compared to infection with Ad5ΔE1+pIX, while in MZ2-MEL3.0/CAR cells the difference was a mere two-fold (figure 4.2 B). The enhanced transgene expression for Ad5ΔE1ΔpIX on the CAR-negative cell line MZ2-MEL3.0 appeared to be not affected by the establishment of protein IX expression in the cells (by using the recombinant lentivirus LV-CMV-pIX-IRES-NPTII [17] prior to the transduction) (result not shown).

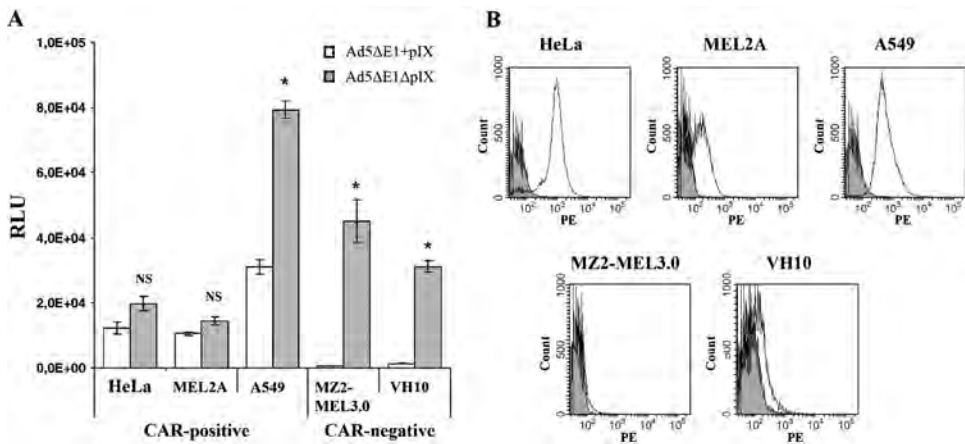


Figure 4.1 (A) Transduction of CAR-positive and CAR-negative cells with the replication-deficient vectors Ad5ΔE1+pIX and Ad5ΔE1ΔpIX. At 24 h post transduction (at 10 pp/cell) the luciferase expression was measured as indicated by the relative luciferase units (RLU) (NS signifies Not Significant, * $p < 0.02$ versus Ad5ΔE1+pIX). Error bars represent SEM ($n = 3$). **(B)** Flow cytometry with anti-CAR antibody and PE-labeled secondary antibody to analyze cell surface expression level of CAR (white histograms). The gray histograms represent incubation with secondary antibody only.

As a next step, the involvement of the C-terminal region of protein IX in the observed phenomenon was investigated. This domain, which is rich in leucine amino acids and is exposed on the HAΔV-5 capsid as an alpha-helical structure [2,3], is highly conserved in human adenoviruses. The biological function of this conserved domain of protein IX is unknown. We analyzed the vector Ad5ΔE1pIX^{ΔLEU}, which lacks a major part of the C-terminal region of protein IX (amino acids 100 to 114) for reporter gene expression in MZ2-MEL3.0 and MZ2-MEL3.0/CAR. Ad5ΔE1pIX^{ΔLEU} demonstrated enhanced transduction of the CAR-negative cell line, very similar to the Ad5ΔE1ΔpIX vector (figure 4.2 C).

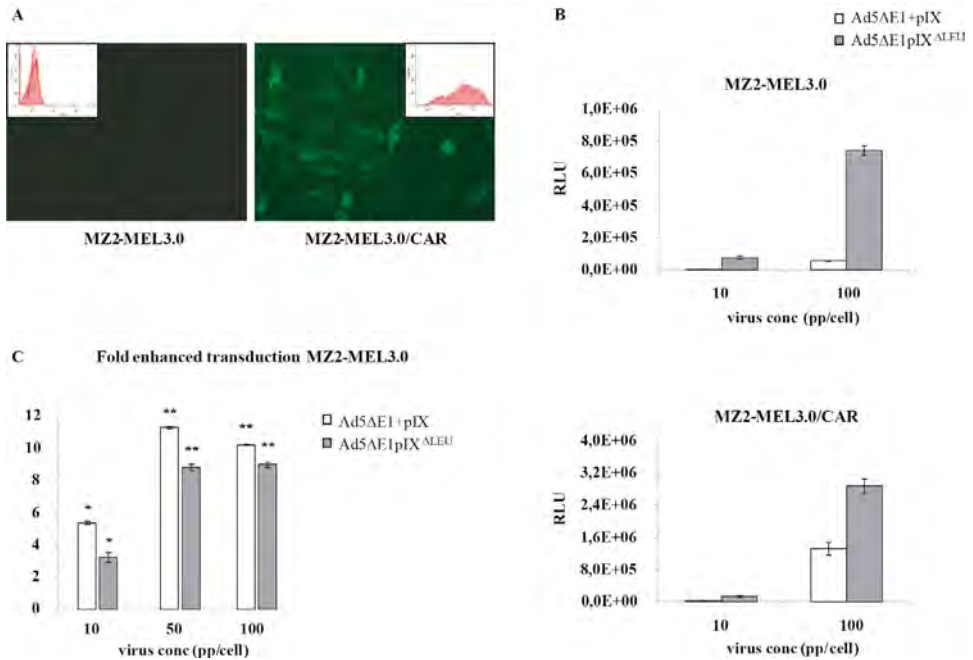


Figure 4.2 Transduction assays on MZ2-MEL3.0 and MZ2-MEL3.0/CAR. (A) Detection of CAR expression in MZ2-MEL3.0 cells by immune-fluorescence staining with anti-CAR antibody and FITC-labeled secondary antibody. The insets represent flow cytometry histograms after staining with anti-CAR antibody and PE-labeled secondary antibody. (B) Luciferase expression in MZ2-MEL3.0 and MZ2-MEL3.0/CAR after Ad5ΔE1+pIX and Ad5ΔE1ΔpIX transduction. Error bars represent SEM (n=3). (C) Fold enhancement of MZ2-MEL3.0 transduction with Ad5ΔE1ΔpIX and Ad5ΔE1pIXΔLEU as compared to the transduction with Ad5ΔE1+pIX. The fold enhancements are normalized to the vector transduction ratios on MZ2-MEL3.0/CAR (*p<0.05, **p<0.005 versus Ad5ΔE1+pIX). Error bars represent SEM (n=3).

To assess the appearance of the vector particles and to check for the absence of microaggregation, electron microscopy was performed on Ad5ΔE1+pIX and Ad5ΔE1ΔpIX vector batches. This showed identically shaped virus particles (figure 4.3 A). No signs of microaggregation were observed. The Ad5ΔE1ΔpIX stock appeared to contain more small particulate matter, possibly virus debris. As previously described, pIX-deficient HAdV-5 particles have an enhanced tendency to partly dissociate into fiber- and penton base- lacking particles [24]. However, our vectors had similar capsid incorporation levels of fiber and hexon proteins, as evident from immunoblot analyses (figure 4.3 B), thus ruling out differences in particle dissociation for the vector preparations.

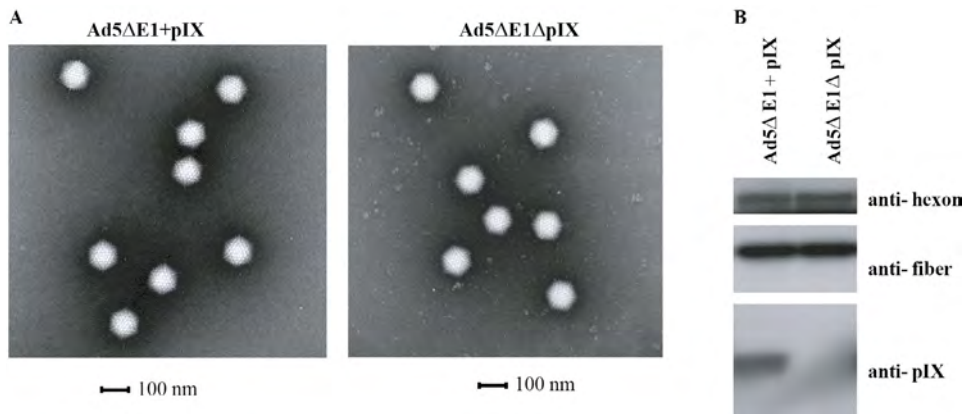


Figure 4.3 (A) Electron microscopy on Ad5ΔE1+pIX and Ad5ΔE1ΔpIX samples with negative staining of the vector particles in phosphotungstic acid. **(B)** Immunoblot detection on Ad5ΔE1+pIX and Ad5ΔE1ΔpIX lysates to analyze capsid incorporation levels of protein IX, hexon, and fiber proteins.

Transduction with Ad5ΔE1ΔpIX is integrin-dependent

Wild-type HAdV-5 enters cells via high affinity binding of the fiber knob domain to CAR [14]. Subsequently low affinity interaction of the penton base with cellular integrins $\alpha_v\beta_3$ and $\alpha_v\beta_5$ promotes virus internalization in clathrin coated pits [25,26]. To answer the question if Ad5ΔE1ΔpIX still uses integrins for cellular uptake, we analyzed Ad5ΔE1+pIX and Ad5ΔE1ΔpIX for transgene expression (GFP) in the presence or absence of bivalent cations, which are necessary for integrin-mediated uptake of wild-type HAdV-5 into cells [26] (figure 4.4 A). This experiment again displayed a stronger reporter gene expression of Ad5ΔE1ΔpIX in MZ2-MEL3.0 cells compared to Ad5ΔE1+pIX. For both vectors the transduction appeared to be totally dependent on the presence of bivalent cations, with a complete reduction to background GFP levels for the cation-negative incubation. This is consistent with integrin-mediated uptake for both vectors. More specifically, the integrin-dependency of Ad5ΔE1ΔpIX was confirmed by a small but significant (approximately two-fold) decrease in transduction after incubation of MZ2-MEL3.0 cells with antibodies directed against $\alpha_v\beta_3$ and $\alpha_v\beta_5$ integrins (figure 4.4 B). Similar antibody-blocking (1.5-fold reduced transduction for anti- $\alpha_v\beta_3$ and anti- $\alpha_v\beta_5$) was observed for Ad5ΔE1+pIX. Incubating the cells with higher concentrations of antibodies did not result in further reductions in transduction levels (data not shown). Anti-integrin mediated blocking of transduction was also observed on A549 cells (figure 4.4 B). From these data we conclude that the vector Ad5ΔE1ΔpIX still uses integrins for cell internalization in CAR-deficient cells.

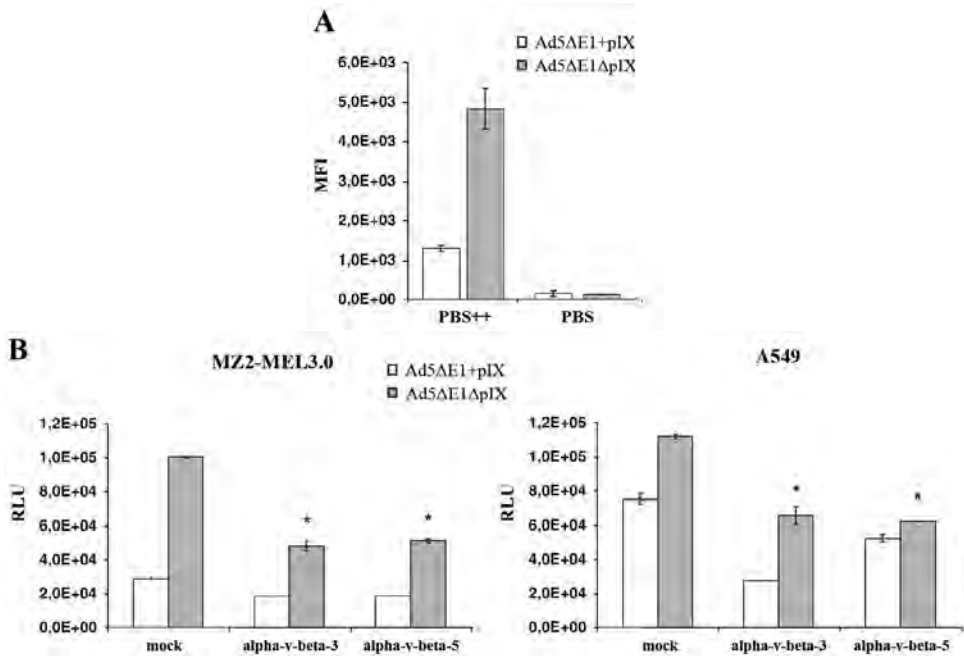


Figure 4.4 The effect of integrin blocking on transduction of cells with **Ad5ΔE1+pIX** and **Ad5ΔE1ΔpIX**. **(A)** MZ2-MEL3.0 cells were treated with EDTA to remove bivalent cations necessary for HAdV-5 interaction with integrins. Subsequent transduction was performed in the presence (PBS⁺⁺) or absence (PBS) of bivalent cations and GFP expression was measured, as indicated by the mean fluorescence intensity (MFI). Error bars represent SEM (n = 3). **(B)** Vector mediated luciferase expression in MZ2-MEL3.0 and A549 cells in the presence or absence of antibodies directed against $\alpha_v\beta_3$ or $\alpha_v\beta_5$ integrins in the infection medium (*p<0.05 versus control treatment). Error bars represent SEM (n = 3).

Reduced virus spread of the replication-competent virus **Ad5ΔpIX**

Our data from the comparative transduction analysis suggest an alternative interaction of HAdV-5 particles lacking protein IX with the cell surface. In parallel to cell tropism extending capsid modifications described for other viruses [27], it is likely that protein IX deletion from a replication-competent HAdV-5 virus would result in a modified ability to spread in monolayer cell cultures. To investigate this, we constructed the replication-competent HAdV-5 viruses Ad5+pIX and Ad5ΔpIX. Both viruses expressed GFP, allowing accurate measurement of plaque size. On A549 cells the plaque size for the Ad5ΔpIX virus (median 30 arbitrary surface units (ASU), range 20–170) appeared to be significantly smaller than

the plaque size for Ad5+E1+pIX (median 100 ASU, range 30–290). A similar difference in plaque size was observed on the CAR-negative cell line VH10, with Ad5ΔpIX (median 50 ASU, range 30–150) yielding much smaller plaques compared to Ad5+pIX (median 100 ASU, range 75–280). From these analyses we conclude that protein IX-gene deletion from the genome of the replication-competent virus results in a decrease in virus spread in CAR-positive (A549) as well as CAR-negative (VH10) monolayer cell cultures.

Enhanced activation of peripheral blood mononuclear cells by Ad5ΔE1ΔpIX

Our findings on the modified transduction characteristics of protein IX-deficient HAdV-5 vectors are of relevance for: (i) fundamental adeno-virology (as the findings point towards a novel biological function of protein IX), and (ii) the development of protein IX-modified HAdV-5 vectors for gene therapies. For both these aspects, it will be highly interesting to determine the effect of protein IX-deletion on the interaction of HAdV-5 vectors with white blood cells. Therefore, we incubated freshly isolated human peripheral blood mononuclear cells with Ad5ΔE1+pIX and Ad5ΔE1ΔpIX, and analyzed GFP expression and the expression of cellular activation markers. This revealed relatively high levels of GFP expression in the monocyte population. The percentage of GFP-positive monocytes was similar for both vectors, varying between 10% and 30% at 100 pp/cell, depending on the donor (data not shown). For both vectors the GFP expression in the T cell, B cell, and NK cell populations was very low (<1% GFP-positive cells). Although Ad5ΔE1+pIX and Ad5ΔE1ΔpIX showed identical GFP expression levels in the monocytes, the incubation with Ad5ΔE1ΔpIX resulted in a remarkably higher level of monocyte activation, as indicated by enhanced CD86 expression (figure 4.5 A). The percentage of CD86 positive monocytes as well as the mean fluorescence intensity for CD86 was significantly higher for the pIX-lacking vector. This enhancement in monocyte activation was observed for monocytes derived from PBMCs of three different donors and with different virus batches. The up-regulated CD86 level involved the entire Ad5ΔE1ΔpIX-incubated monocyte population, not only the GFP-positive cells (figure 4.5 A). Incubation with Ad5ΔE1ΔpIX also resulted in enhanced activation of NK cells, as demonstrated by an increase in CD69 expression (figure 4.5 B). Interferon-gamma (IFN-γ) ELISA of PBMC supernatants revealed higher levels of IFN-γ production after incubation with Ad5ΔE1ΔpIX at the higher input virus levels (figure 4.5 C).

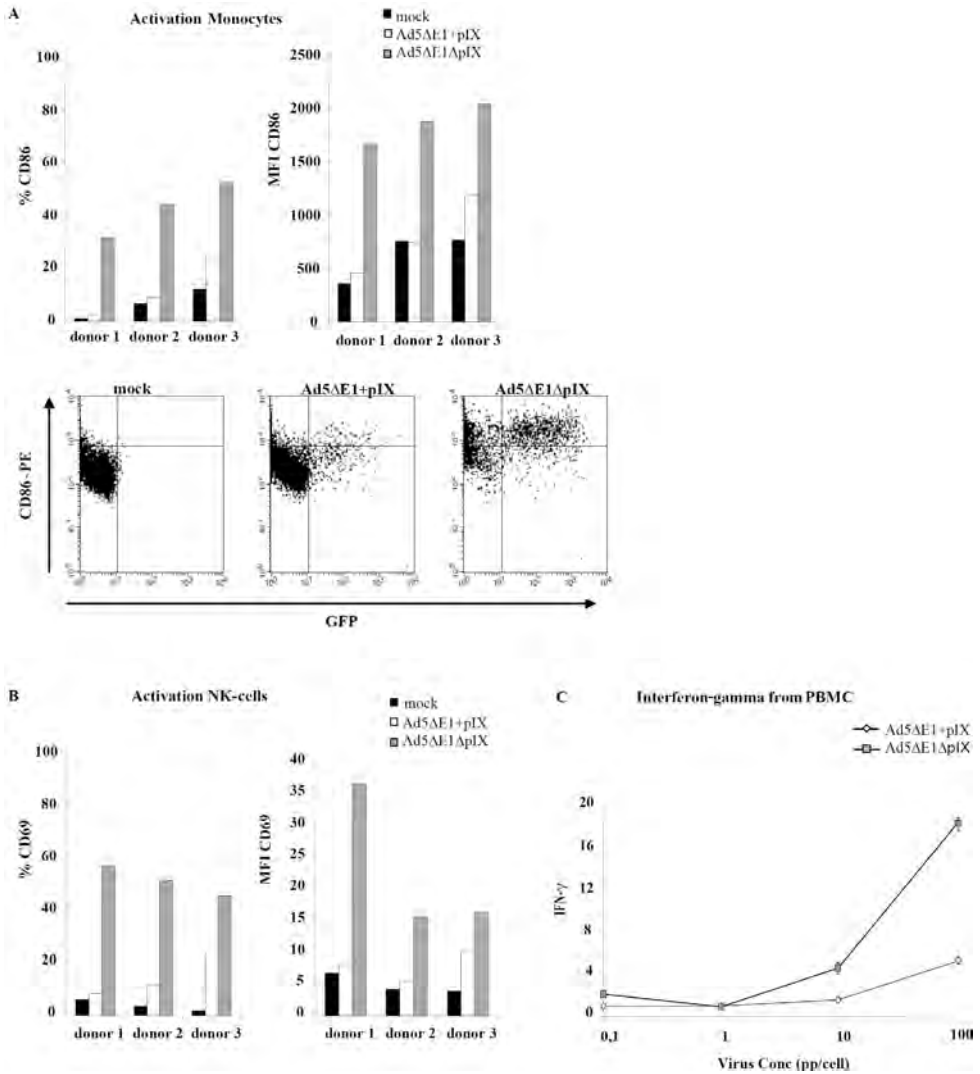


Figure 4.5 Activation of peripheral blood mononuclear cells (PBMCs) after incubation with Ad5ΔE1+pIX and Ad5ΔE1ΔpIX for two days. (A) Activation of the monocyte population. The graphs on the left show the percentage of CD86 positive cells and the mean CD86 expression levels (MFI) for three different donors. The flow cytometry figures on the right illustrate the CD86 up-regulation for transduced (GFP-positive) monocytes and non-transduced (GFP-negative) monocytes (from donor 1). **(B)** Activation of the NK cell population. The percentage of CD69 positive cells and the mean CD69 expression levels (MFI) are shown for three different donors. **(C)** Measurement of IFN-γ levels in PBMC supernatant (from a single donor) after incubation with Ad5ΔE1+pIX and Ad5ΔE1ΔpIX. The data represent mean values of two independent measurements.



Enhanced liver transduction upon intravenous administration of Ad5ΔE1pIX

To study the functional consequences of protein IX-gene deletion on biodistribution in mice, Ad5ΔE1+pIX and Ad5ΔE1ΔpIX viruses were administered via tail vein injection. Luciferase expression in multiple organs was determined at 3 days post injection. The vector lacking protein IX yielded a more than ten-fold higher luciferase activity in the liver (figure 4.6 A). These data show that the absence of protein IX in the viral capsid strongly affected the biodistribution of HAdV-5 particles.

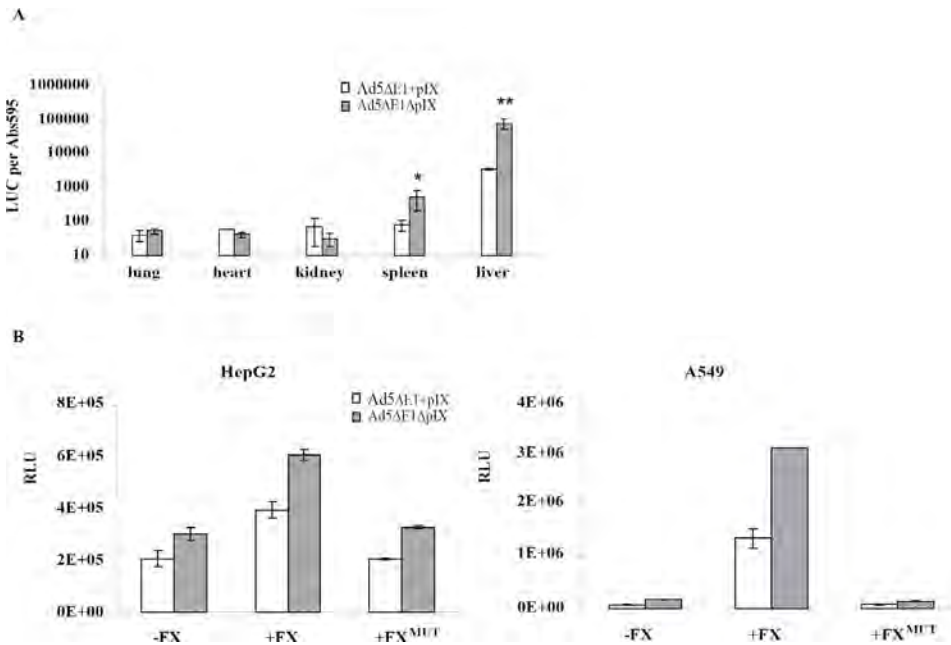


Figure 4.6 (A) Distribution of Ad5ΔE1+pIX and Ad5ΔE1ΔpIX in mice after tail vein injection of 10^9 vector particles. Prior to vector injection, pre-dosing was performed with the vector HAdV-5.CMV to saturate Kupffer cell macrophages. Organs were harvested three days post injection and the luciferase expression per total protein was measured (* $p=0.057$, ** $p=0.006$ versus Ad5ΔE1+pIX). Error bars represent SEM ($n=2$). **(B)** Luciferase expression in HepG2 and A549 cells after transduction with Ad5ΔE1+pIX and Ad5ΔE1ΔpIX in the presence of coagulation factor X (FX), Gla-domainless mutant factor X (FX^{MUT}), or no coagulation factors (mock). Error bars represent SEM ($n=3$).

Recent reports have described the involvement of plasma proteins, such as the blood coagulation factor X (FX), in HAdV-5 transduction of the liver [28,29]. To study whether removal of protein IX influences the effects of clotting-factor binding we compared the FX-mediated transduction for Ad5ΔE1+pIX and

Ad5ΔE1ΔpIX (figure 4.6 B). *In vitro* incubation of A549 cells and HepG2 cells with FX resulted in a similar enhancement in transduction for Ad5+pIX and Ad5ΔpIX. As expected, no effect on transduction was observed after incubation with the mutant FX (FX^{MUT}), which lacks the domain necessary for binding to the HAdV-5 capsid [29]. From these data we conclude that the absence of protein IX does not affect the binding of coagulation factor X.

DISCUSSION

From our data we conclude that the omission of protein IX from HAdV-5 vectors enhances viral transduction of cell lines that are low in expression of the adenovirus receptor CAR. This finding is of relevance for the development and implementation of protein IX-gene modified HAdV-5 vectors. Also, the findings enhance our knowledge on HAdV-5 biology and evolution, which especially becomes clear if stating our conclusion in a 'backwards' manner: the introduction of protein IX in HAdV-5 (making it wild-type HAdV-5) decreases viral transduction of cell lines that are low in CAR expression. Although speculative, it is very well possible that the presence of protein IX in the HAdV-5 capsid negatively interferes with non-specific cell transduction, and thereby plays a role in determining the virus tropism. Noteworthy, the extended cell tropism of the Ad5ΔE1ΔpIX vector, as presented by its enhanced transduction of CAR-negative cells, did not come with a loss in ability of CAR-mediated transduction of cells. This is clear from the comparison on MZ2-MEL3.0 and MZ2-MEL3.0/CAR. Introduction of CAR in the CAR-negative cells significantly increased transduction levels with Ad5ΔE1ΔpIX. It is conceivable that in CAR-expressing cells the protein IX-deficient particles can use either the CAR/fiber-dependent mechanism, or the CAR-independent pIX-dependent mechanism. Quantifying the relative contribution of each of these mechanisms to the total transduction requires tools for specifically blocking the new pathway. Such inhibitors remain to be identified.

Interestingly, the vector Ad5ΔE1pIX^{ΔLEU} had Ad5ΔE1ΔpIX-like properties, implicating the importance of the C-terminal domain of protein IX in inhibiting transgene expression in CAR-negative cell lines. The specificity for the C-terminal domain of protein IX excludes differences in viral capsid stability as a cause for the observed phenomenon, since deletion of this domain does not result in reduced capsid stability [4].

Wild-type HAdV-5 enters cells via high affinity binding of the fiber knob domain to CAR [14], followed by interaction of the RGD motif of the penton base with cellular integrins $\alpha_v\beta_3$ and $\alpha_v\beta_5$ promoting rapid adenovirus cell entry

into clathrin-coated vesicles [25,26]. Similar to the Ad5ΔE1+pIX control virus, Ad5ΔE1ΔpIX requires the presence of bivalent cations for its transgene delivery, indicating the usage of cellular integrins for cell internalization [26]. More specifically, blocking cells with anti-integrin antibodies resulted in a decrease in transduction for Ad5ΔE1ΔpIX, thereby confirming the integrin-dependency. Unfortunately, our efforts to compare the vectors for a general difference in cell-binding affinity, using Alexa488-TFP (tetrafluorophenyl) labeled vector particles, were not conclusive as a result of strong and reproducible negative effects of the labeling procedure on the pIX-deficient vector particles. The effects were not identical for protein IX-positive and protein IX-negative particles, making the results obtained with these particles in comparative binding assays unreliable. Alternative protocols for fluorescent- or radio- labeling of vector particles might be more suitable for comparing the cell-binding affinity. Labeled vector particles might also be used for analyzing differences in cell surface motility between protein IX-containing and protein IX-lacking vectors. Through largely unknown mechanisms HAdV-5 particles migrate on the cell surface and alterations in viral movement can result in modified transduction [30].

The removal of the protein IX gene from a replication-competent HAdV-5 virus results in a small-plaque phenotype on CAR-positive as well as CAR-negative cell lines. This suggests the tropism modifying mutation affects the virus's capacity to spread from cell to cell. Such small-plaque phenotypes of extended tropism mutants is not unprecedented: similar phenotypes have been described for murine corona virus mutants that acquired the capacity to bind heparin [27].

To investigate the effect of protein IX-gene deletion on the interaction of HAdV-5 with human mononuclear leukocytes, we compared the vectors Ad5ΔE1+pIX and Ad5ΔE1ΔpIX for GFP expression in PBMCs. Flow cytometry analyses demonstrated GFP expression almost exclusively in monocytes, with similar expression levels for both vectors. However, increased activation of the entire monocyte population (so not exclusively restricted to the GFP-positive population) was observed for Ad5ΔE1ΔpIX, as demonstrated by an enhancement in CD86 expression. CD86 is an activation marker on antigen-presenting cells such as monocytes, macrophages, dendritic cells, and B cells, and is important for co-stimulation of T cells [31]. The increased activation of monocytes despite similar levels of transduction (GFP expression) could be due to a direct effect on the monocytes themselves or indirectly via a more efficient stimulation of T cells or NK cells. Uptake of the protein IX-deleted vector may be increased and/or may follow different intracellular trafficking routes [32,33]. As a consequence, more

efficient viral antigen loading onto human leukocyte antigen (HLA) molecules, or an increase in CD86 expression, could lead to more T cell activation, and e.g. IFN- γ secretion. Of note, most healthy adult donors have HAdV specific T cells [34]. Indeed, Ad5 Δ E1 Δ pIX incubation resulted in enhanced production of IFN- γ . Protein IX-gene deletion appeared to affect NK cell activation as well, resulting in increased expression levels of CD69, which is an activation marker for lymphocytes including NK cells [35]. Increased T cell activation could have been accompanied by increased levels of other T cell cytokines like interleukin-2 (IL-2). IL-2 is a known activating cytokine of NK cells [36,37]. Alternatively, the increased production of IFN- γ in the supernatant would also be consistent with increased activation of NK cells by the vector lacking pIX, without the involvement of T cells.

Irrespective of the mechanism, the increased activation of monocytes and NK cells as a result of protein IX deletion is likely to have important consequences for the *in vivo* implementation of protein IX modified HAdV-5 vectors, since monocytes (after differentiation to Kupffer macrophages in the liver) as well as NK cells are important players in the sequestration of HAdV-5 vectors from the blood after systemic delivery (reviewed in [38]). Furthermore, the observed differences in PBMC activation between Ad5 Δ E1+pIX and Ad5 Δ E1 Δ pIX suggest a biological function of protein IX in diminishing the immune response against HAdV-5. Further studies will be necessary to fully determine the effects of protein IX deletion from HAdV-5 on the activation of immune cells.

Omission of protein IX from the capsid resulted in a remarkable difference between Ad5 Δ E1+pIX and Ad5 Δ E1 Δ pIX upon intravenous administration in mice. Administration of Ad5 Δ E1 Δ pIX yielded more than ten-fold higher luciferase activity in the liver, for reasons that remain to be clarified. Extensive research has been devoted to defining the molecular mechanisms behind the sequestration of intravenously administered HAdV-5 in the human liver, with the aim to eventually improve the therapeutic efficacy of intravenously delivered HAdV-5 vectors (reviewed in [39]). The uptake of HAdV-5 in the liver has been found to occur in a CAR-independent manner and involves binding of the virus particles in the blood to complement factors and immunoglobulins (mediating uptake in Kupffer cell macrophages) [28,40], and coagulation factors (resulting in hepatocyte transduction) [28,29]. The enhanced transduction of the liver with Ad5 Δ E1 Δ pIX observed in our mouse model seems not to be a result of more efficient binding of the vector to coagulation factor X (FX), as can be concluded from our *in vitro* FX-binding assay. An alternative explanation might be that the absence of protein IX extends the HAdV-5 tropism, enabling the transduction

of cells in the liver that do not present CAR. Of interest, primary human hepatocytes were recently found to have CAR localized at cellular junctions that are inaccessible to the hepatic blood flow [41]. This localization is in contrast to the CAR molecules on hepatocellular carcinoma cells (like HepG2), being highly available for HAdV-5 binding [41,42].

Protein IX is strongly conserved in all primate adenoviruses indicating the importance of the protein. A biological role for protein IX in HAdV-5 capsid stabilization has been proposed, based on *in vitro* heat-stability assays [4]. Our findings point toward other biological functions of protein IX in (i) determining the cell tropism of HAdV-5, and (ii) negatively interfering with the innate immune response against HAdV-5. More insight into the mechanisms by which the presence of protein IX affects gene transfer and activation of immune cells may be of use for enhancing the efficiency of current (e.g. Atencio *et al.*; [43]) and future gene therapies involving protein IX modified HAdV-5 vectors.

ACKNOWLEDGMENTS

We thank Jort Vellinga and Vivien Mautner for valuable scientific discussions and critically reading the manuscript, Steve Cramer for expert technical support, and Martijn Rabelink for producing the viruses used in these studies. This work was supported by the European Union through the 6th Framework Program GIANT (contract no. 512087).

CHAPTER 5

TRUNCATING THE I-LEADER OPEN READING FRAME ENHANCES RELEASE OF HUMAN ADENOVIRUS TYPE 5 IN GLIOMA CELLS

S.K. van den Hengel
J. de Vrij
T.G. Uil
M.L. Lamfers
P.A.E. Sillevius Smitt
R.C. Hoeben

Virology Journal (2011) **8**:162.



INTRODUCTION

The poor prognosis of high grade gliomas with the current treatments prompted an ongoing search for alternative treatments. A new strategy for glioma treatment involves the use of viruses as oncolytic agents, such as Human Adenoviruses (HAdV), Herpes Simplex viruses and, more recently Reoviruses [44-48]. Of these, the use of HAdV has been explored most rigorously, including replication-defective HAdV vectors carrying heterologous transgenes, as well as replication-competent HAdV in which replication is restricted to tumor cells.

HAdV transduce both dividing and quiescent cells with high efficiency, they can be genetically modified with relative ease, and the technology for clinical-grade production is available. Their biology, which is understood in detail, also facilitates modification of the viral genome for creating Conditionally-Replicating Adenoviruses (CRAds). In addition, viral-tissue tropism can be modified by incorporating ligands that target specific receptors on tumor cells, for example by fusing ligands with the fiber [49] or with the minor capsid protein IX [5]. Also modifications have been described that promote interactions with the tumor-specific receptors. Such mutations can be used to increase transduction of target tissues [50-53].

The first phase I clinical trial with a replication-competent HAdV on malignant glioma was performed with ONYX-015 [44], which is based on HAdV-5 and harbors a deletion in the open reading frame encoding the 55 kDa E1B protein [54]. Although ONYX-015 has antitumor activity, the precise mechanism behind its tumorcell preference is still controversial [55]. While the ONYX-015 study provided evidence of the safety of CRAds in glioma-patients [44], the anti-tumor efficacy of this virus was limited, presumably due to inefficient replication and poor intratumoral spread.

To isolate HAdV-5 mutants with improved cytopathic activity, two groups used random mutagenesis and bioselection strategies. Both studies yielded mutants containing point mutations in the *i*-leader region of the late transcription unit [56,57]. The *i*-leader is a 440-nucleotide long sequence that is found between the 2nd and 3rd element of the tripartite-leader sequence in a significant fraction of the major-late transcripts. This sequence contains an open reading frame which encodes a small protein of approximately 16 kDa in size [58]. It has been suggested that it reduces the half-life of L1 mRNAs, however the precise function of the *i*-leader protein is unknown [58,59]. A common point mutation, C8350T, which created a stop codon in the *i*-leader open reading frame, was isolated by Yan *et al.* [57] after bioselection on the HT29 colon carcinoma cell line. Also the C8299T mutation, isolated by Subramanian and coworkers in a screen for

large plaques on A549 adenocarcinomic human alveolar basal epithelial cells, truncated the i-leader open reading frame [56]. Yan and colleagues demonstrated that their mutants ONYX-201 and ONYX-203, which contain next to the i-leader mutation some additional mutations, strongly enhanced the cytopathic activity of HAdV-5 not only in the cells used for bioselection, but in a larger panel of tumor cell lines [57]. Unfortunately, no glioma cell lines were included in their study.

In this study we compared the cytopathic activity of a HAdV-5 virus containing the single i-leader point mutation with that of wtHAdV-5 in glioma cultures. To do so, we created a HAdV-5 that contains the C8350T mutation, which truncates this open reading frame. To facilitate identification of the mutant-virus genomes, an XhoI restriction site was created 6 nucleotides downstream of this mutation. We found the cytopathic activity in glioma cells of the mutant vector (RL-07) to be strongly increased compared to the wild-type vector (wtHAdV-5). While the mutation does not affect timing of viral protein synthesis and virus yields, the mutant virus was found to be released earlier from infected cells. These results demonstrate that improved adenoviruses with enhanced spreading activity in glioma cells can be generated by introduction of a mutation that truncates the i-leader. Such mutations may help enhancing the antitumor efficacy of oncolytic adenoviruses in the treatment of gliomas.

MATERIALS AND METHODS

Cell lines

In this study we used the malignant glioma cell lines U251 and SNB19, the HAdV-5 E1 transformed human embryonic retinoblast cell lines 911 and PER. C6, and the A549 lung carcinoma cell line as described before [60]. Cultures of freshly resected glioma cells were started from resection material of the Dept of Neurosurgery at Erasmus MC and used before the fifth passage. All cell lines were cultured in Dulbecco's modified Eagle's medium (DMEM, Gibco-BRL, Breda, the Netherlands) supplemented with 8% fetal bovine serum (FBS, Gibco-BRL) and penicillin-streptomycin at 37°C in a humidified atmosphere containing 5% CO₂.

Adenovirus vector

We used replication-competent HAdV-5 vectors. The mutant, containing the i-leader mutation C8350T and the extra XhoI restriction site (HAdV-5/RL-07), was generated by homologues recombination in *E. coli* BJ5183, using the pTG3602 plasmid [61] as backbone. The mutated i-leader fragment was generated by mutagenesis PCR using synthetic oligo nucleotides

5'GACAACATCGCGTAGATGACTCGAGTCCATGGTCTGG and 3'-CCAGACCATGGA-CTCGAGTCATCTACGCGATGTTGTC. The nucleotide corresponding to nt 8350 is represented in bold, and the XhoI restriction site is italicized and underlined. The HAdV-5/RL07 virus was rescued on 911 cells, propagated on PER.C6 cells, purified by double CsCl density gradient centrifugation, dialyzed, and stored at -80°C in sucrose buffer. Infectious particle titers were determined by plaque assay on 911 cells. The presence of the C8350T mutation and the XhoI restriction site was verified by restriction and sequence analyses (supplementary figure 5.1 and 5.2). The wtHAdV-5 virus used in this study was recovered in identical manner, using a wt HAdV-5 i-leader fragment, to ensure isogenicity of the RL-07 virus and the wtHAdV-5. The nucleotide sequence of the entire RL-07 virus is available upon request.

Viral titer

Plaque assays were performed to determine the biological titers (as plaque forming units per ml) as described [13]. Briefly, 911 cells were seeded in 6-well plates 1 day prior to viral infection. The cultures were exposed to serial dilutions of the virus. After 4 hrs viral medium was removed and cells were overlaid with 0.5% agar/F15 media supplemented with 2% horse serum. Plaque titers were read at day 10 post infection (p.i.).

The concentrations of viral genome copies were determined by picogreen assay [18]. Purified virus was inactivated in a final concentration of 0.05% SDS in storage buffer and loaded in microtiter plates. After adding picogreen, the fluorescence was measured and viral genomes were calculated using purified bacteriophage λ DNA as a standard.

Propagation on 911 cells

911 cells were seeded in 6-well plates 1 day before infection. Cultures were infected with wtHAdV-5 or RL-07 in parallel MOI=3. 48 hrs p.i. virus was harvested and viral titers were defined by plaque assays as described above.

Cell viability assay

WST-1 reagent (Roche, Woerden, The Netherlands) was used to determine the viability of the cultures after adenoviral infection. Cells were seeded in 96-well plates and infected with various amounts of virus. The cell viability of the cultures was determined 4 days p.i. for the established cell lines, and 7 days p.i. for the primary glioma cultures by adding the WST-1 reagent according to the manufacturer's instructions.

Viral plaque formation

The plaque surfaces were determined on U251 cells according the plaque titration protocol as for 911 cells. The agar was removed 10 days p.i., and the cells were subsequently fixed with methanol and stained with 0.5% crystal violet solution. The relative plaque surfaces were determined with Olympus DP-software.

Viral release

To determine the viral release, media and cells were collected separately at 30 and 48 hrs p.i. of U251 and SNB19 cultures infected with wtHAdV-5 and RL-07 at MOI=3. The titers were determined by plaque titration on 911 cells.

Immunoblot procedure

To study the viral protein synthesis after infection an immunoblot procedure was used. U251 and SNB19 were seeded in 6-well plate o/n and infected with RL-07 or HAdV-5 at MOI=1. Cells were harvested 24, 40, 48, 64, and 70 hrs p.i. in radioimmunoprecipitation assay lysis buffer (Ripa) (50 mM Tris-Cl, pH 7.5, 150 mM NaCl, 0.1% SDS, 0.5% DOC, and 1% NP40) supplemented with protease inhibitors (Complete mini tablets, Roche Diagnostics, Almere, The Netherlands). Per sample 50 µg of protein lysate, defined by the Pierce BCA protein assay kit (Thermo Scientific Rockford, USA), and after addition of western sample buffer (final concentrations: 10% glycerol, 2% SDS, 50 mM Tris-Cl (pH 6.8), 2.5% b-mercaptoethanol and 0.025% bromophenol blue) was loaded onto a SDS-polyacrylamide gel. The proteins were transferred to Immobilon-P (Millipore, Etten-Leur, The Netherlands). Detection of fiber, E1A and ADP was performed with the antibodies 4D2 (anti-fiber tail [23]) and M73 (anti-E1A [62]), a rabbit antiserum raised against an ADP peptide (P63-77 [63]; a kind gift from Dr. W. S. M. Wold), respectively, and visualized by enhanced chemiluminescence. ImmunO anti-actin clone C4 (MP Biomedicals, Amsterdam, The Netherlands) was used as loading control.

Colony-based survival assay

Suspensions of U251 and SNB19 were infected with wtHAdV-5 or RL-07 with a MOI=100 in 2%FBS/ DMEM, non-infected cells were used as control. Cells were incubated for 1 hr at 37°C, washed 3 times with PBS supplemented with 1:500 diluted Immunoglobuline I.V. (stock 60 mg/ml) and plated in a concentration of 500 cells/dish, medium was supplemented with 1:500 dilution of IVIg. After 10 days cells were fixed with methanol and stained with 0.5% crystal violet

solution. Single colonies were counted and number of colonies of wtHAdV-5 was compared to the number RL-07 colonies.

Trypan blue exclusion-based survival assay

This procedure was performed as described by Tollefson *et al.* [64]. In short, U251 and SNB19 were seeded at 4.10^5 cells per well in a 6-well plate. The next morning cells were infected with MOI=100 in 1 ml DMEM/2% FBS. After 2 hr 1 ml DMEM/14%FBS was added to each well. From day 1 up to day 5 media and cells were harvested and trypan blue was added to the cells in a final concentration of 0.02%. A total of 500-600 cells were counted and percentage of viable cells was calculated.

RESULTS

The aim of this study was to evaluate whether truncation of the i-leader open reading frame enhances the cytopathic effect of HAdV-5 in human glioma cell lines. Since the ONYX-234 virus [57], which consists of HAdV-5 with the C8350T mutation, was unavailable to us, we recreated this mutant by site-directed mutagenesis and homologous recombination. To facilitate straightforward identification of this mutant, we inserted an XhoI-restriction site 6 nucleotides downstream of the C8350T mutation (supplementary figure 5.1 and 5.2). From the cloned virus DNA, viruses were generated by transfection of the viral genomes on 911 helper cells. Viral plaques were picked and the viruses expanded and propagated on PER.C6 cells. No consistent differences in viral particle to plaque forming unit (pfu) ratios were observed (table 5.1) in RL-07 and wtHAdV-5 virus batches produced in parallel. Also on 911 cells, the RL-07 viruses could be propagated efficiently, with the kinetics and yields very similar to the wtHAdV-5 (table 5.2).

Table 5.1 Overview viral yield in pfu/ml and vp/ml after CsCl-purification

		Plaque assay (pfu/ml)	Picogreen assay (vp/ml)	vp/pfu ratio
Batch 1	wtHAdV-5	3×10^{11}	5.5×10^{12}	18
	RL-07	1.1×10^{11}	1.6×10^{12}	15
Batch 2	wtHAdV-5	2.8×10^{11}	3.2×10^{12}	11
	RL-07	1.3×10^{11}	1.6×10^{12}	12

Table 5.2 Viral yield (pfu) of wtHAdV-5 and RL-07 on 911 cultures

	wtHAdV-5	RL-07
Culture 1	1.35x10 ⁹	1.24x10 ⁹
Culture 2	1.42x10 ⁹	1.13x10 ⁹
Culture 3	1.25x10 ⁹	1.34x10 ⁹
Average	1.34x10 ⁹	1.23x10 ⁹
SD	8.8x10 ⁷	1.08x10 ⁸

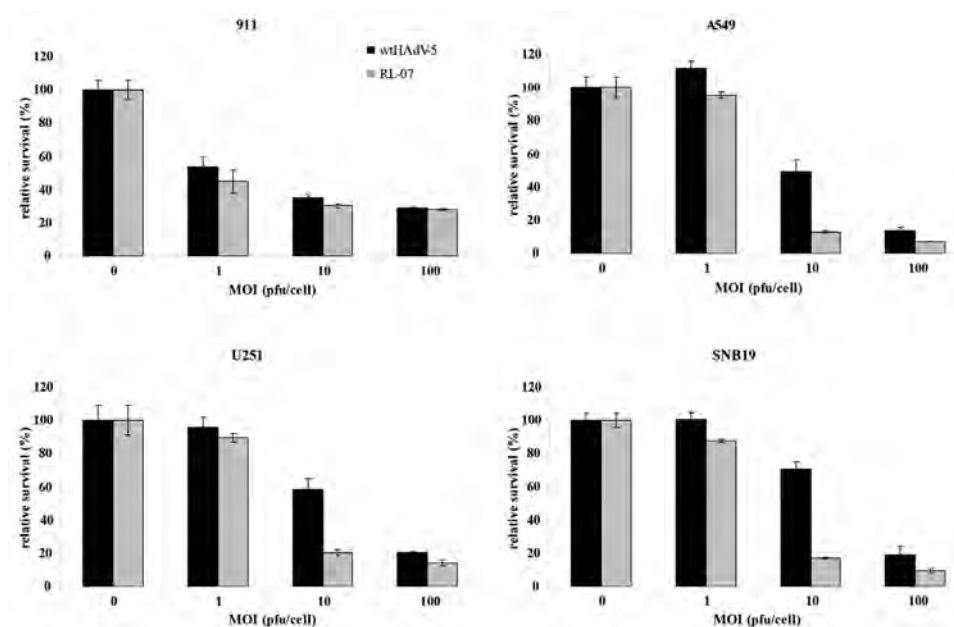


Figure 5.1 Relative survival as determined by WST-1 assay. Cytopathic activity of RL-07 (grey bar) compared to wtHAdV-5 (black bar) is higher on glioma cell lines U251 and SNB19. Error bars represent the SD (n=3). * - statistical significance; *unpaired, two-sided t-test*, $p < 0.01$. Cells were seeded in 96-well plates 1 day before infection with RL-07 and wtHAd5 (MOI range 0-100 pfu/cell). Viability of the cultures was determined 4 days p.i. by WST-1 assay. Very similar results were obtained in a repeat experiment.

To analyze the cytopathic activity of RL-07, two glioma cell lines (U251 and SNB19, both CAR-positive) and two control cell lines (911 and A549) were infected with RL-07 and wtHAdV-5 at multiplicity of infections (MOI) ranging from 0 to 100 pfu/cell. Four days p.i., the cell viability was determined by WST-1 assay (figure 5.1), RL-07 had a significant higher cytopathic effect on glioma cell lines and A549 compared to the control virus wtHAdV-5. On 911 cells, no differences in the induction of cytopathic effects were detected.

To determine whether the decreased viability of RL-07 infected cells in the WST-1 assay correlates with enhanced spread in monolayers of glioma cells, a plaque assay was performed on U251 cells. Monolayers of U251 were infected with RL-07 and wtHAdV-5 with a 10^9 times diluted virus stock (batch 1) and overlaid with agar. Plaque sizes were scored 10 days p.i. (figure 5.2). The plaques formed upon infection with RL-07 are on average 7-fold larger in size than the plaques obtained with wtHAdV-5, demonstrating that the mutation enhances viral spread.

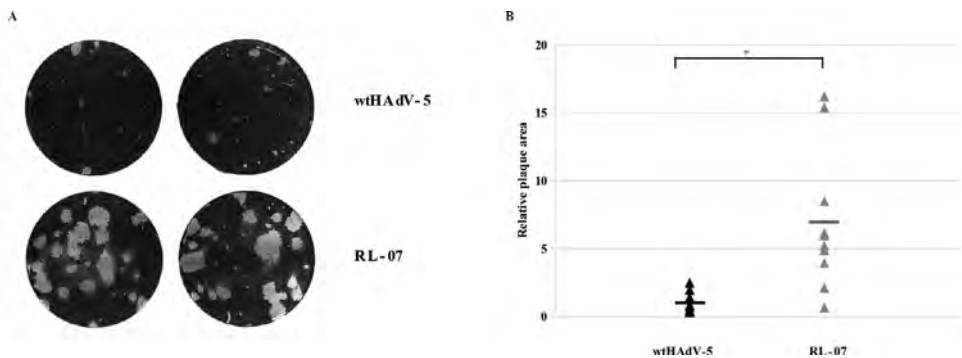


Figure 5.2 Viral plaque formation on U251 cells. Monolayers of U251 were infected with RL-07 or wtHAdV-5 with a MOI of 2.2×10^{-5} and 6×10^5 respectively, and overlaid with 0.5% agar in F15 media supplemented with 2% Horse serum. Ten days p.i. the agar was removed and cells were stained with 0.5% crystal violet solution. (A) Photograph of plaques of wtHAdV-5 and RL-07 on U251 monolayer (B) Relative plaque surface of 10 plaques. *-statistical significance; *unpaired, two-sided, t-test, $p < 0.01$* . wtHAdV-5 - black closed triangles; RL-07 - grey closed triangles.

To compare the kinetics of virus release, U251 and SNB19 cells were infected with either RL-07 or wtHAdV-5. At 30 and 48 hrs p.i. the medium was carefully separated from the adherent cells and both were collected. In both fractions the viral particles were quantified by plaque assays on 911 cells (figure 5.3). In both cell lines approximately 7-fold more virus was found in the medium of the RL-07 infected cells than in the medium of the wtHAdV-5 infected cells at 30 hrs p. i.. At 48 hrs p.i. media of RL-07 infected U251 cells contained approximately 22 times more virus than those infected with wtHAdV-5. Similarly, the amount of RL07 in the media of SNB19 cultures was at least 13 times higher at 48 hrs p.i.. From these data we conclude that the RL-07 virus is released in to the medium earlier than wtHAdV-5.

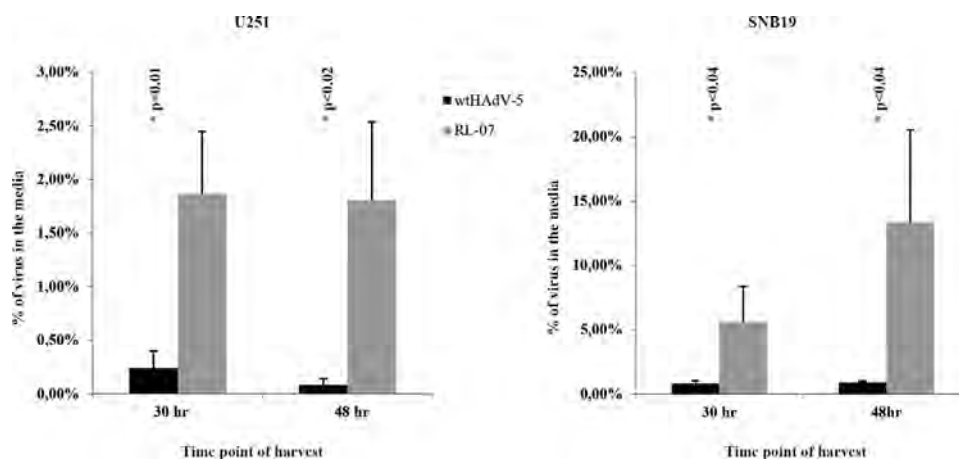


Figure 5.3 Virus releases in culture media. At 30 and 48 hrs p.i. with wtHAdV-5 and RL-07 the cells and the media of the U251 and SNB19 cultures were collected separately and assayed in a plaque assay. The fraction of the total yield recovered in the medium is plotted. Black bars represent wtHAdV-5 and the grey bars RL-07. Error bars represent the SD (n=3) * - statistical significance; *unpaired, two sided t-test*.

Having established that the RL-07 virus was released earlier than wtHAdV-5, we examined the expression pattern of the viral proteins E1A, fiber, and the adenovirus death protein (ADP). U251 and SNB19 cells were infected at MOI=1 and harvested at several time points after infection and viral proteins were visualized by immunoblotting (figure 5.4). In our time series no differences between fiber, E1A and ADP levels were observed between RL-07 and wtHAdV-5. This shows that the rapid release of RL-07 particles does not result from more rapid viral protein synthesis.

In addition to the WST-1 assay, which determines the metabolic activity of the remaining viable cell population, two more direct survival assays were performed. These are the colony-based survival assay and the trypan blue exclusion-based survival assay. The colony-based survival assay measures the number of residual colony-forming cells after exposure of the cells to the virus. In this assay no differences in the number of colonies were noted between wtHAdV-5 and RL-07-infected U251 or SNB19 cells (*data not shown*). With the trypan-blue based assay the fraction of dead cell was assessed by trypan-blue, starting 1 day after infection with MOI=100. Up to day 5 the cell viability of the U251 and SNB19 cultures were determined and plotted (figure 5.5). At one day p.i. there was no increase in cell death discernible. At two days after infection the viability started to decrease. On the U251 cells no differences were observed

between the two viruses. On the SNB19 cell line, from day 2 up to day 5 p.i. a significant higher proportion of dead cells were detected in the cultures infected with RL-07 compared to wtHAdV-5. This indicated that RL-07 accelerates cell death on this cell line.

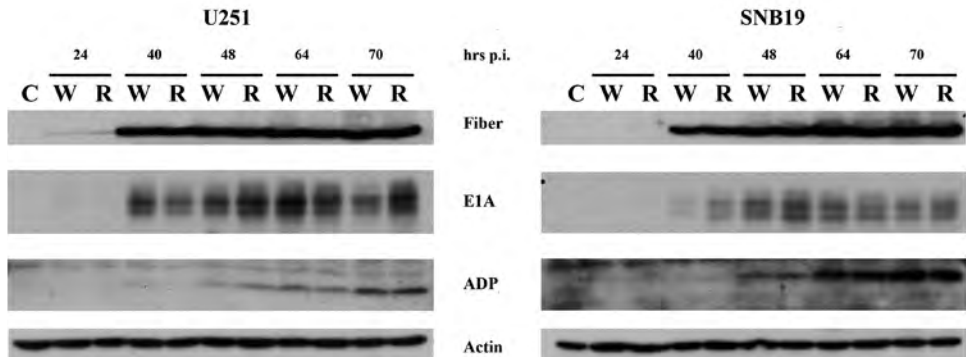


Figure 5.4 Protein immunoblot assay for detection of viral proteins. Fiber, E1A, ADP levels were detected upon infection with RL-07 or wtHAdV-5 at various time points p.i.. Actin was used as loading control. Cells were seeded o/n in a 6-well plate and infected with MOI=1. Cells were harvested 24, 40, 48, 64 and 70 hrs p.i. in Ripa buffer. Protein amounts were determined by BCA protein assay. In each lane 50µg of protein was loaded. C-mock infected control; W- infected with wtHAdV-5; R- infected with RL-07.

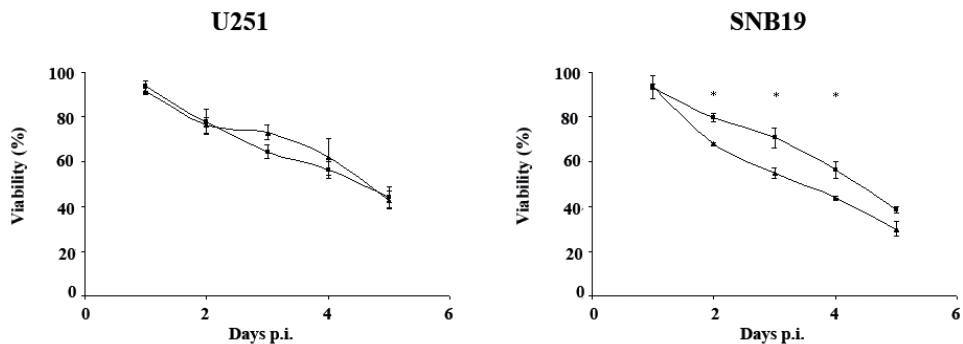


Figure 5.5 Trypan blue-based survival assay. U251 and SNB19 cultures were infected with wtHAdV-5 or RL-07 with a MOI of 100. Cell death in the cultures was determined by trypan blue as described by Tollefson and colleagues [64]. Error bars represent the SD (n=3) * - statistical significance; *unpaired, two sided t-test, p<0.01*. ♦ - wtHAdV-5 infected and Δ - RL-07 infected

Table 5.3 Characteristics primary glioma cell cultures

Tumor specimen	Male/Female	Age	Histology
EMC-1	M	44	Anaplas. Astrocytoma
EMC-3	M	48	Glioblastoma multiform
EMC-9	M	66	Glioblastoma multiform
EMC-24	M	50	Glioblastoma multiform
EMC-26	F	42	Anaplas. Astrocytoma
EMC-29	F	53	Anaplas. Astrocytoma

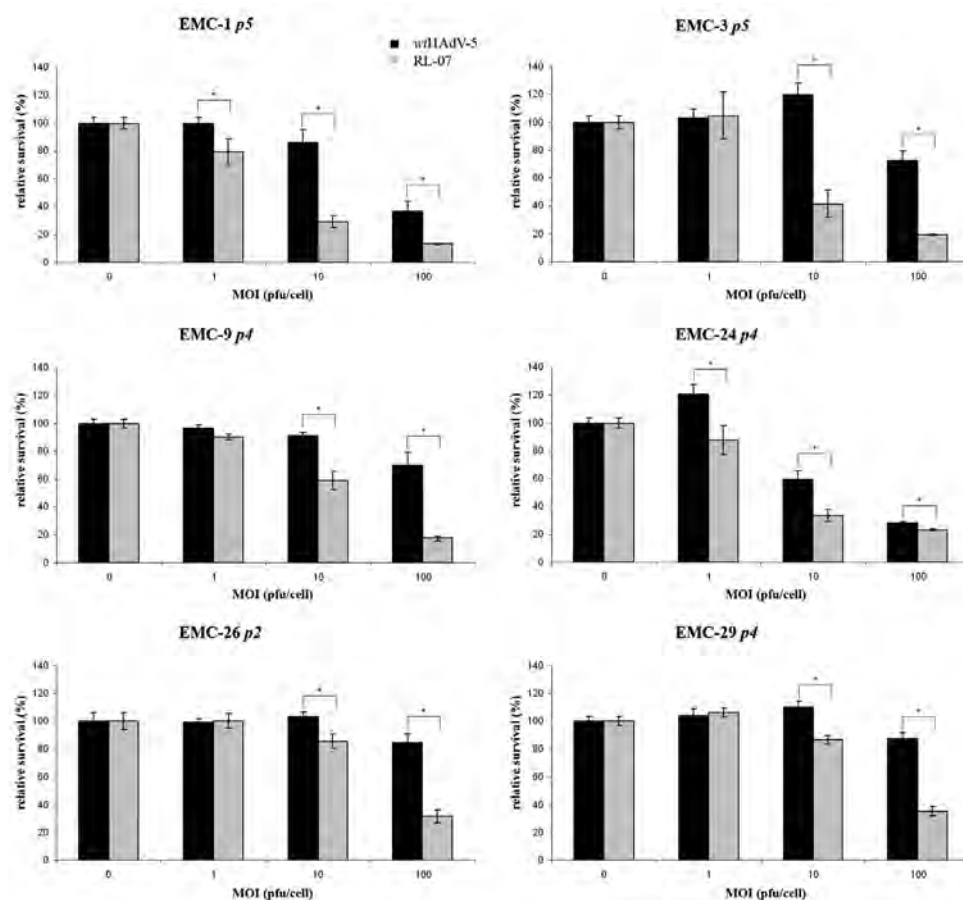


Figure 5.6 Relative survival of infected cells as determined by WST-1 assay. Cytopathic activity of RL-07 (grey bar) compared to wtHAdV-5 (black bar) is higher on primary high grade glioma cell cultures. Error bars represent SD (n = 4). * -statistical significance; paired, two sided *t*-test, $p < 0.01$. Cells were seeded in 96-well plates 1 day prior infection with RL-07 and wtHAdV-5 (MOI range 0-100 pfu/cell). Viability of the cultures was determined by WST-1 assay 7 days p.i..

So far our results demonstrate that the i-leader mutation in RL-07 accelerates virus release and enhances spread in established glioma cell lines. However, the potency of oncolytic HAdV can differ remarkably between established cell lines and cultures derived from resection material. To verify the cytopathic activity of RL-07 in human gliomas, cultures established from resection material of high grade gliomas were used for cytolysis assays. The characteristics of the cultures used in this study are summarized in table 5.3. The cytopathic activities of the viruses were evaluated 7 days p.i. by WST-1 assay. The results are presented in figure 5.6. At MOI=10 and MOI=100 all RL-07-infected cultures showed a significantly increased cytopathic activity in comparison to wtHAdV-5. In three of the cultures, EMC-1, EMC-9 and EMC-24, a significant effect could already observed at MOI=1.

DISCUSSION

In our long term efforts of developing efficacious adenoviruses for gene therapy in glioma [50,60,65-69], we studied the effect of a truncating mutation in the i-leader open reading frame on adenovirus cytopathic activity in glioma cell lines and cell cultures. Our data show that this mutation results in more rapid release of progeny viruses into the culture medium and enhanced spread of the virus in plaque assays. While the precise mechanism for this effect remains to be elucidated, the improved cytopathic activity may be employed in new oncolytic adenoviruses. Our data confirm and extend the results described by Yan *et al.* [57]. These authors isolated the ONYX-201 and ONYX-203 viruses by bioselection on HT29 cells. These viruses harbor several mutations, and share four mutations including the i-leader truncating C8350T mutation. Subsequently these authors generated the ONYX-234 virus that only harbors the C8350T mutation, and show that this mutation enhances the adenovirus's capacity to kill HT29 cells. We confirm and extend these observations and demonstrate that truncation of the open reading frame enhances the adenovirus's cytopathogenicity in glioma cells.

Similar to Subramanian *et al.* [56], we found that the i-leader mutation did not affect virus yield and production kinetics. In addition, no consistent differences in particle to pfu ratios were observed in batches produced in parallel. In a side by side comparison we demonstrated that RL-07 is more cytopathic on A549 and the glioma cell lines U251 and SNB19 than the isogenic wtHAdV-5. The increased cytopathic activity observed on these cell lines is similar to the observations of Yan *et al.* with ONYX-234 on HT29 [57].

Enhanced spread was observed on U251 figure 5.2 with a 7-fold increase in plaque surface. This is in line with published data of the other i-leader mutants [56,57]. There is a broad variation in plaque surfaces for both viruses. As discussed by Subramanian *et al.* this may be attributable to stochastic fluctuations in virus infection and replication [56]. The enhanced spread on U251 can be explained by the more rapid release of RL-07 from the cells. This is not caused by enhanced DNA replication (*data not shown*) confirming observations of Soloway and Shenk [59] and Subramanian [56], nor by a changed kinetics of protein synthesis of fiber, E1A and ADP figure 5.3. These results are similar to the results of Subramanian and co-workers, who also demonstrated that the improved viral spread is independent of ADP expression [56]. In contrast to the data of Yan *et al.* [57], we found no evidence that the truncating i-leader mutation affects virus replication, viral gene expression, or viral yields. The reason for this discrepancy is unclear but may relate to differences in the cell system used (glioma cells vs. colorectal carcinoma cells). It is also conceivable that any of the other six mutations in the ONYX-201 and ONYX-203 viruses have contributed to the differences between the results of the Yan study and ours [57].

Our data provide clear evidence for enhanced cytopathicity of the RL-07 virus in glioma cell cultures. To test whether this is caused by more rapid cell death upon infection or to enhanced virus spread we used several assays to assess cell viability. The WST-1 assay measures the metabolic activity of the residual viable cells in a culture, and is unable to distinguish these two components. The involvement of ADP in early cell death is unlikely since there is no difference between ADP expression in RL-07 and HAdV-5 infected cells. A more direct viability assays is the colony-formation survival assay which yielded very similar results with RL-07 and wtHAdV-5. Also a more direct assessment of cell killing on a per-cell basis is the assay by trypanblue exclusion. This assay revealed that there was no difference in cell death between the two viruses in U251 cells. On SNB19 cells a slightly more rapid cell death was observed in cultures infected with RL-07 compared to wtHAdV-5. The reason for the difference between the U251 cells and the SNB19 cells is unclear. Nevertheless, our data imply that although metabolic viability of U251 cultures infected with RL-07 decreases faster than in wtHAdV-5 infected cultures, this is not reflected in a more rapid cell killing by RL-07. In both cell types there is a strong increase in the release of infectious viral particles early after infection figure 5.3.

In the last set of experiments the cytopathic activity of RL-07 was determined on primary glioma cell cultures. Primary cell cultures resemble the original tumor more than established tumor cell lines. Also in these cultures, we observed

significant increased cytotoxic activity of RL-07 in all the cell lines tested. These results confirm that RL-07 exhibits an increased cytopathic activity in low passage cultures of resected glioma cells.

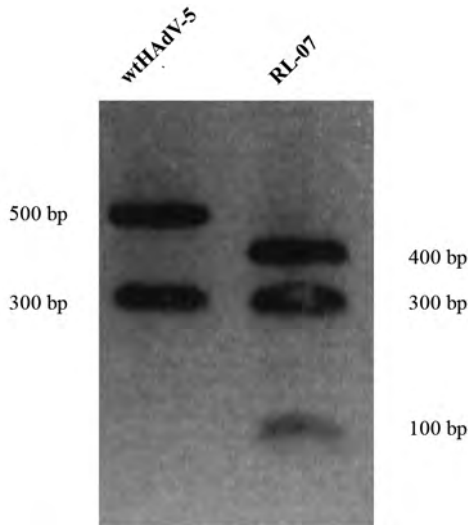
To enhance the potency and reduce the toxicity of adenovirus vectors the replication of HAdV-5 vectors for glioma therapy has been restricted by using promoters that are preferentially expressed in tumor cells for driving expression of key viral genes such as E1A. Also the tropism of the viruses has been modified by fiber modifications to increase the transduction of tumor cells and/or to decrease the transduction in non-target cells. New mutations such as the mutation that truncates the i-leader open reading frame may prove very useful for optimizing such vectors by increasing their the spread. With the fiber-swap mutations [50] and the optimized glial fibrillary acidic protein promoter [60,67], the mutation truncating the i-leader open reading frame protein constitutes a new addition to our arsenal of validated modules for inclusion in new replicating glioma-targeted adenoviruses.



CONCLUSION

In conclusion, truncating the i-leader of HAdV-5 by a single point mutation will give increased cytopathic activity in glioma cells. Introducing this mutation in an oncolytic adenovirus may enhance the antitumor cytopathic efficacy in the treatment of glioblastoma.

SUPPLEMENTARY FIGURES



Supplementary figure 5.1 Identification of RL-07 by PCR analyses. PCR analyses were performed on small freeze-thaw-lysate samples of the viral batches. Samples were heat inactivated and treated with proteinase K prior to PCR analysis. The i-leader region was amplified with the following primer set: Fwd primer 5'-AGACGCTCGGTGCGAGGATGCG; Rev primer 3'-GTCGTCTTCACGCAGAGGCGC. The PCR product was purified according to the SureClean protocol (Bioline, London, UK) and the product was digested using XhoI and loaded on 2% agarose gel. The picture represents the photo-negative image.

		8300		8349
pTG3602	(8300)	AAAGTCCAGATGTCCGCGCGGGCGGTCCGAGCTTGATGACAAACATCGCG		
wtHAdV-5	(314)	AAAGTCCAGATGTCCGCGCGGGCGGTCCGAGCTTGATGACAAACATCGCG		
RL-07	(314)	AAAGTCCAGATGTCCGCGCGGGCGGTCCGAGCTTGATGACAAACATCGCG		
		8350		8399
pTG3602	(8350)	CAGATGGAGCTCTCCATGGTCTGGAGCTCCCGCGGCGTCAGGTCAGGGC		
wtHAdV-5	(364)	CAGATGGAGCTCTCCATGGTCTGGAGCTCCCGCGGCGTCAGGTCAGGGC		
RL-07	(364)	TAGATGACTCGAGTCCATGGTCTGGAGCTCCCGCGGCGTCAGGTCAGGGC		

Supplementary figure 5.2 Alignment i-leader region. Sequencing analyses were performed on PCR products of freeze-thaw samples of virus batches (described by identification RL-07). PCR products were first cleaned with Sureclean (Bioline, London, UK), according to the manual, before direct sequencing. Sequencing was performed at the Leiden Genome Technology Center (LGTC, Leiden, The Netherlands). The sequences of nucleotide 8300-8400 of the parental plasmid pTG3602 and the sequences of the HAdV-5 and RL-07 viruses are represented. The C8350T changes, as well as the XhoI site created in the RL-07 virus, are boxed.

REFERENCES II

ADENOVIRUS



1. **Vellinga, J., van der Heijdt, S., and Hoeben, R.C.** The adenovirus capsid: major progress in minor proteins. *J.Gen.Virol.* 2005; **86**:1581-1588.
2. **Fabry, C.M., Rosa-Calatrava, M., Moriscot, C., et al.** The C-terminal domains of adenovirus serotype 5 protein IX assemble into an antiparallel structure on the facets of the capsid. *J.Virol.* 2009; **83**:1135-1139.
3. **Saban, S.D., Silvestry, M., Nemerow, G.R., and Stewart, P.L.** Visualization of alpha-helices in a 6-angstrom resolution cryoelectron microscopy structure of adenovirus allows refinement of capsid protein assignments. *J.Virol.* 2006; **80**:12049-12059.
4. **Vellinga, J., van den Wollenberg, D.J., van der Heijdt, S., et al.** The coiled-coil domain of the adenovirus type 5 protein IX is dispensable for capsid incorporation and thermostability. *J.Virol.* 2005; **79**:3206-3210.
5. **de Vrij, J., Uil, T.G., van den Hengel, S.K., et al.** Adenovirus targeting to HLA-A1/MAGE-A1-positive tumor cells by fusing a single-chain T-cell receptor with minor capsid protein IX. *Gene Ther.* 2008; **15**:978-989.
6. **Vellinga, J., Rabelink, M.J., Cramer, S.J., et al.** Spacers increase the accessibility of peptide ligands linked to the carboxyl terminus of adenovirus minor capsid protein IX. *J.Virol.* 2004; **78**:3470-3479.
7. **Vellinga, J., de Vrij, J., Myhre, S., et al.** Efficient incorporation of a functional hyper-stable single-chain antibody fragment protein-IX fusion in the adenovirus capsid. *Gene Ther.* 2007; **14**:664-670.
8. **Corjon, S., Wortmann, A., Engler, T., et al.** Targeting of adenovirus vectors to the LRP receptor family with the high-affinity ligand RAP via combined genetic and chemical modification of the pIX capsomere. *Mol.Ther.* 2008; **16**:1813-1824.
9. **Tang, Y., Wu, H., Ugai, H., et al.** Derivation of a triple mosaic adenovirus for cancer gene therapy. *PLoS.One.* 2009; **4**:e8526.
10. **Bayer, W., Tenbusch, M., Lietz, R., et al.** Vaccination with an adenoviral vector that encodes and displays a retroviral antigen induces improved neutralizing antibody and CD4+ T-cell responses and confers enhanced protection. *J.Virol.* 2010; **84**:1967-1976.
11. **Boyer, J.L., Sofer-Podesta, C., Ang, J., et al.** Protective immunity against a lethal respiratory Yersinia pestis challenge induced by V antigen or the F1 capsular antigen incorporated into adenovirus capsid. *Hum.Gene Ther.* 2010; **21**:891-901.
12. **Klein, B., Pastink, A., Odijk, H., et al.** Transformation and immortalization of diploid xeroderma pigmentosum fibroblasts. *Exp.Cell Res.* 1990; **191**:256-262.
13. **Fallaux, F.J., Kranenburg, O., Cramer, S.J., et al.** Characterization of 911: a new helper cell line for the titration and propagation of early region 1-deleted adenoviral vectors. *Hum.Gene Ther.* 1996; **7**:215-222.
14. **Bergelson, J.M., Cunningham, J.A., Droguett, G., et al.** Isolation of a common receptor for Coxsackie B viruses and adenoviruses 2 and 5. *Science* 1997; **275**:1320-1323.
15. **Uil, T.G., de Vrij, J., Vellinga, J., et al.** A lentiviral vector-based adenovirus fiber-pseudotyping approach for expedited functional assessment of candidate retargeted fibers. *J.Gene Med.* 2009; **11**:990-1004.
16. **Carlotti, F., Bazuine, M., Kekarainen, T., et al.** Lentiviral vectors efficiently transduce quiescent mature 3T3-L1 adipocytes. *Mol.Ther.* 2004; **9**:209-217.
17. **Vellinga, J., Uil, T.G., de Vrij, J., et al.** A system for efficient generation of adenovirus protein IX-producing helper cell lines. *J.Gene Med.* 2006; **8**:147-154.



18. **Murakami, P. and McCaman, M.T.** Quantitation of adenovirus DNA and virus particles with the PicoGreen fluorescent Dye. *Anal.Biochem.* 1999; **274**:283-288.
19. **Sittler, A., Gallinaro, H., and Jacob, M.** The secondary structure of the adenovirus-2 L4 polyadenylation domain: evidence for a hairpin structure exposing the AAUAAA signal in its loop. *J.Mol.Biol.* 1995; **248**:525-540.
20. **He, T.C., Zhou, S., da Costa, L.T., et al.** A simplified system for generating recombinant adenoviruses. *Proc.Natl.Acad.Sci.U.S.A* 1998; **95**:2509-2514.
21. **Ono, H.A., Le, L.P., Davydova, J.G., et al.** Noninvasive visualization of adenovirus replication with a fluorescent reporter in the E3 region. *Cancer Res.* 2005; **65**:10154-10158.
22. **Caravokyri, C. and Leppard, K.N.** Constitutive episomal expression of polypeptide IX (pIX) in a 293-based cell line complements the deficiency of pIX mutant adenovirus type 5. *J.Virol.* 1995; **69**:6627-6633.
23. **Hong, J.S. and Engler, J.A.** The amino terminus of the adenovirus fiber protein encodes the nuclear localization signal. *Virology* 1991; **185**:758-767.
24. **Fabry, C.M., Rosa-Calatrava, M., Conway, J.F., et al.** A quasi-atomic model of human adenovirus type 5 capsid. *EMBO J.* 2005; **24**:1645-1654.
25. **Nemerow, G.R. and Stewart, P.L.** Role of alpha(v) integrins in adenovirus cell entry and gene delivery. *Microbiol.Mol.Biol.Rev.* 1999; **63**:725-734.
26. **Wickham, T.J., Mathias, P., Cheresch, D.A., and Nemerow, G.R.** Integrins alpha v beta 3 and alpha v beta 5 promote adenovirus internalization but not virus attachment. *Cell* 1993; **73**:309-319.
27. **de Haan, C.A., Li, Z., Te, L.E., et al.** Murine coronavirus with an extended host range uses heparan sulfate as an entry receptor. *J.Virol.* 2005; **79**:14451-14456.
28. **Kalyuzhniy, O., Di Paolo, N.C., Silvestry, M., et al.** Adenovirus serotype 5 hexon is critical for virus infection of hepatocytes *in vivo*. *Proc.Natl.Acad.Sci.U.S.A* 2008; **105**:5483-5488.
29. **Waddington, S.N., McVey, J.H., Bhella, D., et al.** Adenovirus serotype 5 hexon mediates liver gene transfer. *Cell* 2008; **132**:397-409.
30. **Patterson, S. and Russell, W.C.** Ultrastructural and immunofluorescence studies of early events in adenovirus-HeLa cell interactions. *J.Gen.Virol.* 1983; **64**:1091-1099.
31. **Reiser, H. and Stadecker, M.J.** Costimulatory B7 molecules in the pathogenesis of infectious and autoimmune diseases. *N.Engl.J.Med.* 1996; **335**:1369-1377.
32. **Drouin, M., Cayer, M.P., and Jung, D.** Adenovirus 5 and chimeric adenovirus 5/F35 employ distinct B-lymphocyte intracellular trafficking routes that are independent of their cognate cell surface receptor. *Virology* 2010; **401**:305-313.
33. **McNees, A.L., Mahr, J.A., Ornelles, D., and Gooding, L.R.** Postinternalization inhibition of adenovirus gene expression and infectious virus production in human T-cell lines. *J.Virol.* 2004; **78**:6955-6966.
34. **Heemskerk, B., Veltrop-Duits, L.A., van, V.T., et al.** Extensive cross-reactivity of CD4+ adenovirus-specific T cells: implications for immunotherapy and gene therapy. *J.Virol.* 2003; **77**:6562-6566.
35. **Cambiaggi, C., Scupoli, M.T., Cestari, T., et al.** Constitutive expression of CD69 in interspecies T-cell hybrids and locus assignment to human chromosome 12. *Immunogenetics* 1992; **36**:117-120.
36. **He, X.S., Draghi, M., Mahmood, K., et al.** T cell-dependent production of IFN-gamma by NK cells in response to influenza A virus. *J.Clin.Invest* 2004; **114**:1812-1819.

37. **Trinchieri, G., Matsumoto-Kobayashi, M., Clark, S.C., et al.** Response of resting human peripheral blood natural killer cells to interleukin 2. *J.Exp.Med.* 1984; **160**:1147-1169.
38. **Muruve, D.A.** The innate immune response to adenovirus vectors. *Hum.Gene Ther.* 2004; **15**:1157-1166.
39. **Di Paolo, N.C. and Shayakhmetov, D.M.** Adenovirus de-targeting from the liver. *Curr.Opin.Mol. Ther.* 2009; **11**:523-531.
40. **Xu, Z., Tian, J., Smith, J.S., and Byrnes, A.P.** Clearance of adenovirus by Kupffer cells is mediated by scavenger receptors, natural antibodies, and complement. *J.Virol.* 2008; **82**:11705-11713.
41. **Au, T., Thorne, S., Korn, W.M., et al.** Minimal hepatic toxicity of Onyx-015: spatial restriction of coxsackie-adenoviral receptor in normal liver. *Cancer Gene Ther.* 2007; **14**:139-150.
42. **Bangari, D.S., Shukla, S., and Mittal, S.K.** Comparative transduction efficiencies of human and nonhuman adenoviral vectors in human, murine, bovine, and porcine cells in culture. *Biochem.Biophys.Res.Comm.* 2005; **327**:960-966.
43. **Atencio, I.A., Grace, M., Bordens, R., et al.** Biological activities of a recombinant adenovirus p53 (SCH 58500) administered by hepatic arterial infusion in a Phase 1 colorectal cancer trial. *Cancer Gene Ther.* 2006; **13**:169-181.
44. **Chiocca, E.A., Abbed, K.M., Tatter, S., et al.** A phase I open-label, dose-escalation, multi-institutional trial of injection with an E1B-Attenuated adenovirus, ONYX-015, into the peritumoral region of recurrent malignant gliomas, in the adjuvant setting. *Mol.Ther.* 2004; **10**:958-966.
45. **Forsyth, P., Roldan, G., George, D., et al.** A phase I trial of intratumoral administration of reovirus in patients with histologically confirmed recurrent malignant gliomas. *Mol.Ther.* 2008; **16**:627-632.
46. **Markert, J.M., Medlock, M.D., Rabkin, S.D., et al.** Conditionally replicating herpes simplex virus mutant, G207 for the treatment of malignant glioma: results of a phase I trial. *Gene Ther.* 2000; **7**:867-874.
47. **Pulkkanen, K.J. and Yla-Herttuala, S.** Gene therapy for malignant glioma: current clinical status. *Mol.Ther.* 2005; **12**:585-598.
48. **Sonabend, A.M., Ulasov, I.V., and Lesniak, M.S.** Conditionally replicative adenoviral vectors for malignant glioma. *Rev.Med.Virol.* 2006; **16**:99-115.
49. **Glasgow, J.N., Everts, M., and Curiel, D.T.** Transductional targeting of adenovirus vectors for gene therapy. *Cancer Gene Ther.* 2006; **13**:830-844.
50. **Brouwer, E., Havenga, M.J., Ophorst, O., et al.** Human adenovirus type 35 vector for gene therapy of brain cancer: improved transduction and bypass of pre-existing anti-vector immunity in cancer patients. *Cancer Gene Ther.* 2007; **14**:211-219.
51. **Nandi, S., Ulasov, I.V., Rolle, C.E., et al.** A chimeric adenovirus with an Ad 3 fiber knob modification augments glioma virotherapy. *J.Gene Med.* 2009; **11**:1005-1011.
52. **van Houdt, W.J., Wu, H., Glasgow, J.N., et al.** Gene delivery into malignant glioma by infectivity-enhanced adenovirus: *in vivo* versus *in vitro* models. *Neuro Oncol.* 2007; **9**:280-290.
53. **Zheng, S., Ulasov, I.V., Han, Y., et al.** Fiber-knob modifications enhance adenoviral tropism and gene transfer in malignant glioma. *J.Gene Med.* 2007; **9**:151-160.
54. **Bischoff, J.R., Kirn, D.H., Williams, A., et al.** An adenovirus mutant that replicates selectively in p53-deficient human tumor cells. *Science* 1996; **274**:373-376.

55. **Edwards, S.J., Dix, B.R., Myers, C.J., et al.** Evidence that replication of the antitumor adenovirus ONYX-015 is not controlled by the p53 and p14(ARF) tumor suppressor genes. *J. Virol.* 2002; **76**:12483-12490.
56. **Subramanian, T., Vijayalingam, S., and Chinnadurai, G.** Genetic identification of adenovirus type 5 genes that influence viral spread. *J. Virol.* 2006; **80**:2000-2012.
57. **Yan, W., Kitzes, G., Dormishian, F., et al.** Developing novel oncolytic adenoviruses through bioselection. *J. Virol.* 2003; **77**:2640-2650.
58. **Symington, J.S., Lucher, L.A., Brackmann, K.H., et al.** Biosynthesis of adenovirus type 2 i-leader protein. *J. Virol.* 1986; **57**:848-856.
59. **Soloway, P.D. and Shenk, T.** The adenovirus type 5 i-leader open reading frame functions in cis to reduce the half-life of L1 mRNAs. *J. Virol.* 1990; **64**:551-558.
60. **de Leeuw, B., Su, M., ter Horst, M., et al.** Increased glia-specific transgene expression with glial fibrillary acidic protein promoters containing multiple enhancer elements. *J. Neurosci. Res.* 2006; **83**:744-753.
61. **Chartier, C., Degryse, E., Gantzer, M., et al.** Efficient generation of recombinant adenovirus vectors by homologous recombination in *Escherichia coli*. *J. Virol.* 1996; **83**:4805-4810.
62. **Harlow, E., Franza, B.R., Jr., and Schley, C.** Monoclonal antibodies specific for adenovirus early region 1A proteins: extensive heterogeneity in early region 1A products. *J. Virol.* 1985; **55**:533-546.
63. **Tollefson, A.E., Scaria, A., Saha, S.K., and Wold, W.S.** The 11,600-MW protein encoded by region E3 of adenovirus is expressed early but is greatly amplified at late stages of infection. *J. Virol.* 1992; **66**:3633-3642.
64. **Tollefson, A.E., Scaria, A., Hermiston, T.W., et al.** The adenovirus death protein (E3-11.6K) is required at very late stages of infection for efficient cell lysis and release of adenovirus from infected cells. *J. Virol.* 1996; **70**:2296-2306.
65. **Driesse, M.J., Vincent, A.J., Sillevs Smitt, P.A., et al.** Intracerebral injection of adenovirus harboring the HSVtk gene combined with ganciclovir administration: toxicity study in nonhuman primates. *Gene Ther.* 1998; **5**:1122-1129.
66. **Driesse, M.J., Esandi, M.C., Kros, J.M., et al.** Intra-CSF administered recombinant adenovirus causes an immune response-mediated toxicity. *Gene Ther.* 2000; **7**:1401-1409.
67. **Horst, M., Brouwer, E., Verwijnen, S., et al.** Targeting malignant gliomas with a glial fibrillary acidic protein (GFAP)-selective oncolytic adenovirus. *J. Gene Med.* 2007; **9**:1071-1079.
68. **Sillevis Smitt, P.A., Driesse, M.J., Wolbers, J., et al.** Treatment of relapsed malignant glioma with an adenoviral vector containing the herpes simplex thymidine kinase gene followed by ganciclovir. *Mol. Ther.* 2003; **7**:851-858.
69. **Vincent, A.J., Esandi, M.C., Avezaat, C.J., et al.** Preclinical testing of recombinant adenoviral herpes simplex virus-thymidine kinase gene therapy for central nervous system malignancies. *Neurosurgery* 1997; **41**:442-451.

CHAPTER 6

A STRATEGY FOR GENETIC MODIFICATION OF THE SPIKE-ENCODING SEGMENT OF HUMAN REOVIRUS T3D FOR REOVIRUS TARGETING

D.J.M. van den Wollenberg
S.K. van den Hengel
I.J.C. Dautzenberg
S.J. Cramer
O. Kranenburg
R.C. Hoeben

Gene Therapy (2008) **15**: 1567-1578;



INTRODUCTION

Orthoreovirus Type 3 Dearing (T3D) has been evaluated clinically as oncolytic agent [1,2]. The impetus for these studies has been the observation that reovirus T3D preferentially lyses tumor cells, especially those with an activated Ras signaling pathway [3-7]. The *Reoviridae* (*Respiratory Enteric Orphan viruses*) constitute a family of non-enveloped viruses with segmented double-strand (ds) RNA genomes. The three types of human reoviruses have 10 genome segments and are classified in the genus *orthoreovirus*. These viruses are not associated with disease in humans. In newborn mice, however, these viruses can cause lethal infections [8]. T3D is often studied and serves as a model for the family. Reovirus T3D enters the host cell through the interaction of the spike protein $\sigma 1$ with its cognate receptor, the junction adhesion molecule (JAM-A). In addition, sialic-acid groups at the cell surface can act as receptors [9-13]. The JAM-A-binding amino acids are located in the C-terminal head domain of $\sigma 1$ [12,14-16]. After cell attachment, integrin-binding motifs in the capsid protein $\lambda 2$, which forms the structural base for $\sigma 1$, bind $\beta 1$ -integrins and mediate endocytosis [17]. Following endosomal escape viral replication ensues. Capped plus-strand RNA molecules are formed by transcription of the genome segments by the viral RNA-dependent RNA-polymerase. Plus-strand RNA molecules are used for translation and also associates with viral core proteins in special virus-induced cellular compartments, the so-called “viral factories” [18]. The packaging of the 10 genomic segments must be well orchestrated, as each viral core must contain a single copy of each of the plus-strand transcripts. Recent studies suggest that sequences contained within the 130 nucleotides (nt) at the 5' terminus serve as identity label for each of the segments [19]. Negative-strand synthesis takes place within the newly-formed core, yielding dsRNA segments. These can be further transcribed, or included in maturing virions to be released by the infected cell [20-22]. The plus-strand RNAs contain the tetranucleotide sequence 'GCUA' at the 5' end and the pentanucleotide sequence 'UCAUC' at the 3' end, which may have a role in the encapsidation process [23].

The efficiency of reovirus-based oncolytic therapies is most likely compromised by the scarcity of reovirus receptors on the surface of tumor cells. Freshly isolated colorectal tumor cells resist T3D infection, probably due a lack of JAM-A on their surface [24]. The transduction efficiency and the tumor cell selectivity of oncolytic viruses, such as adenoviruses, has been enhanced by genetically incorporating ligands for alternative receptors [25]. However, genetic modification of reoviruses has been notoriously difficult. A few reports have been published on the genetic modification of member of the *Reoviridae* family

[21,26]. However, these systems are arduous and rather inefficient. Recently, a reverse genetics method has been described that relies on transfection of 10 different expression plasmids encoding all of the viral segments [27]. With this method, a heterologous transgene was engineered into one of the genome segments. However, the genetic modification of capsid components to amend viral tropism was not reported.

Here we describe a new technique for genetically modifying reoviruses. The technique was used for generating targeted T3D variants carrying (His)₆ tags at exposed positions in the head domain of the s1 spike. Reoviruses carrying the s1-(His)₆ spikes, but not wild-type T3D, can infect genetically engineered U118MG glioblastoma cells displaying a single-chain antibody fragment (scFv-His), recognizing the (His)₆ tag as an artificial receptor on their surface. The (His)₆-tagged reoviruses, in combination with the scFv-His-expressing U118MG cells, can serve as a basis for developing tumor-targeted reoviruses.

MATERIALS AND METHODS

Cell lines

The cell line 911 is adenovirus type 5 early region 1-transformed human embryonic retinoblasts [28]. U118MG human glioblastoma cells were obtained from Dr. B. de Leeuw (Erasmus Medical Center, Rotterdam, The Netherlands). All cell lines were cultured in Dulbecco's modified Eagle's medium (DMEM; Invitrogen, Breda, The Netherlands) supplemented with penicillin, streptomycin, glucose, and 8% fetal bovine serum (FBS; Invitrogen), unless otherwise specified. Cells were cultured in a 5% CO₂ atmosphere at 37°C.

Reovirus propagation

The cell line 911 was used to propagate wild-type T3D (American Type Culture Collection, VR-824) as described previously [29]. Briefly, cells were exposed to reovirus in DMEM/2% FBS for 2 hrs at 37°C, 5% CO₂. Subsequently, the inoculum was replaced by DMEM containing 8% FBS. The virus was harvested 48 hrs postinfection by resuspending the cells in phosphate-buffered saline (PBS) with 2% FBS and subjecting the suspension to three cycles of freezing and thawing. The sample was cleared by centrifugation for 10 min at 800x *g*. Where indicated, the virus was further purified by CsCl equilibrium centrifugation essentially as described [28]. In some experiments the R124 clonal isolate was used. This isolate was purified from the VR-824 stock obtained from the ATCC by

two rounds of plaque purification on 911 cells. The infectious reovirus titer was determined by plaque assay on 911 cells.

Cell viability assay

WST-1 reagent (Roche, Woerden, The Netherlands) was used to assay the viability of cells after reovirus infections. Cells were infected with different amounts of reovirus in 96-well plates and WST-1 reagent was added, according to the manufacturer's instructions, at various time points post infection.

Cloning of T3D S1 from infected 911 cells

Cultures of 911 cells were infected with wild-type reovirus T3D at an MOI of ~ 2 plaque-forming units (pfu)/cell. Total cellular RNA was extracted 24 hrs postinfection using the Absolutely RNA miniprep kit (Stratagene, Huissen, The Netherlands). First-strand cDNA synthesis employed the ReoS1 Rev primer, using SuperScript II reverse transcriptase (Invitrogen). *Pfu* polymerase (Promega, Leiden, The Netherlands) was used for template amplification. See table 6.1 for details about the primers and the PCR fragments. The PCR product was purified from a 1% agarose gel using the JetSorb kit (Genomed, ITK Diagnostics, Uithoorn, The Netherlands). The product was digested using *Hind*III and *Not*I, and cloned into the plasmid pCDNA3.1+ (Invitrogen) digested with the same enzymes, yielding plasmid pRT3S1. The sequence of the insert was verified at the Leiden Genome Technology Center.

To insert the codons for the (His)₆ tag at the C-terminus of $\sigma 1$, the $\sigma 1$ -coding region was PCR amplified with primers HisReoS1_Rev and ReoS1_For table 6.1. The PCR product was digested with *Hind*III and ligated to *Hind*III- and *Eco*RV-digested pCDNA3.1+. The resulting plasmid was used as template for PCR amplification with primers SigmaEnd_Rev and ReoS1_For and, after digestion with *Hind*III, ligated into *Hind*III and *Eco*RV-digested plasmid pCDNA3.1+, generating plasmid pRT3S1His.

The sequences of all the constructs described in this study are available on request.

Table 6.1 Primers used in this study

Method	Primer name	Primer number	Sequence	Primer combi	Fragment length (bp)
JAM detection	hJAM For	1	5'-TGGGGACAAAGGCGCAAGTC-3'		
	hJAM_RT Rev	2	5'-CACCAGGAATGACGAGGTC-3'	1+2	928
S1 cloning	ReoS1 For	3	5'-CCAAGCTTGCATTGGTCGGATGATCCTCG-3'		
	ReoS1 Rev	4	5'-ATTGCGGCCGCGATGAAATGCCCCAGTGCCG-3'	3+4	1435
His-tag addition	HisReoS1 Rev	5	5'-GCAGGGTGGTCTGATCCTCAGTATGGT GATGGTATCGCTGAAACTACGCGGGTA-3'	3+5	1423
	SigmaEnd Rev	6	5'-GATGAAATGCCCCAGTGCCGCGGGG TGGTCTGATCCTCA-3'	3+5	1442
S1His RT-PCR	S1endR	7	5'-GATGAAATGCCCCAGTGC-3'	3+7	1442
	His-Rev	8	5'-GTGATGGTGATGGTGATG-3'	3+8	1403
β -actin RT-PCR	Hum_ β -actin For	9	5'-CAAGAGATGGCCACGGCTGCT-3'		
	Hum_ β -actin Rev	10	5'-TCCTTCTGCATCCTGTCTGGGCA-3'	9+10	275
JAM-ECD cloning	JamDP For	11	5'-TGTA CTGCAGTGC ACTCTTCTGAACC TGAAGT-3'		
	JamDP Rev	12	5'-TATGCTGCAGGACCCCCACATTCCGCT-3'	11+12	755

Reverse transcription-PCR

Primers used for the RT-PCR procedures are listed in table 6.1. For the detection of human JAM-A RNA, 911 cells and U118MG cells were seeded on 5 cm dishes and total cellular RNA was isolated using the Absolutely RNA miniprep kit (Stratagene). In all cases, SuperScript II was used to generate first-strand cDNA. For the characterization of the 911S1His cell line, total cellular RNA was extracted from confluent cultures of 911 and 911S1His cells, as described above. For the detection of S1His in reovirus batches, infections of 911 cells were performed. RNA was isolated 24 hrs after infection and used for RT-PCR amplification. The resulting PCR products were cloned into plasmid pTOPO-TA (Invitrogen) and their DNA sequences were determined.

Production of lentiviral vectors

All lentiviral constructs used in this study were based on the pLV-CMV-x-IRES-Neo vector [30] figure 6.3. The S1His region of plasmid pRT3S1His was released by *Eco*105I and *Xba*I digestion and inserted in the same restriction sites of pLV-CMV-x-IRES-Neo. To generate the HA-JAM lentiviral expression vector, plasmid

pCDNA-HA-JAM [31] (kindly provided by Dr. U.P Naik, Delaware, Newark) was digested with *Eco*105I and *Xba*I and inserted in pLV-CMV-BC-Neo. Plasmid pLV-JAM-ECD-IRES-Neo was made by first inserting the codons for the extracellular domain (ECD) of JAM into pDisplay (Invitrogen) and cloning the *Eco*105I-*Xho*I fragment into the same sites of the pLV vector. pCDNA-HA-JAM was used as template to amplify the JAM-ECD (see table 6.1) . To generate pLV-scFvHis-IRES-Neo, encoding the anti-His tag single-chain antibody fragment, pHissFv.rec [32] (a kind gift from Dr. D.T. Curiel, Univ. of Alabama) was digested with *Eco*105I and *Xho*I and inserted in the pLV vector. Production of the lentiviral vectors and transduction of the cells were performed as described previously [30,33]. The LV-S1His vector was used for transducing cultures of 911 cells at an estimated MOI of 0.5. The polyclonal, G418-resistant cell population, referred to as 911S1His cells were used for further studies.

Generation of modified reoviruses carrying the S1His segment

Wild-type reoviruses were used to infect 911S1His cells according to routine procedures. After three rounds of propagation, the resulting σ 1-His containing viruses were harvested by freeze thawing and used to infect U118scFvHis cells. The virus produced in U118scFvHis cells was harvested at the first signs of CPE, and serially passaged several times in U118scFvHis cells.

[³⁵S]Methionine labeling

Infected or mock-infected cells were incubated with Redivue [³⁵S]methionine Pro-mix (200 μ Ci/ml; Amersham, Roosendaal, the Netherlands) for 4 hrs at various time points post infection. Cells were washed once with PBS and lysed in Giordano Lysis Buffer (50 mM Tris-Cl (pH=7.4), 250 mM NaCl, 0.1% Triton, 5 mM EDTA) containing protease inhibitors (Complete mini tablets, Roche Diagnostics, Almere, The Netherlands). All labeling assays were performed in 24-wells plates with 5 μ l Pro-mix per well. The cells were lysed with 100 μ l lysis buffer per well. Fifty μ l of the lysates was loaded on a 10% SDS-polyacrylamide gel after addition of sample buffer. Gels were dried and exposed to a radiographic film to visualize the labeled proteins.

Immunofluorescence assay

For immunofluorescence assays, cells were grown on round glass cover slips in 24-well plates, fixed with methanol, washed with PBS containing 0.05% Tween-20, and incubated with a primary antibody against the oligo (His) tag

primary antibody (Sigma Aldrich, Zwijndrecht, The Netherlands). The coverslips were washed and incubated with secondary fluorescein isothiocyanate (FITC)-conjugated goat anti-mouse serum for 30 min at room temperature. The mounting solution consisted of glycerol containing 0.02 M Tris-HCl (pH=8.0), 2.3% 1,4-diazabicyclo-[2.2.2]-octane and 0,5 µg/ml 4',6-diamidino-2-phenylindole (DAPI) to visualize the nuclei.

Western blot analysis

Cell lysates were made in Giordano lysis buffer supplemented with protease inhibitors. Reovirus lysates were prepared by adding 15 ml of cleared reovirus to 5 ml of Western sample buffer (final concentrations: 10% glycerol, 2% SDS, 60 mM Tris-Cl (pH 6.7), 2.5% b-mercaptoethanol, and 2.5% bromophenol blue). After incubation for 3 min at 100°C, the samples were analyzed on SDS 10% polyacrylamide gels. The proteins were transferred to Immobilon-P (Millipore, Etten-Leur, The Netherlands) and visualized using standard protocols. Primary antibodies used were the Penta-His antibody (Qiagen, The Netherlands) for detection of the (His)₆ tag and 7F4 directed against reovirus protein λ2 [34] (kindly provide by Dr. K. Tyler, University of Colorado Health Science Center, Denver, Colorado). The secondary antibody used was horseradish peroxidase-conjugated Goat anti-Mouse IgG (Santa Cruz Biotechnology, Santa Cruz, USA).

Selective eradication assay

U118MG cells were transduced with a lentiviral vector encoding the eGFP gene [33]. The resulting U118eGFP cells were mixed with U118scFvHis cells and seeded in six-well plates. The mixed cultures were either mock infected, or infected with R124-S1His (MOI of ~1 pfu/cell). At the indicated time points after the infection, the cocultures were trypsinized and the cells were collected in PBS. These cell suspensions were analyzed for eGFP activity using a BD LSRII flow cytometer and BD FACSDiva software (BD Bioscience, Breda, The Netherlands).

RESULTS

The efficacy and specificity of oncolytic-virus approaches can be enhanced by targeting infection to tumor cells. The development of targeted reoviruses has been hampered by the difficulties in applying reverse genetics procedures to the segmented dsRNA genomes of these viruses. Therefore we set out to develop a novel technique for generating such genetically targeted reoviruses (figure 6.1). A cell line was selected that supports reovirus replication but resists infection

due to the absence of reovirus receptors. This cell line was endowed with a cell-surface protein that can function as an artificial receptor. The codons for the peptide ligand were engineered in a suitable position in one of the reovirus capsid proteins. Finally, the genomic segment encoding this modified capsid protein was introduced in the reovirus genome.

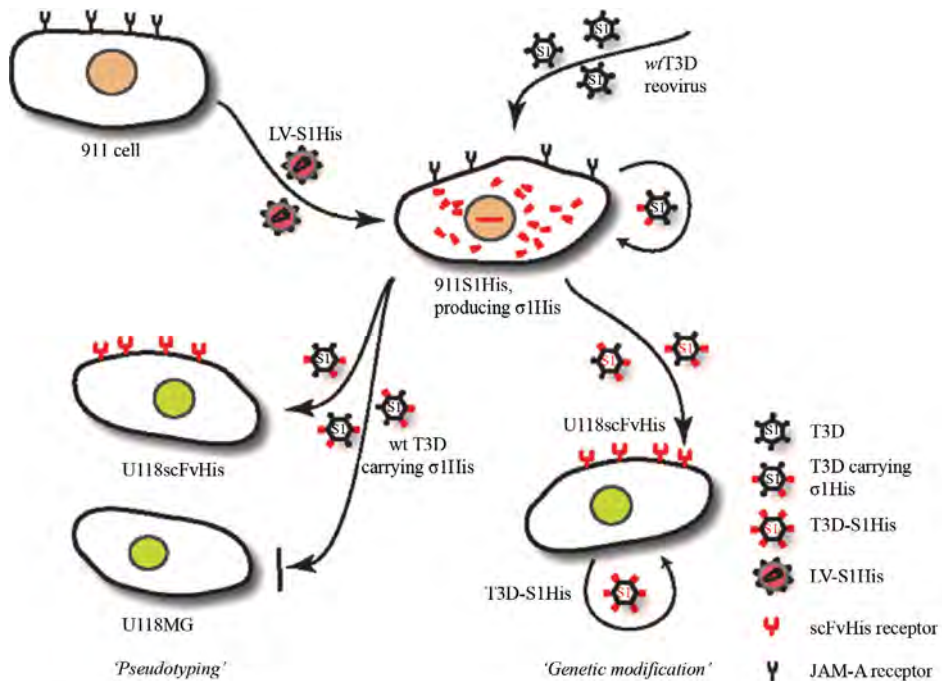


Figure 6.1 Schematic representation of the selection system for a targeted reovirus. The lentivirus vector LV-S1His was used to transfer a reovirus S1-expression cassette into 911 cells. The resulting 911S1His cells produce the $\sigma 1$ protein carrying the (His)₆ tag at its C-terminus. On infection of the 911S1His cells with wild-type T3D, the progeny viruses may carry a mixture of $\sigma 1$ -His and $\sigma 1$ spike proteins in their capsid. As a consequence, these viruses can infect the U118scFvHis cells that display an anti-His-tag single chain-antibody on their cell surface which can serve as an artificial receptor. Unmodified U118MG cells resist reovirus infection. Sequential passaging of virus in U118scFvHis cells selects for viruses in which the wild-type S1 segment has been replaced by the heterologous S1His segment during replication in the 911S1His cells.

JAM-A deficiency underlies U118MG resistance to reovirus infection.

A cell line lacking reovirus receptors and, as a result, resistant to infection, is crucial in the development of genetically retargeted reoviruses. On the basis of published data [35], the human glioblastoma cell line U118MG was selected as a

candidate. To confirm its resistance to reovirus infection, cultures of U118MG cells were exposed to T3D and assayed for cell viability (figure 6.2 A). The viability of U118MG cells was not affected by T3D, up to a multiplicity of infection (MOI) of 100. In contrast, survival of the control cell line 911 declined significantly after infection at a MOI of 0.001. The viability of the cells, as measured by WST-1 assay, strongly correlated with the induction of cytopathic effect (CPE) (data not shown).

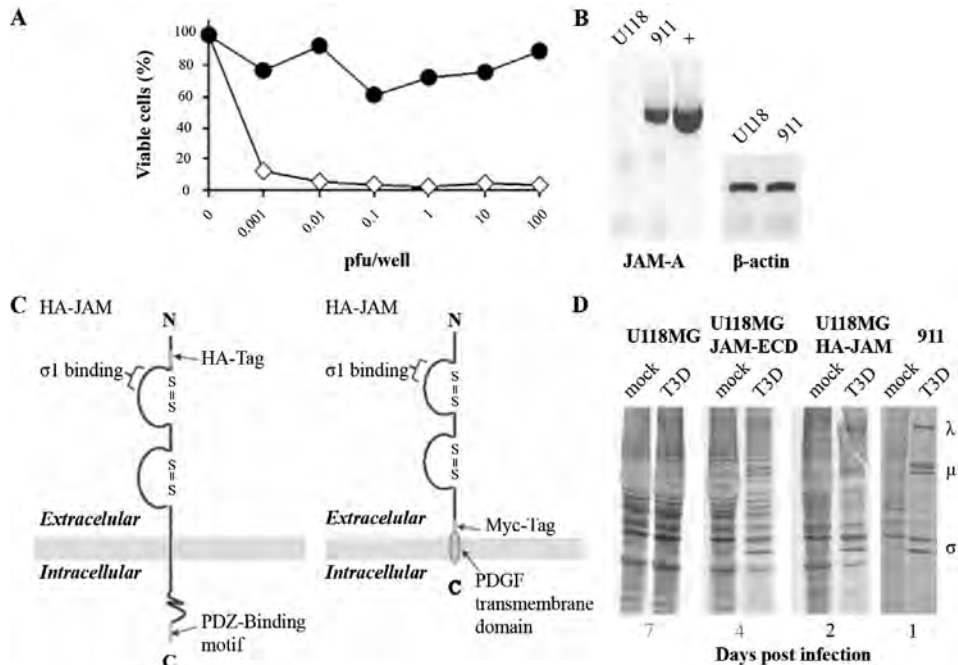


Figure 6.2 U118MG cells resist reovirus infection due to a lack of JAM-A expression.

(A) U118MG cells survive reovirus infection. The viability of cultures of U118MG cells (\bullet) and cultures of 911 cells (\diamond) infected with increasing amounts of reovirus T3D was measured two days post-infection by WST-1 assay. **(B)** hJAM-1 RNA is absent in U118MG cells. RNA from U118MG cells (U118) and 911 cells was isolated and used for cDNA synthesis with primer hJAM_RT rev (see table 6.1). As a positive control (+), a small amount of the pCDNA-HA-JAM plasmid was included in a PCR reaction (product length see table 6.1). A β -actin-specific RT-PCR assay was performed to confirm the integrity of the RNA. **(C)** Schematic representation of the HA-JAM and JAM-ECD proteins displayed at the cell membrane. **(D)** Display of JAM-A or its extracellular domain-sensitized U118MG cells to reovirus T3D. Reovirus T3D-infected cells and mock-infected cells were labeled with [35 S]-methionine once CPE became apparent, and protein samples were analyzed by SDS-PAGE. The positions of the reoviral σ , μ , and λ proteins are indicated. JAM-A, junction adhesion molecule-A; RT-PCR, reverse transcription-PCR

To determine whether the resistance of U118MG cells to T3D is due to the absence of the reovirus receptor JAM-A [9,36,37], RNA isolated from U118MG cells and 911 cells was assayed for the presence of JAM-A mRNA by reverse transcription-PCR (RT-PCR) using a JAM-A-specific primer set. The RNA from U118MG cells yielded no detectable PCR product (figure 6.2 B), confirming the absence of JAM-A. This was further corroborated by immunofluorescence microscopy with JAM-A-specific antisera (data not shown). In contrast, JAM-A mRNA was readily detectable in 911 cell-derived RNA (figure 6.2 B).

To study whether the absence of JAM-A is the sole factor contributing to the resistance of U118MG cells to T3D infection, U118MG cells were transduced with a lentiviral vector encoding hemagglutinin (HA)-tagged JAM-A (figure 6.3). In another vector (LV-JAM-ECD), the extracellular domain (ECD) of JAM-A was linked to a heterologous transmembrane domain to formally rule out JAM-A-mediated signaling (figure 6.2 C). Parental U118MG cells and HA-JAM- or JAM-ECD-expressing U118MG cells were exposed to T3D and metabolically labeled with [³⁵S]-methionine to assess reovirus-protein synthesis, as an indicator for viral replication. No synthesis of reovirus proteins was observed up to 7 days postinfection in U118MG. In contrast, synthesis of the reovirus proteins was detectable in the HA-JAM- and JAM-ECD-expressing U118MG derivatives (figure 6.2 D). Note that host-protein synthesis is not fully shut off by reovirus in U118MG cells. Taken together, these data show that the absence of JAM-A on the surface of U118MG is the only reason for its resistance to reovirus T3D.

Expression of an artificial receptor on the surface of U118MG cells

As an artificial receptor that could be utilized by targeted reoviruses, we exploited a single-chain antibody fragment specific for stretch of six C-terminal histidine residues (scFv-His) [38] as an artificial receptor for the reovirus T3D. This scFv is expressed on the surface of mammalian cells, if linked to a transmembrane domain and has been previously used as an artificial receptor for propagation of recombinant adenoviruses [32]. The codons for scFv-His, linked to the transmembrane domain of the human platelet-derived growth factor receptor and an HA tag, were inserted in the vector pLV-CMV-x-IRES-Neo (Figure 6.3), and the resulting vector was used to transduce U118MG cells. Immunochemical staining confirmed homogeneous expression of the artificial receptor in the transduced U118MG cell population (data not shown).

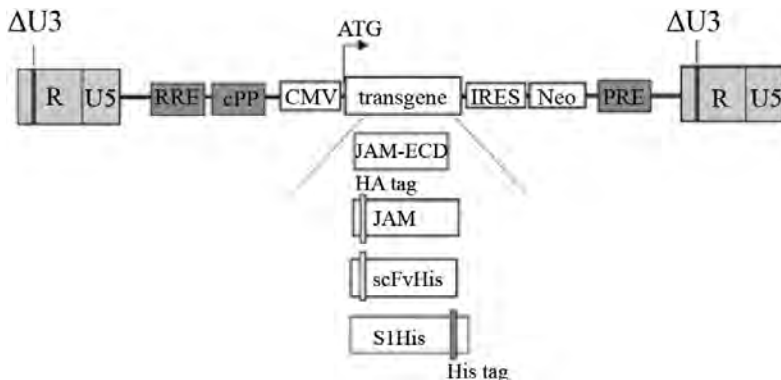


Figure 6.3 Lentiviral vectors used in this study. The scheme represents the integrated lentiviral vectors. The vectors are derived from a self-inactivating third-generation HIV-1 vector. Upon integration, the vector loses its capacity to produce mRNA other than the mRNA derived from the transgene expression cassette. The positions of the Rev-responsive Element (RRE), the central polypurine tract (cPPT), and the post-transcriptional regulatory element (PRE) are indicated. The transgenes were inserted upstream of the internal ribosome entry site (IRES) and the neomycin phosphotransferase (Neo) selection marker. JAM is the cDNA encoding human junction adhesion molecule. JAM-ECD encodes the extracellular domain of JAM-A fused to the PDGF transmembrane domain. scFvHis represents the single-chain antibody directed against the $(\text{His})_6$ tag. S1His is a modified cDNA of the reovirus T3D S1 segment in which the $(\text{His})_6$ tag is fused with $\sigma 1$. PDGF, platelet-derived growth factor.

Modification of $\sigma 1$ by adding a $(\text{His})_6$ tag to its C-terminus

To produce $\sigma 1$ variants, we opted to using a *trans*-complementation approach in which reovirus was propagated on a cell line producing one of the capsid components. The virus may incorporate the modified component in its capsid during virus generation. To generate reoviruses with modified $\sigma 1$ variants in its capsid, 911 cells were generated that stably express a modified S1 gene segments. The S1 genome segment was cloned from wild-type reovirus T3D-infected 911 cells, using primers chosen on the basis of the published S1 sequence [39]. The deduced $\sigma 1$ amino-acid sequence of the S1 genome segment cloned from the ATCC VR-824 T3D reovirus batch was found to differ from the published S1 sequence at two positions, Ile²⁴⁶ to Thr and Thr²⁴⁹ to Ile. These mutations are known to abolish a trypsin-sensitive site in the $\sigma 1$ shaft [40].

The codons for $(\text{His})_6$ tag were inserted by mutation PCR downstream of the triplet encoding the C-terminal Thr of $\sigma 1$. The resulting recombinant S1 genome segment encoding $(\text{His})_6$ -tagged $\sigma 1$ (S1His) was inserted into a lentiviral vector (figure 6.3). This vector was used to generate 911 cells, which stably express S1His. The synthesis of the $(\text{His})_6$ -tagged $\sigma 1$ ($\sigma 1$ -His) in the polyclonal 911S1His

cell lines was verified by immunofluorescence (figure 6.4 A), RT-PCR (figure 6.4 B and C, and table 6.1), and Western-blot analysis (figure 6.4 D). The staining pattern of σ 1-His (figure 6.4 A) is reminiscent of the morphology of the viral factory [8,41]. These data led us to conclude that σ 1-His protein was produced in the transduced cells.

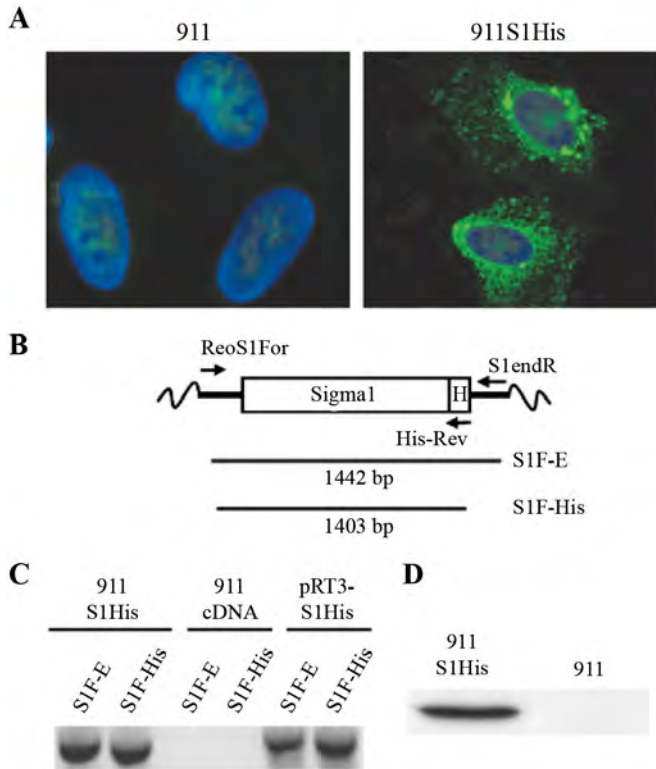


Figure 6.4 Characterization of the 911S1His cell line. (A) Immunofluorescence assay demonstrating the presence of the s-His protein in 911S1His cells. The mouse α -His antibody and FITC-coupled Goat-anti-Mouse sera (green) were used to detect the s1-His protein in the LV-S1His-transduced 911 cells. The nucleus is stained with DAPI (blue). **(B)** Schematic representation of S1His expression cassette after lentivirus-mediated gene transfer. The region coding for s1 is indicated by the open box. The primers used in the PCR assay and the expected PCR products are indicated. H represents the position of the (His)₆ tag (see Table 6.1 for the sequence of the primers). **(C)** RT-PCR to detect S1 RNA in 911S1His cells. Reverse transcription of 911S1His and 911 cell RNA was performed using primer S1endR. The plasmid pRT3S1His was used as a positive control for the PCR analysis which used the primers indicated in (B). The positions of the primers in the S1 segment, as well as the expected PCR products S1F-E and S1F-His, are indicated in (B). **(D)** Western analysis demonstrating the presence of the s1-His protein in 911S1His cell lysates. s1-His protein was detected with the Penta-His antibody. DAPI, 4',6'-diamidino-2-phenylindole; FITC, fluorescein isothiocyanate; RT-PCR, reverse transcription-PCR.



Reovirus pseudotyping by modification of sigma-1

To evaluate whether the σ 1-His protein was incorporated in the capsid, the 911S1His cells were infected with wild-type T3D, and the virus was passaged three times on the 911S1His cells. If σ 1-His is incorporated it could amend the tropism. To test the tropism, U118MG, U118HA-JAM and U118scFvHis cells were infected with either wild-type T3D or T3D from the third passage on 911S1His cells. T3D harvested from 911S1His cells, but not wild-type T3D virus, could infect and lyse U118scFvHis cells (figure 6.5 A). The cell-viability assay confirmed that U118MG cells resist the σ 1-His-containing T3D and showed survival of 10% of the U118HA-JAM cells at 3 days after exposure to the 911S1His-cell derived T3D. U118scFvHis cells exposed to the σ 1-pseudotyped T3D showed a drop of 55% in viability (figure 6.5 B). These data demonstrate that the 911S1His-derived reovirus can infect U118MG cells that express the scFvHis as an artificial receptor. From these results, we conclude that σ 1-His is incorporated in the reovirus capsid, that the (His)₆ tag is accessible to the artificial receptor and that interaction of this tag with its receptor leads to productive infection.

Selecting a genetically modified reovirus

Recent data suggest that the sequence motifs that facilitate assortment and packaging of the reovirus segments are contained within a 130 nt region at the 5' end of reoviral RNAs [19]. This region is also present in the heterologous transcripts produced in 911S1His cells. If the reoviral signals in the LV-S1His-derived σ 1-His-encoding transcripts are functional, these transcripts should associate with newly formed cores and replace the wild-type S1 segment in the progeny virus.

To test this hypothesis, we harvested the virus progeny from the U118scFvHis cells that were infected with s1-pseudotyped T3D. If the particles contain the S1His genome segment, it should be possible to propagate them on U118scFvHis cells. Indeed, a metabolic labeling experiment performed at 3 days postinfection showed that the reovirus particles produced in U118scFvHis cells could again infect U118scFvHis, in contrast to unmodified T3D (figure 6.6 A). The propagated virus, which was named T3D-S1His, was passaged 11 times and maintained the s1-His protein as assayed by Western blotting (figure 6.6 B). The presence of the (His)₆-tag was also confirmed by sequence analysis of cloned RT-PCR products (figure 6.7). These data suggest that S1His segment is incorporated as a genome segment in T3D and expanded its tropism.

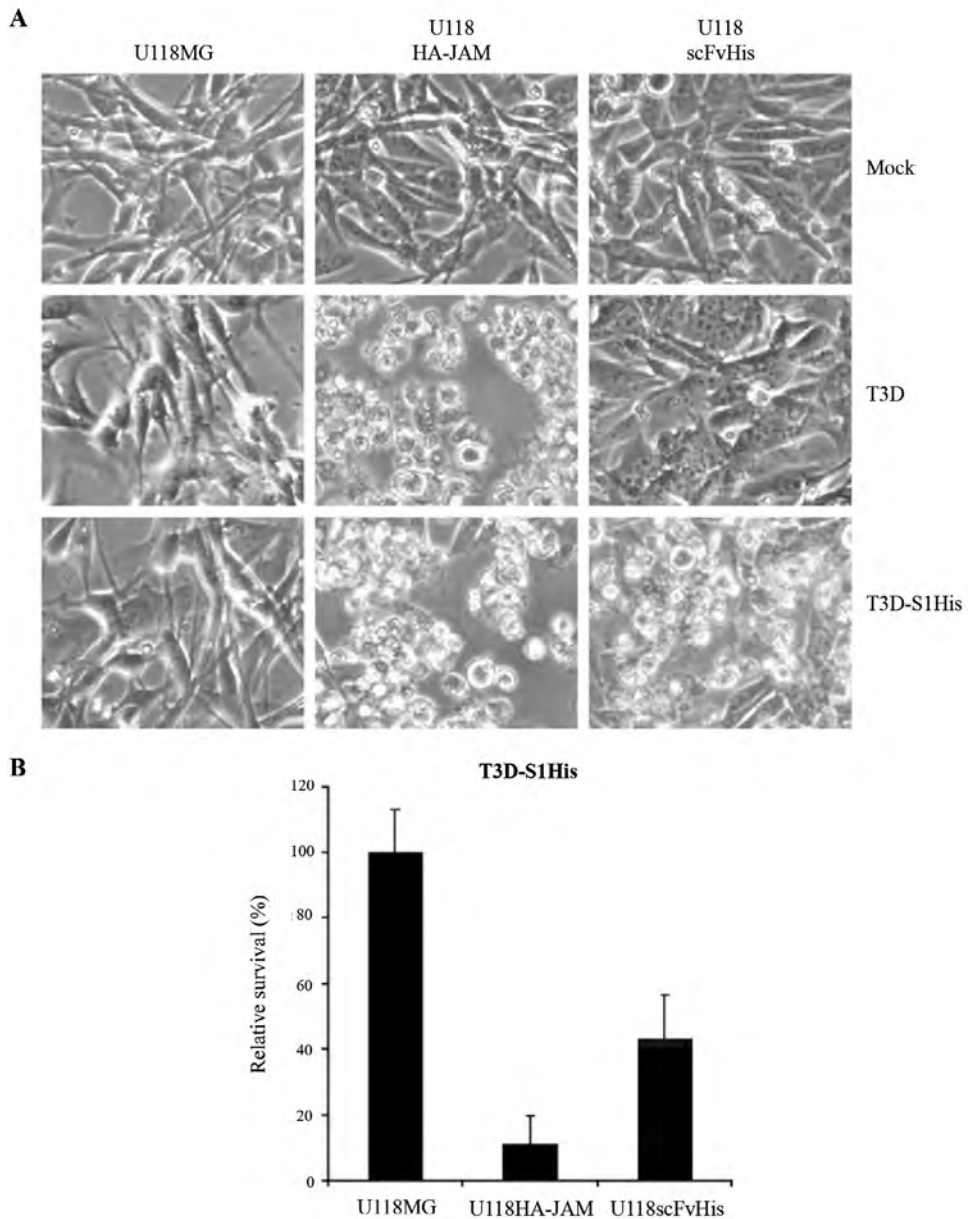


Figure 6.5 Pseudotyping of T3D reovirus after propagation in 911S1His cells. (A) CPE induction in cultures of U118scFvHis and U118HA-JAM cells, but not U118MG cells, infected with reovirus T3D harvested from 911S1His cells. Photos of CPE were taken 3 days post-infection. **(B)** Cell viability of U118MG, U118HA-JAM and U118scFvHis cells, as measured by WST-1 assay, 3 days after infection with reovirus T3D harvested from 911S1His cells. The relative survival is depicted normalized to mock-infected U118MG cells (mean of three measurements).

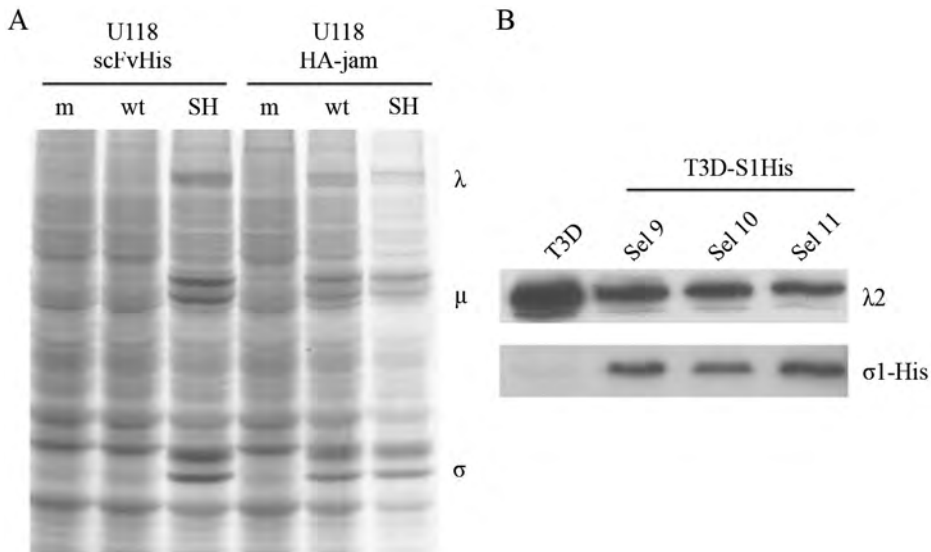


Figure 6.6 Selection of genetically stable T3D-S1His reovirus stock on U118scFvHis cells. (A) U118scFvHis cells synthesize reovirus proteins upon infection with T3D-S1His. [³⁵S]-methionine-incorporation assays were performed 3 days post-infection on U118scFvHis and U118HA-JAM cells infected with wild-type reovirus T3D (wt), T3D-S1His 740 (SH) reoviruses or mock-infected (m), respectively. (B) σ1-His is present in S1His reovirus batches as evidenced by Western analysis of reovirus-containing lysates. Western analyses were performed on different viral lysates for the presence of the (His)₆-modified s1 using the anti-His tag serum. T3D depicts a lysate of the unmodified reovirus T3D. Sel9-11 represents T3D reovirus lysates propagated for 9-11 passages on U118scFvHis cells. Loading controls using the antibody 7F4 against reovirus λ2 are depicted in the upper panel. (His)₆-tagged σ1 detected with Penta-His antibody is shown in the lower panel.

Selection for the (His)₆ tag co-select other alterations in genome segment S1

So far we have demonstrated that the (His)₆ tag of the S1 segment is incorporated in the reovirus. To test whether selection for the presence of the (His)₆ tag could be used for selecting other mutations in the same segment, we repeated the selection experiment with the T3D laboratory strain R124. The nucleotide sequence of S1 from R124 differs in two nucleotides from that used to construct LV-S1His (figure 6.7). This allows distinguishing the origin of the S1 sequences in the resulting T3D-S1His independent of the His tag sequences. After three passages of R124 on 911S1His cells, the virus was harvested and used to infect U118MG, U118HA-JAM and U118scFvHis cells. CPE was observed in U118HA-JAM and U118scFvHis cell cultures but not in the infected U118MG cultures. In contrast, non-speudotyped R124 only induced cell death in U118HA-JAM cells (data not shown).

	1	21		
σ1[pub]	MDPRLREEVVRLIIALTS DN GVSLSKGLESRVSALEKTSQIHS DTILRITQGLDDANKRIIALEQSRDDL			
σ1[R124]	MDPRLREEVVRLIIALTS DN GVSLSKGLESRVSALEKTSQIHS DTILRITQGLDDANKRIIALEQSRDDL			
σ1His[cloned]	MDPRLREEVVRLIIALTS DN GVSLSKGLESRVSALEKTSQIHS DTILRITQGLDDANKRIIALEQSRDDL			
σ1S1HisRT1	MDPRLREEVVRLIIALTS DN GVSLSKGLESRVSALEKTSQIHS DTILRITQGLDDANKRIIALEQSRDDL			
σ1S1HisRT2	MDPRLREEVVRLIIALTS DN GVSLSKGLESRVSALEKTSQIHS DTILRITQGLDDANKRIIALEQSRDDL			
σ1S1HisRT3	MDPRLREEVVRLIIALTS DN GVSLSKGLESRVSALEKTSQIHS DTILRITQGLDDANKRIIALEQSRDDL			
σ1S1HisRT4	MDPRLREEVVRLIIALTS DN GVSLSKGLESRVSALEKTSQIHS DTILRITQGLDDANKRIIALEQSRDDL			
	71	111		
σ1[pub]	VASVSDAQLAISRL ESSIGALQTVVNGLDSSVTQLGARVGQ LETGLAELRV DHDNLVARVDTAERNIGSL			
σ1[R124]	VASVSDAQLAISRL ESSIGALQTVVNGLDSSVTQLGARVGQ LETGLAELRV DHDNLVARVDTAERNIGSL			
σ1His[cloned]	VASVSDAQLAISRL ESSIGALQTVVNGLDSSVTQLGARVGQ LETGLAELRV DHDNLVARVDTAERNIGSL			
σ1S1HisRT1	VASVSDAQLAISRL ESSIGALQTVVNGLDSSVTQLGARVGQ LETGLAELRV DHDNLVARVDTAERNIGSL			
σ1S1HisRT2	VASVSDAQLAISRL ESSIGALQTVVNGLDSSVTQLGARVGQ LETGLAELRV DHDNLVARVDTAERNIGSL			
σ1S1HisRT3	VASVSDAQLAISRL ESSIGALQTVVNGLDSSVTQLGARVGQ LETGLAELRV DHDNLVARVDTAERNIGSL			
σ1S1HisRT4	VASVSDAQLAISRL ESSIGALQTVVNGLDSSVTQLGARVGQ LETGLAELRV DHDNLVARVDTAERNIGSL			
	141	154	163	190
σ1[pub]	TTELSTLTLRV TSIQADFESRI STLERTAV TSAGAPLSIRNNRMTMGLNDGLT LSGNNLAI RLPGNTGLN			
σ1[R124]	TTELSTLTLRV TSIQADFESRI STLERTAV TSAGAPLSIRNNRMTMGLNDGLT LSGNNLAI RLPGNTGLN			
σ1His[cloned]	TTELSTLTLRV TSIQADFESRI STLERTAV TSAGAPLSIRNNRMTMGLNDGLT LSGNNLAI RLPGNTGLN			
σ1S1HisRT1	TTELSTLTLRV TSIQADFESRI STLERTAV TSAGAPLSIRNNRMTMGLNDGLT LSGNNLAI RLPGNTGLN			
σ1S1HisRT2	TTELSTLTLRV TSIQADFESRI STLERTAV TSAGAPLSIRNNRMTMGLNDGLT LSGNNLAI RLPGNTGLN			
σ1S1HisRT3	TTELSTLTLRV TSIQADFESRI STLERTAV TSAGAPLSIRNNRMTMGLNDGLT LSGNNLAI RLPGNTGLN			
σ1S1HisRT4	TTELSTLTLRV TSIQADFESRI STLERTAV TSAGAPLSIRNNRMTMGLNDGLT LSGNNLAI RLPGNTGLN			
	221	246	249	
σ1[pub]	IQNGGLQFR FNTDQFQIVNNNLT LKTTV FDSINSR I GATE EQSYV ASAVT PLRLNS STKVL DML IDS STLE			
σ1[R124]	IQNGGLQFR FNTDQFQIVNNNLT LKTTV FDSINSR I GATE EQSYV ASAVT PLRLNS STKVL DML IDS STLE			
σ1His[cloned]	IQNGGLQFR FNTDQFQIVNNNLT LKTTV FDSINSR I GATE EQSYV ASAVT PLRLNS STKVL DML IDS STLE			
σ1S1HisRT1	IQNGGLQFR FNTDQFQIVNNNLT LKTTV FDSINSR I GATE EQSYV ASAVT PLRLNS STKVL DML IDS STLE			
σ1S1HisRT2	IQNGGLQFR FNTDQFQIVNNNLT LKTTV FDSINSR I GATE EQSYV ASAVT PLRLNS STKVL DML IDS STLE			
σ1S1HisRT3	IQNGGLQFR FNTDQFQIVNNNLT LKTTV FDSINSR I GATE EQSYV ASAVT PLRLNS STKVL DML IDS STLE			
σ1S1HisRT4	IQNGGLQFR FNTDQFQIVNNNLT LKTTV FDSINSR I GATE EQSYV ASAVT PLRLNS STKVL DML IDS STLE			
	281	305	325	
σ1[pub]	INSSGQLTV RSTSPNLRYP IA DVSGG IGMSP NYRFRQSMW IGIV YSGSGLNWRVQVNSD IFIV DDYIHI			
σ1[R124]	INSSGQLTV RSTSPNLRYP IA DVSGG IGMSP NYRFRQSMW IGIV YSGSGLNWRVQVNSD IFIV DDYIHI			
σ1His[cloned]	INSSGQLTV RSTSPNLRYP IA DVSGG IGMSP NYRFRQSMW IGIV YSGSGLNWRVQVNSD IFIV DDYIHI			
σ1S1HisRT1	INSSGQLTV RSTSPNLRYP IA DVSGG IGMSP NYRFRQSMW IGIV YSGSGLNWRVQVNSD IFIV DDYIHI			
σ1S1HisRT2	INSSGQLTV RSTSPNLRYP IA DVSGG IGMSP NYRFRQSMW IGIV YSGSGLNWRVQVNSD IFIV DDYIHI			
σ1S1HisRT3	INSSGQLTV RSTSPNLRYP IA DVSGG IGMSP NYRFRQSMW IGIV YSGSGLNWRVQVNSD IFIV DDYIHI			
σ1S1HisRT4	INSSGQLTV RSTSPNLRYP IA DVSGG IGMSP NYRFRQSMW IGIV YSGSGLNWRVQVNSD IFIV DDYIHI			
	351			
σ1[pub]	CLPAFDGFSI ADGGDLSLNFVT GLLP LLTGDTEPAFHNDVVTYGAQ TVAI GLSSGGAPQYMSKNLWVEQ			
σ1[R124]	CLPAFDGFSI ADGGDLSLNFVT GLLP LLTGDTEPAFHNDVVTYGAQ TVAI GLSSGGAPQYMSKNLWVEQ			
σ1His[cloned]	CLPAFDGFSI ADGGDLSLNFVT GLLP LLTGDTEPAFHNDVVTYGAQ TVAI GLSSGGAPQYMSKNLWVEQ			
σ1S1HisRT1	CLPAFDGFSI ADGGDLSLNFVT GLLP LLTGDTEPAFHNDVVTYGAQ TVAI GLSSGGAPQYMSKNLWVEQ			
σ1S1HisRT2	CLPAFDGFSI ADGGDLSLNFVT GLLP LLTGDTEPAFHNDVVTYGAQ TVAI GLSSGGAPQYMSKNLWVEQ			
σ1S1HisRT3	CLPAFDGFSI ADGGDLSLNFVT GLLP LLTGDTEPAFHNDVVTYGAQ TVAI GLSSGGAPQYMSKNLWVEQ			
σ1S1HisRT4	CLPAFDGFSI ADGGDLSLNFVT GLLP LLTGDTEPAFHNDVVTYGAQ TVAI GLSSGGAPQYMSKNLWVEQ			
	421	455	461	
σ1[pub]	WQDGV LRLRVEGGGS ITH SNSKWPAMTVS Y PRSFT -----			
σ1[R124]	WQDGV LRLRVEGGGS ITH SNSKWPAMTVS Y PRSFT -----			
σ1His[cloned]	WQDGV LRLRVEGGGS ITH SNSKWPAMTVS Y PRSFT HHHHHH			
σ1S1HisRT1	WQDGV LRLRVEGGGS ITH SNSKWPAMTVS Y PRSFT HHHHHH			
σ1S1HisRT2	WQDGV LRLRVEGGGS ITH SNSKWPAMTVS Y PRSFT HHHHHH			
σ1S1HisRT3	WQDGV LRLRVEGGGS ITH SNSKWPAMTVS Y PRSFT HHHHHH			
σ1S1HisRT4	WQDGV LRLRVEGGGS ITH SNSKWPAMTVS Y PRSFT HHHHHH			



Figure 6.7 Amino-acid sequence of different $\sigma 1$ and $\sigma 1$ -His proteins. The amino-acid sequence alignment of $\sigma 1$ (455 aa) and $\sigma 1$ His (461 aa) is shown. The upper sequence (s1[pub]) is the published sequence of $\sigma 1$ (accession number gi|333742|gb|M10262.1). R124 is our lab strain of reovirus T3D. The isolate was purified from the VR-824 stock obtained from the ATCC by two rounds of plaque purification on 911 cells. $\sigma 1$ His (cloned) is the sequence in pRT3S1His. $\sigma 1$ His RT1 and -2 are two RT-PCR amplified clones from the ATCC-T3D-derived T3D-S1His viruses. $\sigma 1$ His RT3 and -4 are amplified clones from the R124-S1His virus. The amino-acid changes are color-coded. RT-PCR, reverse transcription-PCR.

The virus produced in the U118scFvHis cells was passaged for six times on this cell line. The resulting virus, named R124-S1His, was used again to infect U118scFvHis cells. After confirming the presence of the (His)₆-tagged $\sigma 1$ (figure 6.8 A), RNA was isolated from infected cells and the S1 segments were cloned after RT-PCR amplification. Sequence analysis confirmed the presence of the (His)₆-tag encoding sequence. All clones have a sequence identical to the cloned S1His, rather than the R124-S1, at the positions which differ between isolates (figure 6.8 B en C). These data suggest that selection for the presence of the (His)₆ tag leads to incorporation of the entire S1 segment into reovirus particles. A few additional changes were found in the s1 encoded by the S1 of R124-S1His (figure 6.7). This can be attributed to the RNA-dependent RNA polymerase's relative lack of fidelity [42]. The fact that all the clones contained a S325Y mutation suggest that this mutation occurred early during passaging on U118scFvHis cells. Taken together, our data are consistent with a mechanism in which the entire S1 genome segment is replaced by the S1His segment.

Selective infection of cells in a mixed population by a targeted reovirus

To verify that genetically targeted reoviruses could be used to selectively eradicate specific cells in a mixed population, U118scFvHis cells were plated with U118-eGFP cells to represent target and non-target cells, respectively. A number of these mixed cultures were exposed to the R124-S1His virus at an MOI of 1.5. At various time points after infection the relative number of eGFP-positive cells was determined by flow-cytometry (figure 6.8 D). The relative number of eGFP-positive cells increased more than 5.4-fold in comparison with mock-infected cultures at 96 hrs post infection. These data demonstrate selective eradication of sensitized cells by a genetically targeted reovirus.

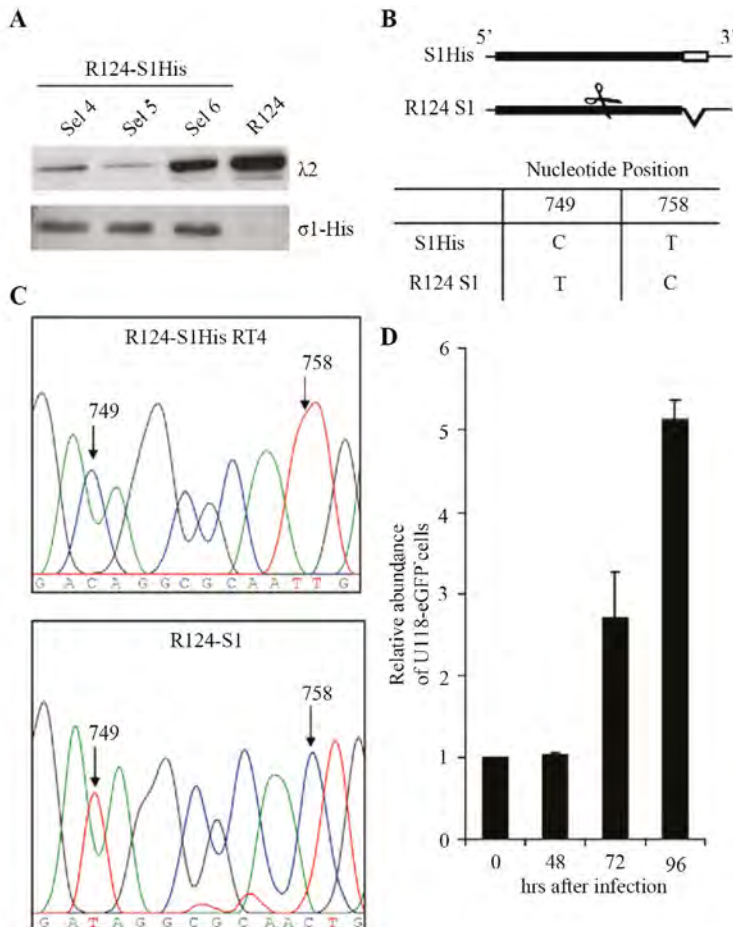


Figure 6.8 Selection of R124-S1His reoviruses on U118scFvHis cells. (A) The s1-His protein is present in lysates of R124-S1His reoviruses serially passaged on U118scFvHis cells. R124 is a lysate of the plaque-purified T3D reovirus. Sel4-6 depict R124-S1His reovirus lysates isolated after the indicated number of passages on U118scFvHis cells. Upper panel: Western blot analysis for λ2. The presence of λ2 was confirmed by western blotting using the 7F4 specific for λ2. Lower panel: Western blotting demonstrates the presence of (His)₆-tagged σ1 with the Penta-His antibody in the R124-S1His virus. (B) Nucleotide differences distinguish the cloned S1His sequence and the R124 S1 sequence. The amino acids coded by codons at positions 749 and 758 of the R124-S1 create a trypsin-cleavable site in σ1 ("). (C) Sequence analyses depict the differences at nucleotides 747-760 of RT-PCR clone R124-S1His RT4 and R124. Arrows represent the nucleotide differences at position 749 and 758. (D) The R124-S1His reovirus specifically eradicates the U118scFvHis cells from a mixed population. A mixture of U118scFvHis and U118-eGFP cells were infected with R124-S1His reovirus at an MOI of 2, and samples were taken for flow-cytometric analyses at the indicated times after the infection. Represented is relative frequency of GFP-positive cells in the virus-infected cultures relative to mock-infected cultures. These data show that the relative frequency of the R124-S1His-*resistant* eGFP-positive cells increased more than 10-fold upon selective eradication of the cells which are sensitive to the targeted reovirus. GFP, green fluorescent protein; MOI, multiplicity of infection; RT-PCR, reverse transcription-PCR.

DISCUSSION

Reverse genetics in RNA viruses with segmented genomes has been technically challenging. For Reoviridae, this is due, at least in part, to the difficulties in achieving sufficient quantities of non-polyadenylated plus-strand reovirus RNAs in the cytoplasm of mammalian cells. The previously described methods to manipulate reovirus genomes either involve transfection of RNA synthesized *in vitro* or employ T7 polymerase-driven expression cassettes [21,26,27]. In these techniques, ribozymes generate transcripts with 3' ends, which are identical to normal segment termini. In general, such transcripts are unstable since they lack a poly-A tract [21,26,27]. Here we show that also polyadenylated transcripts generated with a conventional RNA polymerase II expression cassette can be used to replace a genome segment. A transcript containing a modified copy of the reovirus T3D S1 segment, encoding a (His)₆-tagged version of the spike protein $\sigma 1$, was stably expressed. This protein was capable of binding a single-chain antibody fragment for oligo (His) tags. Propagation of wild-type T3D on cells producing s1-His led to its incorporation into reovirus capsids. A similar strategy has been previously used for other capsid proteins of reoviruses [43] and other non-enveloped viruses such as adenoviruses [44,45]. However, if the genetic sequences encoding the modified capsid protein are not encapsidated, the altered targeting specificity would be lost after a single round of replication.

The transcripts encoded by the lentivirus vector LV-S1His contain all genetic information and most likely also the structural information contained within the S1 segment, for example the motifs regulating plus- and minus-strand synthesis. We hypothesized that these transcripts would be targeted to the 'viral factories' and here associate with newly formed viral cores. Furthermore, if the signals for minus-strand synthesis [22,46] are functional, the S1 part of the lentiviral transcript should be converted in dsRNA. Secondary transcription of this dsRNA would lead to S1 segments with authentic termini. Our results propagating the T3D-S1His variant support these hypotheses.

Based on our hypothesis, we anticipated that the entire LV-S1His-derived genome segment, rather than only the region encoding the (His)₆ tag, would become incorporated into the virion. This was confirmed using the R124 strain in the selection. The reovirus selected after infection of the U118scFvHis with the R124 strain propagated in 911S1His cells contained the sequence of the (His)₆-tagged s1-encoding segment instead of the S1 from R124 at the isolate-specific positions. These findings are consistent with the model that the entire S1His segment is derived from the transcript specified by LV-S1His.

This approach may prove useful for improving reoviruses as oncolytic agents. To date, only wild-type T3D has been used in clinical trials [2,6,47]. The results of this approach are encouraging and the procedure is well tolerated. However, the scarcity or inaccessibility of reovirus receptors on the surface of tumor cells may limit the efficacy of wild-type reoviruses as oncolytic agents. We recently reported that cultures of colorectal tumor cells isolated from resected tumor material resist reovirus infection, despite the presence of JAM-A [48]. This is likely attributable to the insufficient expression of reovirus receptors at their plasma membranes since T3D-derived infectious subviral particles, which are known to enter cells independent of JAM-A and sialic acid, efficiently infect and lyse these cells. Further development of the approach presented here should allow modification of reoviruses to enhance tumor cell transduction and reduce the infection of non-target cells. This will increase the safety and efficacy of anticancer strategies using reoviruses as oncolytic agents.

We have developed a simple technique to genetically modify reoviruses, and identified the C-terminus of $\sigma 1$ as a good location for insertion of a targeting oligopeptides. Moreover, the (His)₆ tag at the C-terminus of $\sigma 1$, in combination with the U118scFvHis cells allowed the construction of reoviruses that do not depend on JAM-A for attachment and cell entry. Furthermore, the development of tumor-targeted reoviruses can benefit from the experience with targeted adenoviruses, especially as the spatial structure of the reovirus spike is remarkably similar to the adenovirus fiber [49].

This reovirus genetic-modification technique developed in this study may be widely applicable. It may be adapted for other reovirus genome segments [50]. This would allow generation of defined mutants for gaining insight in the intricate interactions between the reoviruses and their hosts, and to address questions about virus structure, function, and pathogenesis. The strategy may be amendable for use in other Reoviridae. Although from the family name one may get the impression that all its members are 'orphan' viruses, some of them cause severe diseases and have considerable economic impact. Members of its genera *Orbivirus* and *Coltivirus* cause diseases of humans, for example Colorado tick fever, and of domestic livestock, for example African horse sickness and blue-tongue disease [51]. Moreover, members of the genus *Rotaviruses* are the major etiologic agents of serious diarrhea in children under 2 years of age [52]. In these genera, too, this reverse genetics technique may be very useful.

ACKNOWLEDGEMENTS

We thank Martijn Rabelink and Cynthia Sitaram for their expert technical assistance. We gratefully acknowledge Drs Lee Fradkin, Hans Tanke, Danijella Koppers-Lalic, and Twan de Vries for their helpful discussions and critically reading the manuscript.

CHAPTER 7

ISOLATION OF REOVIRUS T3D MUTANTS CAPABLE OF INFECTING HUMAN TUMOR CELLS INDEPENDENT OF JUNCTION ADHESION MOLECULE-A

D.J.M. van den Wollenberg*

I.J.C. Dautzenberg*

S.K. van den Hengel

S.J. Cramer

R.J. de Groot

R.C. Hoeben

* These authors contributed equally to this work.

PLoS One. (2012) **7**:e48064



INTRODUCTION

The *Reoviridae* constitute a family of viruses with a non-enveloped icosahedral capsid and a segmented double-stranded RNA genome. Prototypes of the mammalian *orthoreoviruses* were isolated from the human respiratory and enteric tracts and have not been associated with serious human disease. The human reovirus type 3 Dearing (T3D) is frequently studied and often serves as a model for the family. The reoviruses have a lytic replication cycle and preferentially induce cell death and apoptosis in tumor cells but not in diploid, non-transformed cells [2,3,53]. In transformed cells reovirus uncoating and replication are stimulated [7,8,54-56]. In addition, Ras signalling sensitizes the cells to reovirus-induced apoptosis [57]. Based on these observations, reovirus T3D is a promising candidate for use as oncolytic agent, and is currently evaluated in a variety of clinical cancer therapy trials [1,58-60].

Reovirus attachment to cells is a multi-step process. The reovirus spike protein $\sigma 1$ binds with a region of its shaft domain to cell surface-bound sialic acids with low-affinity, before the head domain of $\sigma 1$ engages the high affinity receptor junction adhesion molecule-A (JAM-A, also known as JAM-1) [10,61]. Following receptor binding, virions become internalized by a mechanism involving the capsid protein $\lambda 2$ binding to $\beta 1$ integrins [17,62]. An alternative entry pathway can be employed upon proteolytic removal of the reovirus outer capsid protein $\sigma 3$ and cleavage of $\mu 1/\mu 1C$, yielding intermediate (or infectious) subviral particles (ISVPs). The ISVPs can directly penetrate the cellular membrane independent of the presence of JAM-A [63,64]. The ISVPs are similar to the disassembly intermediates formed during cellular entry via the endocytosis pathway.

The reovirus receptor JAM-A is expressed in epithelial and endothelial cells of several tissues including lung, kidney, pancreas, heart, brain, intestine and lymph nodes [65] but some tumor cells have down-regulated the JAM-A receptors on their cell surface, thereby limiting the susceptibility to reovirus T3D. JAM-A expression was found significantly down-regulated in clear-cell renal carcinoma cells [66]. Also, cells grown from freshly isolated colorectal tumor metastases resist reovirus infection. Immunohistochemistry demonstrated that JAM-A is not accessible at the cell surface, although JAM-A is detectable intracellularly [67]. Furthermore, there is an inverse correlation of JAM-A expression in breast cancer cells and their ability to migrate. JAM-A is expressed in normal human mammary epithelial cells but in metastatic breast cancer tumors the expression is down-regulated [68].

Here we describe the isolation and characterization of reovirus T3D mutants that are adapted to propagation in JAM-A negative, reovirus-T3D resistant cell

lines. The first was identified as a spontaneously occurring mutant in one of our batches genetically retargeted reovirus [69]. Subsequently two other mutants were isolated by selection on JAM-A negative human glioblastoma cells. We demonstrate that these JAM-A-independent (*jin*) mutants employ an as yet unidentified, but apparently ubiquitous receptor, which is present on a wide variety of cell types. Their potential use as novel oncolytic tools against tumor cells in which JAM-A is absent or inaccessible is discussed.

MATERIALS AND METHODS

Cell lines

Cell lines 911 (generated previously in our lab, see reference [28]), U118MG (obtained from ATCC), U2OS (obtained from ATCC, see reference [70]), CHO (obtained from ATCC), Eoma (obtained from ATCC, see reference [71]) and VH10 (primary human foreskin fibroblasts, provided by B. Klein [72]) were cultured in Dulbecco's Modified Eagle Medium (DMEM) containing high glucose (Invitrogen, Breda, The Netherlands), supplemented with penicillin, streptomycin (pen-strep) and 8% fetal bovine serum (FBS) (Invitrogen, Breda, The Netherlands). The U118-HAJAM cells were cultured in DMEM plus 8% FBS and pen-strep, supplemented with 200 µg/ml G418. LMH cells (obtained from ATCC, see reference [73]) were grown on collagen I coated dishes (Rat Tail collagen, 2.5 µg/cm², Invitrogen, Breda, The Netherlands) in DMEM plus 8%FBS and pen-strep. STAET2.1 cells were grown on collagen I coated dishes (5.0 µg/cm²) in RPMI 1640 medium (Invitrogen, Breda, The Netherlands), supplemented with pen-strep and 10% FBS. Lec2 cells (derived from ATCC, see reference [74]) were cultured in alpha-MEM (Invitrogen, Breda, The Netherlands) with 8% FBS. All cells are cultured in an atmosphere of 5% CO₂ at 37°C.

Reovirus propagation

The wild-type T3D virus strain R124 (see accession numbers) was isolated from a reovirus T3D stock obtained from the American Type Culture Collection (stock VR-824) by two rounds of plaque purification on 911 cells. The 911 cells were used to propagate R124 (referred to as wt T3D in the text) as described previously [29]. Briefly, cells were exposed to reovirus in DMEM plus 2% FBS for 2 hrs at 37°C, 5% CO₂. Subsequently, the inoculum was replaced by DMEM containing 8% FBS. The virus was harvested 48 hrs post infection by resuspending the cells in phosphate-buffered saline (PBS) with 2% FBS and subjecting the suspension to three cycles of freezing and thawing. The sample

was cleared by centrifugation for 10 min at 800x g. For the mutant *jin* viruses, U118MG cells were used to propagate the viruses after one round of plaque purification on 911 cells. The *jin* viruses were routinely harvested from U118MG cells 72 hrs post infection. The experiments were done with virus-containing freeze-thaw lysates, unless otherwise indicated. The infectious reovirus titers of the strains were determined by plaque assay on 911 cells.

Origin of the *jin*-mutants

jin-1 is derived from U118scFvHis cells during our experiments on genetically modifying reovirus [69]. The *jin-1* virus was first grown on U118scFvHis cells for two propagations, before three passages on U118MG cells (first point of S1-sequence analysis). The virus was subjected to one round of plaque purification on 911 cells to obtain a homogenous population. This was further propagated on U118MG cells for 11 rounds before analysis of the complete genome sequence (table 7.1).

jin-2 was isolated from U118scFvHis cells infected with wt T3D reovirus and passaged twice in these cells. The S1 segment was sequenced from this passage. Subsequently it was passaged 10 times on U118MG cells. After plaque purification, the complete genome sequence was determined (table 7.1).

jin-3 was isolated from U118MG cells exposed to wt T3D virus followed by blindly passaging the virus for 6 rounds. From the resulted preparation a virus was isolated by plaque purification and following by 10 additional passages on the U118MG cells (table 7.1).

Yield determinations

To determine the replication of wt T3D, *jin-1*, *jin-2* and *jin-3* in U118MG and VH10 cells (figure 7.3), cells were seeded in 24-well plate with a cell density of 1×10^5 cells/well. Viruses (in DMEM plus 2% FBS) were added to the cells with an MOI of 10, two wells per virus. After an exposure of one hr in incubator (37°C, 5% CO₂) the inoculum was removed and the cells were washed once with PBS and fed by fresh DMEM plus 2% FBS. Reoviruses were harvested from medium and cells by 3 cycles of freeze-thawing, 72 hrs after infection. Yields were determined by plaque assays on 911 cells.

For the replication of wt T3D or *jin-1* in 911, U118MG, LMH, U2OS, CHO and Lec2 cells (figure 7.7 B and figure 7.8 B), cells were seeded in 6 well plates with a density of 1.5×10^6 cells/well. Wild-type T3D or *jin-1* was added to 4 wells in case of 911 cells and 3 wells for the other cell lines with an MOI of 10 (in DMEM plus 2% FBS). After one hr of exposure in incubator, the viruses were washed

from cells and medium was replaced. From one well, immediately after washing once with PBS, cells in medium were collected and subjected to freeze-thaw cycles (1 hr time point). 32 Hrs (911 cells only), 48 and 72 hrs after infection cells and medium were collected and subjected to freeze-thaw cycles. Viral yields were determined by plaque assays on 911 cells.

Table 7.1 Amino acid differences in reovirus proteins of the *jin* mutants and the wt T3D reovirus strains

RNA segment (protein)	AA position	wt	<i>jin-1</i>	<i>jin-2</i>	<i>jin-3</i>
S1 (σ 1)	187	Gly		Arg	
	193	Thr	Met		
	196	Gly			Arg
	336	Gln	Arg	Arg	
S2 (σ 2)	254	Ser	Phe		
S3 (σ NS)	No changes				
S4 (σ 3)	177	Ser	Phe		
	198	Gly	Glu		
	357	Met	Thr		
M1 (μ 2)	No changes				
M2 (μ 1)	388	Lys	Arg		
	530	Thr	Ala		
M3 (μ NS)	705	Ala	Val		
	706	Asp	Ala		
	708	Val	Ala		
L1 (λ 3)	413	Ile	Ser		
L2 (λ 2)	1101	Met	Ile		
L3 (λ 1)	201	Thr	Ala		
	703	Arg			Gly
	1164	Ser			Phe

Cell viability assay

WST-1 reagent (Roche, Almere, The Netherlands) was used to assay the viability of cells after reovirus infections. U118MG and 911 cells in 96-well plate were mock-infected or infected with wt T3D or *jin-1* with an MOI of 10, in triplo. Six days post infection WST-1 reagent was added, according to the manufacturer's manual. The viability measurements in mock-infected cell cultures, were set to 100%.

[³⁵S]Methionine labelling

Infected cells (911 cells infected at MOI=1; U118MG and U118-HAJAM with MOI=5) or mock-infected cells were incubated with TRAN³⁵S -LABEL™ (10mCi/ml; MP Biomedicals, Eindhoven, The Netherlands) for 4 h; one day (911 cells) or two days (U118MG and U118HA-JAM cells) post infection. Cells were washed once with phosphate-buffered saline and lysed in Giordano Lysis Buffer (50 mM Tris HCl pH 7.4, 250 mM NaCl, 0.1% Triton, 5 mM EDTA) containing protease inhibitors (Complete mini tablets, Roche Diagnostics, Almere, The Netherlands). The labelling assays were performed in 24-well plates with 5 ml (50 µCi) TRAN³⁵S -LABEL™ per well. The cells were lysed with 100 µl lysis buffer. After addition of sample buffer, 50 µl per lysate was loaded in the wells of a 10% SDS-polyacrylamide gel. Gels were dried and exposed to a radiographic film to visualize the labeled proteins.

Immunofluorescence assay

For immunofluorescence assays, U118MG and 911 cells were grown on glass coverslips in 24-well plates before infection with wt T3D or *jin-1* with an MOI of 5 or no virus. One day post infection the cells were fixed with cold methanol (15 min, 4°C), washed with PBS containing 0.05% Tween-20, and incubated with antibody 4F2 directed against reovirus σ3 (monoclonal antibody developed by T.S. Dermody [34]; obtained from the Developmental Studies Hybridoma Bank developed under the auspices of the NICHD and maintained by The University of Iowa, Department of Biology, Iowa City, IA 52242), diluted in PBS containing 3% BSA. After incubation at room temperature the cells were washed (PBS, 0.05% Tween-20) and incubated with secondary fluorescein isothiocyanate (FITC)-conjugated goat antimouse serum for 30 min at room temperature. The mounting solution consisted of glycerol containing 0.02 M Tris HCl pH8.0, 2.3% 1,4-diazabicyclo-[2.2.2]-octane and 0,5 µg/ml 49,6-diamidino-2-phenylindole (DAPI) to visualize the nuclei.

RT-PCR and sequencing

Total RNA was isolated (Absolutely RNA miniprep kit; Stratagene, Agilent Technologies, Amstelveen, The Netherlands) from U118MG cells infected with the different reovirus mutants (*jin-1* or *jin-3*), one day post infection. For wt T3D total RNA was isolated from infected 911 cells. Primers used for the RT-PCR procedures are listed in Supplementary_table 7.1. DNA synthesis of all the segments started with the unique endR primer designed for every segment,

using SuperScript III (Invitrogen, Woerden, The Netherlands) for the reverse transcription process. For the PCR, *Pfu* polymerase (Promega, Leiden, The Netherlands) was used with the primer combinations unique for every segment. PCR products were first cleaned with Sureclean (Bioline, London, UK), according to the manual, before direct analysis of the sequence. In some cases the resulting PCR products were cloned into plasmid pJet1 (GeneJet, PCR cloning kit; Stratagene, Agilent Technologies, Amstelveen, The Netherlands) and their DNA sequences were determined. All sequence data were generated by The Leiden Genome Center (LGTC, Leiden, The Netherlands).

***In vitro* transcription-translation and trimerization assay**

All primer sequences can be found in Supplementary_table 7.1. With DualSHFor and DualSHRev primers, S1 PCR product was generated from plasmid pCDNART3S1 [69], according to manual of the pDual-GC vector (Stratagene, Agilent Technologies, Amstelveen, The Netherlands). The resulting construct (pDualS1His) contained no stop codon, meaning that the Myc-His tag was present behind S1. To introduce a stop codon behind the S1 ORF in pDualS1His, the DualS1st for and rev primers were used in a mutation PCR, with EXL polymerase (Stratagene, Agilent Technologies, Amstelveen, The Netherlands). This resulted in the plasmid pDGC-S1delTag, which was used for the trimerization assay and as start to generate the pDGC-S1QR and pDGC-S1Y313A (with S1-QRmut2Rev and For combi or S1Y313AmRev and For combi, respectively) also with EXL polymerase. For the *in vitro* transcription-translation (ITT) part, TNT[®] T7 Quick Coupled Transcription/Translation kit (Promega, Leiden, The Netherlands) was used. Input for the ITT assays were the plasmids pDGC-S1delTag, pDGC-S1QR and pDGCS1Y313A. The total reaction volume was 15 μ l, scaled according to the manual (in the presence of 6 μ Ci TRAN³⁵S-LABEL[™]; MP Biomedicals, Eindhoven, The Netherlands). For the trimerization Assay, one fifth of every ITT reaction per construct was used and incubated with Sample buffer (final concentrations: 10% glycerol, 2% SDS, 60 mM Tris HCl pH 6.7, 2.5% β -mercaptoethanol and 2.5% bromophenol blue) for 30 min at 37°C to stabilize the trimers or boiled for 5 min 96°C to disrupt the trimers. After incubation the samples were loaded on a 10% SDS-polyacrylamide gel, which was kept at 4°C during the run. Gels were dried and exposed to a radiographic film to visualize the labeled proteins.

Plaque assay and size measurements

Plaque assays were performed in a standard assay as previous described for adenoviruses [28] with minor modifications. Briefly, virus stocks were serially diluted in DMEM containing 2% FBS. The dilutions were added to near-confluent 911 cells in six-well plates. Four hrs after infection, medium was replaced with agar-medium. Agar-medium consists of (final concentrations) 0.5% agarose (Ultrapure™, Invitrogen, The Netherlands), 16 minimal essential medium (MEM), 2% FBS, 12.5 mM MgCl₂, 2 mM GlutaMAX™ (Invitrogen, Almere, The Netherlands) and 1x pen-strep antibiotic mixture (Invitrogen, Almere, The Netherlands). Plaques are counted six days post infection. Plaque sizes were measured four days post infection. For the measurements a CKX41 Olympus microscope was used and the plaque area was measured with the software of Olympus: Olympus DP-soft.

Western analysis

Cell lysates were made in Giordano Lysis Buffer supplemented with protease inhibitors (Complete mini tablets, Roche Diagnostics, Almere, The Netherlands). Total amount of protein in the lysates was measured (Bradford, Biorad, Veenendaal, The Netherlands) and the same amount of lysate (30 µg) was loaded into the wells of a 10% SDS-polyacrylamide gel after addition of western sample buffer (final concentrations: 10% glycerol, 2% SDS, 50 mM Tris HCl pH 6.8, 2.5% β-mercaptoethanol and 0.025% bromophenol blue). The proteins were transferred to Immobilon-P (Millipore, Etten-Leur, The Netherlands) and visualized using standard protocols. Antibodies used in this study: 4F2 directed against reovirus σ3; β-Actin antibody: ImmunO anti-Actin clone C4 (MP Biomedicals, Eindhoven, The Netherlands).

E64d inhibition

E64d (Sigma Aldrich, Zwijndrecht The Netherlands) was dissolved in DMSO before use. U118MG and 911 cells were seeded in 24 well plates; half of the cells were exposed to 100 µM E64d at 37°C, 5% CO₂ for one hr. Purified wt T3D or *jin-1* virus and ISVPs (approximately 2x10³ particles per cell) were added to the cells and left for one hr at 4°C; cells were washed with PBS and transferred back to 37°C, 5% CO₂ in the absence or presence of E64d, for 36 hrs. Lysates were made as described in Western analysis. For the immunodetection the anti-σ3 antibody (4F2) and β-Actin antibody were used.

Generation of ISVPs

Wild-type T3D or *jin-1* virus ISVPs are freshly prepared by treating CsCl purified virions [29] with chymotrypsin. Purified viruses were diluted to a concentration of 10^{11} pfu/ml in Reovirus Storage Buffer (10 mM Tris HCl pH 7.5, 150 mM NaCl, 10 mM $MgCl_2$) and treated with 200 μ g/ml Chymotrypsin (TLCK treated, Sigma Aldrich, Zwijndrecht The Netherlands; C3142) at 37°C for 1 hr. Reaction was stopped by adding 5 mM phenylmethyl-sulfonyl fluoride (Sigma Aldrich, Zwijndrecht The Netherlands).

Wheat germ agglutinin (WGA) binding and competition experiment

For the detection of sialic acids in the different cell lines, FITC labeled WGA (Sigma Aldrich, Zwijndrecht The Netherlands) was used. Cells (grown on round glass coverslips in 24-well plate) were fixed with ice-cold Methanol (15 min, 4°C) and washed with PBS containing 0.05% Tween-20. WGA-FITC was added to the cells at a concentration of 5 μ g/ml in PBS containing 3% BSA and incubated for 1 hr at room temperature. Excess of unbound WGA-FITC was washed away with PBS containing 0.05% Tween-20. Nuclei were visualized by DAPI in the same mounting solution as is described for the immunofluorescence assay.

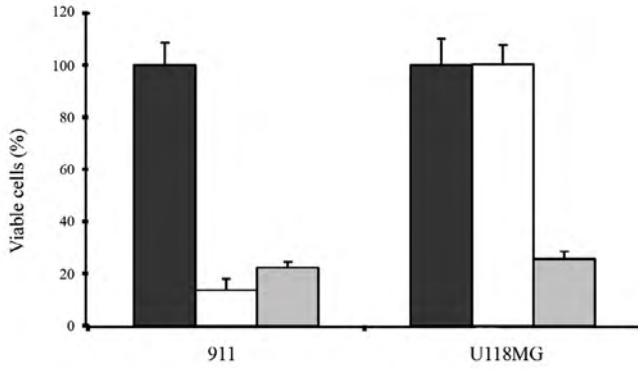
WGA competition experiment was done by exposing cells (in 24-well plate wells) to WGA at a concentration of 100 μ g/ml in culture medium for one hr in CO₂ incubator at 37°C. The preincubation medium was removed and wt T3D or *jin-1* virus was added to the cells with an MOI of 10 in DMEM containing 2% FBS at 4°C for one hr. Cells were washed with ice-cold PBS and normal culture medium was added to the cells. Cells were left for 32 hr in CO₂ incubator (37°C) before lysates were made as described in Western analysis. For the immunodetection the anti- σ 3 antibody (4F2) and β -Actin antibody were used.

RESULTS

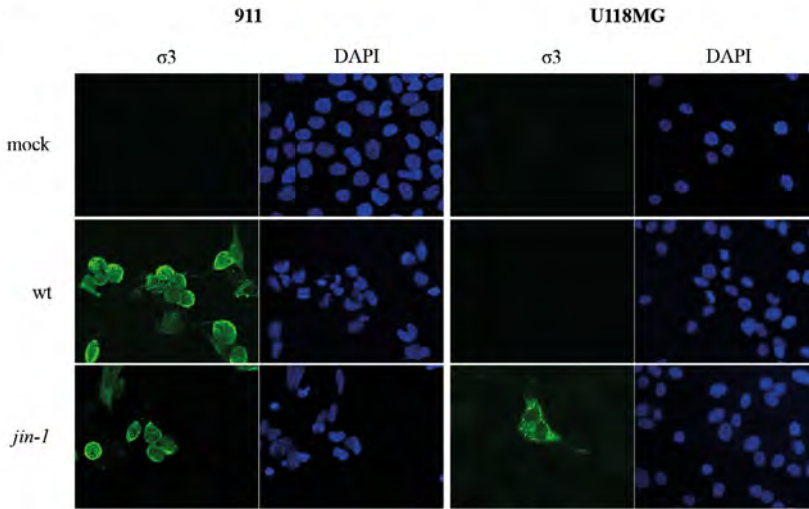
Isolation of a JAM-A independent reovirus mutant

Previously we described a system for generating genetically modified reoviruses. The modification strategy relies on the exchange of a genome segment encoding the spike protein σ 1 by a segment encoding a his-tagged spike. The modified viruses can be selected and propagated on U118scFvHis cells. This cell line is a derivative of the JAM-A negative human glioblastoma cell line U118MG and expresses a single-chain Fv (scFv) on its surface that is capable of binding the His-tag. The scFv serves as an artificial receptor for the σ 1-His containing viruses [69].

A



B



C

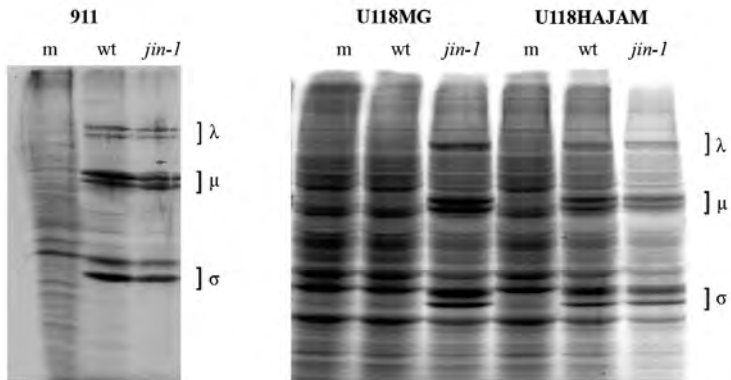


Figure 7.1 Reovirus mutant *jin-1* is able to infect the JAM-A negative cell line U118MG. (A) Viability assay (WST-1) on 911 and U118MG cells. Cells were mock infected (black bar) or infected with wt T3D (white bar) or *jin-1* virus (grey bar) with an MOI of 10, six days post infection. Means (\pm standard deviation) from three wells. **(B)** Detection of outer capsid protein $\sigma 3$ in 911 and U118MG cells after addition of wt T3D or *jin-1* virus with an MOI of 5. 40 hrs post infection cells were stained with a monoclonal antibody directed against $\sigma 3$ (4F2) and visualized with a fluorescein isothiocyanate (FITC)-conjugated goat-anti-mouse secondary antibody. The nuclei are visualized with 49,6-diamidino-2-phenylindole (DAPI). **(C)** Assessment of reoviral protein synthesis in *jin-1* or wt T3D infected cells. Indicated cells were infected with wt T3D or *jin-1* virus and labeled with [35 S]methionine once CPE became apparent. 911 cells were infected with an MOI of 1 and U118MG or U118HAJAM cells with MOI of 5. Indicated are the positions of the reoviral λ , μ and σ proteins. m represents mock infected cells; *wt*: wt T3D infected cells and *jin-1*: *jin-1* infected cells.

In one of the batches of $\sigma 1$ -His modified reoviruses, we noted that a cytopathic effect (CPE) was not only induced in the U118scFvHis cells, but also in the parental U118MG cells. This suggested that this batch contains viruses that are capable of infecting cells independent of the presence of JAM-A and independent of the artificial scFv-His receptor.

The first mutant virus isolated, which was called *jin-1* (JAM-A independent), was further propagated on U118MG cells. The *jin-1* mutant virus was compared to our lab reference wt T3D reovirus. In contrast to the wt T3D reovirus, the *jin-1* virus induces CPE in U118MG cells as is evident from a WST-1 cell viability assay (figure 7.1 A). Both viruses are equally cytolytic to 911 cells which do contain JAM-A [69]. Immunofluorescence assays using an antibody against the major capsid protein $\sigma 3$ confirmed the presence of $\sigma 3$ in U118MG cells infected with *jin-1*, but not with wt T3D (figure 7.1 B). To further verify that U118MG cells support the replication of the *jin-1* mutant, a metabolic labelling with [35 S]methionine was performed. As a positive control the U118HA-JAM cell line was included. This U118MG-derived cell line had been transduced with a lentivirus to overexpress an HA-tagged version of the JAM-A receptor. In U118-HAJAM and in 911 cells, exposure to the *wt* T3D as well as to *jin-1* reoviruses established infection as is evident from the synthesis of reovirus proteins. In contrast, in U118MG cells the reoviral protein synthesis was only detectable upon infection with the *jin-1* virus but not with our wt T3D (figure 7.1 C). These data demonstrate that the *jin-1* reovirus, in contrast to wt T3D, is capable of infecting and replicating in the JAM-A negative cell line U118MG.

Sequence analysis of the reovirus mutants

The *jin-1* mutant originated from the U118scFvHis cell line. Since this mutant can infect JAM-A negative U118MG cells, we speculated that the attachment protein $\sigma 1$ was altered. After one round of plaque purification and further propagation for eleven passages on U118MG cells, the complete genome was sequenced. The primers used (for this) are listed in Supplementary_table 7.1. The PCR products were purified and used for sequence analysis. In the S1 segment two mutations occurred. The mutation led to a threonine-to-methionine change at position 193 (T193M) and a glutamine-to-arginine change at position 336 of the protein (Q336R). Also in other segments mutations were found (table 7.1).

To expand the pool of mutants, we repeated the procedure and exposed the U118scFvHis cells with our wild-type virus before further expansion on U118MG cells. After the first selection rounds in the U118scFvHis cells, we again found the Q336R mutation in the $\sigma 1$ head domain. Upon prolonged propagation (10 passages) on U118MG cells an additional mutation was found in S1, resulting in a G187R change. This mutant strain, carrying mutations resulting in a Q336R and G187R change was named *jin-2*. Based on the findings in *jin-2* S1 in the earlier passage, we analyzed S1 of an earlier passage of *jin-1* as well (prior to plaque purification) and also in this S1 segment the only mutation present was the one resulting in the Q336R change in $\sigma 1$.

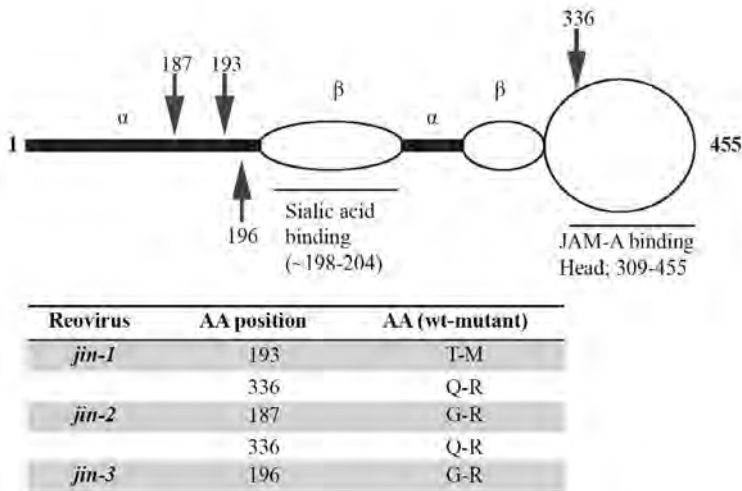


Figure 7.2 Schematic representation of mutations in Sigma-1. Model of the $\sigma 1$ protein (adapted from Chappel *et al.*, 1997 [75]). Arrows indicate the positions of the mutations.

Another mutant reovirus (*jin-3*) was obtained after direct exposure of U118MG cells at very high MOI to wt T3D reovirus. This virus was blindly passaged (i.e. the cells were lysed without signs of overt CPE at the time of virus harvest) for 6 rounds on U118MG cells. After 6 rounds in U118MG cells, CPE became apparent. After plaque purification on 911 cells and 10 additional passages on U118MG the complete genome of the *jin-3* mutant was sequenced. Only one mutation was found in the S1 segment, resulting in a G196R alteration. Table 7.1 gives a summary of all the amino acid changes found in the mutants, compared to our wt T3D. A schematic overview of the amino acid changes in $\sigma 1$ is depicted in figure 7.2. In all *jin* mutants the amino-acid alterations in the shaft of $\sigma 1$ are located close to the sialic acid (SA) binding motif [10,55,75,76].

Primary human fibroblasts (VH10 Cells) do not support replication of the *jin* mutants or wt T3D

To study whether the *jin* mutants acquired the capacity to replicate in normal, non-transformed human cells, we exposed diploid human foreskin fibroblasts (VH10 cells) to wt T3D and to the *jin*-mutants. The skin fibroblasts were chosen because primary human fibroblasts do not express JAM-A [77]. We studied the yields of the *jin* viruses and compared these with the yields of wt T3D on VH10 fibroblasts and on U118MG cells. As expected U118MG cells yielded high titers of the *jin* reoviruses, while wt T3D virus yields were below the amounts of virus added to the cells (figure 7.3 A). On VH10 fibroblasts, neither the wt T3D reovirus nor the three *jin*-mutants yielded significant titers (figure 7.3 B). Furthermore in the VH10 cell cultures no apparent signs of cell death were observed (data not shown). These data suggest that, like wt T3D our *jin* mutants do not replicate in normal non-transformed diploid fibroblasts.

During the plaque assays on 911 cells for the determination of viral yields, we noted that the plaques formed by the *jin-1* virus and *jin-3* virus were consistently smaller than those of the wt T3D virus; the plaque surface area of the initial *jin-1* virus and *jin-3* virus is approximately 10-fold lower (figure 7.3 C), suggesting reduced cell-to-cell spread of the mutants.

The *jin-2* virus also has a reduced plaque size compared with the wt virus, but the variation within the population is larger, which suggests heterogeneity in the population. Sequence analysis of the S1 segment of both the smaller and the larger *jin-2* plaques revealed that the smaller plaques contained the mutations for the G187R and Q336R change, while the larger plaques only contained the mutation that yield the Q336R alteration in $\sigma 1$ (data not shown).

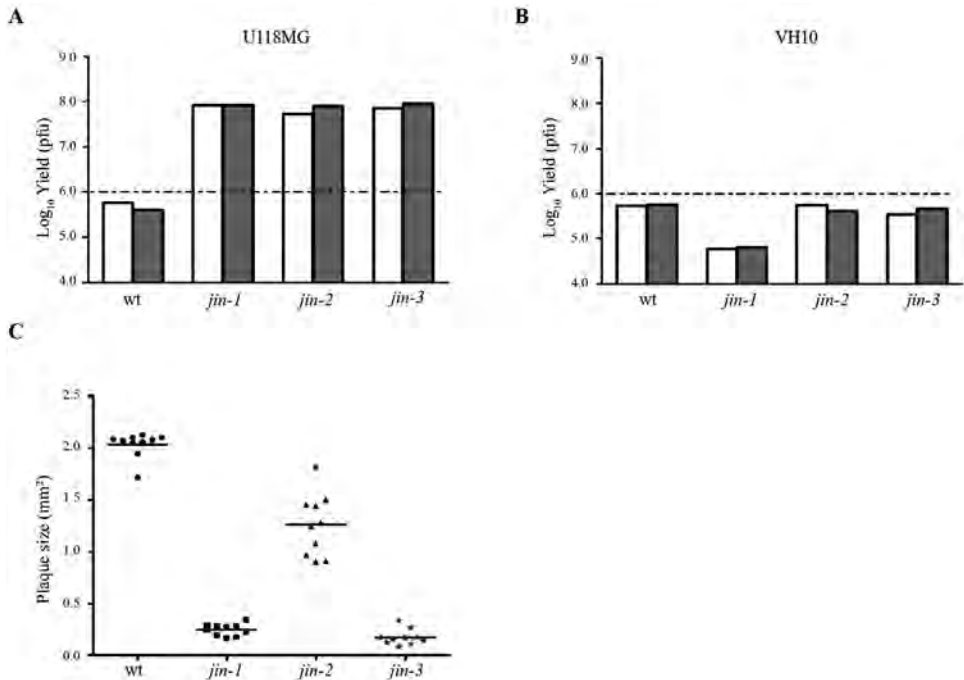


Figure 7.3 Comparison of wt T3D with *jin*-viruses in terms of plaque size, yield in U118MG cells and primary human fibroblasts (VH10 cells). (A) Yield of wt T3D and *jin-1*, *jin-2* and *jin-3* mutants from U118MG cells infected with MOI 10 per virus. Yields were determined 72 hours post infection by plaque assays on 911 cells. The graph shows yields (Log₁₀ pfu) of two independent U118MG cell infections: first one is shown as a white bar and second as a grey bar. The dashed line represents the input amount of the initial infection. **(B)** Yield of wt T3D and *jin-1*, *jin-2* and *jin-3* mutants from VH10 cells infected with MOI 10 per virus. Yields were determined 72 hours post infection by plaque assays on 911 cells. The graph shows yields (Log₁₀ pfu) of two independent VH10 cell infections: first one is shown as a white bar and second as a grey bar. The dashed line represents the input amount of the initial infection. **(C)** Plaque sizes of wt T3D and *jin-1*, *jin-2* and *jin-3* mutants in 911 cells. Surface areas of 10 plaques per virus were measured four days post infection with Olympus DP-software.

Protease inhibitor E64d blocks entry of *jin-1* virus

Reoviruses enter cells by receptor-mediated endocytosis after attachment of the $\sigma 1$ protein to the JAM-A receptor [9,63]. Subsequently, the viral $\lambda 2$ protein binds cellular integrins leading to endocytosis. In the endosomes the particle undergoes conformational changes by partial proteolysis, leading to intermediate subviral particles (ISVPs). The outer capsid proteins $\sigma 3$ and $\mu 1/\mu 1C$ are cleaved by cellular proteases and $\sigma 1$ undergoes a conformational change. *In vitro*, this process can be mimicked by proteolytic treatment of complete virions. The generated ISVPs

are capable to enter cells independent of the JAM-A receptor by penetration of the cytoplasmic membrane [63,64,78]. One possible explanation for the JAM-A independent entry of the *jin-1* virus could be a premature transition to ISVPs prior to entry into the cell. To test whether the *jin-1* virus is still dependent on cellular proteases the protease inhibitor E64d was used. If cells are exposed to E64d prior to infection, intact virions are trapped in the endosome while ISVPs can complete the replication cycle [79,80]. To confirm that wt ISVPs are JAM-A independent we exposed the U118MG cells to wt T3D ISVPs and to intact T3D virions (figure 7.4 A). As expected, only in the cells exposed to the ISVPs, viral protein $\sigma 3$ synthesis is detected, evidencing virus entry and viral virus are inhibited by E64d (figure 7.4 B), while $\sigma 3$ was detected in both the *jin-1* and wt ISVP infected cells. Also in the U118MG cells, the *jin-1* virus entry is blocked by the presence of E64d, but not the *jin-1* ISVP entry. These data demonstrate that like wt T3D reovirus, the reovirus mutant *jin-1* exploits the endocytotic pathway to enter U118MG cells.

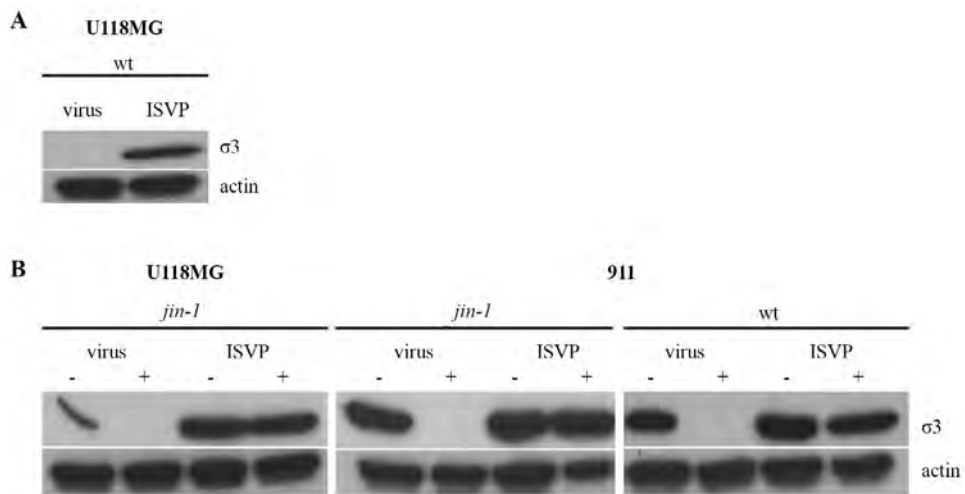


Figure 7.4 Effect of the cysteine protease inhibitor E64d on *jin-1*, wt T3D virus, and ISVP entry into cells. (A) U118MG cells were exposed to purified wt T3D virus and wt T3D ISVP (2×10^3 particles per cell). Lysates were made 24 hours post-infection and analyzed by SDS-PAGE and western-blotting. The reovirus $\sigma 3$ proteins were detected by the anti-reovirus $\sigma 3$ antibody 4F2 and an anti-Actin serum was used to detect actin as a loading control. (B) Effect of 100 μM E64d on the entry of particles compared to entry of ISVPs. Cells, treated (+) or untreated (-) with 100 μM E64d, were exposed to *jin-1* (U118MG and 911 cells) or wt T3D (911 cells) virus or ISVPs (2×10^3 particles per cell). Lysates were made 24 hours post-infection. Equal amounts of protein were loaded on 10% SDS-polyacrylamide gel and detected with anti-reovirus $\sigma 3$ antibody (4F2), and anti-Actin as a loading control.

***jin-1* $\sigma 1$ forms trimers**

The change at amino-acid position 336 is located close to the domain that has been implicated in trimerization of $\sigma 1$ [81]. Although the Q336R alteration is located at the outward surface-exposed side of every monomer in the trimeric conformation (figure 7.5 A, R336 is shown in red) it is essential to confirm that the Q336R alteration does not interfere with trimer formation. To this end an *in vitro* trimerization assay was performed as described by Leone *et al.* [74]. For this wt $\sigma 1$, $\sigma 1$ -Q336R and $\sigma 1$ -Y313A proteins were synthesized *in vitro*. The Y313A change abolishes the capacity of $\sigma 1$ to form trimers [81]. The $\sigma 1$ products were analysed by mild PAGE at 4°C (figure 7.5 B). Whereas the $\sigma 1$ -Y313A protein does not form mature trimers, both the wt T3D $\sigma 1$ and $\sigma 1$ -Q336R do. Intermediate trimers, which consist of $\sigma 1$ molecules in which only the shaft is trimerized while the head domain is in a monomeric configuration, are detectable in all $\sigma 1$ variants tested. Our data show that the Q336R alteration that occurs in the *jin-1* and *jin-2* viruses does not affect the formation of mature $\sigma 1$ -trimers *in vitro*.

***jin-1* and *jin-2* have selective advantages over wt reovirus in U118MG cells**

To confirm that *jin-1* and *jin-2* viruses have a selective advantage over wt T3D in U118MG cells, we mixed *jin-1* or *jin-2* with a 100-fold excess of wt T3D prior to infection of cells. Cultures of 911 cells were infected at an MOI 10 with the mixtures to allow reassortment of genome segments to take place. Two days post-infection, the virus was harvested by three freeze-thaw cycles and used to infect U118MG cells. While no CPE for *jin-1*/wt T3D mixtures was observed at 7 days post-infection in the U118MG cells, the cells were freeze-thawed and the lysate was used to infect fresh U118MG cultures. In U118MG cells infected with *jin-2*/wt T3D mixture the virus was harvested after 4 days, with visible signs of CPE. This procedure was repeated for two more times. At passage 3 clear CPE was observed four days post infection in both *jin-1*/wt and *jin-2*/wt selections. Sequencing of PCR products after reverse transcription PCR of the S1 segment after the third selection on U118MG cells were compared with the S1 sequences of wt T3D, *jin-1* and *jin-2* (figure 7.6). S1 of the *jin-1*/wt end population contains a T at nucleotide position 590 and a G at position 1019, identical to the *jin-1* S1 segment. Sequence results for S1 of the *jin-2*/wt end population revealed an A at position 571 and a G at position 1019 and this is identical to *jin-2* S1 sequence. From these findings we conclude that in U118MG cells $\sigma 1$ proteins from *jin-1* or *jin-2* provide a strong selective advantage over wt T3D $\sigma 1$. These data provide evidence that the amino-acid alterations in $\sigma 1$ provide the *jin* mutants with the capacity to infect and replicate in JAM-A-negative cells.

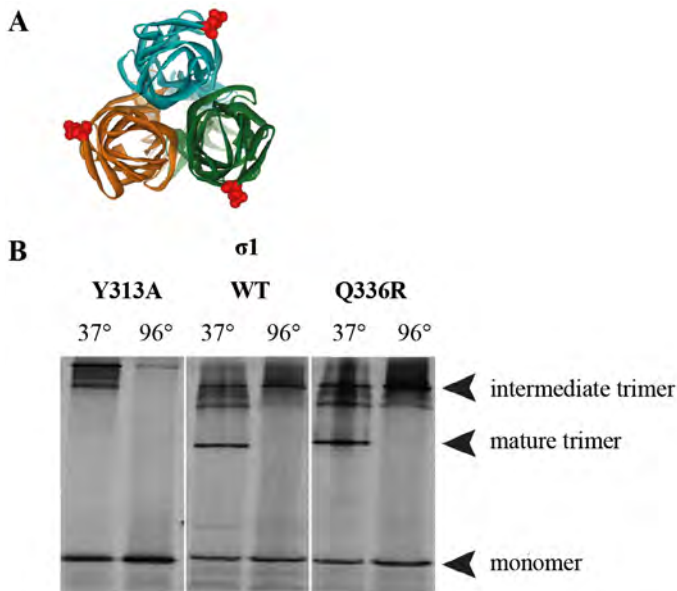


Figure 7.5 Analysis of Sigma-1 trimers synthesized *in vitro*. **(A)** Top view of σ 1-trimer, with colored monomer units (green, turquoise, orange). Position of the Q336R mutation in each monomer is indicated as red CPK symbol [86] PDB ID: 1KKE. The software used for the 3D graphs is Viewerlite 5.0 from Accelrys. **(B)** [35 S] methionine labelled *in vitro* transcribed and translated products of plasmids pDGC-S1wt (S1wt), pDGC-S1Q336R (S1Q336R) and pDGCS1Y313A (S1Y313A) were incubated for 30 minutes at 37°C (to stabilize the mature trimers) or boiled for 5 minutes (to disrupt the trimers), before loading on a 10% SDS-polyacrylamide gel at 4°C. The position of the three different conformations is indicated.

***j*in-1 reoviruses infect cells that are non-permissive for wt T3D**

To study whether the *j*in-1 mutant has expanded its tropism beyond the U118MG cell line, we evaluated whether this virus can replicate in a panel of cell lines that resists infection with wt T3D virus. These cell lines include chicken hepatoma cell line LMH [73] murine endothelioma cell line Eoma [71], human bone osteosarcoma cell line U2OS [70] and human Ewing sarcoma cell line STA-ET2.1 [82]. In parallel the cell lines 911 and U118HA-JAM were included as positive controls for infection. Each of the cell lines were exposed to wt T3D or *j*in-1 viruses with an amount of virus corresponding to 8 PFU/cell as determined in 911 cells. While no major capsid protein σ 3 was detected in the wt T3D-resistant cell lines exposed to wt T3D, exposure of these cells to *j*in-1 resulted in the detection of the σ 3 protein at 36 hr post infection (figure 7.7 A). In 911 and U118HA-JAM cells, the σ 3 protein is present in wt T3D infected cells as well as in the *j*in-1 infected cells.

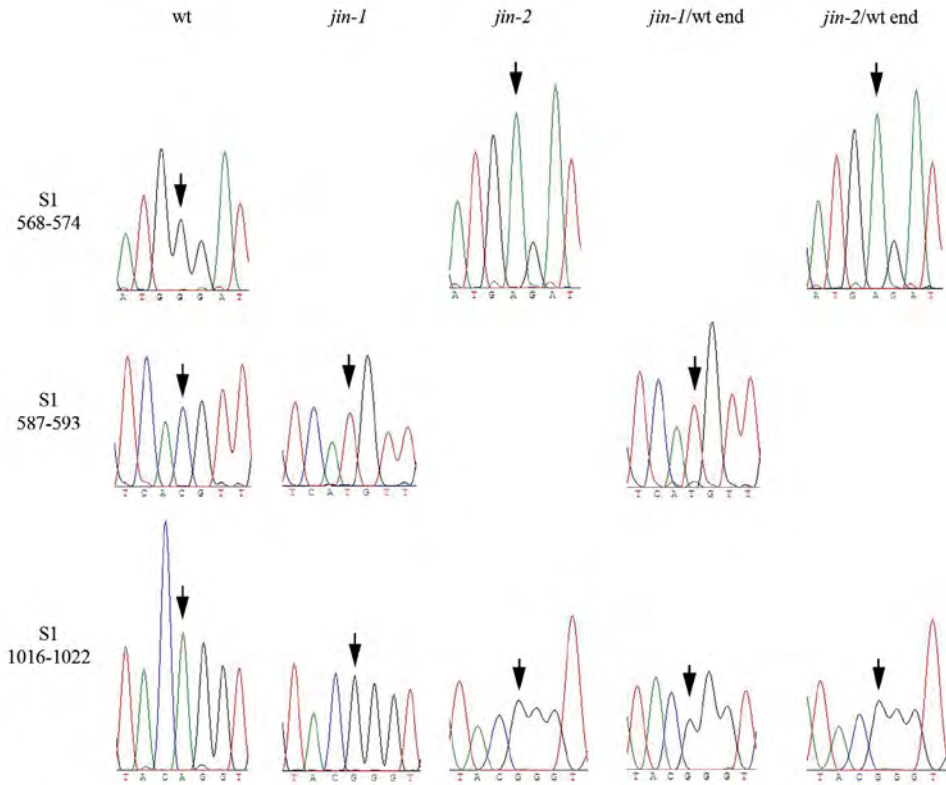


Figure 7.6 S1-sequence analysis of the *jin-1/wt* T3D and *jin-2/wt* T3D selection assay on U118 MG cells. The *jin-1* or *jin-2* viruses were mixed with a 100-fold excess of wt T3D virus with regards to MOI. 911 cells were exposed to the mixtures first, before propagation on U118MG cells for three more passages. Reovirus RNA was isolated from the virus derived from the third passage on U118MG cells and subjected to RT-PCR to obtain the S1 products from the total population (*jin-1/wt end* or *jin-2/wt end*). Sequence histograms of the indicated regions were compared to the S1 sequences of the input reoviruses. Arrows indicate the nucleotide differences between the wt T3D and *jin-1* or *jin-2*. (S1 nucleotide positions 571, 590 and 1019).

To verify that wt T3D resistant cells could support replication of the *jin-1* virus, the virus yields were determined in some of these cell lines (figure 7.7 B). In 911 cells both viruses give a similar yield, but in three other cell lines (U118MG, U2OS and LMH) more progeny virus was produced with the *jin-1* virus than with wt virus. The amount of wt T3D produced per cell did not rise above the amount added to the cells (MOI of 10, dashed lines). From these data we conclude that the *jin-1* virus is able to productively infect our panel of wt T3D resistant cells.

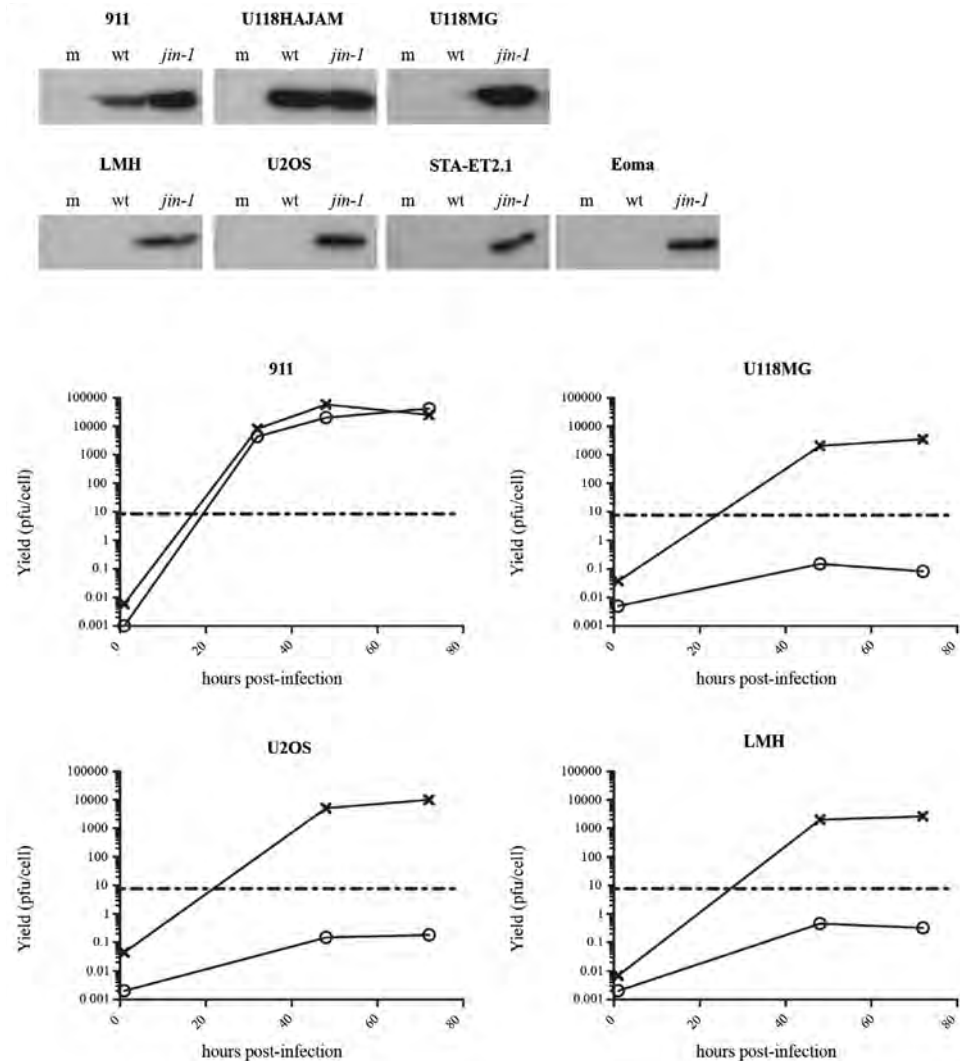


Figure 7.7 Reovirus mutant *jin-1* can infect cell lines that resist wt T3D reovirus infection. **(A)** Several cell lines were infected with wt T3D or *jin-1* and 32 hr post-infection cells were lysed. Protein samples (30 μ g) were analyzed by 10% SDS-polyacrylamide gel electrophoresis. For the immunodetection anti-reovirus σ 3 (4F2) was used. The cell lines 911 and U118-HAJAM are included to serve as positive controls for the infectivity of wt T3D. The cells were mock-infected (m); wt T3D infected, or *jin-1* infected. **(B)** Virus production of wt T3D and *jin-1* in the different cell lines. Cells were exposed to virus at MOI of 10 for one hr, washed with PBS and immediately lysed (1 hour time point) or left for 48 or 72 hrs. For 911 cells an additional harvest point at 32 hrs post-infection was included. The viral titers in the samples were determined by plaque assays on 911 cells. The graph shows a representative example of the assay. Open circles: wt T3D (o), crosses: *jin-1* (x). The dashed line represents the input amount of the initial infection (10 pfu/cell).

Cell entry of reovirus *jln-1* and *jln-3* relies on sialic acids

Apart from the Q336R mutation, the other mutations found in the S1 segments of the *jln* mutants are located close to the region involved in SA binding [10,55]. Recently the crystal structure of the sialic acid- $\sigma 1$ complex was elucidated [76]. There is a remarkable heterogeneity in the amino acid sequence of the SA-binding domains of different T3D and T1L strains. Some isolates cannot bind SA as determined on JAM-A negative murine erythroleukemia (MEL) cells. The forced selection of such strains yielded mutants that could infect MEL cells probably via the interaction with SA [83].

The wt T3D that was used in our studies has an amino-acid sequence of the sialic-acid binding pocket that is identical to strains capable of binding sialic acid. The S1 mutations found in the *jln* mutants are not located in the region coding for the SA-binding pocket of $\sigma 1$ (viz. amino acids 198–204; ref [10,76]), but are located in close proximity of this region.

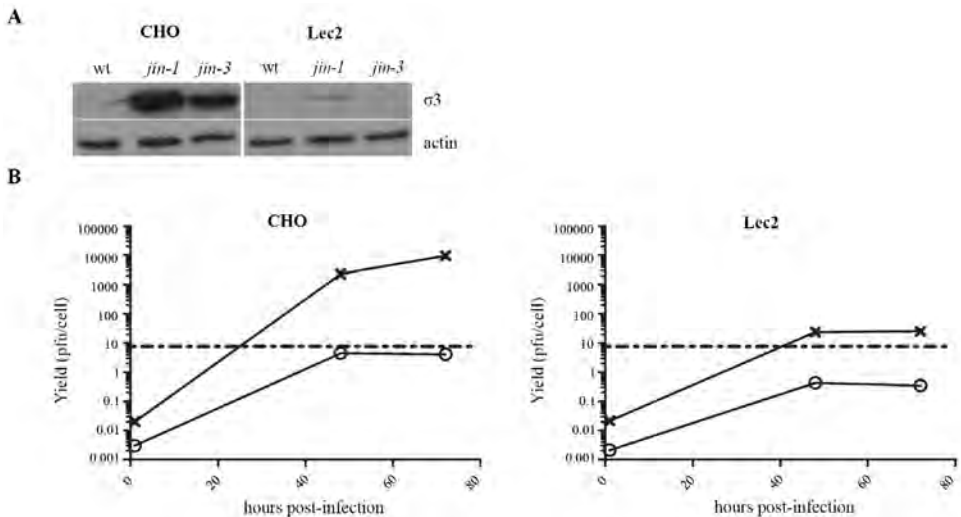


Figure 7.8 Lec2 cells are poorly infected by reovirus mutant *jln-1* and *jln-3*. (A)

CMP-sialic acid transporter defective Lec2 cells and parental cell line, CHO, were exposed to wt T3D, *jln-1*, and *jln-3* at MOI of 10. Protein lysates were made 32 hrs post-infection and analyzed by SDS-polyacrylamide gel electrophoresis. For the immunodetection of $\sigma 3$ the anti-reovirus $\sigma 3$ antiserum 4F2 was used, and anti-actin (human) was used to detect actin as a loading control. (B) Virus production of wt T3D and *jln-1* in CHO and Lec2 cells. Cells were exposed for one hour to the viruses at MOI of 10, washed with PBS and immediately lysed (1 hour time point), or incubated at 37°C for 48 hrs and 72 hrs. Virus yields were determined by plaque assays on 911 cells. The graph shows a representative example of the assay. Open circles: wt T3D(o), crosses: *jln-1*(x). The dashed line represents input amount of virus used at the initial infection (10 pfu/cell).

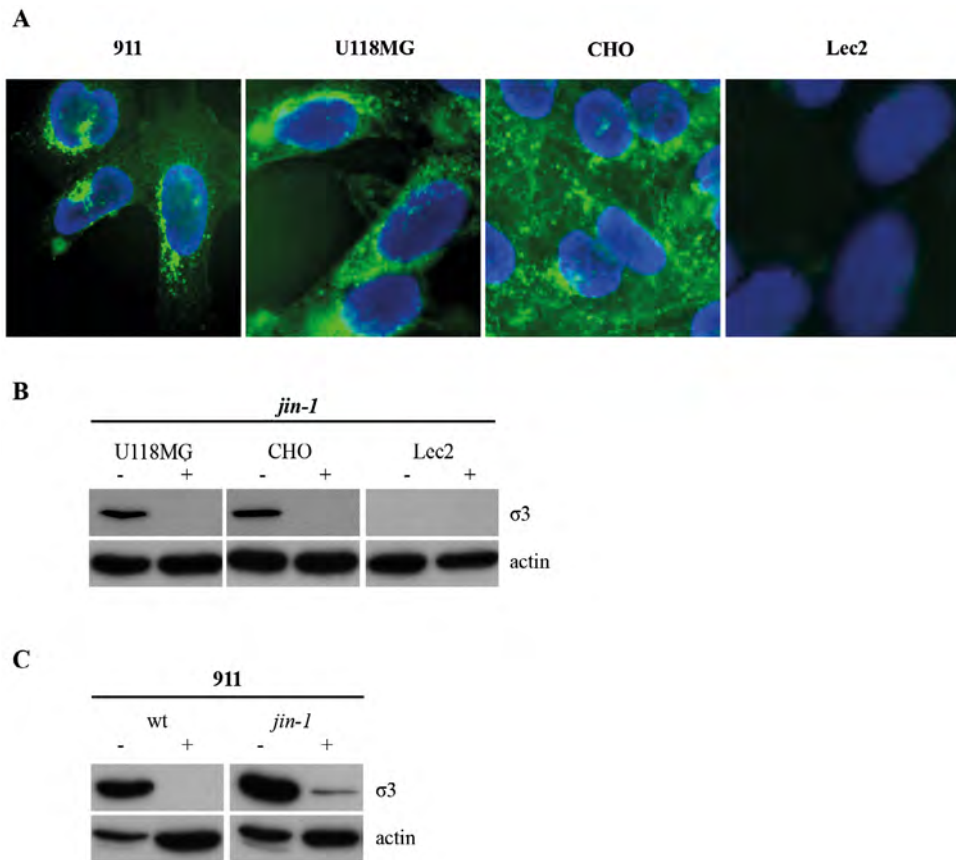


Figure 7.9 WGA inhibits binding of reovirus to cells. (A) Detection of sialic acids in cell lines (911, CHO, U118MG and Lec2) by FITC-labeled WGA immunofluorescence. **(B)** WGA inhibition of reovirus infection. Prior to exposure of reovirus *jin-1*, the cells (U118MG, CHO, and Lec2) were mock-treated (-) or treated with 100 $\mu\text{g}/\text{ml}$ WGA for 1 hr. at 37°C (+). After exposure of the cells to the virus at 4°C the cells were washed with PBS and incubated for an additional 32 hours in a CO₂ incubator before protein lysates were made. For the immunodetection of the $\sigma 3$ protein the anti-reovirus $\sigma 3$ (4F2) was used and anti-actin was used as a loading control. **(C)** WGA inhibition of *wt* T3D and *jin-1* reovirus infection in 911 cells.

Nevertheless, it is conceivable that the amino acid alterations in the *jin* mutants affect the affinity or avidity of SA binding. To investigate the involvement of SA in binding of our mutant viruses we used Lec2 cells. Lec2 cells have a strongly reduced (by about 90%) amount of sialic acids on their cell surface [84,85]. Lec2 cells are mutants derived from Chinese Hamster ovary (CHO) cells, which are poorly infected by *wt* T3D reovirus [11,36]. In contrast, both the *jin-1* and *jin-3* mutants efficiently infect CHO cells (figure 7.8 A). The *wt* T3D nor *jin-1*

and *jin-3* infect Lec2 cells, as is evidenced by lack of detectable $\sigma 3$ in the cells exposed to these viruses (figure 7.8 A). Also the replication of *jin-1* in the Lec2 cells is markedly reduced compared with the yields obtained in the parental CHO cells (figure 7.8 B). This suggests that the expanded tropism of *jin* is dependent on the presence of SA on the cell surface. To support the utilization of SA by the *jin-1* mutant, we shielded the SA on the surface of the cells by pre-incubating the cells with wheat germ agglutinin (WGA). WGA is a lectin with a strong affinity to a broad range of sialoconjugates. To confirm that WGA effectively binds to the cell lines 911, U118MG and CHO, but not to Lec2, we employed FITC-labeled WGA on fixed cells grown on cover slips (figure 7.9 A). For the competition experiments we blocked the sialic acids with WGA prior to the binding of *jin-1* to the cells. The addition of WGA to the cells inhibited entry of *jin-1* in U118MG and CHO cells (figure 7.9 B). Also in 911 cells, *jin-1* and wt T3D infection are inhibited (figure 7.9 C). This confirms the dependency of wt T3D on SA for cell binding and entry. Our data demonstrate that also the *jin-1* mutant relies on SA binding for cellular entry.

DISCUSSION

The use of tumor-selective oncolytic viruses for killing tumor cells that resist conventional therapeutic approaches is conceptually attractive. Human reoviruses are one of the promising candidates for use as replicating oncolytic agent [6,56,87]. Reoviruses preferentially induce cell death and apoptosis in tumor cells, but not in diploid, non-transformed cells [2,3,53]. However, in some tumor cells expression of the JAM-A receptors is down-regulated and absent on the cell surface, thereby limiting the susceptibility of the cells to reovirus T3D infection.

Here we report the isolation of JAM-A independent T3D reoviruses with an expanded tropism. These mutants, designated as *jin* mutants, may be considered as oncolytic agents in those tumor types that lack accessible JAM-A on their surface [66-68,88] Although we encountered the first *jin* mutant in a batch of S1-His modified reovirus after selection in the U118MG-scFvHis cell line [69], the *jin* mutants are not genetically modified viruses in the formal sense since they resulted from spontaneous mutations in T3D viruses.

In three independent virus batches we identified *jin* mutants. Two of these (*jin-1* and *jin-2*) carried an identical mutation in the head domain of the spike protein $\sigma 1$. The mutation replaces the glutamine (Q) residue at position 336 by an arginine (R). The amino acid 336 is located at a surface exposed position, close to the region involved in the trimerization of the $\sigma 1$ spikes [81]. The alteration renders the area more positively charged. This could potentially result

in conformational changes that may disturb the formation of $\sigma 1$ -trimers. However, the results of a trimerization assay (depicted in figure 7.3) revealed that altered $\sigma 1$ of *jin-1* still forms mature trimers, showing that the Q336R alteration in S1 of the *jin-1* and *jin-2* viruses does not affect trimer formation of this domain.

While the *jin* mutants were isolated on human glioblastoma cell line U118MG, we found that the *jin-1* mutant efficiently infects a variety of reovirus T3D resistant cell lines, including the chicken hepatoma cell line LMH, but not non-transformed primary human skin fibroblasts (VH10). This expanded tropism, together with the small-plaque phenotype observed in the JAM-A positive cell line 911, is reminiscent of changes observed in other virus families. Adaptation to cell culture conditions can result in selection of viruses that acquired the capacity to bind heparan sulfates [89-91]. Variants of foot-and-mouth disease virus (FMDV) which bind strongly to heparan sulfate *in vitro*, show small plaques on BHK cells and these variants are attenuated in cattle. Furthermore, they have a decreased ability to spread from the site of inoculation [91]. Alternatively, mutants of Sindbis Virus that exhibit a reduced binding to heparan sulfate give rise to larger plaques *in vitro* and are more virulent *in vivo* with slower clearance from the circulation [89]. However, the Q336R change in *jin-1* and *jin-2* does not yield a typical linear heparin-binding domain consensus -X-B-B-X-B-X-and -X-B-B-B-X-X-B-X-in which B is a basic residue (mainly K or R) and X a hydrophobic residue [92-94]. It should be noted that the presence of a linear consensus sequence is not a strict prerequisite for glycosaminoglycan binding. Some of Venezuelan equine encephalitis virus (VEE) mutants bind heparan sulfates (HS) through a conformational domain and do not contain the linear HS-binding domain [95]. Our observation that reovirus *jin-1* entry into U118MG cells cannot be inhibited by incubation with heparin or heparan sulphate (data not shown) suggests that binding to glycosaminoglycans is not responsible for the broadened tropism of *jin-1* and *jin-2*. It therefore remains to be established if and how the Q336R change contributes to the expanded tropism. Also with respect to sialic acid binding, in some DNA viruses mutations in the SA-binding pocket resulted in changes in plaque morphology [96,97].

Upon continued serial passaging of *jin* mutants in U118MG cells, additional amino acid alterations accumulated in spike protein $\sigma 1$, T193M in *jin-1* and G187R in *jin-2*. For the *jin-3* mutant, a single mutation in S1 resulted in G196R substitution in $\sigma 1$. Those changes are located in close proximity of the region implicated in sialic acid binding [10,55,75,76]. This is in line with the previous observation that passaging of reoviruses incapable of binding SA on mouse erythroleukemia cells yielded mutants capable of binding sialic acids [83]. In

co-crystalization experiments of $\sigma 1$ in complex with SA it was shown that the changes were mapped in the $\sigma 1$ region between amino acids 198 and 204 [76].

Also outer capsid protein $\sigma 3$ plays an important role in the process of reoviral entry [62,63,98,99]. A mutation found in so-called persistent-infection reoviruses leads to an amino acid change Y354H in the $\sigma 3$ protein. This alteration has been linked to the reoviral resistance to the protease inhibitor E64d [100]. A mutation in *jin-1* results in M357T in $\sigma 3$, which is in close proximity of position 354. However, no such mutations are found in *jin-2* and *jin-3*. Moreover, *jin-1* is sensitive to E64d, demonstrating that the *jin-1* virus still depends on cysteine proteases for uncoating and infection. This suggests that the *jin-1* virus enters JAM-A negative cells via the endocytic pathway, like wt T3D in JAM-A expressing cells.

So far, we have evaluated the *jin* mutants in *in vitro* studies only and it remains to be elucidated what the effect will be *in vivo*, both with regards to safety, as well as to their oncolytic efficacy.

While we cannot exclude the possibility of the recruitment of secondary receptors, our data suggest that the *jin* mutants rely on sialic acid binding for internalization. It is tempting to speculate that a changed affinity for sialic acids underlies the changed tropism of our *jin* viruses, since they show a decreased ability to spread in cultured cells, exhibit a small plaque phenotype, and shielding SA moieties with WGA prevents the *jin* viruses to enter cells. It remains to be established if the mutation in S1 affects reovirus pathology in mice. In this respect, it is noteworthy that the pathology of reoviruses is, in part, dependent on the $\sigma 1$ protein [101].

ACKNOWLEDGMENTS

The authors thank Dr. Marco Schilham and Jens Pahl in the LUMC Department of Pediatrics for providing the STA-ET2.1 cells, and Binie Klein in the LUMC Department of Toxicogenetics for providing the VH10 cells.

SUPPLEMENTARY TABLE

Supplementing table 7.1 List of primers used in this study.

RT-PCR primers	Sequence (5'-3')	Length
S1for	GCTATTGGTCGGATGGATCCTCG	23
S1end R	GATGAAATGCCCCAGTGC	18
S2for	GCTATTCGCTGGTCAGTTATGGC	23
S2endR	GATGAATGTGTGGTCAGTCGTGAGG	25
S3for	GCTAAAGTCACGCCTGTCGTC	21
S3endR	GATGATTAGGCGTCACCCACCACCAAG	27
S4for	GCTATTTTTGCCTCTTCCCAG	21
S4endR	GATGAATGAAGCCTGTCCCACGTCA	25
M1for	GCTATTCGCGGTCATGGCTTA	21
M1endR	GATGAAGCGCGTACGTAGTCTTAG	24
M2for	GCTAATCTGCTGACCGTTACTC	22
M2endR	GATGATTTGCCTGCATCCCTTAAC	24
M3for	GCTAAAGTGACCGTGGTCATGGCT	24
M3endR	GATGAATGGGGGTCGGGAAGGCTTA	25
L1for	GCTACACGTTCCACGACAATG	21
L1endR	GATGAGTTGACGCACCACGACCCATG	26
L2for	GCTAAATGGCGCGATGGCGA	20
L2endR	GATGAATTAGGCGCGCTCACGAGGGA	26
L3for	GCTAATCGTCAGGATGAAGCGG	22
L3endR	GATGAATCGGCCCACTAGCATTG	24
Additional sequence primers		
L1midSQ1 For	GCTAGCTCAAGTTATTCATGGTTTA	25
L1midSQ2 Rev	GCTATGTCATATTTCCATCCGAATTC	26
L1midSQ3 For	GTGAAACTATTCAGAACGATCTAG	24
L1seq3 For	GTCTGGACGAGCGGCCCT	19
L1seq4 Rev	CGCGCTTCTTATCATTGG	19
L1seq5 For	GTCTGGTAGTGCGGTCATTGAG	22
L2midFor	GAACAGAAGATCTTGCCCAA	20
L2midRev	GTCTCGATACCAGTCACGGA	20
L2seq2 Rev	TGGTATAGATTCTGCGTCG	20
L2seq3 For	TGGACGCATGACTCTTCAGC	20
L2seq4Rev	CTGAGGAAGTTCCGATGAAAGCA	23
L2sq6For	CTCTAGTGGGATCTAATGCT	20
L3mdSQ6_REV	CGTCTGCCATTGTACTGCTG	21

Supplementing table 7.1 Continued

Additional sequence primers		
L3midSQ7_FOR	GGACTTCACCAATGAGTTAAC	21
L3midSQ1 For	GTTCAAGTTTCGGCTGATGTCG	22
L3midSQ2 Rev	CGTGGCCACGTGTGAGGCGTTG	22
L3seq4 For	ATGACCCTAGCCAACATG	18
L3seq5 Rev	TGCAGATACATTGGTGTC	18
L3seq8Rev	CAAATGTGTCGACTGAACACG	21
M1midSQ1_For	AATCTTGTTATATGCTCC	18
M1midSQ2_Rev	TGAGCGAATGTTAGCAATC	19
M1midSQ3_Rev	CATGATTTGGATTCTAAT	19
M2midFor	GGAACTAATTGGCATCTCAA	20
M2midRev	TTGCCGTTTGGATCCCAGCT	20
M3midSQ1 For	GATCCTGAAATCTATAACGAG	21
M3midSQ2 Rev	CTGCTGCAACACAGGACATTC	21
M3midSQ3_For	TTGCTTGACGCTGTGCGTGTCG	22
S4midFor	AGCCTTAAACCTGATGATCG	20
S4midRev	AGAATTGGGTTTGACGAGCA	20
Dual-GC primers		
DualS1st rev	AGCGCGGCCGAGTGTTAAACTTCACGTGAAACTACGCGGGT	43
DualS1st for	ACCCGCGTAGTTTCACGTGAAGTTTAAACACTGCGGCCGCGCT	43
DualSH rev	GCCTCTTCTAAGCGTGAAACTACGCGG	27
DualSH for	GCCTCTCCATGGATCCTCGCCTACGT	27
S1-QRmut2Rev	AATGTCGGAGTTCACCCGTACCCTCCAATTCAGC	34
S1-QRmut2For	GCTGAATTGGAGGGTACGGGTGAACTCCGACATT	34
Y313A S1mrev	GCTCTGCCTAAACCTAGCATTGGACTCATTCCGATA	37
Y313A S1mfor	TATCGGAATGAGTCCAATGCTAGGTTTAGGCAGAGC	37

First part of the table contains the primers used for the Reverse Transcription PCR experiments. Middle part contains the additional primers used to sequence the different segments. The last part contains the primers used to clone the S1 and S1mutants in the Dual-GC system for the trimerization experiments

CHAPTER 8

HETEROGENEOUS REOVIRUS SUSCEPTIBILITY IN HUMAN GLIOBLASTOMA STEM-LIKE CELL CULTURES

S.K. van den Hengel

R.K. Balvers

I.J.C. Dautzenberg

D.J.M. van den Wollenberg

J.J. Kloezeman

M.L. Lamfers

P.A.E. Sillevius Smitt

R.C. Hoeben

Cancer Gene Therapy (2013), 20:507-513



INTRODUCTION

Treatment of glioblastoma (GB) remains a significant clinical challenge. Despite intensive treatment, which includes surgical resection, followed by chemoradiation therapy, the prognosis remains infaust. This is largely due to the high tumor recurrence rate caused by the highly infiltrative and aggressive nature of these tumors. Despite the extensive research in the past decades, the patient survival rates have only incrementally improved [102]. An important role in the recurrence of GBs has been assigned to a small population of cells, the GB stem-like cells (GSC) [102-104]. These cells possess high resistance to radio- and chemotherapy [105-107] and can self-renew and differentiate into the heterogeneous cell types that drive tumorigenesis [103,108,109]. Additionally, genotypic and phenotypic analyses of cultured GSC revealed that they retain the molecular characteristics of the parental tumors better than cells cultured in conventional serum-containing media [108,109].

The notion that GSCs are relatively resistant to the conventional radiation and chemotherapies stresses the importance of exploring other means of eliminating these cells. An approach that has gained much interest for cancer treatment over the past decades is virotherapy. So far, at least fifteen different viruses have been evaluated in preclinical studies. Of these, at least four, that is, herpes simplex virus, human adenovirus, Newcastle disease virus and mammalian reovirus, have been evaluated in clinical studies for the treatment of GB. The results demonstrated that the approach is safe and well tolerated, and provided anecdotal evidence of anti-tumor efficacy (as reviewed in Wollman *et al.* [110] and Zemp *et al.* [111]) Nevertheless, these studies revealed that the therapeutic efficacy needs further improvement. One way to accomplish this is to focus the treatment modalities by identifying those tumors and patients who are more likely than others to respond to a specific therapy.

Here we evaluated the susceptibility of a panel of cultured GSCs, isolated from tumor resections of GB patients, to mammalian reovirus Type 3. Reovirus Type 3 Dearing (T3D) has been evaluated extensively as oncolytic agent. It has a segmented double-stranded RNA genome. Reovirus attachment and entry are mediated by the junction adhesion molecule-A (JAM-A), which is an integral tight junction protein [9,36]. Research indicates that the absence or incorrect expression of JAM-A on colorectal tumor cells inhibits reovirus infection [112]. In addition, upon infection, reoviruses preferentially lyse cells with an activated RAS/RalGEF/p38 pathway [7,29,53]. This tumor cell preference leads to the initiation of at least 30 clinical studies involving the use of wild-type (wt) T3D as oncolytic agent [113]. So far, one phase-I clinical trial involving intratumoral

administration of reovirus to patients with recurrent malignant glioma was completed. This study showed that this approach is safe and well tolerated, but anti-tumor efficacy has been limited [1].

To evaluate the capacity of reovirus to establish a lytic infection in brain tumor stem cells, we assessed the cytolytic capacity of reoviruses in GSC cultures. First, the expression of the canonical mammalian reovirus receptor, JAM-A [9] was analyzed by flow cytometry. A wide heterogeneity in JAM-A expression between the GSC cultures was observed. Therefore, the susceptibility to wt T3D was compared with the susceptibility to the T3D mutant *jin-1*. This mutant, in contrast to wt T3D, can infect cells independent of JAM-A expression [114]. To evaluate the susceptibility of the GSCs, early viral protein synthesis, the virus-induced cytopathic effect and progeny virus yields were determined. Progeny virus yields are relevant, as virus spread and amplification are dependent on progeny production. Moreover, virus penetration and spread in 3-dimensional (3D) GSC spheroid cultures were determined. The 3D cultures serve as an intermediate between monolayer cultures and animal model systems, and these 3D cultures may mimic the intratumoral environment more than monolayer cultures [115,116]. Moreover, distribution, spread and oncolysis can be studied in 3D spheroid models [117]. Our data reveal a wide heterogeneity in reovirus susceptibility among the different GSC cultures and that the reovirus replication can be hampered at various stages of infection. In addition, we demonstrate that the *jin-1* mutant infects cells more efficient in GSCs in monolayer cultures, is more cytolytic and produces more progeny virus upon GSC infection. However, in 3D GSC spheroid cultures, the pattern of viral spread and infection of *jin-1* was similar to wt T3D.

MATERIALS AND METHODS

Cell lines

The established cell lines 911 and U118MG were cultured in high glucose Dulbecco's modified Eagle medium (DMEM) (Invitrogen, Breda, The Netherlands), supplemented with penicillin, streptomycin (pen-strep) and 8% fetal bovine serum (Invitrogen, Bleiswijk, The Netherlands). A detailed protocol for establishment of GSC cultures from glioma resection specimens is described elsewhere [118]. In brief, GSCs were grown on growth factor-reduced extracellular matrix-(Cultrex BME Reduced Growth Factor, R&D systems, Abingdon, UK) coated dishes and cultured in DMEM/F12 supplemented with 1% pen-strep, B27 (Invitrogen), human EGF (5 µg/ml), human basic FGF (5

µg/ml) (both Tebu-Bio, Heerhugowaard, The Netherlands) and heparin (5 mg/ml) (Sigma-Aldrich, Zwijndrecht, The Netherlands). The tumor material was acquired with informed consent from patients as approved by the Institutional Review Board of the Erasmus Medical Center, Rotterdam. All cell cultures were cultured in humidified atmosphere of 5% CO₂ at 37°C.

Reovirus

The wt mammalian reovirus Type 3 Dearing strain R124 (referred in the text as wt T3D), and the *jin-1* mutant were propagated as described before [114]. Cultures of 911 cells were exposed to wt T3D in DMEM 2% fetal bovine serum. At 4 hrs post infection, the medium was replaced with DMEM 8% fetal bovine serum. The wt T3D virus was harvested 48 hrs after infection by collecting the cells in 2% fetal bovine serum/phosphate-buffered saline and the virus was released by three cycles of freeze-thawing. The *jin-1* virus was propagated on the JAM-A-deficient cell line, U118MG, and was harvested at 72 hrs post infection. Infectious titers of both viruses were determined by plaque assay on 911 cell cultures.

Cell viability assay

Cells were infected in suspension with wt T3D or *jin-1* at a multiplicity of infection (MOI) range 0-100 pfu₉₁₁ per cell. Subsequently cells were transferred to an EMC growth factor-reduced pre-coated 96-well plate in which 1x10⁴ cells per well were seeded. The viability of the cultures was measured 72 hrs post infection by CellTiter-Glo Luminescent Cell Viability assay, according to manufacturer's instructions (Promega, Leiden, The Netherlands). Briefly, the reagent was added to the cell cultures and incubated at room temperature in the dark for 10 min. Next, samples were transferred to black 96-well plates and luminescence was measured by a plate reader (Tecan Infinite M200, Tecan Group Ltd, Männedorf, Switzerland). Luminescence count data of the plate reader were transferred to Microsoft office Excel and half maximal effective concentration (EC₅₀) values were calculated from the mean residual luminescence from three independent samples.

Flow cytometry analysis

Anti-JAM-A immunostaining. GSC cultures, 911 cells and U118MG cells, in suspension as single cells, were incubated with mouse monoclonal anti-JAM-A antibody (clone M.Ab.F11, Cat. No. ab17261, Abcam, Cambridge, UK) for 1 hr on ice. Subsequently, the cells were incubated in the dark with PE fluorochrome-

conjugated rat anti-mouse serum (Cat. No. 340270, BD Bioscience, Erembodegem, Belgium) for 30 min on ice. After washing, the samples were taken up in FACS buffer (phosphate-buffered saline, 0.5% BSA, 2 mM EDTA) and assayed on a BD LSRII flow cytometer. Data were analyzed with FACSDiva software (BD Bioscience).

Anti-Sigma 3 immunostaining. Cells were infected in suspension with wt T3D or *jin-1* at an MOI 3 pfu₉₁₁ per cell and transferred to a 6-well plate at 2x10⁴ cells per well. After 30 hr, the cells were harvested and fixed in 4% formaldehyde for 10 min. Subsequently, cells were washed and permeabilized with Perm/Wash buffer (Cat. No. 554714, BD Cytfix/Cytoperm Fixation Permeabilization kit, BD Bioscience) followed by incubation with the anti-Sigma 3 mouse antibody (4F2, monoclonal antibody, Developmental Studies Hybridoma Bank (DSHB), University of Iowa, Iowa, IA, US) for 1 hr at 4°C. After washing twice with Perm/Wash buffer, the samples were incubated in the dark with the PE fluorochrome-conjugated rat anti-mouse serum (Cat. No. 340269, BD Bioscience) for 30 min. Subsequently, the samples were washed extensively, resuspended in FACS buffer and assayed on a BD LSRII flow cytometer and data of a gated population of 1x10⁴ cells were analyzed with FACSDiva software (BD Bioscience).

Viral progeny

Cells were exposed in suspension at 37°C for 1 hr with wt T3D or *jin-1*, MOI 3 pfu₉₁₁ per cell. Next, unbound virus was removed by centrifugation, removal of the medium and plating the cells in fresh medium in 24-well plates. After 72 hrs, cells and media were collected and freeze-thawed three times to release virus from the cells. Viral titers were determined by plaque assays on 911 cells as described [28]. The plaque titration conditions used have an inter-experimental variation of <15%. The virus production by the cell cultures was expressed as the fold-increase and calculated by dividing the total yield by the amount of virus used to infect the culture.

Spheroid 3D cultures

Multicellular spheroids were generated by seeding 1x10⁴ cells per well in a non-adherent 96-well round-bottom plate in culture media supplemented with 2.4% methylcellulose (Sigma-Aldrich). After 1 day, the multicellular spheroids were washed three times and placed in fresh media. Two days later, the spheroids were mock infected or exposed to wt T3D or *jin-1* at a MOI 10 pfu₉₁₁ per cell. Three days after infection, the spheroids were fixed overnight with 4% formaldehyde and embedded in paraffin. Analyses of 6 mm paraffin sections were performed

by 3,3'-Diaminobenzidine immunocytochemistry. First, sections were incubated overnight with the primary antibody against Sigma 3 (4F2, DSHB) followed by a wash and subsequent incubation with the secondary horse radish peroxidase-conjugated antibody (Cat. no. P0447, Dako, Glostrup, Denmark).

RESULTS

The aim of our research is to develop an oncolytic virus-based therapy for glioblastoma. To assess the susceptibility, we defined the sensitivity of GSCs to reovirus by measuring five parameters. A panel of seven independent serum-free GSC cultures [118] was evaluated in parallel to the highly reovirus-susceptible human embryonic retinoblast cell line 911 [28,114] and the JAM-A negative U118MG cell line [114]. All of the serum-free GSC cultures are derived from GB resections, five from primary tumor specimens, and two from recurrent disease cases. The characteristics of the patients from whom the GSC cultures were derived are summarized in table 8.1. The expression of the JAM-A reovirus receptor was assessed in each of these cultures by flow cytometry. The expression is heterogeneous and could be categorized in four groups. The GS187 and GS249 cultures were JAM-A negative whereas the GS184 and GS186 have only a low-level of JAM-A expression. Moderate JAM-A expression was measured in GS79 and GS245 cultures, respectively, with between 30 and 50% of the cell population expressing JAM-A. The highest expression was observed in GS224, in which almost the entire population expressed JAM-A (figure 8.1 and table 8.2). The latter closely resembled the JAM-A expression of the control cell line 911. The high variation in JAM-A expression prompted us to include in our studies the T3D reovirus *jln-1*. In contrast to the wt T3D, the *jln-1* mutants can infect cells independent of JAM-A expression [114].

Table 8.1 Patient Characteristics of Glial Stem-like Cells cultures

GSC Cultures	Male/Female	Age	Type
GS79	F	74	GB
GS184	M	50	GB
GS186	F	48	GB
GS187	F	63	GB recurrent
GS224	M	49	GB recurrent
GS245	M	70	GB
GS249	M	43	GB

Abbreviations: F, female; GB, glioblastoma; M, male

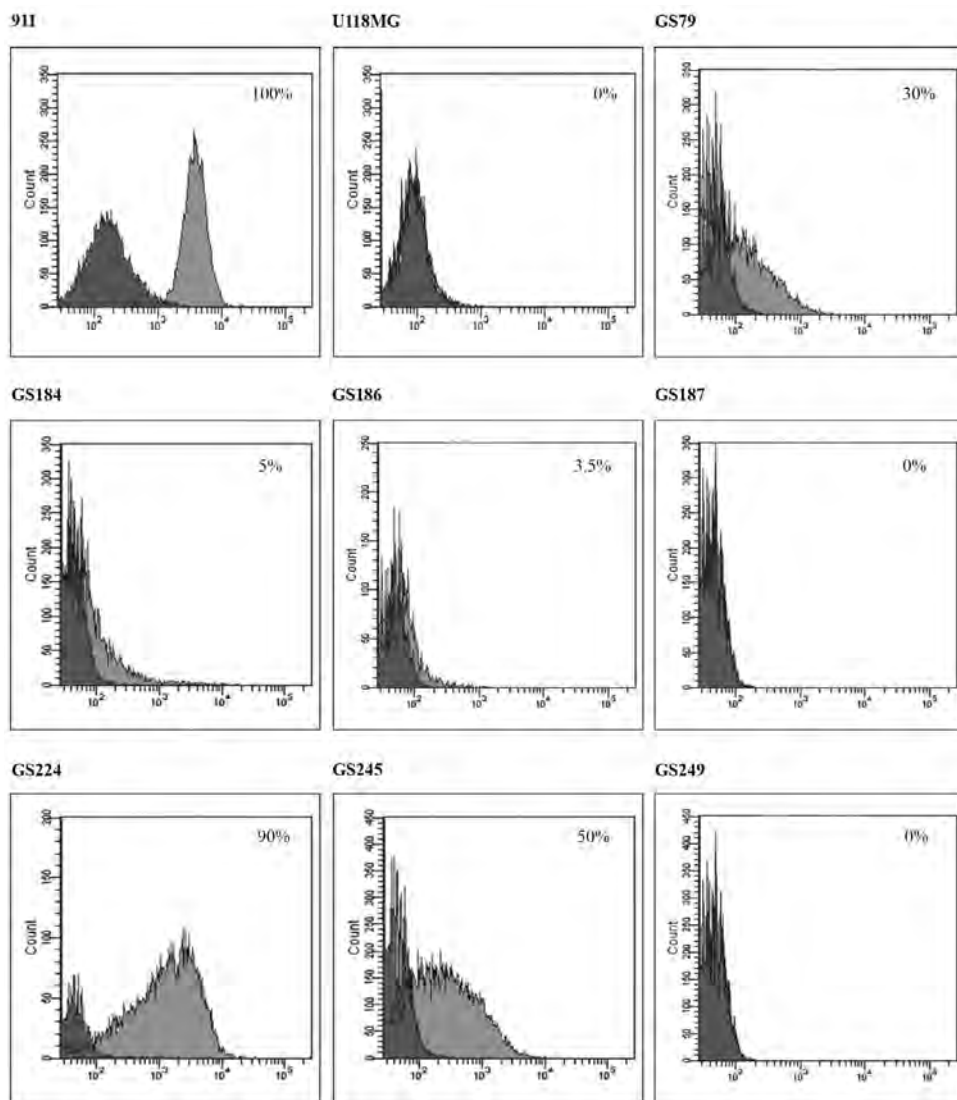


Figure 8.1 Flow cytometry analyses of JAM-A expression on GSC cultures and 911 and U118MG cells. Staining was performed with an anti-JAM-A mouse monoclonal antibody followed by a secondary rat anti-mouse PE-conjugated antibody (light grey histograms). The dark grey histograms represent the incubation with secondary antibody only. The analysis was performed on a gated population of 10,000 cells. The percentages represent the JAM-A positive population in respect to only secondary antibody treated cells.

Table 8.2 GSC cultures exposed to wt T3D or jin-1 reovirus.

GSC culture	JAM-A expression	Fraction of reovirus σ 3-positive cells (%)		EC50 (pfu/cell)		Reovirus yield - fold increase over input		Reovirus yield per σ 3-positive cell (pfu/cell)	
		wt T3D	jin-1	wt T3D	jin-1	wt T3D	jin-1	wt T3D	jin-1
911	High	88	59	0.2	0.1	430	700	15000	36000
U118MG	Negative	0.2	1.3	Insensitive	>100	0.33	14.1	5000	33000
GS79	Moderate	22	99	64	4.1	20	30	300	90
GS184	Low	0.8	19	>100	26	0.5	15	200	9100
GS186	Low	0.6	66	9.3	<1	21	570	10 500	2600
GS187	Negative	0.4	62	Insensitive	8.2	2	250	1 500	1200
GS224	High	54	89	7.6	1.2	11	14	60	50
GS245	Moderate	0.5	16	>100	40	3.7	108	2 200	2000
GS249	Negative	0.4	67	Insensitive	>100	3.7	670	2 800	3000

Abbreviations: GSC, glioblastoma stem-like cells; JAM-A, junction adhesion molecule-A; T3D, Type 3 Dearing; WT, wild type.



Within the GSC cultures, a highly variable sensitivity to wt T3D reovirus infection was observed (table 8.2). In five out of seven GSC cultures, the fraction of reovirus-positive cells did not exceed 1%. This indicates that virus entry in these cultures is inhibited or that the infection is blocked prior to the initiation of reovirus protein synthesis. In contrast, upon wt T3D reovirus exposure, approximately 20% of the GS79 cells were positive for $\sigma 3$, whereas in GS224, more than 50% of the cells synthesized $\sigma 3$ (table 8.2).

To establish the EC_{50} , each culture was exposed to serial dilutions of the wt T3D reovirus stocks and the viability was determined. No clear cytopathic effects were observed in four GSC cultures. The viability assay demonstrated that GS187 and GS249 are fully resistant to wt T3D. The GS184 and the GS245 cultures exhibited a minimal reduction in viability at the highest MOI used and therefore their EC_{50} values were scored as >100 pfu₉₁₁ per cell. Infection of wt T3D was clearly discernible in GS79, GS186 and GS224 cultures (table 8.2). In GS186 cultures, the reovirus cytolysis was not accompanied by reovirus protein synthesis.

To study whether GSC infection results in the production of infectious progeny reovirus, the viral yields were determined at 72 hr post infection. From these data, the fold-increase in progeny was calculated (table 8.2). Significant amounts of progeny virus particles were obtained in six out of the seven GSC cultures. Only from the GS184 culture the amount of reovirus recovered was below the amount used to infect the cultures. The highest yields were collected from GS79 and GS186, with a 20-fold-increase in infectious titer. A 10-fold-increase was produced by GS224. The cultures of GS245 and GS249 both yielded almost four times more virus particles. A doubling of the infectious virus particle number was achieved by GS187. From these data we conclude that several of the GSC cultures are productively infected with wt T3D, albeit with highly variable yields.

In order to determine the virus production per cell, the data of the $\sigma 3$ -positive population was combined with the virus yields (table 8.2). The viral yield per cell obtained from GS79, GS184 and GS224 was low, and does not exceed the 300 pfu₉₁₁ per cell. The production per cell from GS187, GS245 and GS249 cultures ranged from 1.5×10^3 to 3×10^3 pfu₉₁₁ per cell. The highest yields were produced by GS186 with approximately 10^4 pfu₉₁₁ per cell. These data show that, whereas some cultures are susceptible to reovirus infection, they do not replicate reoviruses to high titers.

The GSC cultures were grown as spheroids to study the reovirus spread in 3D cultures that mimic the tumor structure more faithfully than monolayer cultures [116,119]. Immunocytochemistry revealed the presence of reovirus-infected cells in all GSC spheroid cultures. The distribution and the abundance of the reovirus-infected cells differed within the GSC spheroids (figure 8.2). In GS184,

only a few reovirus-positive cells were detected throughout the spheroid. In GS79 and GS245, the entire outer rim of the spheroids was infected. Already at visual inspection of the spheroid cultures cellular debris was observed surrounding the spheroids. These detached cells were lost during sample processing prior to analysis. In GS187 and GS249, the wt T3D infected cells were concentrated at a single side of the spheroids, suggesting that the virus infection was initiated at a single point near the outer rim, and then spread inward from there. Additionally, visual inspection of GS187 spheroids revealed abnormal blown-up cell structures on the edge of the spheroid, indicative of reovirus infection. The GS224 spheroids showed a mixed pattern of infection with the entire outer layer being reovirus infected in combination with inward spread on one side of the spheroids. On GS186 spheroids, the $\sigma 3$ staining revealed that all cells of the spheroids were infected with the exception of the core cells in a few spheroids. Taken together, these data show that there is a high variation in the extent of reovirus infection and pattern of spreading in the different GSC spheroid cultures.

To study whether the *jln-1* mutant is more effective in the GSC cultures, we repeated the experiments described above with this mutant virus. Overall, the fraction of positive cells exceeded the fraction of reovirus positive cells after infection with wt T3D. The cultures with the lowest number of reovirus $\sigma 3$ -positive cells included GS184 and GS245. In the GS186, GS187 and GS249 cultures, more than 60% of the cell population stained positive for $\sigma 3$ reovirus protein. Most susceptible to *jln-1* were GS79 and GS224 with, respectively, 99 and 89% of the cells being reovirus positive (table 8.2).

Similar to the experiments with wt T3D reovirus, the EC_{50} values were determined (table 8.2). All values of *jln-1* infection were found to be lower than after infection with wt T3D. On GS249, a moderate cytopathic effect of *jln-1* was seen at $MOI=100$. In all the other six cultures, cytopathic effects were clearly seen in higher dilution ranges. The EC_{50} determined on GS245 and GS184 was 40 and 26 pfu_{911} per cell, respectively. The remaining four cultures scored an EC_{50} below 10 pfu_{911} per cell. The culture most sensitive to *jln-1* was GS186, in which an effect was already observed at $MOI=0.1$.

The lowest effective viral progeny yield was obtained from GS79, GS184 and GS224 with less than a hundred-fold-increase in virus titer. Higher yields were obtained in GS245 and GS187 with a 200 and 500-fold amplification, whereas in the GS186 and GS249 cultures the yields exceeded the input dose by three orders of magnitude (table 8.2). Moreover, the calculated yield per infected cell in four of the seven cultures was similar for the *jln-1* and wt T3D viruses. In three cultures, the yields per cell were different from those of wt T3D and *jln-1*. In GS79 and GS186, the yield of progeny virus is higher for wt T3D than

for *jin-1*, whereas in GS184 the yield of the *jin-1* was 45-fold higher than in wt T3D-exposed cultures.

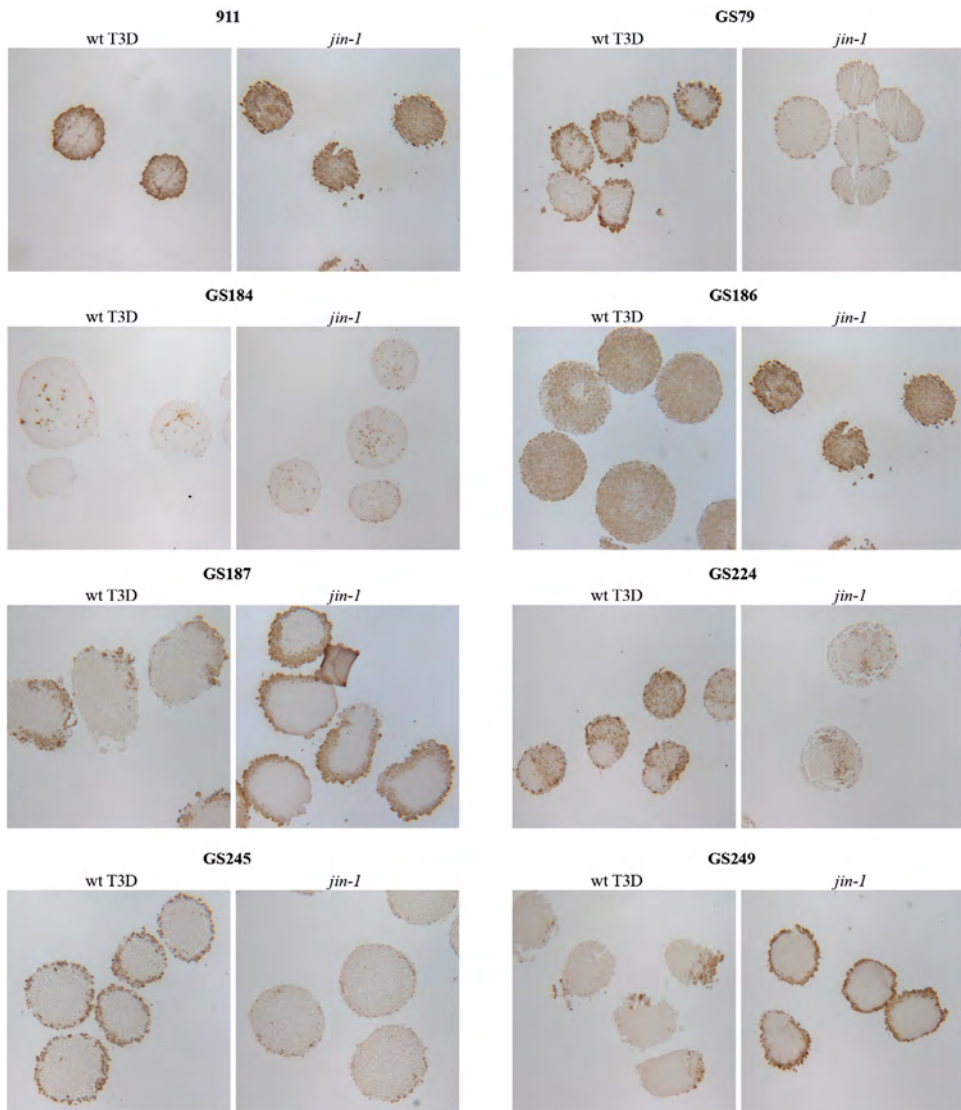


Figure 8.2 wt T3D and *jin-1* reovirus infection pattern in GSC spheroids. GSC spheroids generated of 10,000 cells were incubated with wt T3D or *jin-1* at MOI =10. After 72 hrs, the spheroids were fixed and processed into paraffin sections. To analyze the $\sigma 3$ pattern, sections were incubated with the monoclonal antibody 4F2 against $\sigma 3$ followed by secondary antibody horse radish peroxidase (HRP)-conjugated polyclonal Goat anti-Mouse immunoglobulins. HRP activity was visualized by 3,3'-Diaminobenzidine staining. The brown color indicates the presence of $\sigma 3$ protein indicative of reovirus infection.

To study the distribution and abundance of reovirus-infected cells in 3D cultures, GSC spheroids were exposed to *jin-1* (figure 8.2). Similar to wt T3D, variable results were obtained upon exposure to *jin-1*. In four GSC spheroids, the cells at the outer rim stained positive for $\sigma 3$, although at varying levels. GS187 and GS249 were more effectively infected than GS79 and GS245. Viral spread into the core of the spheroids was seen in GS184, GS186 and GS224. In GS184 and GS224, only some isolated reovirus-infected cells were seen, whereas in GS186 spheroids, $\sigma 3$ -stained cells were found throughout the spheroid.

DISCUSSION

The identification of GSCs, their role in tumor recurrence, metastases and therapy resistance, stresses their importance in brain cancer research. Treatment procedures aiming at eliminating these cells may improve brain cancer outcomes [102,120]. The aim of this study was to test the susceptibility of GSC cultures to the wt mammalian reovirus T3D and the JAM-A-independent *jin-1* mutant. In previous studies, the susceptibility to reovirus was tested in tumor cells in serum-supplemented cultures [35,121], which lose their parental tumor characteristics during culturing [108,109] and therefore may be less representative for the clinical situation.

In this study, we measured the GSC cultures on four parameters - reoviral protein synthesis, the induction of cytopathic effects, the production of progeny virus and the spread and penetration of the virus in a 3D spheroid culture of the GSC. These parameters are all independently evaluated in addition to cell lysis, production and spread. Moreover, because the expression of the high-affinity reovirus receptor JAM-A varied on the GSC cells, we evaluated if *jin-1* was more potent in this regard than wt T3D.

From this study we conclude that there is marked heterogeneity between the GSC cultures in their sensitivity to reovirus-mediated cytolysis. The differences in reoviral $\sigma 3$ protein synthesis may reflect variation differences in reovirus binding to the cells, reovirus egress from endosomes or differences in positive-strand messenger RNA generation [122,123]. The efficiency of reovirus $\sigma 3$ protein synthesis does not correlate with the sensitivity to reovirus-mediated cytolysis. While GS186 is poorly susceptible to wt T3D reovirus synthesis, as evidenced by the fraction of cells that produces $\sigma 3$ proteins, it is relatively sensitive to reovirus-induced cytolysis. In contrast, GS79 synthesizes $\sigma 3$ -proteins in a relatively high percentage of the cells, while it is relatively insensitive and requires a high MOI for induction of cytopathic effects by wt T3D. Similarly, we see a highly variable capacity to support reovirus propagation. The amount of

progeny reovirus produced per productively infected cells varies over 2 orders of magnitude with the GS186 culture being the most effective wt T3D producer, and the GS224 being least effective. With the use of the *jln-1* reovirus, we see a similar heterogeneity. Whereas minor variation is seen in fraction of reovirus-infected cells in the different GSC cultures, the sensitivity to reovirus-induced cytolysis, as well as the capacity to produce progeny reovirus is much more heterogeneous.

The infection efficiency, the reovirus-induced cytolysis and the virus production in the monolayer cultures are more efficient with *jln-1* than with wt T3D. In contrast, the distribution and abundance of $\sigma 3$ -positive cells in spheroid cultures is similar with these viruses. This suggests that the JAM-A receptor expression is not a prime determinant of the reoviruses' capacity to spread in spheroid cultures. Although this was unexpected, it is not unprecedented. Recently it was established that wt T3D infects and spreads efficiently in 3D tumor spheroids established from JAM-A-deficient U118MG cells. In contrast, wt T3D infection of U118MG cells in monolayer cultures is dependent on JAM-A expression [124]. This demonstrates that the canonical T3D entry route, which starts by the reovirus $\sigma 1$ protein's engagement of JAM-A, is not essential in 3D cultures, and that under these growth conditions alternative entry routes can be used by the reovirus.

Spread of the oncolytic viruses within the tumor is essential for anti-tumor efficacy. The compartmentalization brought about by depositions of extracellular matrix presents itself as a physical barrier [125]. Also, the vasculature and the tumor-stroma may impose limitations to viral spread [126]. An appealing option for enhancing the spread of the oncolytic viruses is the use of carrier cells loaded with oncolytic viruses [127-129]. The carrier cells need to possess the capacity to home to tumors. Several cell types have been identified that can home to tumors, such as dendritic cells, T cells, macrophages and several types of stem cells. After loading, the virus should hitchhike on these cells and be released in the tumor [128,129]. If the viruses are associating with the cells in a manner that shields them from neutralizing antibodies, the approach may also be effective in those patients with pre-existing neutralizing immunity against reovirus. That this strategy can be applied for reovirus delivery was shown by Ilett *et al.* [130,131], who showed that reovirus can hitchhike onto dendritic cells and T cells. Additionally, internalization of reovirus by dendritic cells protected the virus from neutralizing antibodies [131].

So far, only single GSC cultures were established and studied from the individual patients. It therefore remains to be established whether the

heterogeneity observed between different cultures faithfully reflects phenotypic inter-patient or inter-tumor variations, or whether the heterogeneity is the result of intratumor heterogeneity [132] or even phenotypic drift in the cultures. The latter could result from the preferential outgrowth of specific populations of cells in the tumor cell cultures. Such culture bias could limit the predictive value as model for the clinical tumors *in situ*. It would therefore be extremely useful if clinical studies on the efficacy of oncolytic reovirus therapy were paralleled with *in vitro* studies on reovirus sensitivity in cultures of tumor cells derived from the same patients. Such studies may eventually reveal which of the *in vitro* parameters would best predict the efficiency of therapeutic reovirus replication *in vivo*.

CONFLICT OF INTEREST

The authors declare no conflict of interest.

CHAPTER 9

MESENCHYMAL STROMAL CELLS AS CARRIERS FOR ONCOLYTIC REOVIRUSES: AN *IN VITRO* FEASIBILITY STUDY

S.K. van den Hengel
I.J.C. Dautzenberg
D.J.M. van den Wollenberg
R.K. Balvers
M.L. Lamfers
P.A.E. Sillevius Smitt
R.C. Hoeben

In preparation



INTRODUCTION

A promising oncolytic agent for the treatment of a variety of cancer types is the mammalian *orthoreovirus* type 3 Dearing (T3D) [8]. The mammalian *orthoreoviruses* were first isolated from the respiratory and enteric tract. Infections proceed usually asymptotically and the majority of the human population possess neutralizing antibodies against reovirus [133,134]. Already in the late 1970's, the human reoviruses' preference for lytic replication in transformed cells was noted [47,135,136]. Strong and coworkers were the first to implicate activation of the RAS signaling pathway in the sensitization of cells to reovirus replication and cytolysis [53]. Subsequently, more details were unraveled and the sensitivity of cells to reovirus mediated cytolysis was related to an activated RAS/RaGGEF/p38 signaling pathway [7,47,57]. This pathway is constitutively activated in many human tumors [8,47,137]. The virus' preference for transformed cells, together with the absence of reovirus-associated clinical pathology, led to studies on the feasibility of using wild-type (wt) reovirus T3D as oncolytic agent.

Phase I and II clinical trials involving the use of reovirus T3D have been initiated for a variety of tumor types [113]. These studies demonstrated that reovirus-administration to humans is generally safe and well tolerated [1,58,59,138]. Despite evidence of antitumor efficacy, the overall effect of reovirus as single therapeutic agent has been limited. Currently the use of reoviruses in combination with conventional therapies is being explored in phase I-III clinical trials [113,138,139]. The first results of these combination trials demonstrate that also this strategy is safe and well tolerated [138,140-142], and there is evidence for anti-tumor efficacy [143]. Although these data are encouraging, the deposition of the reovirus into the tumor upon systemic virus delivery is limited and should be improved to enhance therapeutic efficacy.

The presence of neutralizing antibodies reduces the transduction of tumor cells, especially upon systemic administration [128,138]. In addition, other soluble factors, including complement and pre-immune IgM, as well as non-specific binding of the viruses to blood cells, and uptake by non-target tissues, hamper therapeutic virus delivery [144]. To enhance oncolytic virus therapy efficacy, various virus-shielding strategies to improve the viral transfer to the tumors have been explored [113]. One of these strategies involves the use of cellular delivery vehicles. Migration of cells to tumors may facilitate chaperoning and delivery of the viruses to the tumor site. In addition, during transport the carrier cells may shield the virus from neutralizing antibodies [128,145-147]. There are a number of cell types which have been investigated as oncolytic-virus

delivery vehicles including cytokine induced-killer cells, tumor-antigen-specific T cells, dendritic cells, macrophages, and various stem cells [129,148].

In this study we explored the possibility of loading human bone marrow-derived mesenchymal stromal cells (MSC) with reovirus with the prospect of using them as delivery vehicles for therapeutic viruses. The procedure of isolating MSC is relatively straightforward and the cells can be cultured and expanded *in vitro*. Studeny and coworkers [149] were the first to show that MSC could be used as a delivery vehicle for tumor targeting. They transduced MSC with an adenoviral vector expressing IFN- β and administered these cells to tumor bearing mice. Although the therapeutic effect was transient, tumor growth was significantly delayed compared to human IFN- β administration [149]. Subsequent studies explored the delivery of oncolytic viruses such as adenovirus and measles virus to both immune-deficient as well as in immune-competent tumor bearing-mice [147,150,151]. These studies further encouraged exploration of MSC for reovirus delivery.

Here, we evaluated loading of MSC with wt T3D and with the mutant reovirus *jin-1*, which can infect cells independent of the expression of the junction adhesion molecule-A (JAM-A) [114]. Our data demonstrate that human MSC could be successfully loaded with wt T3D and with *jin-1*, and that loaded MSC could successfully hand-off virus to both monolayer as well as in 3-dimensional tumor cell spheroids. In addition, the reoviruses could also be handed off to JAM-A negative U118MG cells in spheroid cultures, consistent with our earlier observations that reovirus infections in tumor cells spheroids do not depend on JAM-A expression [124]. Taken together these data warrant further exploration of MSC-mediated oncolytic reovirus delivery in experimental tumor models.

MATERIAL AND METHODS

Cell lines

The human adenovirus type 5 (HAdV-5) E1 transformed human embryonic retinoblast cell lines 911 and the malignant glioma cell lines U118MG and U87MG were cultured in Dulbecco's modified Eagle's medium (DMEM, Gibco-BRL, Breda, the Netherlands) supplemented with 10% fetal bovine serum (FBS, Gibco-BRL). Human bone-marrow derived Mesenchymal Stromal Cells (MSC) (a kind gift from H. Roelofs, LUMC) were cultured in DMEM supplemented with 10% FBS and penicillin-streptomycin. All cell lines were maintained at 37°C in humidified atmosphere with 5% CO₂.

MSC expressing eGFP were generated by lentivirus-mediated transfer of the eGFP expression cassette. Production of the lentiviral vector containing the human Cytomegalovirus immediate early enhancer/promoter driven eGFP-cassette, and the transduction of MSC were performed as described previously [30,33].

Reoviruses

The isolation and propagation methods of the wt T3D and *jin-1* reoviruses were performed as described before [69,114]. In brief, propagation of wt T3D performed on 911 cultures. Cells were exposed to the virus in DMEM with 2% FBS and after 4 hrs, the infection medium was replaced by DMEM with 8% FBS. The wt T3D was harvested 48 hrs after infection by collecting the cells in PBS/2% FBS and released by freeze-thawing the cells three times [69]. The *jin-1* was routinely propagated on the JAM-A-negative cell line U118MG as previously described [114]. The final production was performed on 911 cells and the virus was harvested 72 hrs post-infection. Infectious titers of both viruses were determined by plaque assays on 911-cell cultures and expressed as pfu₉₁₁/ml [69].

Reverse transcription PCR

Total cellular RNA was isolated from MSC with the Absolutely RNA miniprep kit (Stratagene, Agilent Technologies, Amstelveen, The Netherlands). Copy DNA synthesis of JAM-A or GAPDH RNA was started with the synthetic primers hJAM_RT Rev 5'-CACCAGGAATCACGAGGTC-3' or GAPDH Rv 5'-AATGAAGGGGTCATTGATGG-3' using SuperScript III (Invitrogen, Woerden, The Netherlands) for reverse transcription. For the PCR Pfu polymerase (Promega, Leiden, the Netherlands) was used with the primer combination unique for hJAM-A forward hJAM For 5'-ATGGGGACAAAGGCGCAAGTC-3' and hJAM_RT Rev 5'-CACCAGGAATGACGAGGTC-3' or unique for GAPDH Fw 5'-ACAGTCAGCCGCATCTTCTT-3'; GAPDH Rv 5'-AATGAAGGGGTCATTGATGG-3'. The plasmid pLV-JAM-ECD-IRES-Neo [69] encoding huJAM was used as positive control.

Flow cytometry analysis

Anti-JAM-A immunostaining

MSC cultures, as single cells in suspension, were incubated for one hr on ice with mouse monoclonal anti-JAM-A antibody (clone M.Ab.F11, Cat. No. ab17261,

Abcam, Cambridge, UK). Subsequently, the cells were incubated in the dark with PE fluorochrome-conjugated rat anti-mouse serum (Cat. No. 340270, BD Bioscience, Erembodegem, Belgium) for 30 min on ice. After washing, the samples were taken up in FACS buffer (PBS, 0.5% BSA, 2 mM EDTA) and assayed on a BD LSRII flow cytometer. Data was analyzed with FACSDiva software (BD Bioscience).

Anti-sigma-3 immunostaining

Adhered MSC cultures of 10^5 cells were infected with wt T3D or *jin-1* at a multiplicity of infection (MOI) $10 \text{ pfu}_{911}/\text{cell}$, or mock infected. After 72 hrs the MSC were harvested and fixed in 4% formaldehyde (FA) for 10 min. Subsequently, cells were washed and permeabilized with Perm/Wash buffer (Cat. No. 554714, BD Cytotfix/Cytoperm, Fixation Permeabilization kit, BD Bioscience) followed by incubation with the anti-sigma3 ($\sigma 3$) mouse antibody (4F2, monoclonal antibody, Developmental Studies Hybridoma Bank (DSHB), University of Iowa, Iowa, US) for one hr at 4°C. After washing twice with Perm/Wash buffer the samples were incubated in the dark with the PE fluorochrome conjugated rat anti-mouse serum (Cat. No. 340269, BD Bioscience) for 30 min. Subsequently, the samples were washed extensively, resuspended in FACS buffer and assayed on a BD LSRII flow cytometer and data of a gated population of 1×10^4 cells were analyzed with FACSDiva software (BD Bioscience).

Immunofluorescence

MSC were plated in 24-well plates on glass coverslips at a concentration of 10^5 cells/well. The next day cells were exposed to MOI=10 wt T3D or *jin-1* per cell. The MSC were fixed 72 hrs post infection (pi) in ice-cold methanol and subsequently washed with phosphate-buffered saline containing 0.05% Tween-20. The fixed cells were incubated with the primary antibody against reovirus capsid protein $\sigma 3$ (4F2). After thoroughly washing, the cells were incubated with a goat anti-mouse fluorescein isothiocyanate (FITC)-conjugated serum. After 30 min incubation at RT, the secondary antibody was removed and the nuclei were stained with Hoechst 33342 (Molecular Probes, Leiden, The Netherlands). After washing the coverslips were mounted in Vectashield (Vector Laboratories, Inc. Burlingame, US).

Virus yield determination

MSC (10^5 cells) were exposed to reoviruses at a MOI=10 with wt T3D or *jin-1*. After 4 hrs the medium was replaced by fresh medium. At 72 hrs pi conditioned media and cells were harvested and the virus was released from the cells by three cycles of freeze-thawing. The reovirus titers were determined by plaque assays on 911-cell cultures.

Neutralization of wt T3D by IVIg

A monolayer of 911-cells was infected with wt T3D, MOI=3, or Mock. The infection media was supplemented with human intravenous immunoglobulin (IVIg), 10 ng/ml, 1 ng/ml or 0 ng/ml. 48 hrs after infection the viability of the cultures was assayed by adding WST-1 reagent (Roche, Woerden, The Netherlands) according to the manufacturer's instructions.

Virus release assay - monolayer

MSC were exposed to MOI=3 of either wt T3D or *jin-1*. At 72 hrs pi the MSC cultures were harvested by brief trypsinization, washed and incubated in DMEM containing 10% FBS with or without 60 mg/ml IVIg for 30 min at 37°C. Subsequently, the MSC were washed in DMEM containing 10% FBS and counted before they were mixed in increasing concentrations with 911 cultures. The cytopathic effects (CPE) in these mix cultures were scored at day 7 post mixing.

Real-time imaging

In an experimental set up similar to the hand-off assay, the mixed cultures of reovirus-exposed MSC.eGFP and 911-indicator cells were analyzed by bright-field and fluorescence microscopy every hr up to 64 hrs after initiation of the co-culture by IncuCyte life-cell microscopy (Bucher Biotech AG, Basel, Switzerland).

Virus release assay - spheroid cultures

Spheroids cultures of 911, U118MG, and U87MG cells were generated by seeding 10^4 cells/well in a non-adherent 96-well round-bottom plate in DMEM containing 10% FBS supplemented with 2.4% methylcellulose (MC) (Sigma-Aldrich). Two days post seeding, the spheroids were washed three times with media to remove the MC. At day three the spheroids were treated with one of the following conditions; 1) Mock infection; 2) exposed to wt T3D at 2500 pfu₉₁₁/well; 3) exposed to *jin-1* at 2500 pfu₉₁₁/well, 4) addition of 500-mock

infected MSC.eGFP; 5) addition of 500 wt T3D-infected MSC.eGFP; 6) addition of 500 *jin-1* infected MSC.eGFP. The MSC.eGFP had been mock infected or were exposed to MOI=10 wt T3D or *jin-1*, three days earlier. Three days after mixing the spheroids were fixed in 4% formaldehyde (FA), and embedded in paraffin. Microtome sections of 6 μm thickness were deparaffinized, rehydrated, and incubated overnight with the primary antibodies against $\sigma 3$ (4F2) or against GFP (Cat. No. A11122, rabbit polyclonal, Invitrogen, Eugene, Oregon, USA). After thoroughly washing, the secondary Horse Radish Peroxidase (HRP) conjugated antibody (Dako Netherlands bv. Belgium) signals was used to visualize the antigens by 3,3'-diaminobenzidine (DAB) immunohistochemistry.

RESULTS

To assess the ability of reovirus to hitch-hike on MSC to target cells, we studied the reovirus loading onto MSC and the efficiency of MSC-mediated reovirus delivery in different culture systems. In these studies we evaluated loading of wt T3D and of the *jin-1* mutant, which is capable of infecting cells independent of the presence of the high-affinity reovirus receptor junction adhesion molecule-A (JAM-A) [114].

Oncolytic reovirus infection of MSC

An essential cell property for productive infection in monolayer is the expression of JAM-A on the cell surface [9,114,152]. JAM-A expression on MSC was determined by reverse-transcription PCR on total cellular RNA and anti-JAM flow cytometric analysis of the MSC population. No JAM-A cDNA could be amplified (figure 9.1 A) and flow cytometry detected only a small subpopulation (3.3%) of MSC expressing JAM-A (figure 9.1 B). Next, the MSC cultures were exposed to wt T3D or *jin-1* at multiplicity of infection (MOI) 1, 10 and 100 to determine the sensitivity to both reovirus isolates. Three-days post-infection the cells were visually inspected. No overt cytopathic effects (CPE) were apparent in the virus-exposed MSC cultures of MOI=1 and 10. Cultures exposed to MOI=100 clearly suffered from the high virus dose. Immune fluorescence microscopy with an antiserum directed against the reovirus capsid protein $\sigma 3$ did not detect this protein in MSC exposed to MOI=1, and only very few cells exposed to MOI=10 were positive for $\sigma 3$. Additionally only a slightly higher percentage of cells displayed $\sigma 3$ proteins upon *jin-1* exposure than upon wt T3D exposure, 0.8% and 0.2% respectively.

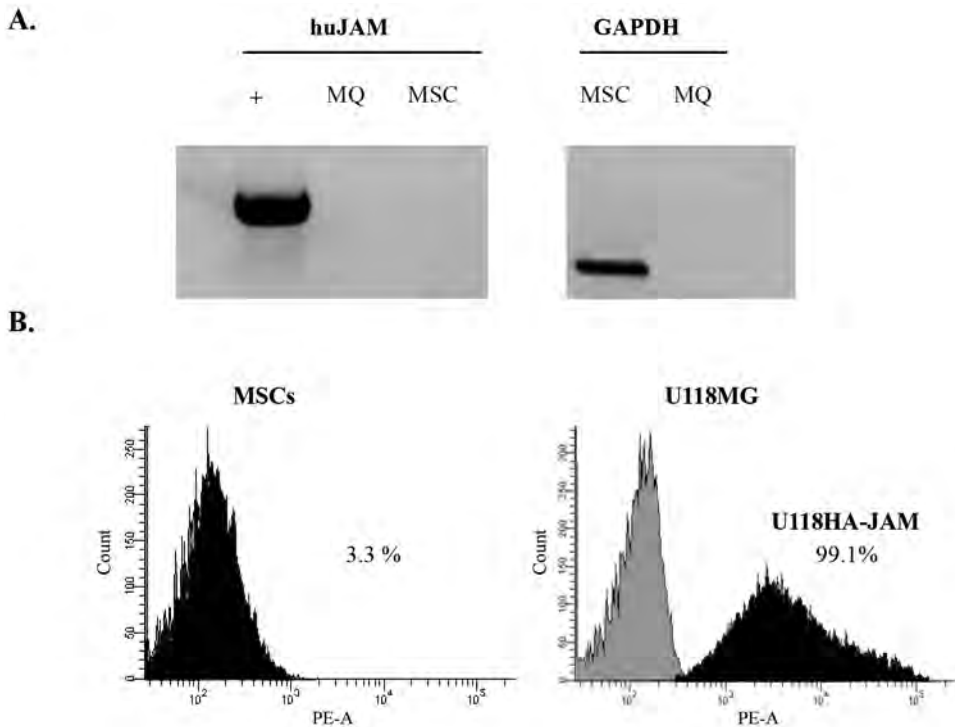


Figure 9.1 A small population of MSC express junction adhesion molecule-A (A) rtPCR analysis was performed on total RNA extract of MSC. Copy DNA (cDNA) synthesis and PCR amplification was performed with specific synthetic oligonucleotides directed against human JAM-A or, as control, GAPDH. A plasmid encoding human JAM-A was used as positive control for the PCR reaction. **(B)** Flow cytometric analyzes of JAM-A expression on MSC – 3.3% of the MSC expressed JAM-A. U118MG, negative for JAM-A, and U118hJAM, 99.1% of the cells expressed JAM-A, were implemented as respectively negative and positive control for the JAM-A staining. Staining was performed with an anti-JAM-A mouse monoclonal antibody followed by a secondary rat anti-mouse PE-conjugated antibody shown in the black histograms. The percentages represent the JAM-A positive population in respect to secondary antibody treated cells only, represented in the grey histograms. Analysis was performed on a gated population of 10,000 cells.

Infectious reovirus particles obtained from MSC

Infected cells were harvested and subjected to several freeze-thaw cycles before total viral progeny yields were determined by plaque assay. No significant differences in the viral production were seen between wt T3D and *jin-1* (figure 9.2). In addition, of both viruses the total yields did not exceed the input titer. Previously similar yields of both viruses were obtained from diploid human skin fibroblasts (VH10 cells), which are also non-transformed cells [114]. This confirmed the poor permissiveness of MSC for wt T3D and *jin-1* reoviruses.

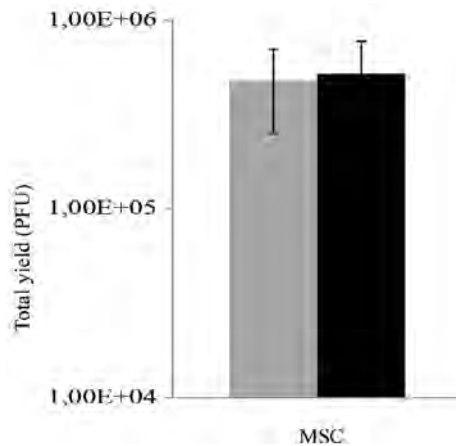


Figure 9.2 The reovirus yield of wt T3D in a MSC culture is comparable to the *jin-1* yield. A total of 10^5 MSC were incubated with reovirus, wt T3D or *jin-1*, $MOI=10$ $pfu_{911}/cell$. After 72 hrs cells and medium were harvested and freeze-thawed three times to release the virus. Virus titers were determined by plaque assays on 911-cell cultures. Grey bar - wt T3D, Black bar - *jin-1*, dashed line - the input titer of the initial infection. The experiments were performed in triplicate.

MSC hand-off oncolytic reovirus

Viruses can use several mechanisms when hitch-hiking with cellular vehicles [129]. The first is that the virus productively infects the carrier cell and produces progeny viruses, which are released at the target site. Alternatively, the viruses may associate non-productively with the cells and be released at the destination site. Either way, the viruses must be released by their cellular vehicle to infect the target cells. To determine the ability of MSC to hand-off reoviruses to sensitive cells, a co-culture experiment was set-up. MSC were exposed for 72 hrs to reovirus either wt T3D or *jin-1* before the loaded MSC were added to reovirus-sensitive 911-cell cultures. Already 48 hrs after mixing the first signs of CPE were observed and over time the CPE became apparent in the higher dilutions as well. At day seven the CPE per mix culture was scored visually, from 0 (no CPE) to 4 (full CPE) (figure 9.3 A). Total CPE was discernible in the 911-cell cultures to which 10^4 and 10^3 wt T3D-loaded MSC were added. If 100 wt T3D-loaded MSC were added, only in one of three cultures full CPE was exhibited while in the other mix-cultures viable cells were still detectable. In the 911 cell cultures mixed with *jin-1*-loaded MSC total CPE was apparent after addition of as few as 10 and 100 loaded-MSC.

The experiment was repeated using eGFP-marked MSC to allow tracking and monitoring of the reovirus-exposed MSC in the co-cultures. In this experiment

the reovirus-loaded eGFP-MSK were mixed with reovirus-sensitive 911 cells and imaged every hr by IncuCyte bright-field and fluorescence microscopy. While in many of the co-cultures the 911 cells exhibit clear CPE for both viruses, no apparent infection signs were seen in the cultures exposed to mock-infected eGFP-labeled MSC for the entire observation period of 64 hrs. Disintegration of eGFP-labeled MSC was regularly noticed. During this process eGFP-labeled vesicle-like fragments were released. Eventually some of these MSC collapsed and completely fragmented, usually between 48 and 60 hrs after initiation of the co-culture (figure 9.3 B). This process was more frequently seen in reovirus-loaded MSC, but also sporadically by mock-loaded MSC.

Viruses can associate with the MSC in several ways. Most straight-forward is that the viruses are associated at the outside of the MSC surface. In this case the viruses would be sensitive to neutralizing antibodies. Alternatively, the virus could be taken up by the MSC and associate with the cell in an internal location. This could be in a manner that allows the virus to replicate, or alternatively, the virus could be taken up in a vesicle, and subsequently released at the tumor site, without any viral replication. In either of the latter two models, the virus would be protected against neutralizing immunity. To discriminate between these models we performed a hand-off assay in which the reovirus-loaded MSC were incubated for 30 min in the presence of a high titer neutralizing antibodies. To this end we used a human intravenous immunoglobulin (IVIg) preparation. The IVIg is derived from blood from over 10^4 healthy donors, and as a consequence has a high titer of neutralizing activity to human reoviruses. The batch IVIg of 1 $\mu\text{g}/\text{ml}$ used in this study contains a neutralizing titer against human reovirus T3D as is shown in figure 9.3 C. IVIg treatment of reovirus loaded MSC delayed, but did not fully block, the induction of cytopathicity for wt T3D as well as *jin-1* (figure 9.3 D). At day seven post-mixing, IVIg treatment inhibited hand-off of the virus in comparison to the untreated controls. These data demonstrate that, at least, part of the viruses carried by the MSC is physically shielded against the neutralizing activity of human immunoglobulins.

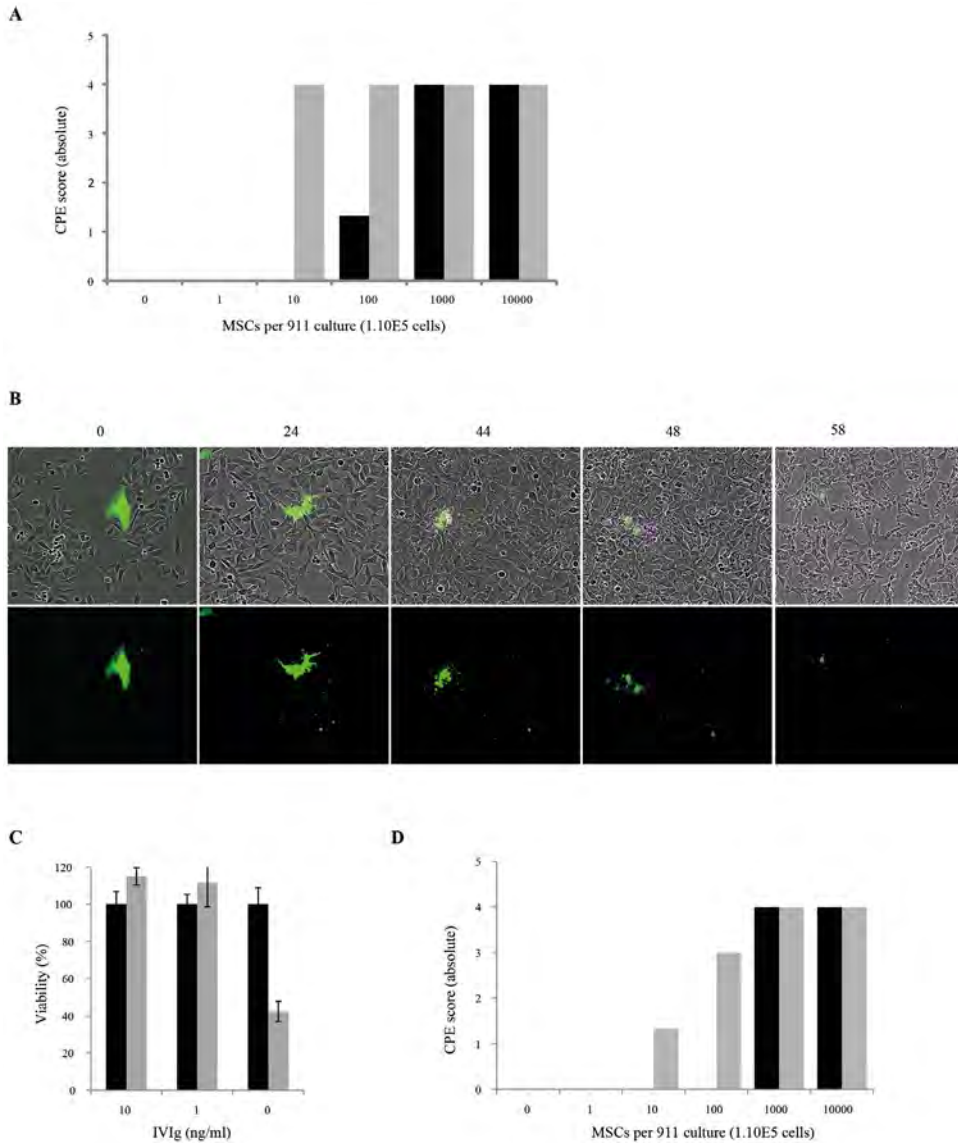


Figure 9.3 Reovirus-loaded MSC can transfer reoviruses to surrounding cells.

Increasing amounts of reovirus-loaded MSC were mixed with reovirus-sensitive 911 cells. **(A)** Mean CPE score over 3 wells at 7 days post mixing. CPE was scored by microscopic inspection on a scale ranging from 0, indicating no CPE visible, 1 - one plaque visible per culture, 2 - several of plaques visible per culture, 3- all cells rounded but still attached to the bottom, and 4- almost all cells detached, the culture in total CPE. **(B)** Bright-field and fluorescent online imaging microscopy. Reovirus-loaded, eGFP expressing MSC were co-cultured with 911-cells. From the start of the experiment up to 64 hrs post mixing every hour photomicrographs were taken using an IncuCyte life-cell imaging system.

Figure represents *jin-1*-loaded MSC co-culture, at 24 hrs the *jin-1* loaded MSC start to form vesicles. At 44 hrs and 48 hrs post mixture the MSC is fragmented and the 911 cells start to show signs of infection and at 58 hrs CPE of 911 cells is clearly visible. **(C)** Neutralization of wt T3D by IVIg. A monolayer of 911-cells was incubated with MOI=3 of wt T3D in IVIg supplemented media, as infection control no IVIg was added. 48 hrs after infection a viability assay was performed. The experiment was performed in triplicate. Black-bar – mock (no virus), Grey bar – wt T3D MOI=3. **(D)** Mean CPE score over 3 wells 7 days post mixing. Reovirus-loaded MSC were washed with IVIg prior to their addition to the indicator cells. CPE was scored visually.

Reovirus hand-off in 3-dimensional tumor cell spheroid models

The data above demonstrated that MSC hand-off reoviruses to reovirus-sensitive 911 indicator cells in monolayer. To investigate whether the MSC could also hand-off reovirus to cells in a 3-dimensional (3D) cell culture, reovirus delivery was evaluated in spheroids generated from 3 different cell lines. The cell lines included are the reovirus-sensitive JAM-A positive 911 cells, JAM-A-deficient U118MG cells, and the JAM-A positive U87MG cells.

MSC expressing eGFP were loaded with wt T3D or with *jin-1* at a MOI=10 and cultured for three days. Subsequently, 500 reovirus-loaded MSC were added to a preformed spheroid. As controls, spheroids were exposed directly to 2500 pfu₉₁₁ wt T3D or *jin-1* per spheroid. The viral titer used was equated to the viral load of 500 MSC. The spheroids were fixed and embedded in paraffin three days after addition of the MSC. Subsequently sections were analyzed for reovirus-infected cells and MSC by antibody staining against reovirus $\sigma 3$ and eGFP, respectively (figure 9.4).

MSC were detected throughout the spheroids in all cell lines (figure 9.4). The MSC were incorporated in the spheroids, as is evident from the eGFP signal at different depths within the spheroids. Mock-treated and reovirus-loaded MSC showed no differences in level and depth of incorporation, suggesting that the capacity of MSC to penetrate the spheroids is not affected by reovirus exposure.

Minimal infection was observed in the 911-cell spheroids exposed to the wt T3D and the *jin-1* (figure 9.4, top panel). In contrast, significant infection occurred when these spheroids were co-cultured with reovirus-loaded MSC. Infection was evident throughout the spheroid, and also included the cores of the spheroids. The reovirus infection initiated by wt T3D-loaded MSC was more pronounced than with *jin-1*-loaded MSC. Since two consecutive sections were used for the analyses, overlay of the pictures allow assessing co-localization of MSC with reovirus infection. This revealed that there were areas in the spheroid that stained positive for reovirus $\sigma 3$ as well as for eGFP. Taken together these data indicate that viral infection was initiated in the spheroids composed of 911 cells by exposure to reovirus loaded MSC.

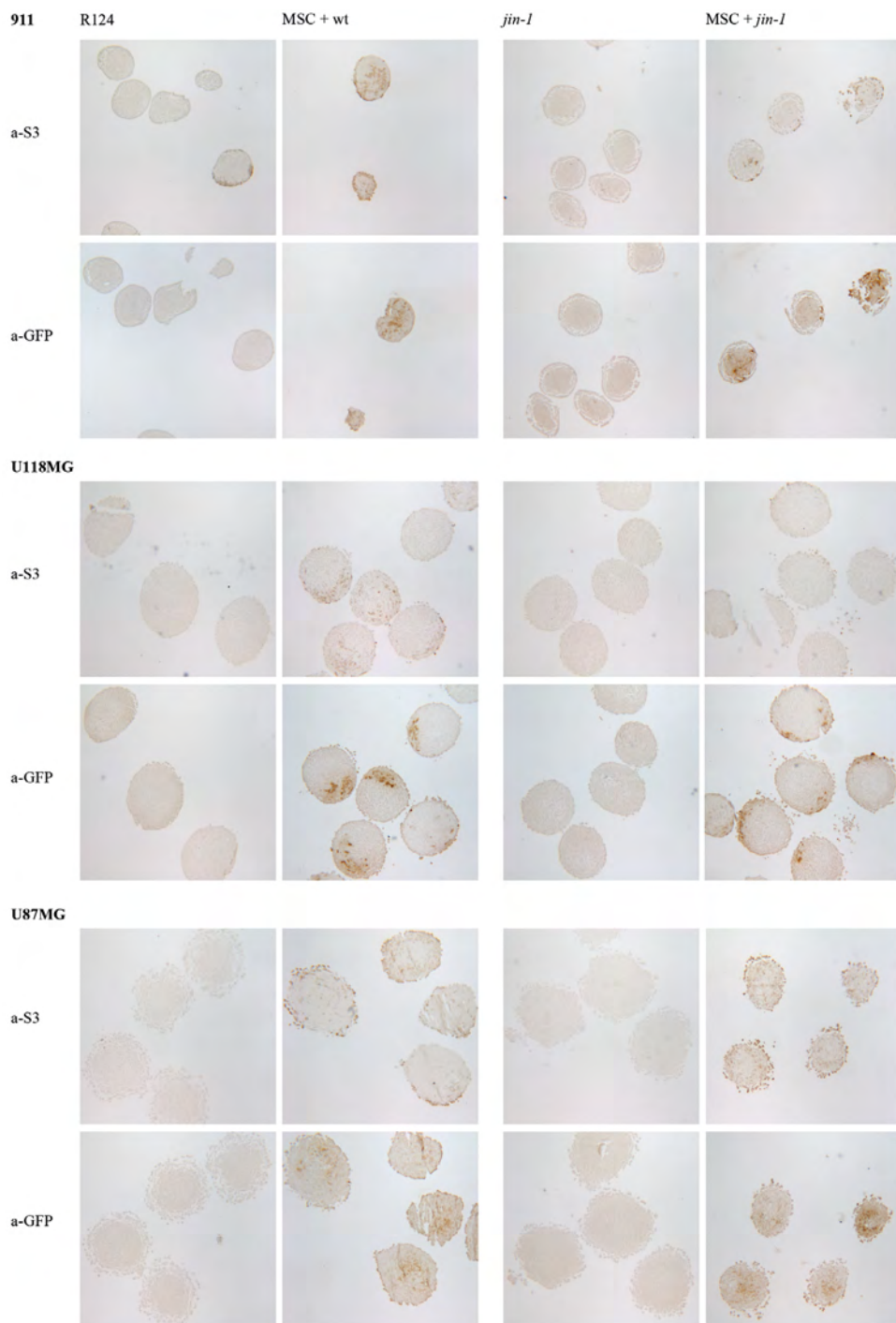


Figure 9.4 Distribution of reovirus infections in tumor-cell spheroids initiated by reovirus or reovirus-loaded MSC. Tumor-cell spheroids generated by 911, U118MG, and U87MG cells were incubated with 2500 pfu₉₁₁ reovirus or 500 reovirus-loaded, eGFP-expressing MSC. 72 hrs post exposure, the spheroids were fixed, paraffinized, and sectioned. Analysis of the sections was performed by DAB-immunocytochemistry with antibody 4F2 against reovirus capsid protein $\sigma 3$ or an antibody against eGFP, followed incubation with a Horse Radish Peroxidase (HRP)-conjugated antibody. HRP activity was visualized by DAB-staining. Representative spheroids are depicted.

No infection was observed in spheroids of U118MG cells exposed to only reovirus (figure 9.4, middle panel). When the spheroids were co-cultured with wt T3D-loaded MSC reovirus, $\sigma 3$ -positive cells were detected throughout the spheroid. In most areas there is no or limited eGFP signal, suggesting that the $\sigma 3$ -staining is derived from reovirus infected U118MG cells. The absence of eGFP signal can be explained by the fact that they are already lysed or fragmented in vesicle-like structures with a weaker eGFP signal. In spheroids incubated with *jln-1*-loaded MSC the $\sigma 3$ signal was weaker, suggesting that *jln-1* spreads less efficient in the spheroids than wt T3D reovirus.

No reovirus protein synthesis was observed when U87MG spheroids were infected with wt T3D or with *jln-1* only. Spheroids co-cultured with reovirus-loaded MSC demonstrated reovirus synthesis at various layers of the spheroid and the infection efficiency of wt T3D and *jln-1* was similar. At the core of the spheroid the $\sigma 3$ signal was weaker, and there was limited eGFP signal discernible suggesting that MSC did not reach the core of the spheroid.

Overall, the spread and penetration of reovirus into the spheroids upon exposure to reovirus-loaded MSC was higher than upon exposure to reovirus only. In these assays the efficiency of wt T3D was similar or higher than of the *jln-1*.

DISCUSSION

In the last decade the concept of using carrier cells for delivery of oncolytic viruses to solid tumors has gained momentum [128,129,153,154]. Several cell types have been considered, including T cells, natural killer cells, macrophages, dendritic cells (DCs), neural stem cells, and mesenchymal stromal cells (MSC) [129,148]. Here we have evaluated MSC as carriers of oncolytic reovirus. MSC have been shown to be capable of homing to tumor sites [149], they can be employed in autologous as well as in allogeneic transplantations, and they have an excellent safety record in clinical transplantation [155]. This supports their use for oncolytic virus delivery. Here we demonstrate that MSC can be loaded with reoviruses and that these viruses can be efficiently handed-off to target cells in monolayer and 3D cultures.

In the last decade much progress has been made in elucidating the molecular mechanisms of the reovirus infectious cycle. Reovirus can associate with cells via low-affinity binding to sialic-acid residues [75], internalization proceeds after engagement of the high-affinity receptor JAM-A. Absence of JAM-A on the cell surface provides resistance to reoviruses, as was seen by colorectal tumor cell cultures [156], chicken fibroblasts [9], and several tumor cell lines [114]. JAM-A independent entry into monolayer cultures can be achieved by the *jin*-mutants, which harbor mutations in the S1 segment encoding the viral spike protein [114]. Such mutants may have advantages over wt T3D reoviruses as oncolytic agent in tumors lacking JAM-A expression on their cell surface.

While flow-cytometry analyses revealed slightly higher number of MSC with $\alpha 3$ synthesis upon *jin-1* infection compared to wt T3D, the viral yield of both viruses is lower than the amount required for infection, confirming the earlier results on human diploid skin fibroblasts [114]. These data are consistent with a mechanism that MSC inhibits reovirus replication at a post-entry level. While many of the mechanistic details involved in lytic reovirus replication are still enigmatic, the stimulating effects of activating the Ras/RalGEF/p38 signaling pathway [7,53] are well established. In addition, many other cellular factors have been implicated in various aspects of the lytic replication cycle (reviewed in [47,148]).

Although virus replication in carrier cells can be considered as advantage to increase the virus load however it is not a prerequisite for efficient cell-mediated delivery, as was demonstrated for reovirus loaded onto T cells, DCs, or blood cells [130,131,157]. These studies demonstrated efficient delivery to target cells in the absence of viral replication in the carrier cells.

In our studies the mechanism of reovirus MSC association and release need to be further elucidated. The real-time-imaging microscopy data demonstrated that reovirus-loaded MSC eventually fragment (figure 9.3 B), releasing the cellular matter to the cultures. The fragmentation was mostly seen in the reovirus-exposed MSC co-cultures and at a much lower frequency, in mock-infected MSC co-cultured with indicator cells. The pathways leading to the fragmentation of the MSC have not yet been delineated. It is attractive to speculate that the vesicles released by the disintegrating reovirus-loaded MSC may facilitate reovirus dissemination to neighboring sensitive cells.

Pre-existing immunity reduces the efficacy of oncolytic virus therapy after intravenously administration [158,159]. This is of relevance as the human population has been exposed to reovirus [134]. The presence of a strong reovirus neutralizing activity in patients was evident in a phase I clinical trial

where neutralizing anti-reovirus antibody titers were further increased upon intravenous reovirus administration [60]. Shielding the virus would prevent neutralization of the virus. Our data suggest that reoviruses loaded onto MSC are at least partially protected from neutralizing antibodies. Although we noted a small reduction in efficiency, reovirus hand-off is not blocked by high doses of intravenous immunoglobulins (IVIg). This suggests that the reoviruses associate with the MSC in a concealed environment, where they are protected from neutralizing immunity. Two mechanisms can be envisioned 1) the reoviruses productively infect the MSC and the progeny virus is released at the target site and infect the sensitive cells or 2) part of the viruses may be taken up by the cells in endosomes or other vesicles but do not establish a productive infection, but may still be subsequently released as infectious viruses. Such mechanism has been proposed for immature DCs [131]. In absence of efficient and specific inhibitors of reovirus replication, it is difficult to distinguish these mechanisms.

While the monolayer cultures are often used in the development of new anticancer agents, the cultures do not faithfully mimic the 3D cellular architecture of the tumor. Spheroid cultures composed of cancer cells are more similar to tumors [116,119]. Oncolytic viruses testing in spheroid models demonstrated that penetration and distribution of the viral anticancer agents can be easily monitored [117,160]. Our studies demonstrate that the reovirus-loaded MSC can associate and become incorporated within tumor cell spheroids. No difference in MSC incorporation was noted between reovirus-loaded MSC and mock-loaded MSC, demonstrating that the reovirus infection does not negatively affect the MSC capacity to integrate into the spheroids. The addition of the reovirus-loaded MSC to the tumor cell-spheroids led to efficient infection of the tumor cells within the spheroid. Almost no infection was observed when spheroids were incubated with 2500 pfu₉₁₁ reovirus, which is comparable to the virus load of the reovirus pre-incubated MSC. Applying higher viral titers to the spheroids causes predominantly infections of the outer rim of the spheroids [124], while the addition of reovirus-loaded MSC to the spheroids resulted in reovirus infection deeper into the spheroids. Remarkably, efficient MSC-mediated infection wt T3D and *jin-1* in 911-cell spheroids, U87MG-cell spheroids, as well as in U118MG-cell spheroids was seen, even though the latter cells lack JAM-A expression. The infection of spheroids in absence of JAM-A can be attributed to secretion of active cellular proteases which convert the reovirus particles to infectious subviral particles [124]. This demonstrates that JAM-A expression can be dispensable for reovirus infection in 3D cultures. Taken together, these data suggest that the reoviruses do not depend on JAM-A for cell entry into 3-D cultures. The increased

efficiency of *jin-1* in infecting JAM-A negative cells in monolayer culture does not correspond to an increased efficiency in 3D cell cultures. Therefore it remains to be established which mechanisms are employed by reoviruses to infect JAM-A negative cells in 3D cell cultures.

Taken together our data demonstrate that human MSC can be used for delivery of reovirus T3D. It was shown that reovirus loaded MSC can efficiently hand-off the virus to sensitive cells in monolayer and 3D cultures and that the reovirus does not inhibit the MSC's capacity to become incorporated into tumor-cell spheroids. In addition, the reoviruses associated with the MSC are partially protected from neutralizing immunoglobulins. Therefore, our data warrant further evaluation of MSC as carrier cells of oncolytic reoviruses in animal models for human cancer.

REFERENCES III

REOVIRUS



1. **Forsyth, P., Roldan, G., George, D., et al.** A phase I trial of intratumoral administration of reovirus in patients with histologically confirmed recurrent malignant gliomas. *Mol. Ther.* 2008; **16**:627-632.
2. **Norman, K.L. and Lee, P.W.** Not all viruses are bad guys: the case for reovirus in cancer therapy. *Drug Discov. Today* 2005; **10**:847-855.
3. **Coffey, M.C., Strong, J.E., Forsyth, P.A., and Lee, P.W.** Reovirus therapy of tumors with activated Ras pathway. *Science* 1998; **282**:1332-1334.
4. **Etoh, T., Himeno, Y., Matsumoto, T., et al.** Oncolytic viral therapy for human pancreatic cancer cells by reovirus. *Clin. Cancer Res.* 2003; **9**:1218-1223.
5. **Kilani, R.T., Tamimi, Y., Hanel, E.G., et al.** Selective reovirus killing of bladder cancer in a co-culture spheroid model. *Virus Res.* 2003; **93**:1-12.
6. **Norman, K.L. and Lee, P.W.** Reovirus as a novel oncolytic agent. *J. Clin. Invest* 2000; **105**:1035-1038.
7. **Norman, K.L., Hirasawa, K., Yang, A.D., et al.** Reovirus oncolysis: the Ras/RalGEF/p38 pathway dictates host cell permissiveness to reovirus infection. *Proc. Natl. Acad. Sci. U.S.A* 2004; **101**:11099-11104.
8. **Tyler, K. L. and B. N. Fields.** 2001. Mammalian Reoviruses, p. 1729-1745. *In*: D. M. Knipe and P. M. Howely (eds.), *Fields Virology*. 4 th ed. Lippincott, Williams & Wilkins, Philadelphia.
9. **Barton, E.S., Forrest, J.C., Connolly, J.L., et al.** Junction adhesion molecule is a receptor for reovirus. *Cell* 2001; **104**:441-451.
10. **Barton, E.S., Connolly, J.L., Forrest, J.C., et al.** Utilization of sialic acid as a coreceptor enhances reovirus attachment by multistep adhesion strengthening. *J. Biol. Chem.* 2001; **276**:2200-2211.
11. **Danthi, P., Hansberger, M.W., Campbell, J.A., et al.** JAM-A-independent, antibody-mediated uptake of reovirus into cells leads to apoptosis. *J. Virol.* 2006; **80**:1261-1270.
12. **Forrest, J.C., Campbell, J.A., Schelling, P., et al.** Structure-function analysis of reovirus binding to junctional adhesion molecule 1. Implications for the mechanism of reovirus attachment. *J. Biol. Chem.* 2003; **278**:48434-48444.
13. **Lee, P.W. and Leone, G.** Reovirus protein sigma 1: from cell attachment to protein oligomerization and folding mechanisms. *Bioessays* 1994; **16**:199-206.
14. **Lee, P.W. and Gilmore, R.** Reovirus cell attachment protein sigma 1: structure-function relationships and biogenesis. *Curr. Top. Microbiol. Immunol.* 1998; **233**:137-153.
15. **Nibert, M.L., Dermody, T.S., and Fields, B.N.** Structure of the reovirus cell-attachment protein: a model for the domain organization of sigma 1. *J. Virol.* 1990; **64**:2976-2989.
16. **Turner, D.L., Duncan, R., and Lee, P.W.** Site-directed mutagenesis of the C-terminal portion of reovirus protein sigma 1: evidence for a conformation-dependent receptor binding domain. *Virology* 1992; **186**:219-227.
17. **Maginnis, M.S., Forrest, J.C., Kopecky-Bromberg, S.A., et al.** Beta1 integrin mediates internalization of mammalian reovirus. *J. Virol.* 2006; **80**:2760-2770.
18. **Nibert, M. L. and L. A. Schiff.** 2001. Reovirus and their replication, p. 1679-1728. *In*: D. M. Knipe and P. M. Howely (eds.), *Field Virology*. 4th ed. Lippincott Williams & Wilkins, Philadelphia.
19. **Roner, M.R. and Steele, B.G.** Localizing the reovirus packaging signals using an engineered m1 and s2 ssRNA. *Virology* 2007; **358**:89-97.

20. **Chen, D., Zeng, C.Q., Wentz, M.J., et al.** Template-dependent, *in vitro* replication of rotavirus RNA. *J. Virol.* 1994; **68**:7030-7039.
21. **Komoto, S., Sasaki, J., and Taniguchi, K.** Reverse genetics system for introduction of site-specific mutations into the double-stranded RNA genome of infectious rotavirus. *Proc. Natl. Acad. Sci. U.S.A* 2006; **103**:4646-4651.
22. **Patton, J.T. and Spencer, E.** Genome replication and packaging of segmented double-stranded RNA viruses. *Virology* 2000; **277**:217-225.
23. **Roner, M.R., Bassett, K., and Roehr, J.** Identification of the 5' sequences required for incorporation of an engineered ssRNA into the Reovirus genome. *Virology* 2004; **329**:348-360.
24. **Van Houdt, W.J., Smakman, N., van den Wollenberg, D.J., et al.** Transient infection of freshly isolated human colorectal tumor cells by reovirus T3D intermediate subviral particles. *Cancer Gene Ther.* 2008; **15**:284-292.
25. **Wahler, R., Russell, S.J., and Curiel, D.T.** Engineering targeted viral vectors for gene therapy. *Nat. Rev. Genet.* 2007; **8**:573-587.
26. **Roner, M.R. and Joklik, W.K.** Reovirus reverse genetics: Incorporation of the CAT gene into the reovirus genome. *Proc. Natl. Acad. Sci. U.S.A* 2001; **98**:8036-8041.
27. **Kobayashi, T., Antar, A.A., Boehme, K.W., et al.** A plasmid-based reverse genetics system for animal double-stranded RNA viruses. *Cell Host. Microbe* 2007; **1**:147-157.
28. **Fallaux, F.J., Kranenburg, O., Cramer, S.J., et al.** Characterization of 911: a new helper cell line for the titration and propagation of early region 1-deleted adenoviral vectors. *Hum. Gene Ther.* 1996; **7**:215-222.
29. **Smakman, N., van den Wollenberg, D.J., Elias, S.G., et al.** KRAS(D13) Promotes apoptosis of human colorectal tumor cells by ReovirusT3D and oxaliplatin but not by tumor necrosis factor-related apoptosis-inducing ligand. *Cancer Res.* 2006; **66**:5403-5408.
30. **Vellinga, J., Uil, T.G., de Vrij, J., et al.** A system for efficient generation of adenovirus protein IX-producing helper cell lines. *J. Gene Med.* 2006; **8**:147-154.
31. **Naik, U.P., Naik, M.U., Eckfeld, K., et al.** Characterization and chromosomal localization of JAM-1, a platelet receptor for a stimulatory monoclonal antibody. *J. Cell Sci.* 2001; **114**:539-547.
32. **Douglas, J.T., Miller, C.R., Kim, M., et al.** A system for the propagation of adenoviral vectors with genetically modified receptor specificities. *Nat. Biotechnol.* 1999; **17**:470-475.
33. **Carlotti, F., Bazuine, M., Kekarainen, T., et al.** Lentiviral vectors efficiently transduce quiescent mature 3T3-L1 adipocytes. *Mol. Ther.* 2004; **9**:209-217.
34. **Virgin, H.W., Mann, M.A., Fields, B.N., and Tyler, K.L.** Monoclonal antibodies to reovirus reveal structure/function relationships between capsid proteins and genetics of susceptibility to antibody action. *J. Virol.* 1991; **65**:6772-6781.
35. **Wilcox, M.E., Yang, W., Senger, D., et al.** Reovirus as an oncolytic agent against experimental human malignant gliomas. *J. Natl. Cancer Inst.* 2001; **93**:903-912.
36. **Campbell, J.A., Schelling, P., Wetzell, J.D., et al.** Junctional adhesion molecule a serves as a receptor for prototype and field-isolate strains of mammalian reovirus. *J. Virol.* 2005; **79**:7967-7978.
37. **Stehle, T. and Dermody, T.S.** Structural similarities in the cellular receptors used by adenovirus and reovirus. *Viral. Immunol.* 2004; **17**:129-143.

38. **Lindner, P., Bauer, K., Krebber, A., et al.** Specific detection of his-tagged proteins with recombinant anti-His tag scFv-phosphatase or scFv-phage fusions. *Biotechniques* 1997; **17**:140-149.
39. **Cashdollar, L.W., Chmelo, R.A., Wiener, J.R., and Joklik, W.K.** Sequences of the S1 genes of the three serotypes of reovirus. *Proc.Natl.Acad.Sci.U.S.A.* 1985; **82**:24-28.
40. **Chappell, J.D., Barton, E.S., Smith, T.H., et al.** Cleavage susceptibility of reovirus attachment protein sigma1 during proteolytic disassembly of virions is determined by a sequence polymorphism in the sigma1 neck. *J.Virol.* 1998; **72**:8205-8213.
41. **Yin, P., Keirstead, N.D., Broering, T.J., et al.** Comparisons of the M1 genome segments and encoded mu2 proteins of different reovirus isolates. *Virology* 2004; **1**.
42. **Castro, C., Arnold, J.J., and Cameron, C.E.** Incorporation fidelity of the viral RNA-dependent RNA polymerase: a kinetic, thermodynamic and structural perspective. *Virus Res.* 2005; **107**:141-149.
43. **Jane-Valbuena, J., Nibert, M.L., Spencer, S.M., et al.** Reovirus virion-like particles obtained by re-coating infectious subvirion particles with baculovirus-expressed sigma3 protein: an approach for analyzing sigma3 functions during virus entry. *J.Virol.* 1999; **73**:2963-2973.
44. **Vellinga, J., Rabelink, M.J., Cramer, S.J., et al.** Spacers increase the accessibility of peptide ligands linked to the carboxyl terminus of adenovirus minor capsid protein IX. *J.Virol.* 2004; **78**:3470-3479.
45. **Vellinga, J., de Vrij, J., Myhre, S., et al.** Efficient incorporation of a functional hyper-stable single-chain antibody fragment protein-IX fusion in the adenovirus capsid. *Gene Ther.* 2007; **14**:664-670.
46. **Chen, D. and Patton, J.T.** Rotavirus RNA replication requires a single-stranded 3' end for efficient minus-strand synthesis. *J.Virol.* 1998; **72**:7387-7396.
47. **Shmulevitz, M., Marcato, P., and Lee, P.W.** Unshackling the links between reovirus oncolysis, Ras signaling, translational control and cancer. *Oncogene* 2005; **24**:7720-7728.
48. **Van Houdt, W.J., Smakman, N., van den Wollenberg, D.J., et al.** Transient infection of freshly isolated human colorectal tumor cells by reovirus T3D intermediate subviral particles. *Cancer Gene Ther.* 2008; **15**:284-292.
49. **Stehle, T. and Dermody, T.S.** Structural evidence for common functions and ancestry of the reovirus and adenovirus attachment proteins. *Rev.Med.Virol.* 2003; **13**:123-132.
50. **Kobayashi, T., Chappell, J.D., Danthi, P., and Dermody, T.S.** Gene-specific inhibition of reovirus replication by RNA interference. *J.Virol.* 2006; **80**:9053-9063.
51. **Roy, P.** 2001. Orbiviruses, p. 1835-1869. *In*: D. M. Knipe and P. M. Howely (eds.), *Fields Virology*. Lippincott Williams and Wilkins, Philadelphia.
52. **Kapikian, A. Z., Y. Hoshino, and R. M. Chanock.** 2001. Rotaviruses, p. 1787-1833. *In*: D. M. Knipe and P. M. Howely (eds.), *Fields Virology*. Lippincott Williams and Wilkins, Philadelphia.
53. **Strong, J.E., Coffey, M.C., Tang, D., et al.** The molecular basis of viral oncolysis: usurpation of the Ras signaling pathway by reovirus. *EMBO J.* 1998; **17**:3351-3362.
54. **Barton, E.S., Chappell, J.D., Connolly, J.L., et al.** Reovirus receptors and apoptosis. *Virology* 2001; **290**:173-180.
55. **Connolly, J.L., Barton, E.S., and Dermody, T.S.** Reovirus binding to cell surface sialic acid potentiates virus-induced apoptosis. *J.Virol.* 2001; **75**:4029-4039.



56. **Kim, M., Chung, Y.H., and Johnston, R.N.** Reovirus and tumor oncolysis. *J.Microbiol.* 2007; **45**:187-192.
57. **Smakman, N., van den Wollenberg, D.J., Borel Rinkes, I.H., et al.** Sensitization to apoptosis underlies KrasD12-dependent oncolysis of murine C26 colorectal carcinoma cells by reovirus T3D. *J.Virol.* 2005; **79**:14981-14985.
58. **Gollamudi, R., Ghalib, M.H., Desai, K.K., et al.** Intravenous administration of Reolysin, a live replication competent RNA virus is safe in patients with advanced solid tumors. *Invest New Drugs* 2010; **28**:641-649.
59. **Vidal, L., Pandha, H.S., Yap, T.A., et al.** A phase I study of intravenous oncolytic reovirus type 3 Dearing in patients with advanced cancer. *Clin.Cancer Res.* 2008; **14**:7127-7137.
60. **White, C.L., Twigger, K.R., Vidal, L., et al.** Characterization of the adaptive and innate immune response to intravenous oncolytic reovirus (Dearing type 3) during a phase I clinical trial. *Gene Ther.* 2008; **15**:911-920.
61. **O'Donnell, S.M., Hansberger, M.W., and Dermody, T.S.** Viral and cellular determinants of apoptosis induced by mammalian reovirus. *Int.Rev.Immunol.* 2003; **22**:477-503.
62. **Guglielmi, K.M., Johnson, E.M., Stehle, T., and Dermody, T.S.** Attachment and cell entry of mammalian orthoreovirus. *Curr.Top.Microbiol.Immunol.* 2006; **309**:1-38.
63. **Alain, T., Kim, T.S., Lun, X., et al.** Proteolytic disassembly is a critical determinant for reovirus oncolysis. *Mol.Ther.* 2007; **15**:1512-1521.
64. **Borsa, J., Morash, B.D., Sargent, M.D., et al.** Two modes of entry of reovirus particles into L cells. *J.Gen.Virol.* 1979; **45**:161-170.
65. **Mandell, K.J. and Parkos, C.A.** The JAM family of proteins. *Adv.Drug Deliv.Rev.* 2005; **57**:857-867.
66. **Gutwein, P., Schramme, A., Voss, B., et al.** Downregulation of junctional adhesion molecule-A is involved in the progression of clear cell renal cell carcinoma. *Biochem. Biophys.Res.Commun.* 2009; **380**:387-391.
67. **Smakman, N.** 2006. [University Utrecht](#).
68. **Naik, M.U., Naik, T.U., Suckow, A.T., et al.** Attenuation of junctional adhesion molecule-A is a contributing factor for breast cancer cell invasion. *Cancer Res.* 2008; **68**:2194-2203.
69. **van den Wollenberg, D.J., van den Hengel, S.K., autzenberg, I.J., et al.** A strategy for genetic modification of the spike-encoding segment of human reovirus T3D for reovirus targeting. *Gene Ther.* 2008; **15**:1567-1578.
70. **Ponten, J. and Saksela, E.** Two established *in vitro* cell lines from human mesenchymal tumours. *Int.J.Cancer* 1967; **2**:434-447.
71. **Obeso, J., Weber, J., and Auerbach, R.** A hemangioendothelioma-derived cell line: its use as a model for the study of endothelial cell biology. *Lab Invest* 1990; **63**:259-269.
72. **Klein, B., Pastink, A., Odijk, H., et al.** Transformation and immortalization of diploid xeroderma pigmentosum fibroblasts. *Exp.Cell Res.* 1990; **191**:256-262.
73. **Kawaguchi, T., Nomura, K., Hirayama, Y., and Kitagawa, T.** Establishment and characterization of a chicken hepatocellular carcinoma cell line, LMH. *Cancer Res.* 1987; **47**:4460-4464.

74. **Leone, G., Maybaum, L., and Lee, P.W.** The reovirus cell attachment protein possesses two independently active trimerization domains: basis of dominant negative effects. *Cell* 1992; **71**:479-488.
75. **Chappell, J.D., Gunn, V.L., Wetzel, J.D., et al.** Mutations in type 3 reovirus that determine binding to sialic acid are contained in the fibrous tail domain of viral attachment protein sigma1. *J.Virol.* 1997; **71**:1834-1841.
76. **Reiter, D.M., Frierson, J.M., Halvorson, E.E., et al.** Crystal structure of reovirus attachment protein sigma1 in complex with sialylated oligosaccharides. *PLoS.Pathog.* 2011; **7**:e1002166.
77. **Morris, A.P., Tawil, A., Berkova, Z., et al.** Junctional Adhesion Molecules (JAMs) are differentially expressed in fibroblasts and co-localize with ZO-1 to adherens-like junctions. *Cell Commun.Adhes.* 2006; **13**:233-247.
78. **Borsa, J., Sargent, M.D., Lievaart, P.A., and Copps, T.P.** Reovirus: evidence for a second step in the intracellular uncoating and transcriptase activation process. *Virology* 1981; **111**:191-200.
79. **Connolly, J.L. and Dermody, T.S.** Virion disassembly is required for apoptosis induced by reovirus. *J.Virol.* 2002; **76**:1632-1641.
80. **Van Houdt, W.J., Smakman, N., van den Wollenberg, D.J., et al.** Transient infection of freshly isolated human colorectal tumor cells by reovirus T3D intermediate subviral particles. *Cancer Gene Ther.* 2008; **15**:284-292.
81. **Schelling, P., Guglielmi, K.M., Kirchner, E., et al.** The reovirus sigma1 aspartic acid sandwich: a trimerization motif poised for conformational change. *J.Biol.Chem.* 2007; **282**:11582-11589.
82. **Kovar, H., Jug, G., Aryee, D.N., et al.** Among genes involved in the RB dependent cell cycle regulatory cascade, the p16 tumor suppressor gene is frequently lost in the Ewing family of tumors. *Oncogene* 1997; **15**:2225-2232.
83. **Rubin, D.H., Wetzel, J.D., Williams, W.V., et al.** Binding of type 3 reovirus by a domain of the sigma 1 protein important for hemagglutination leads to infection of murine erythroleukemia cells. *J.Clin.Invest* 1992; **90**:2536-2542.
84. **Arnberg, N., Edlund, K., Kidd, A.H., and Wadell, G.** Adenovirus type 37 uses sialic acid as a cellular receptor. *J.Virol.* 2000; **74**:42-48.
85. **Eckhardt, M., Gotza, B., and Gerardy-Schahn, R.** Mutants of the CMP-sialic acid transporter causing the Lec2 phenotype. *J.Biol.Chem.* 1998; **273**:20189-20195.
86. **Chappell, J.D., Prota, A.E., Dermody, T.S., and Stehle, T.** Crystal structure of reovirus attachment protein sigma1 reveals evolutionary relationship to adenovirus fiber. *EMBO J.* 2002; **21**:1-11.
87. **Kelly, K., Nawrocki, S., Mita, A., et al.** Reovirus-based therapy for cancer. *Expert. Opin.Biol.Ther.* 2009; **9**:817-830.
88. **Koshiba, H., Hosokawa, K., Kubo, A., et al.** Junctional adhesion molecule A [corrected] expression in human endometrial carcinoma. *Int.J.Gynecol.Cancer* 2009; **19**:208-213.
89. **Byrnes, A.P. and Griffin, D.E.** Large-plaque mutants of Sindbis virus show reduced binding to heparan sulfate, heightened viremia, and slower clearance from the circulation. *J.Virol.* 2000; **74**:644-651.
90. **Hulst, M.M., van Gennip, H.G., and Moormann, R.J.** Passage of classical swine fever virus in cultured swine kidney cells selects virus variants that bind to heparan sulfate due to a single amino acid change in envelope protein E(rns). *J.Virol.* 2000; **74**:9553-9561.

91. **Sa-Carvalho, D., Rieder, E., Baxt, B., et al.** Tissue culture adaptation of foot-and-mouth disease virus selects viruses that bind to heparin and are attenuated in cattle. *J. Virol.* 1997; **71**:5115-5123.
92. **Cardin, A.D. and Weintraub, H.J.** Molecular modeling of protein-glycosaminoglycan interactions. *Arteriosclerosis* 1989; **9**:21-32.
93. **Hileman, R.E., Fromm, J.R., Weiler, J.M., and Linhardt, R.J.** Glycosaminoglycan-protein interactions: definition of consensus sites in glycosaminoglycan binding proteins. *Bioessays* 1998; **20**:156-167.
94. **Vives, R.R., Lortat-Jacob, H., and Fender, P.** Heparan sulphate proteoglycans and viral vectors : ally or foe? *Curr. Gene Ther.* 2006; **6**:35-44.
95. **Bernard, K.A., Klimstra, W.B., and Johnston, R.E.** Mutations in the E2 glycoprotein of Venezuelan equine encephalitis virus confer heparan sulfate interaction, low morbidity, and rapid clearance from blood of mice. *Virology* 2000; **276**:93-103.
96. **Bauer, P.H., Cui, C., Liu, W.R., et al.** Discrimination between sialic acid-containing receptors and pseudoreceptors regulates polyomavirus spread in the mouse. *J. Virol.* 1999; **73**:5826-5832.
97. **Lopez-Bueno, A., Rubio, M.P., Bryant, N., et al.** Host-selected amino acid changes at the sialic acid binding pocket of the parvovirus capsid modulate cell binding affinity and determine virulence. *J. Virol.* 2006; **80**:1563-1573.
98. **Chandran, K. and Nibert, M.L.** Animal cell invasion by a large nonenveloped virus: reovirus delivers the goods. *Trends Microbiol.* 2003; **11**:374-382.
99. **Jane-Valbuena, J., Breun, L.A., Schiff, L.A., and Nibert, M.L.** Sites and determinants of early cleavages in the proteolytic processing pathway of reovirus surface protein sigma3. *J. Virol.* 2002; **76**:5184-5197.
100. **Wilson, G.J., Nason, E.L., Hardy, C.S., et al.** A single mutation in the carboxy terminus of reovirus outer-capsid protein sigma 3 confers enhanced kinetics of sigma 3 proteolysis, resistance to inhibitors of viral disassembly, and alterations in sigma 3 structure. *J. Virol.* 2002; **76**:9832-9843.
101. **Tyler, K.L.** Pathogenesis of reovirus infections of the central nervous system. *Curr. Top. Microbiol. Immunol.* 1998; **233**:93-124.
102. **Ricard, D., Idbah, A., Ducray, F., et al.** Primary brain tumours in adults. *Lancet* 2012; **379**:1984-1996.
103. **Galli, R., Binda, E., Orfanelli, U., et al.** Isolation and characterization of tumorigenic, stem-like neural precursors from human glioblastoma. *Cancer Res.* 2004; **64**:7011-7021.
104. **Vescovi, A.L., Galli, R., and Reynolds, B.A.** Brain tumour stem cells. *Nat. Rev. Cancer* 2006; **6**:425-436.
105. **Bao, S., Wu, Q., McLendon, R.E., et al.** Glioma stem cells promote radioresistance by preferential activation of the DNA damage response. *Nature* 2006; **444**:756-760.
106. **Eramo, A., Ricci-Vitiani, L., Zeuner, A., et al.** Chemotherapy resistance of glioblastoma stem cells. *Cell Death. Differ.* 2006; **13**:1238-1241.
107. **Liu, G., Yuan, X., Zeng, Z., et al.** Analysis of gene expression and chemoresistance of CD133+ cancer stem cells in glioblastoma. *Mol. Cancer* 2006; **5**:67.
108. **Lee, J., Kotliarova, S., Kotliarov, Y., et al.** Tumor stem cells derived from glioblastomas cultured in bFGF and EGF more closely mirror the phenotype and genotype of primary tumors than do serum-cultured cell lines. *Cancer Cell* 2006; **9**:391-403.

109. **Vik-Mo, E.O., Sandberg, C., Olstorn, H., et al.** Brain tumor stem cells maintain overall phenotype and tumorigenicity after *in vitro* culturing in serum-free conditions. *Neuro.Oncol.* 2010; **12**:1220-1230.
110. **Wollmann, G., Ozduman, K., and van den Pol, A.N.** Oncolytic virus therapy for glioblastoma multiforme: concepts and candidates. *Cancer J.* 2012; **18**:69-81.
111. **Zemp, F.J., Corredor, J.C., Lun, X., et al.** Oncolytic viruses as experimental treatments for malignant gliomas: using a scourge to treat a devil. *Cytokine Growth Factor Rev.* 2010; **21**:103-117.
112. **Van Houdt, W.J., Smakman, N., van den Wollenberg, D.J., et al.** Transient infection of freshly isolated human colorectal tumor cells by reovirus T3D intermediate subviral particles. *Cancer Gene Ther.* 2008; **15**:284-292.
113. **Russell, S.J., Peng, K.W., and Bell, J.C.** Oncolytic virotherapy. *Nat.Biotechnol.* 2012; **30**:658-670.
114. **van den Wollenberg, D.J., Dautzenberg, I.J., Van Den Hengel, S.K., et al.** Isolation of reovirus T3D mutants capable of infecting human tumor cells independent of junction adhesion molecule-A. *PLoS.One.* 2012; **7**:e48064.
115. **Elliott, N.T. and Yuan, F.** A review of three-dimensional *in vitro* tissue models for drug discovery and transport studies. *J.Pharm.Sci.* 2011; **100**:59-74.
116. **Hirschhaeuser, F., Menne, H., Dittfeld, C., et al.** Multicellular tumor spheroids: an underestimated tool is catching up again. *J.Biotechnol.* 2010; **148**:3-15.
117. **Grill, J., Lamfers, M.L., van Beusechem, V.W., et al.** The organotypic multicellular spheroid is a relevant three-dimensional model to study adenovirus replication and penetration in human tumors *in vitro*. *Mol.Ther.* 2002; **6**:609-614.
118. **Balvers, R.K., Kleijn, A., Kloezeman, J.J., et al.** Serum-free culture success of glial tumors is related to specific molecular profiles and expression of extracellular matrix-associated gene modules. *Neuro.Oncol.* 2013; **15**:1684-1695.
119. **Herrmann, R., Fayad, W., Schwarz, S., et al.** Screening for compounds that induce apoptosis of cancer cells grown as multicellular spheroids. *J.Biomol.Scren.* 2008; **13**:1-8.
120. **Nduom, E.K., Hadjipanayis, C.G., and Van Meir, E.G.** Glioblastoma cancer stem-like cells: implications for pathogenesis and treatment. *Cancer J.* 2012; **18**:100-106.
121. **Alloussi, S.H., Alkassar, M., Urbschat, S., et al.** All reovirus subtypes show oncolytic potential in primary cells of human high-grade glioma. *Oncol.Rep.* 2011; **26**:645-649.
122. **Coombs, K.M.** Reovirus structure and morphogenesis. *Curr.Top.Microbiol.Immunol.* 2006; **309**:117-167.
123. **Schiff, L.A.** Reovirus capsid proteins sigma 3 and mu 1: interactions that influence viral entry, assembly, and translational control. *Curr.Top.Microbiol.Immunol.* 1998; **233**:167-183.
124. **Dautzenberg, I.J., van den Wollenberg, D.J., Van Den Hengel, S.K., et al.** Mammalian orthoreovirus T3D infects U-118 MG cell spheroids independent of junction adhesion molecule-A. *Gene Ther.* 2014.
125. **Kuriyama, N., Kuriyama, H., Julin, C.M., et al.** Pretreatment with protease is a useful experimental strategy for enhancing adenovirus-mediated cancer gene therapy. *Hum.Gene Ther.* 2000; **11**:2219-2230.
126. **Kuppen, P.J., van der Eb, M.M., Jonges, L.E., et al.** Tumor structure and extracellular matrix as a possible barrier for therapeutic approaches using immune cells or adenoviruses in colorectal cancer. *Histochem.Cell Biol.* 2001; **115**:67-72.

127. **Lamfers, M.L., Idema, S., van Milligen, F., et al.** Homing properties of adipose-derived stem cells to intracerebral glioma and the effects of adenovirus infection. *Cancer Lett.* 2009; **274**:78-87.
128. **Power, A.T. and Bell, J.C.** Taming the Trojan horse: optimizing dynamic carrier cell/oncolytic virus systems for cancer biotherapy. *Gene Ther.* 2008; **15**:772-779.
129. **Willmon, C., Harrington, K., Kottke, T., et al.** Cell carriers for oncolytic viruses: Fed Ex for cancer therapy. *Mol.Ther.* 2009; **17**:1667-1676.
130. **Ilett, E.J., Prestwich, R.J., Kottke, T., et al.** Dendritic cells and T cells deliver oncolytic reovirus for tumour killing despite pre-existing anti-viral immunity. *Gene Ther.* 2009; **16**:689-699.
131. **Ilett, E.J., Barcena, M., Errington-Mais, F., et al.** Internalization of oncolytic reovirus by human dendritic cell carriers protects the virus from neutralization. *Clin. Cancer Res.* 2011; **17**:2767-2776.
132. **Sottoriva, A., Spiteri, I., Piccirillo, S.G., et al.** Intratumor heterogeneity in human glioblastoma reflects cancer evolutionary dynamics. *Proc.Natl.Acad.Sci.U.S.A* 2013; **110**:4009-4014.
133. **Rosen, L., Evan, H.E., and Spickard, A.** Reovirus infections in human volunteers. *Am.J.Hyg.* 1963; **77**:29-37.
134. **Tai, J.H., Williams, J.V., Edwards, K.M., et al.** Prevalence of reovirus-specific antibodies in young children in Nashville, Tennessee. *J.Infect.Dis.* 2005; **191**:1221-1224.
135. **Hashiro, G., Loh, P.C., and Yau, J.T.** The preferential cytotoxicity of reovirus for certain transformed cell lines. *Arch.Virol.* 1977; **54**:307-315.
136. **Theiss, J.C., Stoner, G.D., and Kniazeff, A.J.** Effect of reovirus infection on pulmonary tumor response to urethan in strain A mice. *J.Natl.Cancer Inst.* 1978; **61**:131-134.
137. **Downward, J.** Targeting RAS signalling pathways in cancer therapy. *Nat.Rev.Cancer* 2003; **3**:11-22.
138. **Harrington, K.J., Vile, R.G., Melcher, A., et al.** Clinical trials with oncolytic reovirus: moving beyond phase I into combinations with standard therapeutics. *Cytokine Growth Factor Rev.* 2010; **21**:91-98.
139. **Pandha, H.S., Heinemann, L., Simpson, G.R., et al.** Synergistic effects of oncolytic reovirus and cisplatin chemotherapy in murine malignant melanoma. *Clin. Cancer Res.* 2009; **15**:6158-6166.
140. **Comins, C., Spicer, J., Protheroe, A., et al.** REO-10: a phase I study of intravenous reovirus and docetaxel in patients with advanced cancer. *Clin.Cancer Res.* 2010; **16**:5564-5572.
141. **Harrington, K.J., Karapanagiotou, E.M., Roulstone, V., et al.** Two-stage phase I dose-escalation study of intratumoral reovirus type 3 dearing and palliative radiotherapy in patients with advanced cancers. *Clin.Cancer Res.* 2010; **16**:3067-3077.
142. **Lolkema, M.P., Arkenau, H.T., Harrington, K., et al.** A phase I study of the combination of intravenous reovirus type 3 Dearing and gemcitabine in patients with advanced cancer. *Clin.Cancer Res.* 2011; **17**:581-588.
143. **Karapanagiotou, E.M., Roulstone, V., Twigger, K., et al.** Phase I/II trial of carboplatin and paclitaxel chemotherapy in combination with intravenous oncolytic reovirus in patients with advanced malignancies. *Clin.Cancer Res.* 2012; **18**:2080-2089.

144. **Prestwich, R.J., Harrington, K.J., Pandha, H.S., et al.** Oncolytic viruses: a novel form of immunotherapy. *Expert.Rev.Anticancer Ther.* 2008; **8**: 1581-1588.
145. **Iankov, I.D., Blechacz, B., Liu, C., et al.** Infected cell carriers: a new strategy for systemic delivery of oncolytic measles viruses in cancer virotherapy. *Mol. Ther.* 2007; **15**: 114-122.
146. **Ong, H.T., Hasegawa, K., Dietz, A.B., et al.** Evaluation of T cells as carriers for systemic measles virotherapy in the presence of antiviral antibodies. *Gene Ther.* 2007; **14**: 324-333.
147. **Power, A.T., Wang, J., Falls, T.J., et al.** Carrier cell-based delivery of an oncolytic virus circumvents antiviral immunity. *Mol. Ther.* 2007; **15**: 123-130.
148. **van den Wollenberg, D.J., Van Den Hengel, S.K., Dautzenberg, I.J., et al.** Modification of mammalian reoviruses for use as oncolytic agents. *Expert.Opin.Biol. Ther.* 2009; **9**: 1509-1520.
149. **Studeny, M., Marini, F.C., Champlin, R.E., et al.** Bone marrow-derived mesenchymal stem cells as vehicles for interferon-beta delivery into tumors. *Cancer Res.* 2002; **62**: 3603-3608.
150. **Komarova, S., Kawakami, Y., Stoff-Khalili, M.A., et al.** Mesenchymal progenitor cells as cellular vehicles for delivery of oncolytic adenoviruses. *Mol.Cancer Ther.* 2006; **5**: 755-766.
151. **Mader, E.K., Maeyama, Y., Lin, Y., et al.** Mesenchymal stem cell carriers protect oncolytic measles viruses from antibody neutralization in an orthotopic ovarian cancer therapy model. *Clin.Cancer Res.* 2009; **15**: 7246-7255.
152. **Van Houdt, W.J., Smakman, N., van den Wollenberg, D.J., et al.** Transient infection of freshly isolated human colorectal tumor cells by reovirus T3D intermediate subviral particles. *Cancer Gene Ther.* 2008; **15**: 284-292.
153. **Ferguson, S.D., Ahmed, A.U., Thaci, B., et al.** Crossing the boundaries: stem cells and gene therapy. *Discov.Med.* 2010; **9**: 192-196.
154. **Nakashima, H., Kaur, B., and Chiocca, E.A.** Directing systemic oncolytic viral delivery to tumors via carrier cells. *Cytokine Growth Factor Rev.* 2010; **21**: 119-126.
155. **Parekkadan, B. and Milwid, J.M.** Mesenchymal stem cells as therapeutics. *Annu. Rev.Biomed.Eng* 2010; **12**: 87-117.
156. **Van Houdt, W.J., Smakman, N., van den Wollenberg, D.J., et al.** Transient infection of freshly isolated human colorectal tumor cells by reovirus T3D intermediate subviral particles. *Cancer Gene Ther.* 2008; **15**: 284-292.
157. **Adair, R.A., Roulstone, V., Scott, K.J., et al.** Cell carriage, delivery, and selective replication of an oncolytic virus in tumor in patients. *Sci.Transl.Med.* 2012; **4**: 138ra77.
158. **Chen, Y., Yu, D.C., Charlton, D., and Henderson, D.R.** Pre-existent adenovirus antibody inhibits systemic toxicity and antitumor activity of CN706 in the nude mouse LNCaP xenograft model: implications and proposals for human therapy. *Hum. Gene Ther.* 2000; **11**: 1553-1567.
159. **Tsai, V., Johnson, D.E., Rahman, A., et al.** Impact of human neutralizing antibodies on antitumor efficacy of an oncolytic adenovirus in a murine model. *Clin. Cancer Res.* 2004; **10**: 7199-7206.
160. **Lamfers, M.L. and Hemminki, A.** Multicellular tumor spheroids in gene therapy and oncolytic virus therapy. *Curr.Opin.Mol. Ther.* 2004; **6**: 403-411.

PART IV

SUMMARY, DISCUSSION AND CONCLUSION



CHAPTER 10

SUMMARY AND DISCUSSION



The main aim of this thesis is to provide knowledge which can improve oncolytic virus therapy with adenovirus and reovirus vectors. The concept of using viruses for the treatment of malignancies was already investigated in the 1950s. Due to the disappointing results, the interest in this approach faded away from the general public. Renewed interest was gained around the 90s when molecular techniques became more advanced. This allowed approaches to increase the potency and the safety of viral vectors. In addition this also provided researcher tools to modify virus genomes [1,2]. During this period oncolytic virus therapy was seen as promising treatment. Now more than two decades down the road it can be concluded that generating effective oncolytic viruses has been more challenging than initially thought. Major bottlenecks are the efficiency and selectivity. In the recent years many research groups focused their research on improving oncolytic virus vectors.

Adenovirus can infect quiescent and dividing cells and drive the cells into S-phase. This allows the virus to propagate efficiently. Although adenovirus does not have a natural preference for transformed cells it is still one of the best studied viruses for oncolytic virus therapy. A brief overview on the general virus biology and the modifications required for endowing the adenovirus with a tumor-cell preference can be found in **chapter 2**. In **chapter 3** a similar overview is given for reovirus. In contrast to adenovirus the reovirus has an intrinsic preference for transformed cells. However, further modification of the genome of reovirus is challenging due to its segmented, double stranded RNA (dsRNA) genome. In part II and III different strategies for improving the oncolytic virus therapy with adenoviruses and reoviruses are discussed. In part III a section is dedicated to defining the susceptibility to reovirus of a cell type which has an important role in tumor genesis.

ADENOVIRUS

Adenovirus capsid protein modifications have been researched in depth to enhance the tumor cell specificity and decrease transfection of non-target tissue. The focus was to a large extent on fiber modifications, but also the other capsid proteins have been subjected to modification strategies to alter the tropism and shield the virus particle [3-6]. For instance protein IX turned out to be a useful anchor for small polypeptides to modify the cell tropism [7,8]. Protein IX is a minor capsid protein, and despite the much research to the functionality it remains enigmatic. Yet it is suggested that its function is important since the region is conserved in all primate adenoviruses [8]. Previous studies analyzing

the effect of the removal of protein IX already showed that the stability of the particles was negatively influenced [9]. In **chapter 4** we show that removal of protein IX yields an adenovirus vector with enhanced transgene delivery in coxsackie and adenovirus receptor (CAR) negative cells. In addition protein IX deletion caused an enhanced activation of peripheral blood mononuclear cells (PBMC) and sequesters in the liver after intravenous delivery in a mouse model. These data give more insight in the function of protein IX in determining the cell tropism and the activation of the immune system. In addition this knowledge may be important for the development of future clinical oncolytic vectors.

In the quest to improved adenovirus vectors for the use as oncolytic agents not only retargeting strategies are of interest but also modifications aiming at increasing the oncolytic efficiency and specificity are of concern. Since adenovirus has been popular as a model system in viral entry, transcription and replication studies and is well-investigated as an oncolytic vector, a lot of knowledge was gathered about gene functions and modification strategies. Therefore rational design was mainly the basis to the improved vectors that have been generated. However, literature exists showing that random approaches can also be effective for generating adenovirus vectors with improved cytopathic activity [10-13]. For example, two of these studies isolated mutants with mutations in the i-leader region after random mutagenesis and bioselection strategies [11,13]. The i-leader is present in the adenovirus major-late transcripts [14]. Unfortunately the exact function of this region is still unknown, partly because of that this region was not subjected earlier in modification studies. In the study of Yan *et al.* two mutants with multiple single-base-pair-mutations, including a shared mutation in the i-leader, were isolated after mutagenesis and bioselection on the human colorectal cancer cell line HT29. Further analysis confirmed that the shared i-leader truncating mutation was essential for the improved cytolytic activity [13]. The purpose of **chapter 5** was to determine the cytopathic effect of an adenovirus vector with the i-leader mutation on glioma cells in comparison to wild-type adenovirus. A replication competent adenovirus vector containing the i-leader truncating mutation (RL-07) was constructed by site directed mutagenesis and homologous recombination. The comparison studies were performed on established cell lines and on primary high grade glioma cultures. These studies showed that RL-07 had a higher cytopathic effect on transformed cell cultures but not on non-transformed cell lines. The expression pattern of E1A, fiber and adenovirus death protein (ADP) was similar to wild-type, however RL-07 was released earlier from the cells enhancing, the spread in the cultures. Although further research has to confirm that the function of the i-leader protein

is related to early release of the virus from cells, this mutation may be useful in future vectors.

REOVIRUS

Viral transduction of target cells may be hampered by the scarcity or inaccessibility of the viral receptors on the target cell. For reovirus is the junction adhesion molecule-A (JAM-A) receptor the high affinity receptor. The first genetic modification strategies in reovirus were published several years ago [15-17]. However retargeting of reovirus by genetic modifications is still a laborious and challenging process (see also chapter 1.3). The major challenges of modifying the reovirus genome is caused by the segmented double stranded RNA (dsRNA) genome. A description of one of the modification strategies, which may be applicable for the improvement of human reoviruses as oncolytic agents, is presented in **chapter 6**. The chapter focuses on the modification of the spike-encoding segment which anchors to the cognate receptor JAM-A. The generation of retargeted virus is performed on cells expressing a modified σ 1-encoding segment embedded in a conventional RNA polymerase II transcript. The wild-type σ -1 segment is replaced by the modified σ 1-encoding segment upon propagation. This was shown by infection of a resistant cell line expressing the receptor for the modified σ 1-protein. Further analysis confirmed that the modified σ -1 segment was also incorporated into the genome. From these data it can be concluded that 1) the modification strategy described is feasible for the modification of reovirus 2) the C-terminus of the spike-protein is a potential place to incorporate small polypeptides which can alter the cell tropism. However, additional experiments need to be performed to show which polypeptide would be suitable to introduce.

The lack of proofreading of the polymerase of RNA viruses, including reovirus, results in a high mutation rate [18]. Forcing reovirus propagation to resistant cell cultures which do not express the JAM-A receptor expands the cell tropism. This strategy is described in **chapter 7**. Briefly, wild-type reovirus was forced to propagate for several consecutive replication rounds on U118MG, a glioblastoma cell line which does not express JAM-A. Reovirus isolates which induce the cytopathic effect were further characterized. The isolated mutants, JAM-A independent (*jin*) mutants, could infect a wide range of cell lines that resisted wild-type, but infection on human fibroblasts was inhibited. Sequencing results of the S1 segment, encoding for the spike-protein, revealed that the *jin* mutants harbored mutations located close to the sialic-acid binding domain in the shaft

and two of the *jin* mutants also displayed a mutation in the head-domain, which is the JAM-A binding domain. Further analysis of the *jin* mutants indicated that infection relies on binding to sialic acid. Although these results indicate that the *jin* mutants may be useful as oncolytic vectors for the treatment of tumors which lack JAM-A on their surface, additional *in vitro* and *in vivo* studies need to confirm this.

The aim of **chapter 8** was to evaluate reovirus susceptibility of glioblastoma stem-like cells (GSC). A GSC culture is established from a fresh surgical specimen of a glioblastoma (GB). GSC represent a small population of a GB which possess high resistance to radio- and chemotherapy. In addition, these cells acquire the capacity to self-renew and differentiate into heterogeneous cells types that drive tumorigenesis [19-24]. Further analysis revealed that cultures of GSC more closely mirror the clinical features of GB than cells cultured in conventional serum-containing media or established glioblastoma cell lines [22,24]. Flow cytometry analyses of seven GSC cultures showed large variation of JAM-A expression. For that reason, susceptibility studies were performed with both the wild-type reovirus and the *jin-1* mutant. Four parameters were analyzed including infection, oncolytic efficacy, reovirus yield and infection of GSC spheroids. These three dimensional (3D) cultures mimic the tumor structure more faithfully than conventional two dimensional monolayer cultures [25,26]. The susceptibility to both wild-type and *jin-1* reovirus differed between the seven GSC cultures. Furthermore, on monolayer *jin-1* reovirus seems to perform better than wild-type while on the spheroids both viruses performed similarly. This difference, which is also demonstrated by Dautzenberg *et al.* [27], indicates that JAM-A expression may not be essential for infection in 3D cultures and that another alternative entry route may be involved. It is unclear whether the differences between the cultures faithfully reflect the status of the individual patients or that the heterogeneity is due to culturing conditions.

Efficient transduction of the tumor cells, especially after systematic administration, can be hampered by neutralizing antibodies. Other factors involved include scavenging by non-target tissue, non-specific binding by blood cells and soluble factors such as complement and pre-immune IgM that can reduce the uptake by target tissue [28,29]. In the oncolytic virus field different virus shielding and delivery strategies have been described. These studies suggest that delivery of significant amounts of oncolytic virus may be feasible [28,30,31]. The goal of **chapter 9** was to investigate if reovirus could be loaded onto human bone marrow-derived mesenchymal stromal cells (MSC), as these cells have the ability to home to tumors [32]. In addition different studies have

already described the use of MSC as carrier cells for oncolytic viruses [33,34]. In this study it was shown that wild-type reovirus and *jin-1* reovirus can be loaded onto MSC and that MSC are able to hand-off the virus to neighboring cells, in monolayer cultures and in spheroids. Furthermore incubation of the reovirus loaded MSC with neutralizing IgG only partly inactivated the virus suggesting that virus is, to some degree, shielded. Just as in chapter 8 *jin-1* performed slightly better on monolayer compared to wild-type. However this difference disappeared again in 3D cultures. The differences between the monolayer and spheroid cultures show that reliable model systems to test oncolytic viruses are urgently needed. In conclusion these data showed that MSC are potential cell carriers for reovirus, although future *in vitro* and *in vivo* research need to confirm this.

Finally, despite of anecdotic evidence of oncolytic viruses as effective oncolytic agents, it seems that viruses as single agents are not powerful enough to become the ultimate oncolytic treatment. However, an enhanced antitumor efficacy is seen when oncolytic viruses are combined with conventional treatment strategies [35]. Since this is a relatively new development future research need to confirm the safety of this approach.

CHAPTER 11

CONCLUSION



In **conclusion**, the work presented in this thesis shows that:

- Modification of capsid proteins can change the cell tropisms and these modifications may provide more insight into the function of the capsid proteins.
- Random and rational modification strategies both obtain modified vectors with increased oncolytic efficiency.
- The structure of a culture, monolayer (2D) or spheroids (3D), may result in differences determination of the oncolytic efficacy of the viral vector
- GSC cultures show a heterogeneous susceptibility to reovirus which may reflect the clinical variation.

CHAPTER 12

NEDERLANDSE SAMENVATTING



Het voornaamste doel van het onderzoek dat beschreven is in dit proefschrift is het verbeteren van oncolytisch virustherapie met adenovirus en reovirus vectoren. Het concept om virussen te gebruiken ter bestrijding van tumoren heeft al een lange geschiedenis en werd voor het eerst onderzocht rond 1950. Helaas ging belangstelling bij het grote publiek verloren door het uitblijven van grote doorbraken. Rond 1990 ontstond er hernieuwde interesse in virussen als anti-tumor therapie. Dit werd gekenmerkt door ontwikkeling van nieuwe technieken en kennis op het gebied van de moleculaire biologie. Deze nieuwe technieken en kennis leidden tot hernieuwde aanpakken die de effectiviteit en de veiligheid van het gebruik van virale vectoren verhoogden. Daarnaast gaven de moleculaire technieken de onderzoekers de mogelijkheid om het virusgenoom te modificeren [1,2]. Mede hierdoor werd in de jaren 90 oncolytische virustherapie beschouwd als een veelbelovende behandeling van tumoren. Nu, twee decennia verder, kan geconcludeerd worden dat de ontwikkeling van effectieve oncolytische virussen een grotere uitdaging is dan destijds werd aangenomen. Op dit moment zijn de effectiviteit en de selectiviteit van het virus ten opzichte van de tumor de belangrijkste knelpunten. Afgelopen jaren hebben dan ook vele onderzoeksgroepen zich gericht op het ondervangen van o.a. deze knelpunten ter verbetering van de effectiviteit van oncolytische virus vectoren.

Adenovirus is het best bestudeerde virus voor het gebruik als oncolytisch virus vector ondanks dat het geen voorkeur heeft voor getransformeerde cellen. Het virus kan cellen in rust maar ook actief-delende cellen infecteren waarna het adenovirus ervoor zorgt dat cellen in de S-fase van de celcyclus overgaan. De S-fase is de ideale omgeving voor adenovirus om zich efficiënt te repliceren. Een aanvullende beschrijving van adenovirus biologie is gegeven in **hoofdstuk 2**. In dit hoofdstuk is ook aandacht voor modificatie strategieën die ervoor zorgen dat adenovirus een voorkeur krijgt voor getransformeerde cellen. Naast adenovirus wordt in dit proefschrift een tweede virus beschreven als oncolytisch vector, te weten reovirus. In **hoofdstuk 3** is een gelijksoortig overzicht van de reovirus biologie en modificatie strategieën gegeven als voor adenovirus. In tegenstelling tot het adenovirus heeft reovirus wel een voorkeur voor getransformeerde cellen, maar is de modificatie van het genoom een grotere uitdaging. Dit wordt veroorzaakt doordat het genoom van een reovirus bestaat uit tien dubbel-strengs (ds) RNA segmenten. In de twee opeenvolgende secties worden verschillende strategieën beschreven die de oncolytische virustherapie met adenovirus (sectie 2) of reovirus (sectie 3) vectoren kunnen verbeteren. In sectie 3 is daarnaast nog een hoofdstuk gewijd aan de gevoeligheid van een tumorceltype, dat een belangrijke rol speelt in het ontstaan van tumoren en uitzaaiingen.

ADENOVIRUS

In het verleden heeft het adenovirusonderzoek zich voornamelijk gericht op het modificeren van capsid-eiwitten met als doel de selectiviteit voor getransformeerde cellen te verbeteren en het verlagen van de infectie van 'non-target' weefsel. Het onderzoek richtte zich op fiber-modificaties maar ook modificaties van de andere capsid-eiwitten zijn onderzocht. Deze strategieën focusten zich op het veranderen van het tropisme, maar ook op de afscherming van het virus door middel van het integreren van een extra eiwitstructuur in een capsid-eiwit [3-6]. Uit een van die onderzoeken kwam naar voren dat onder andere eiwit IX (pIX) een geschikte kandidaat is voor de 'verankering' van kleine polypeptiden die het cel-tropisme veranderen [7,8]. Eiwit IX is een klein capsid-eiwit met een vooralsnog raadselachtige functie. Toch wordt gesuggereerd dat pIX van belang is aangezien de regio coderende voor pIX geconserveerd is in alle primaat adenovirussen [8]. Daarnaast hebben eerdere studies laten zien dat verwijdering van pIX de stabiliteit van het virus aantast [9]. Hier kan aan toegevoegd worden dat de verwijdering van pIX een adenovirus-vector oplevert met een verhoogde transgene afgifte in coxsackievirus en adenovirus receptor (CAR) negatieve cellen. Dit wordt beschreven in **hoofdstuk 4**. Bovendien veroorzaakt de deletie van pIX een verhoogde activatie van perifere bloed mononucleaire cellen (PBMC) en opname in de lever na intraveneuze toediening in een muismodel. Samengevat, de gepresenteerde data geven meer inzicht in de functie van pIX; zij suggereren een rol van pIX bij de bepaling van het cellulaire tropisme en in de activatie van het immuun systeem. De verkregen kennis kan van belang zijn in de ontwikkeling van toekomstige oncolytische adenovirus vectoren.

In de zoektocht naar strategieën ter verbetering van adenovirus vectoren voor het gebruik als oncolytisch geneesmiddel zijn niet alleen 'retargeting' strategieën belangrijk maar ook modificaties die de infectie-efficiëntie en cel-specificiteit verbeteren. De populariteit van adenovirus als modelvirus voor infectie, transcriptie, replicatie en als oncolytische vector resulteerde in niet alleen virus-specifieke maar ook algemene virale kennis over functies en genetische modificatie strategieën. Dit leidde het tot rationeel ontwerpen van adenovirus-vectoren als basisstrategie. Daarnaast zijn er studies die laten zien dat ook 'random' modificatie ook effectief kan zijn voor het verkrijgen van vectoren met verhoogde cytopatische activiteit [10-13]. Voorbeelden hiervan zijn twee afzonderlijke studies waarin wordt beschreven dat na 'random' mutagenesis en bioselectie adenovirus-mutanten kunnen worden geïsoleerd die mutaties hebben in de i-leader regio [11,13]. De i-leader wordt tot expressie gebracht

tijdens adenovirus 'major-late' transcriptie [14]. Toch is tot op heden de exacte functie van deze regio nog niet bekend, mede daardoor is deze regio niet eerder onderwerp van modificatiestudies geweest. In de eerst gepubliceerde studie beschrijven Yan *et al.* twee adenovirus mutanten die geïsoleerd zijn op de humane colorectale kanker cellijn HT29 na mutagenese en bioselectie. Deze twee mutanten bevatten beide meerdere puntmutaties waaronder een gedeelde i-leader mutatie. Analyse bevestigde dat deze gemeenschappelijke mutatie essentieel is voor de verbeterde cytolytische activiteit [13]. Het doel van de studie beschreven in **hoofdstuk 5** was het determineren van het cytopatische effect van de adenovirus met i-leader mutatie op glioma-cellen in vergelijking met het wild-type virus. In deze studie werd doormiddel van gerichte mutagenese en homologe recombinatie een replicatie-competent adenovirus vector gecreëerd die de i-leader mutatie (RL-07) bevatte. Vergelijkingsstudies op gestandaardiseerde (established) cellijnen en primaire hooggradige glioma tumorcel kweken toonden aan dat RL-07 een hogere cytopatische activiteit heeft op getransformeerde celculturen dan wild-type adenovirus, maar dat dit niet werd gezien op niet-getransformeerde cellijnen. Hoewel het expressie patroon van E1A, fiber en 'adenovirus death protein' (ADP) in vergelijking tot wild-type gelijk was, kwam RL-07 toch eerder vrij uit de cellen. Hierdoor verbeterde de spreiding van dit virus in de culturen. Ondanks dat toekomstige studies nog moeten bevestigen dat de functie van de i-leader gerelateerd is aan de vervroegde afgifte van het virus kan dit een interessante mutatie zijn voor toekomstige vectoren.

REOVIRUS

Virale transductie kan belemmerd worden door afwezigheid of door het niet-toegankelijk zijn van specifieke receptoren op de target-cel. Voor reovirus is de junction adhesion molecule-A (JAM-A) receptor van groot belang voor efficiënte transductie; modificatie van virus-attachment eiwitten kan deze specificiteit veranderen. Al zijn de eerste genetische modificatie strategieën voor reovirus enkele jaren geleden gepubliceerd [15-17], toch blijft het 'retargeten' van reovirus door middel van genetische modificatie een uitdagend proces. Dit wordt veroorzaakt door het gesegmenteerde dsRNA genoom (hoofdstuk 3). In **hoofdstuk 6** wordt een modificatie strategie beschreven die zich richt op de modificatie van het S1 segment coderend voor het spike-eiwit ($\sigma 1$). De spike bindt de JAM-A receptor. De productie van het 'geretargette' virus wordt uitgevoerd met gemodificeerde cellen die het $\sigma 1$ coderend-segment, ingebed

in een conventionele RNA polymerase II transcript, tot expressie brengen. Het wild-type sigma-1 eiwit en genoom-segment, worden gedurende de replicatie vervangen door het gemodificeerde sigma-1. Dit werd bevestigd door 1) infectie van een resistente cellijn die de receptor voor de verankering van het gemodificeerde $\sigma 1$ tot expressie brengt en 2) moleculaire analyse die aantoonde dat het gemodificeerde segment in het genoom was geïncorporeerd. Uit deze studie kan geconcludeerd worden, 1) dat modificatie van reovirus doormiddel van de bovenstaande strategie mogelijk is en 2) dat de C-terminus van de spike-eiwit $\sigma 1$ een geschikte locatie is voor het incorporeren van kleine polypeptiden die het cellulaire tropisme kunnen aanpassen. Vervolgexperimenten kunnen bepalen welke polypeptiden geschikt zijn voor de introductie van nieuwe sequenties in het reovirus genoom en capside.

De hoge mutatiesnelheid in RNA virussen waaronder het reovirus wordt veroorzaakt door het ontbreken van de 'proof-reading' capaciteit van de RNA polymerasen [18]. In **hoofdstuk 7** staat beschreven dat oncolytische vectoren kunnen worden verkregen door gebruik te maken van de ontbrekende 'proof-reading'. Waar het op neer komt is dat wild-type reovirus replicatie wordt geforceerd op JAM-A negatieve celculturen. In deze studie werd gebruik gemaakt van de JAM-A negatieve glioblastoma cellijn U118MG. Dit resulteerde in een virus met een aangepast cellulair tropisme. Na enkele geforceerde replicatiecycli werden de reovirus-isolaten die een verhoogd cytopathisch-effect induceerden verder gekarakteriseerd. De geïsoleerde mutanten, hier genaamd JAM-A onafhankelijke (*jin*) mutanten, kunnen een grote range aan cellen infecteren die resistent zijn voor wild-type reovirus. Infectie van humane fibroblast cellen bleef geblokkeerd. De resultaten van het nucleotide-sequencing van het S1 segment, coderend voor het spike-eiwit, onthulde dat in de *jin* mutanten mutaties zijn opgetreden dicht bij het sialzuur-bindingsdomein. Aanvullende experimenten lieten zien dat deze mutanten tijdens infectie afhankelijk zijn van binding aan sialzuur i.p.v. binding aan JAM-A. Tot slot, resultaten uit deze studie laten zien dat de *jin* mutanten van betekenis kunnen zijn als oncolytische vectoren voor de behandeling van tumoren die JAM-A niet tot expressie brengen op hun celoppervlak. Om dit te bevestigen Zijn aanvullende *in vitro* en *in vivo* studies zijn nodig.

In **hoofdstuk 8** wordt de gevoeligheid van glioblastoma stem-like cells (GSC) voor reovirus beoordeeld. De gebruikte GSC-culturen zijn verkregen uit chirurgische specimen van glioblastomas (GB) van verschillende patiënten. De GSC representeren een kleine populatie cellen in een GB die een hoge weerstand hebben tegen radio- en chemotherapie. Daarnaast bevatten deze cellen de

eigenschap om zichzelf te vermenigvuldigen en te differentiëren in heterogene celtypen die de tumorgenese aansturen [19-24]. Studies hebben uitgewezen dat de eigenschappen van GSC culturen meer overeenkomsten hebben met de klinische eigenschappen van GB dan de cellen die gekweekt worden in de conventionele serum-bevattende media of gestandaardiseerde (established) GB cellijnen [22,24]. Met behulp van flowcytometrie werd de expressie van JAM-A van de zeven geselecteerde GSC-culturen bepaald. Hieruit kwam naar voren dat er een grote variatie in JAM-A expressie bestaat tussen deze GSC-culturen. Mede hierdoor werd er besloten dat de studie zou worden uitgevoerd met wild-type reovirus en de *jin-1* mutant. Vier parameters werden geanalyseerd, inclusief infectie-efficiëntie op monolaagculturen, oncolytische effectiviteit, virusopbrengst en infectie van GSC sferoïden. In literatuur staat beschreven dat driedimensionale (3D) culturen de tumorstructuur beter nabootsen dan de conventionele tweedimensionale monolaagculturen [25,26]. Uit deze studie kan geconcludeerd worden dat de gevoeligheid van de GSC culturen voor beide virussen, wild-type en *jin-1*, niet gelijkwaardig was. Bovendien lijkt het effect van *jin-1* op de monolaagculturen groter dan dat van wild-type, terwijl op de sferoïden beide virussen vergelijkbare resultaten gaven. Het gegeven dat reovirus zich anders gedraagt in monolaag dan in 3D culturen is kort geleden gepubliceerd door Dautzenberg *et al.* In deze publicatie staat beschreven dat in 3D culturen JAM-A expressie niet essentieel is voor infectie en dat er alternatieve infectie-routen zijn [27]. In een vervolgstudie zou moeten worden onderzocht of het effect van reovirus op de geselecteerde GSC een waardig beeld geeft van de individuele variatie tussen patiënten of dat deze verschillen voortkomen uit variaties in kweekcondities.

Het efficiënt transduceren van tumorcellen, zeker na systemische toediening, kan belemmerd worden door neutraliserende antilichamen. Andere factoren die een negatieve invloed kunnen hebben op de transductie-efficiëntie zijn o.a. het wegvangen van virussen door andere weefsels en niet-specifieke binding van virussen aan bloedcellen of oplosbare factoren zoals complementeiwitten en pre-immuun IgM [28,29]. In de oncolytische onderzoekswereld worden verschillende strategieën beschreven waarbij virussen hiervoor worden afgeschermd. Deze studies suggereren dat de aflevering van significante hoeveelheden oncolytische virussen uitvoerbaar kan zijn [28,30,31]. Het doel van **hoofdstuk 9** was het onderzoeken van de mogelijkheid om reovirus te laden op mesenchymale stamcellen (MSC) geïsoleerd uit humaan beenmerg. Van MSC is bekend dat ze het vermogen hebben om naar tumoren te migreren [32]. Daarnaast hebben verschillende studies laten zien dat MSC gebruikt kunnen worden als drager-

cellen voor oncolytische virussen [33,34]. In deze studies is onderzocht 1) of wild-type reovirus en *jin-1* reovirus kunnen worden geladen op MSC en 2) of de MSC het virus ook weer kunnen doorgeven aan buurcellen, zowel in monolaag als in sferoiden. Nadat de MSC werden geladen met reovirus, werd onderzocht of MSC het virus kon beschermen tegen uitwendige factoren. Hiervoor werden de reovirus-beladen MSC geïncubeerd met neutraliserende IgG antilichamen. Dit gaf een gedeeltelijke inactivatie van het virus. Dit suggereert dat het virus in beperkte mate beschermt is. Zoals eerder vermeld in hoofdstuk 8 is het effect van *jin-1* in vergelijking met wild-type iets beter op monolaag culturen. Echter dit verschil is niet meer waarneembaar in de 3D culturen. Het verschil tussen monolaag en 3D culturen in zowel deze studie, als ook in de vorige, laat zien dat het van belang is om een goed modelsysteem te hebben die betrouwbaar effectiviteit van oncolytische virussen in een klinisch-relevante omgeving representeert. Hiervoor zouden in de toekomst vergelijkingsstudies tussen modelsystemen en klinische studies gedaan moeten worden. De data uit hoofdstuk 9 laat verder zien dat MSC potentiële dragers zijn voor reovirus en dat uitgebreide *in vitro* en *in vivo* studies een logisch vervolg kunnen zijn.

Ten slotte, ondanks anekdotisch bewijs dat oncolytische virussen effectief kunnen zijn als oncolytisch geneesmiddel, lijkt het erop dat virussen als monotherapie niet krachtig genoeg zijn om de ultieme behandelmethodete worden. Echter een verbeterd antitumoreffect is beschreven wanneer oncolytische virussen worden gecombineerd met de conventionele behandelingsstrategieën [35]. Aangezien dit een relatief nieuwe ontwikkeling is zal er meer onderzoek moeten plaatsvinden om uit te zoeken hoe veilig en effectief deze combinatiestrategie is.

CONCLUSIE

Uit de data gepresenteerd in dit proefschrift kan geconcludeerd worden dat:

- Modificatie van een capside eiwit kan leiden tot het veranderen van het cellulaire tropisme. Tevens kan deze modificatie meer inzicht geven in de biologische functie van het eiwit;
- Willekeurige en rationele modificatie strategieën kunnen beide leiden tot virale vectoren met een verhoogd oncolytisch-rendement;
- De structuur van de cultuur, monolaag (2D) of sferoïde (3D), kan voor een verschil zorgen in de beoordeling van de oncolytische activiteit van een vector; en
- De gevoeligheid van GSC culturen op reovirus laat een grote variatie zien, dit zou de klinische variatie kunnen weergeven.

REFERENCES IV

SUMMARY, DISCUSSION
AND CONCLUSION



1. **Hammill, A.M., Conner, J., and Cripe, T.P.** Oncolytic virotherapy reaches adolescence. *Pediatr. Blood Cancer* 2010; **55**:1253-1263.
2. **Kelly, E. and Russell, S.J.** History of oncolytic viruses: genesis to genetic engineering. *Mol. Ther.* 2007; **15**:651-659.
3. **Bachtarzi, H., Stevenson, M., and Fisher, K.** Cancer gene therapy with targeted adenoviruses. *Expert. Opin. Drug Deliv.* 2008; **5**:1231-1240.
4. **Glasgow, J.N., Everts, M., and Curiel, D.T.** Transductional targeting of adenovirus vectors for gene therapy. *Cancer Gene Ther.* 2006; **13**:830-844.
5. **Nandi, S. and Lesniak, M.S.** Adenoviral virotherapy for malignant brain tumors. *Expert. Opin. Biol. Ther.* 2009; **9**:737-747.
6. **Toth, K., Dhar, D., and Wold, W.S.** Oncolytic (replication-competent) adenoviruses as anticancer agents. *Expert. Opin. Biol. Ther.* 2010; **10**:353-368.
7. **Vellinga, J., Rabelink, M.J., Cramer, S.J., et al.** Spacers increase the accessibility of peptide ligands linked to the carboxyl terminus of adenovirus minor capsid protein IX. *J. Virol.* 2004; **78**:3470-3479.
8. **Vellinga, J., van der Heijdt, S., and Hoeben, R.C.** The adenovirus capsid: major progress in minor proteins. *J. Gen. Virol.* 2005; **86**:1581-1588.
9. **Vellinga, J., van den Wollenberg, D.J., van der Heijdt, S., et al.** The coiled-coil domain of the adenovirus type 5 protein IX is dispensable for capsid incorporation and thermostability. *J. Virol.* 2005; **79**:3206-3210.
10. **Gros, A., Martinez-Quintanilla, J., Puig, C., et al.** Bioselection of a gain of function mutation that enhances adenovirus 5 release and improves its antitumoral potency. *Cancer Res.* 2008; **68**:8928-8937.
11. **Subramanian, T., Vijayalingam, S., and Chinnadurai, G.** Genetic identification of adenovirus type 5 genes that influence viral spread. *J. Virol.* 2006; **80**:2000-2012.
12. **Uil, T.G., Vellinga, J., de Vrij, J., et al.** Directed adenovirus evolution using engineered mutator viral polymerases. *Nucleic Acids Res.* 2011; **39**:e30.
13. **Yan, W., Kitzes, G., Dormishian, F., et al.** Developing novel oncolytic adenoviruses through bioselection. *J. Virol.* 2003; **77**:2640-2650.
14. **Symington, J.S., Lucher, L.A., Brackmann, K.H., et al.** Biosynthesis of adenovirus type 2 i-leader protein. *J. Virol.* 1986; **57**:848-856.
15. **Kobayashi, T., Antar, A.A., Boehme, K.W., et al.** A plasmid-based reverse genetics system for animal double-stranded RNA viruses. *Cell Host. Microbe* 2007; **1**:147-157.
16. **Roner, M.R., Sutphin, L.A., and Joklik, W.K.** Reovirus RNA is infectious. *Virology* 1990; **179**:845-852.
17. **van den Wollenberg, D.J., van den Hengel, S.K., Dautzenberg, I.J., et al.** A strategy for genetic modification of the spike-encoding segment of human reovirus T3D for reovirus targeting. *Gene Ther.* 2008; **15**:1567-1578.
18. **Domingo, E. and Holland, J.J.** RNA virus mutations and fitness for survival. *Annu. Rev. Microbiol.* 1997; **51**:151-178.
19. **Bao, S., Wu, Q., McLendon, R.E., et al.** Glioma stem cells promote radioresistance by preferential activation of the DNA damage response. *Nature* 2006; **444**:756-760.

20. **Eramo, A., Ricci-Vitiani, L., Zeuner, A., et al.** Chemotherapy resistance of glioblastoma stem cells. *Cell Death.Differ.* 2006; **13**:1238-1241.
21. **Galli, R., Binda, E., Orfanelli, U., et al.** Isolation and characterization of tumorigenic, stem-like neural precursors from human glioblastoma. *Cancer Res.* 2004; **64**:7011-7021.
22. Lee, J., Kotliarova, S., Kotliarov, Y., et al. Tumor stem cells derived from glioblastomas cultured in bFGF and EGF more closely mirror the phenotype and genotype of primary tumors than do serum-cultured cell lines. *Cancer Cell* 2006; **9**:391-403.
23. **Liu, G., Yuan, X., Zeng, Z., et al.** Analysis of gene expression and chemoresistance of CD133+ cancer stem cells in glioblastoma. *Mol.Cancer* 2006; **5**:67.
24. **Vik-Mo, E.O., Sandberg, C., Olstorn, H., et al.** Brain tumor stem cells maintain overall phenotype and tumorigenicity after in vitro culturing in serum-free conditions. *Neuro.Oncol.* 2010; **12**:1220-1230.
25. **Herrmann, R., Fayad, W., Schwarz, S., et al.** Screening for compounds that induce apoptosis of cancer cells grown as multicellular spheroids. *J.Biomol.Screen.* 2008; **13**:1-8.
26. **Hirschhaeuser, F., Menne, H., Dittfeld, C., et al.** Multicellular tumor spheroids: an underestimated tool is catching up again. *J.Biotechnol.* 2010; **148**:3-15.
27. **Dautzenberg, I.J., van den Wollenberg, D.J., van den Hengel, S.K., et al.** Mammalian orthoreovirus T3D infects U-118 MG cell spheroids independent of junction adhesion molecule-A. *Gene Ther.* 2014; **21**:609-17
28. **Power, A.T. and Bell, J.C.** Taming the Trojan horse: optimizing dynamic carrier cell/oncolytic virus systems for cancer biotherapy. *Gene Ther.* 2008; **15**:772-779.
29. **Prestwich, R.J., Harrington, K.J., Pandha, H.S., et al.** Oncolytic viruses: a novel form of immunotherapy. *Expert.Rev.Anticancer Ther.* 2008; **8**:1581-1588.
30. **Kreppel, F. and Kochanek, S.** Modification of adenovirus gene transfer vectors with synthetic polymers: a scientific review and technical guide. *Mol.Ther.* 2008; **16**:16-29.
31. **Nakashima, H., Kaur, B., and Chiocca, E.A.** Directing systemic oncolytic viral delivery to tumors via carrier cells. *Cytokine Growth Factor Rev.* 2010; **21**:119-126.
32. **Studený, M., Marini, F.C., Champlin, R.E., et al.** Bone marrow-derived mesenchymal stem cells as vehicles for interferon-beta delivery into tumors. *Cancer Res.* 2002; **62**:3603-3608.
33. **Komarova, S., Kawakami, Y., Stoff-Khalili, M.A., et al.** Mesenchymal progenitor cells as cellular vehicles for delivery of oncolytic adenoviruses. *Mol.Cancer Ther.* 2006; **5**:755-766.
34. **Mader, E.K., Maeyama, Y., Lin, Y., et al.** Mesenchymal stem cell carriers protect oncolytic measles viruses from antibody neutralization in an orthotopic ovarian cancer therapy model. *Clin.Cancer Res.* 2009; **15**:7246-7255.
35. **Russell, S.J., Peng, K.W., and Bell, J.C.** Oncolytic virotherapy. *Nat.Biotechnol.* 2012; **30**:658-670.

LIST OF PUBLICATIONS



Publications

de Vrij, J., Uil, T.G., van den Hengel, S.K., Cramer, S.J., Koppers-Lalic, D., Verweij, M.C., Wiertz, E.J., Vellinga, J., Willemsen, R.A., Hoeben, R.C. Adenovirus targeting to HLA-A1/Mage-A2-positive tumor cells by fusing a single-chain T-cell receptor with minor capsid protein IX. *Gene Ther.* 2008; **15**:978-989

van den Wollenberg, D.J., van den Hengel, S.K., Dautzenberg, I.J., Cramer, S.J., Kranenburg, O., Hoeben, R.C. A strategy for genetic modification of the spike-encoding segment of human reovirus T3D for reovirus targeting. *Gene Ther.* 2008; **15**:1567-1578

van den Wollenberg, D.J., van den Hengel, S.K., Dautzenberg, I.J., Kranenburg, O., Hoeben, R.C. Modification of mammalian reoviruses for use as oncolytic agents. *Expert.Opin.Biol.Ther.* 2009; **9**:1509-1520

de Vrij, J., van den Hengel, S.K., Uil, T.G., Koppers-Lalic, D., Dautzenberg, I.J., Stassen, O.M., Barcena, M., Yamamoto, M., de Ridder, C.M., Kraaij, R., Kwappenberg, K.M., Schilham, M.W., Hoeben, R.C. Enhanced transduction of CAR-negative cells by protein IX-gene deleted adenovirus 5 vectors. *Virology* 2011; **410**:192-200

Uil, T.G., Vellinga, J., de Vrij, J., van den Hengel, S.K., Rabelink, M.J., Cramer, S.J., Eekels, J.J., Ariyurek, Y., van Galen, M., Hoeben, R.C. Directed adenovirus evolution using engineered mutator viral polymerase. *Nucleic Acids Res.* 2011; **39**:e30

van den Hengel, S.K., de Vrij, J., Uil, T.G., Lamfers, M.L., Sillevius Smitt, P.A., Hoeben, R.C. Truncating the i-leader open reading frame enhances release of human adenovirus type 5 in glioma cells. *Virol.J.* 2011; **8**:162

de Vrij, J., Dautzenberg, I.J., van den Hengel, S.K., Magnusson, M.K., Uil, T.G., Cramer, S.J., Vellinga, J., Verissimo, C.S., Lindholm, L., Koppers-Lalic, D., Hoeben, R.C. A cathepsin-cleavage site between the adenovirus capsid protein IX and tumor-targeting ligands improves targeted transductions. *Gene Ther.* 2012; **19**:899-906

van den Wollenberg, D.J., Dautzenberg, I.J., van den Hengel, S.K., Cramer, S.J., de Groot, R.J., Hoeben, R.C. Isolation of reovirus T3D mutants capable of infecting human tumor cells independent of junction adhesion molecule-A. *PLoS One* 2012; **7**:e48064

van den Hengel, S.K., Balvers, R.K., Dautzenberg, I.J., van den Wollenberg, D.J., Kloezeman, J.J., Lamfers, M.L., Sillevius Smitt, P.A., Hoeben, R.C. Heterogeneous reovirus susceptibility in human glioblastoma stem-like cell cultures. *Cancer Gene Ther.* 2013; **20**(9):507-513

Dautzenberg, I.J., van den Wollenberg, D.J., van den Hengel, S.K., Limpens, R.W., Bárcena, M., Koster, A.J., Hoeben, R.C. Mammalian orthoreovirus T3D infects U-118 MG cell spheroids independent of junction adhesion molecule-A. *Gene Ther.* 2014; **21**:609-617

Balvers, R.K., Belcaid, Z., van den Hengel, S.K., Kloezeman, J.J., de Vrij, J., Wakimoto, H., Hoeben, R.C., Debets, R., Leenstra, S., Dirven, C., Lamfers, M.L. Locally-derived T-cell-derived cellular vehicles efficiently track and deliver adenovirus delta24-RGD infiltrating glioma. *Viruses* 2014; **6**: 3080-96

van den Wollenberg, D.J., Dautzenberg, I.J., Ros, W., Lipińska, A.D., van den Hengel, S.K., Hoeben, R.C. Replicating reoviruses with a transgene replacing the codons for the head domain of the viral spike. *Gene Ther.* 2015; **22**:51-63

Book chapter

van den Hengel, S.K., Dautzenberg, I.J., van den Wollenberg, D.J., Sillevius Smitt, P.A., Hoeben, R.C. Genetic modification in mammalian orthoreoviruses. 2013; p.289-317. *In: A. Bridgen (ed.), Reverse Genetics of RNA Viruses.* Wiley-Blackwell

PHD PORTFOLIO



COURSES (13 ECTS)

- 2008 The animal Imaging Workshop by AMIE, Molecular Medicine, Rotterdam, The Netherlands
- 2009 Data-analysis ESP03, Nihes, Rotterdam, The Netherlands
- 2009 Basic and Translational Oncology, Molecular Medicine, Rotterdam, The Netherlands
- 2009-2010 Biomedical English Writing and Communication, ErasmusMC, Rotterdam, The Netherlands
- 2010 The Photoshop CS3 Workshop for PhD-students and other researchers, Molecular Medicine, Rotterdam, The Netherlands
- 2010-2011 Proefdierkunde (art. 9), LUMC, Leiden, The Netherlands
- 2012 BioBusiness Summer School, Hyphen Projects, Amsterdam, The Netherlands

PRESENTATIONS AND CONGRESS VISITS (8.5 ECTS)

Oral:

- 2010 Department Retrovirus & Comparative Pathology, University of Lyon 1, Lyon, France
- 2012 Nederlandse Vereniging voor Gen and Celtherapie (NVGCT), Heeze, The Netherlands

Poster

- 2008 European Society for Gene and Cell Therapy, Brugge, Belgium
- 2009 9th International Adenovirus Meeting, Dobogókő, Hungary

Congress visits

- 2007 European Society for Gene and Cell Therapy, Rotterdam, The Netherlands
- 2011 British society for Gene Therapy, Brighton, UK
- 2007-2011 Dutch Annual Virology Symposium, KNAW, Amsterdam, The Netherlands

TEACHING (7 ECTS)

Students

2009-2011 Supervising Master students Biotechnology, Wageningen
University and Research
(*L. Fanchi and B. van Ravenstein*)

Lecturing

2010-2012 Practical course Molecular Techniques, LUMC

ABOUT THE AUTHOR





Sanne Klaassiena van den Hengel werd geboren op 1 april 1983 te Groningen. Na het behalen van haar havo diploma aan het C.S.G.'t Liudger te Drachten begon ze in 2000 met de hbo-opleiding Biotechnologie aan de Noordelijke Hogeschool Leeuwarden/Van Hall Instituut. Haar onderzoeksstage getiteld *het effect van (-)-hydroxycitric acid op vet absorptie* doorliep ze met goed gevolg aan de Rijksuniversiteit Groningen, afdeling neuroendocrinologie onder leiding van dr. PY Wielinga en Prof. dr. AJW Scheurink. Haar afstudeerstage genaamd *The Optimisation of a high throughput screening assay for the therapy of Friedreich Ataxia* voldeed ze met succes in het Murdoch Childrens Research Institute in Melbourne, Australië onder leiding van dr. JP Sarsero, Ms. L Li en Prof. dr. PA Ioannou. Na het behalen van haar Bachelor diploma in 2005 startte ze met haar Master Biotechnologie aan de Universiteit Wageningen met als specialisatie cellulaire en moleculaire biotechnologie. Het onderwerp van haar onderzoeksstage was *De identificatie van butanol-derivaten die minder schadelijk zijn voor C.acetobutylicum dan butanol en de modificatie van de bacteriën om deze derivaten te gaan produceren*. Dit onderzoek werd uitgevoerd aan de universiteit Wageningen, afdeling microbiologie onder leiding van dr. MAJ Siemerink en Prof. dr. J van der Oost. Haar afstudeeronderzoek met de titel *Rat insulin Promoter II; a potetial tool for a gene therapy based strategy towards the curing of Diabetes Mellitus* heeft ze uitgevoerd aan het Leids Universitair Medisch Centrum (LUMC), afdeling moleculaire celbiologie (MCB), sectie virus- en stamcelbiologie. Tijdens deze periode werd ze begeleidt door dr. A Zaldumbide en Prof. dr. RC Hoeben.

In 2007 behaalde ze haar MSc waarna ze direct startte met haar promotieonderzoek aan het Erasmus Medisch Centrum (ErasmusMC), afdeling Neurologie in nauwe samenwerking met het LUMC, afdeling MCB, sectie VSB. Het onderwerp van haar promotieonderzoek was het verbeteren van virale vectoren voor oncolytische virus therapie en werd uitgevoerd onder leiding van Prof. dr. Sillevius Smitt (afdeling Neurologie, ErasmusMC) en Prof. dr. RC Hoeben (LUMC, afdeling MCB, sectie VSB). In 2011, in het kader van voortzetting van haar promotieonderzoek, kreeg ze een aanstelling als onderzoeker aan het LUMC, afdeling MCB, sectie VSB. De resultaten van deze onderzoeksperiodes zijn gepresenteerd in dit manuscript.

Sinds april 2013 is ze werkzaam als onderzoeker bij Wetsus, European centre of excellence for sustainable water technology in Leeuwarden en is daar betrokken bij het onderzoek naar 1) antibioticaresistentie in ziekenhuisafvalwater en 2) virus-inactivatie en verwijdering uit drinkwater.

DANKWOORD



Hier zit ik dan met een leeg stuk papier voor mijn neus. Ik heb moeite om de eerste woorden op papier te krijgen, want ja... het dankwoord moet nog geschreven worden. En zoals jullie misschien wel weten, het uitdrukken van mijn gedachten in woorden is niet mijn sterkste eigenschap. Toch wil ik mijn gebundelde werk afsluiten met een mooi dankwoord waar ik trots op ben.

Het liefst zou ik iedereen persoonlijk willen bedanken en elke herinnering die nu naar boven komt op willen schrijven, zoals nagellakken aan de virus en stamcel biologie koffietafel. Maar het moet een dankwoord blijven en geen terugblik daarom heb mij beperkt tot de meest memorabele herinneringen. BEDANKT!! Aan iedereen die een bijdrage heeft geleverd aan mijn proefschrift of aan mijn welzijn gedurende mijn promotie, dit promotiehoofdstuk van mijn leven wordt hier nu afgesloten, maar ik hoop jullie allemaal weer terug te zien in de komende hoofdstukken van mijn leven.

Eerst wil ik het woord richten tot mijn promotoren Prof. dr. Peter Sillevius Smitt en Prof. dr. Rob Hoeben. Jullie hebben veel geduld moeten hebben voordat jullie dit boekje in handen kregen. Heel erg bedankt voor jullie geduld, steun en snelle reacties op mijn berichten. Peter, onze eerste ontmoeting was op het ErasmusMC. Het was een kennismakingsgesprek, ik herinner mij dat je een vraag stelde over hoe ik de toekomst voor me zag. Geen idee meer wat ik precies heb geantwoord, maar je hebt me aangenomen. Bedankt voor je vertrouwen en wetenschappelijke input in de afgelopen jaren. Rob, mijn eerste ontmoeting met jou was in de zomer van 2006, ruim 8 maanden voordat mijn promotiestudie startte. Ik kwam op jouw afdeling voor een afstudeerstage. Naast het inspirerende onderzoek hing er ook een prettige sfeer. Ik was ook ontzettend blij dat jij een PhD-project voor mij creëerde door je netwerk in te schakelen. Rob, al die jaren ben ik mij blijven verbazen over de parate kennis die je hebt. Promoveren onder jouw toezicht was een unieke ervaring.

Beste Prof. dr. Dirven, Prof. dr. Bangma en dr. van der Pluijm bedankt dat jullie mijn manuscript wilden beoordelen door plaats te nemen in de leescommissie. Daarnaast wil ik jullie en dr. Debets, dr. Lamfers, dr. Van Hall en dr. Van der Hoog bedanken dat jullie tijdens mijn verdediging aan de andere zijde van de tafel willen plaatsnemen.

Lieve Iris, super bedankt dat je mijn paranif wilt zijn. Onze eerste samenwerking voert terug naar onze studietijd in Wageningen. In Leiden kwam jij naast mij te zitten; jij ging ook aan reovirus werken. Naast onze samenwerking en jouw intellectuele verrijking van mijn werk gingen onze gemeenschappelijke interesses verder, nu.nl-achterklap, telegraaf-privé, happy-hardcore (Q-music foute uur). Ook ons tripje naar Lyon, op jouw verjaardag naar de Keukenhof en

nog andere legendarische momenten schieten nou door mijn hoofd. Bedankt! Wat ik je wil meegeven: 'doorzetten! Als ik (en de rest) het kan (kunnen), kan jij het zeker'.

Lieve Anna, mijn steun en toeverlaat en niet alleen tijdens deze promotie. Onze geschiedenis gaat ver terug. Als kleine meisjes waren wij al bij elkaar te vinden, maar door de jaren heen is onze band alleen maar sterker geworden. Ik weet dat ik op jou kan rekenen.

Mijn collega's op de afdeling Virus en Stamcel Biologie, bedankt! Jullie maakten het een feest om naar mijn werk te gaan. Arnaud, jij was mijn begeleider tijdens mijn afstudeerstage. Af en toe begreep ik je niet, maar jij inspireerde mij. Het enthousiasme waarmee je jouw kennis deelde maakte mijn beslissing om een PhD te gaan doen gemakkelijk. Diana, kamergenoot, reovirus specialist, bedankt voor het delen van je kennis. Maarten, al onze vroege koffieuurtjes en jouw geintjes ☺. Jolande, je hoort officieel niet in dit rijtje, maar je hoort bij Maarten, bedankt voor je ongekende interesse in mijn werk en leven, we houden contact! Jeroen ons schaatstochtje komt als eerste naar boven. En ik ben je nog steeds dankbaar dat ik een tijdje in je huisje heb mogen bivakkeren. Natuurlijk mogen in dit rijtje Steve – vraagbaak, iemand met jouw kennis mis ik op mijn nieuwe werkplek, Martijn – Lentivirus specialist, maar ook Hester, Françoise, Selina, Erik, Taco, Lianne, Harald, Dirk, Jim, Manuel, Anabel, Twan, Kim, Danijela, Laetitia en Ietje niet gemist worden in dit rijtje. Bedankt voor alles. Aan deze lijst voeg ik tevens Bram en Lorenzo toe, twee studenten die ik heb mogen begeleiden in het begin van hun carrière. Dank voor jullie inzet.

Mijn Rotterdamse collega's Rutger en Jenneke, het was super om met jullie en op jullie afdeling te mogen werken. Martine, naast dat je in de commissie hebt willen plaatsnemen, wil ik je ook bedanken voor onze samenwerking die ik erg prettig vond. Ik ging graag bij jou langs in Rotterdam om data en ideeën te bespreken.

Aan al mijn korfbalvrienden, zowel van VKC, Débaldéruit en Harga (nou Nexus), bedankt voor jullie interesse in mijn werk en voor alle ontspannende momenten die ik met jullie heb mogen beleven. Diane, onze bijna maandelijkse etentjes waren altijd super gezellig. Na onze etentjes was ik weer helemaal op de hoogte van de nieuwste roddels. Dit mis ik, nou ik in Leeuwarden zit.

Het is alweer ruim 2 jaar geleden dat ik bij Wetsus in dienst ben getreden. Het voelde als een warm bad en binnen de kortste keren voelde ik mij er helemaal thuis. Bedankt fijne collega's en een speciaal dank aan mijn oud-kamergenoten Heleen, Lucia en Hester. Bianca ondanks dat jij er nog geen jaar rondloopt, heb ik het gevoel dat we elkaar al heel lang kennen. Jouw zonnige en energieke

karakter is fantastisch. Daarnaast wil ik Johannes, Cees en Bert bedanken voor het vertrouwen dat jullie in mij hebben. Wetsus haalt het beste in mij naar boven!

Naast collega's en korfbalvrienden wil ik ook nog twee andere speciale vrienden bedanken. Lotte onze promotietrajecten liepen bijna synchroon, hierdoor begrepen we elkaars frustraties. Bedankt voor het je luisterend oor en steun. Liane al hebben we niet meer zo close-contact als vroeger toch blijf je een vriendin waar ik van weet dat die er altijd zal zijn.

Aangezien ik ruim 12,5 jaar samen ben met mijn grote liefde betekend dat ik ook ruim 12,5 jaar een fantastische schoonfamilie heb. Een basis in Driesum waar wij rust vinden, die ons af en toe even uit onze sleur halen. Bedankt voor de afleiding en onvoorwaardelijke steun.

Oma met haar sterke wil, ik herken eigenschappen van haar in mijzelf (al weet ik niet of ik daar altijd even blij mee ben). Jij hebt geen idee waar ik mij mee bezig heb gehouden, en dat is ook niet erg. Ik bewonder je vechtlust en positieve levenshouding en ben super blij dat je dit nog mag lezen.

Ik heb een speciale band met mijn broeders, Herwin, Gerbrant en Arjo, ondanks dat wij allemaal niet even spraakzaam zijn, kunnen we elkaar toch altijd vinden. Tegenwoordig behoren wij tot dezelfde vriendengroep (oud-VKC) en dat is fijn. Fantastische tijden (feesten en weekenden) met VKC staan nog steeds in mijn geheugen, geheimen die wij verborgen hielden voor vader en moeder (al gooide André wel eens roet in het eten). Betere broeders kan ik mij niet wensen. Annelien jij vult dit uitstekend aan.

Pap en mam, nou zijn jullie aan de beurt. Zoals ik net al heb proberen te beschrijven kom ik uit een fantastisch gezin, dat is jullie verdienste. Daarnaast hebben jullie mij altijd gesteund, mij mijn eigen weg laten kiezen en mij gemotiveerd om me verder te ontwikkelen. Jullie hebben mij losgelaten door me als 18 jarig meisje op kamers te laten wonen. En nog geen twee jaar later ging ik alleen naar Australië voor ruim 6 maanden. Ik ben jullie daar enorm dankbaar voor. Ik kan mij geen betere ouders wensen. Ruim twee jaar geleden toen ik bij Wetsus werd aangenomen, mocht ik zo weer thuis-thuis komen wonen. Al was het onder het mom van tijdelijk, ik woon er nog steeds. En al het huishoudelijk werk wat voornamelijk jij mam mij uithanden hebt genomen, heeft mij de rust gegeven om deze promotie af te maken. Bedankt voor jullie onvoorwaardelijk liefde en steun.

Last but not least, mijn grote liefde André, wij zijn samen begonnen aan dit avontuur 'promoveren' en gaan het samen afsluiten. Een droom die in vervulling komt. In de onderstaande tekst heb ik geprobeerd om mijn gedachten aan, en

gevoelens voor jou op papier te krijgen, maar mijn woorden schieten te kort. Al ruim 12,5 jaar samen, in die tijd hebben wij elkaar altijd vrij gelaten om ons verder te ontwikkelen. Jouw steun en vertrouwen in mij hebben mij doen groeien tot deze vrouw. En nog steeds leer ik veel van jou. Jij helpt mij om verder te komen en daar ben ik je enorm dankbaar voor. Samen sluiten wij dit hoofdstuk af en beginnen wij aan het volgende deel van ons boek. Een toekomstdroom van ons is om plaats te kunnen nemen onder onze appelboom en samen genieten van de ondergaande zon. Laten wij nu eerst genieten van dit feest en de nabije toekomst.

- The best has yet to come -
Scorpions

Liefs Sanne

